BIOPHYSICAL INVESTIGATION OF BACTERIAL AGGREGATION

KEVIN EFOSA EBOIGBODIN B.Sc, M.Sc

Thesis submitted for the degree of Doctor of Philosophy

To the University of Sheffield, Sheffield, UK

On completion of research in the Biological and Environmental Systems Group within the Department of Chemical and Process Engineering

January, 2008

This thesis is dedicated to my family, especially my parents (Engr. and Mrs Eboigbodin), my brother (Osagie Eboigbodin) and my wife (Mrs Lisa Eboigbodin)

Declaration

The thesis is a testimony of the author's work completed at The University of Sheffield, UK, except where acknowledgements are made. This work has not been submitted for any other degrees.

Kevin Efosa EBOIGBODIN (Candidate)

Acknowledgements

A special acknowledgement goes to my supervisors Dr. Catherine Biggs and Dr. Alex Routh, for their excellent supervision, without whose support and guidance this project would never have been completed. Special thanks also go to the postdoctoral researcher, Dr. Jillian Newton, for her support and guidance through this project.

General appreciation goes to members of the Biological and Environmental Systems Group in the Department Chemical and Process Engineering, and the Cell-Mineral Interface group, in the Kroto Research Institute – a cheerful and supportive group.

Special thanks go to Dr. María Romero González and Mr. Jesus Ojeda from the EPRSC funded Cell-Mineral Interface group, Kroto Research Institute (GR/S72467/01) for their support and guidance, and access to the FTIR and potentiometric titrator.

A special thanks to Robert Bachmann, of the Groundwater Protection & Restoration Group, Kroto Research Institute for his training, guidance and advice.

I would also like to extend my appreciation to all members of the Department of Chemical and Process Engineering, both staff and students, who in one way or another helped me, progress through this project.

Special thanks also go to all my colleagues, especially those in my office (Ian Gabbott for making cups of tea for 3 years and IT support), Adela Khor, Kel Win Chua, David Hernandez-Atonal, and Ngoc Anh Phan for their advice and support.

Thanks to Prof. Paul Williams (University of Nottingham) and his research group for providing the bacterial strains. Special thanks also to Dr. Klaus Winzer for his support and guidance on quorum sensing.

Special thanks go to both the BBSRC (through grant number BB/C505391/14) and the EPSRC (studentship).

Finally, special thanks go to my family, especially my parents and wife, for their endless support and love.

List of publications

Parts of the work in this thesis have been published as below:

(J-journal paper, O-oral presentataion, P-poster presentation, PE-public engagement).

(J1) Eboigbodin, K. E., J. R. Newton, A. F. Routh, and C. A. Biggs (2005). Role of nonadsorbing polymers in bacterial aggregation. *Langmuir* **21**:12315-12319.

(J2) Eboigbodin, K. E., J. R. A. Newton, A. F. Routh, and C. A. Biggs (2006). Bacterial quorum sensing and cell surface electrokinetic properties. *Applied Microbiology and Biotechnology* **73**:669-675.

(J3) Eboigbodin K.E, Ojeda, J and C.A Biggs (2007). Investigating the effect of glucose on *Escherichia coli* cell surface properties, and the inhibition of aggregation. *Langmuir* **23**:6691-6697

(J4) Eboigbodin K.E and C. A. Biggs (2008). Characterisation of the Extracellular Polymeric Substances produced by *Escherichia coli* using Infra-Red Spectroscopic, Proteomic and Aggregation Studies. *Biomacromolecules*. DOI 10.1021/bm701043c

(O1) Role of non-adsorbing polymers in bacterial aggregation, 10th UK Polymer Colloids Forum April 2005, University of Sheffield

(O2) Cell-to-cell communication in *E.coli*: Who is listening? Seminar series on environmental microbiology, Department of Civil and Structural Engineering December 2006, University of Sheffield.

(O3) Bacterial aggregation "The Royal Society" for bacteria. Departmental Seminar, Department of Chemical and Process Engineering, April 2007, University of Sheffield.

(P1) Bacterial quorum sensing and cell surface electrokinetic properties. NERC scientific meeting on quorum sensing co-sponsored by BBSRC, EPSRC, MRC and the Wellcome Trust, 7th December 2005.

(P2) Role of depletion interaction in bacterial aggregation. Cell-Mineral Interface Annual Steering Committee Jan 2006, University of Sheffield.

(P3) Surface Properties of Bacteria: Does Quorum Sensing Play a Role? American Society of Microbiology (ASM) 106th General Meeting, Orlando USA 21-25th May 2006.

(PE1) Invited Press Release for ASM. "Bacteria are talking with electric charge". 106th General Meeting of the American Society for Microbiology, Orlando USA 21-25th May 2006.

(PE2) Interview for ASM Radio: MicrobeWorld: June 2006 A 90-second radio feature being heard across the U.S. on primarily public radio stations on "snapshot" of the latest developments or historical viewpoint on microbes.

CONTENT

Abbreviations

2-DE	Two-dimensional gel electrophoresis
AI-2	Autoinducer-2
Da	Dalton (molecular mass)
DLVO	Derjaguin, Landau, Verwey, Overbeek
E.coli	*Escherichia coli*
ECP	Extracellular proteins
EPS	Extracellular polymeric substances
FTIR	Fourier transform infrared spectroscopy
HSL	*N*-acyl homoserine lactones
LB	Luria-Bertani media
LBG	Luria-Bertani media supplemented with 0.5 % (w/v) glucose at the beginning of growth phase
LC-MS/MS	Liquid chromatography coupled to tadem mass spectrometer
luxS	*S*-Riboylhomocysteinase
MATH	Microbial adhesion to hydrocarbon
MIC	Microbiologically Influenced Corrosion
O.D	Optical density
PALS	Phase Analysis Light Scattering
PCR	Polymerase chain reaction
SDS-PAGE	Sodium dodecyl sulfate polyacrylamide gel electrophoresis
SPS	Sodium polystyrene sulphonate
w/v	weight per volume

Abstract

In nature, bacteria usually exist as aggregates, in order to withstand changes in environmental conditions. Bacterial aggregation is of great significance in the field of biotechnology, environmental studies and medicine. Bacterial aggregation is thought to be governed by physical forces such Van der Waals and electrostatic interaction. However, extracellular polymeric substances (EPS), and the ability of bacteria to participate in cell-to-cell communication via quorum sensing molecules have also been implicated in the bacterial aggregation process. Despite the wealth of knowledge available, a detailed understanding of bacterial aggregation still remains unclear. The overall aim of this work therefore, is to understand bacterial aggregation at the cellular and sub-cellular level using existing colloidal characterisation techniques and post genomic methods. This will enable both the biological and the physical aspects of aggregation to be studied together.

E.coli strains (AB1157, MG1655 and MG1655 *luxS*) were cultivated in Luria-Bertani (LB) medium at 30^0C supplemented with or without 0.5 w/v (%) glucose at the beginning of growth phase. Depletion aggregation studies were carried out using *E.coli* AB1157 and *E.coli* MG1655 harvested at different growth phases using a non-adsorbing polymer, sodium polystyrene sulphonate (SPS) and biological produced extracellular polymeric substances (EPS) respectively. The content of EPS produced by *E.coli* MG1655 during their growth in different media was quantified and characterized using Fourier transformation infrared spectroscopy (FTIR), SDS-PAGE and an electrospray ionization-tandem mass spectrometry. The changes in cell surface properties of *E.coli* strains during growth, changes in media composition and quorum sensing were elucidated using potentiometric titration, FTIR and electrophoretic mobility.

Neither quorum sensing, nor the addition of 0.5 w/v (%) glucose affected the growth pattern for the strains. However, the addition of 0.5 w/v (%) glucose to the medium affected the measurable amount of quorum sensing molecule present in the supernatant. Aggregation of *E.coli* was found to be dependent on the

concentration and type of polymer used, as well as the surface chemistry of the cell. The cell surface functional groups, such as such as, hydroxyl, phosphoryl, amines and carboxylate groups varied with respect to different growth phase and changes in media. The protein content of free-EPS was found to significantly increase due to changes in growth phase and media composition. The growth phase, changes in media and quorum sensing all affected the cell surface properties and hence played a role in the aggregation capability of *E.coli*.

Chapter 1 Introduction

1.1. Introduction

In nature, bacteria do not usually exist as a single entity but are either attached to each other (i.e. aggregates) and/or surfaces (i.e. a biofilm). Bacteria that exist in aggregates or a biofilm, are able to respond and adapt to changes in the environment or perform highly specialised tasks similar to multicellular organisms (1). Recently, studies have shown that over 90% of bacteria that exist in the environment are aggregates attached to a surface, forming sessile communities (2). Figure 1.1 demonstrates the variety of environments in which aggregated cells can be found.

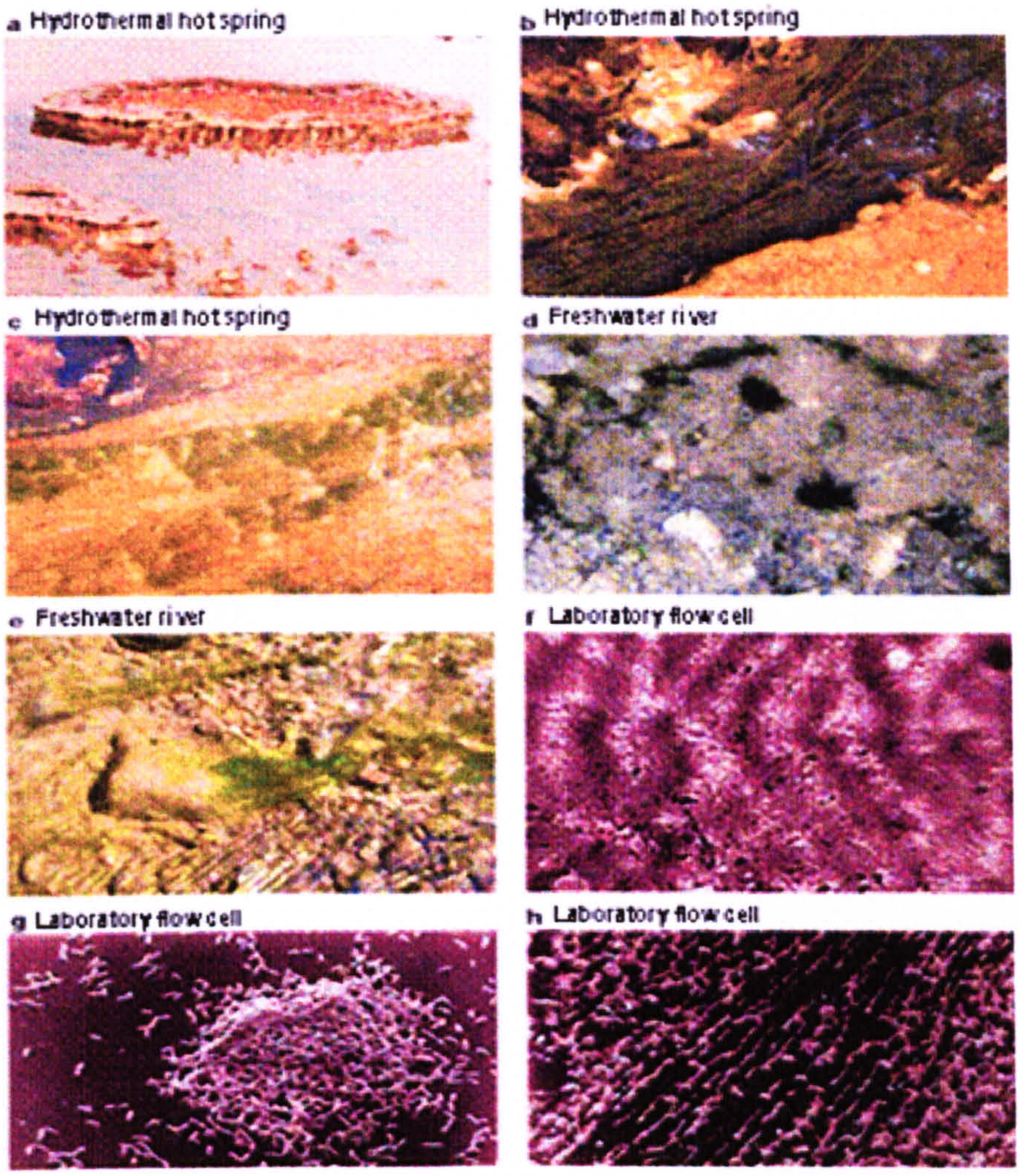

Figure 1.1 Bacteria exist as aggregates or biofilm in the natural environment and laboratory (reproduced from Hall-Stoodley *et al* (3))

Research into the field of bio-aggregation/biofilm formation can be found as early as the 1870s, where Pasteur first described yeast aggregation (flocculation) in the production of beer (4). Aggregation of brewing yeast usually occurred when the sugar component of the liquor in the brewery bioreactor had been converted into alcohol by the yeast. Hence the ability of the yeast to flocculate is desirable in the brewery industry, since it facilitates an efficient and easy way of separating the yeast cells from the beer produced. The aggregation phenomena have also been shown to occur in other biological systems such as bacteria, fungi, blood cell and algae (5-7).

Microbial aggregation is of great significance in the biotechnology field, environmental applications and medicine. There are several well known aggregation systems, which include (i) aggregation of the activated sludge microbial community in wastewater treatment, (ii) flocculation of yeast in the brewery industries (8-10), (iii) coaggregation of oral bacteria in dental plaque (iv) coaggregation of aquatic bacteria into biofilms (11-13), (v) aggregation of myxobacteria (14), (vi) formation of aggregate during conjugation in *Escherichia coli* (15), (vii) aggregation of bacteria onto a various solid surfaces (biofilm formation), and (viii) formation of clumps in liquid cultures.

Some of the advantages of microbial aggregation include: enhancing the selective separation of microbes, and allowing a high amount of microbes to be used in continuous fermentors. Conversely, bacterial aggregation can also have a detrimental effect to the environment. Unwanted microbes can attach to an artificial surface, and if the surface is in contact with water for a period of time, a phenomenon known as biofouling occurs. They can corrode metal such as pipes, a process generally termed Microbiologically Influenced Corrosion (MIC) or biocorrosion. Biocorrosion or biofouling can lead to contamination of industrial processes. The annual worldwide process engineering cost for aggregation or biofilm related problems is in the region of hundreds of millions of pounds (16).

Several pathogenic bacteria have also been shown to be able to form aggregates in order to withstand unfavorable environmental conditions, such as phagocytosis, antibiotics or biocides in their host organisms (17-20). Hence, pathogens which are able to form aggregates are less susceptible to antibiotics than bacteria that exist as a single entity. Bacteria can also colonize on medical devices, paving the way for dangerous sources of infection (21), which is now responsible for approximately 65% of hospital infections (22).

The process of bacterial cell-to-cell interaction leading to aggregation, or cell-to-surface interaction forming biofilms involves several biological and physical processes (23). Bacterial aggregation has been suggested to be controlled by biological factors like growth conditions (24), the presence of extracellular polymeric substances (EPS) (25, 26) and the ability to communicate among themselves (quorum sensing) (27, 28). Physical factors have also been linked to aggregation, such as Van der Waals and electrostatics interactions (29, 30). These interactions are governed by the presence of macromolecules such as outer membrane proteins, lipoproteins and lipopolysaccharides on the cell surface (31). Hence from a linked bio-physical point of view, bacterial aggregation consists of different stages which are controlled by biological and/or physical factors (Figure 2.1). Firstly, bacteria in a dispersed solution may come into close proximity due to Brownian motion, convectional transportation of microbes as a result of air and liquid flow, and/or the active motion of the microbes with their flagella (Figure 2.1a). Once bacteria are in close proximity, the next stage is the initial cell-to-cell adhesion, which may be reversible or irreversible (Figure 2.1b). Initial adhesion is thought to be governed by physical interactions such as Van der Waals and electrostatic interactions (29, 30). The third stage involves bacteria becoming firmly attached to themselves (or a surface) mainly by secreting extracellular polymeric substances (EPS) (32, 33) (Figure 2.1c). The final step is the increase in cell growth and further aggregation. Aggregation involves an increase in cell's proximity to each other and hence the cell-to-cell interaction within the bacteria communities may occur via a cell density dependent process, termed quorum sensing (Figure 2.1d). This cell-to cell communication allows the bacterial

community to perform several metabolic activities such as gene expression, antibiotic resistance, gene expression and bioluminescence (34-38).

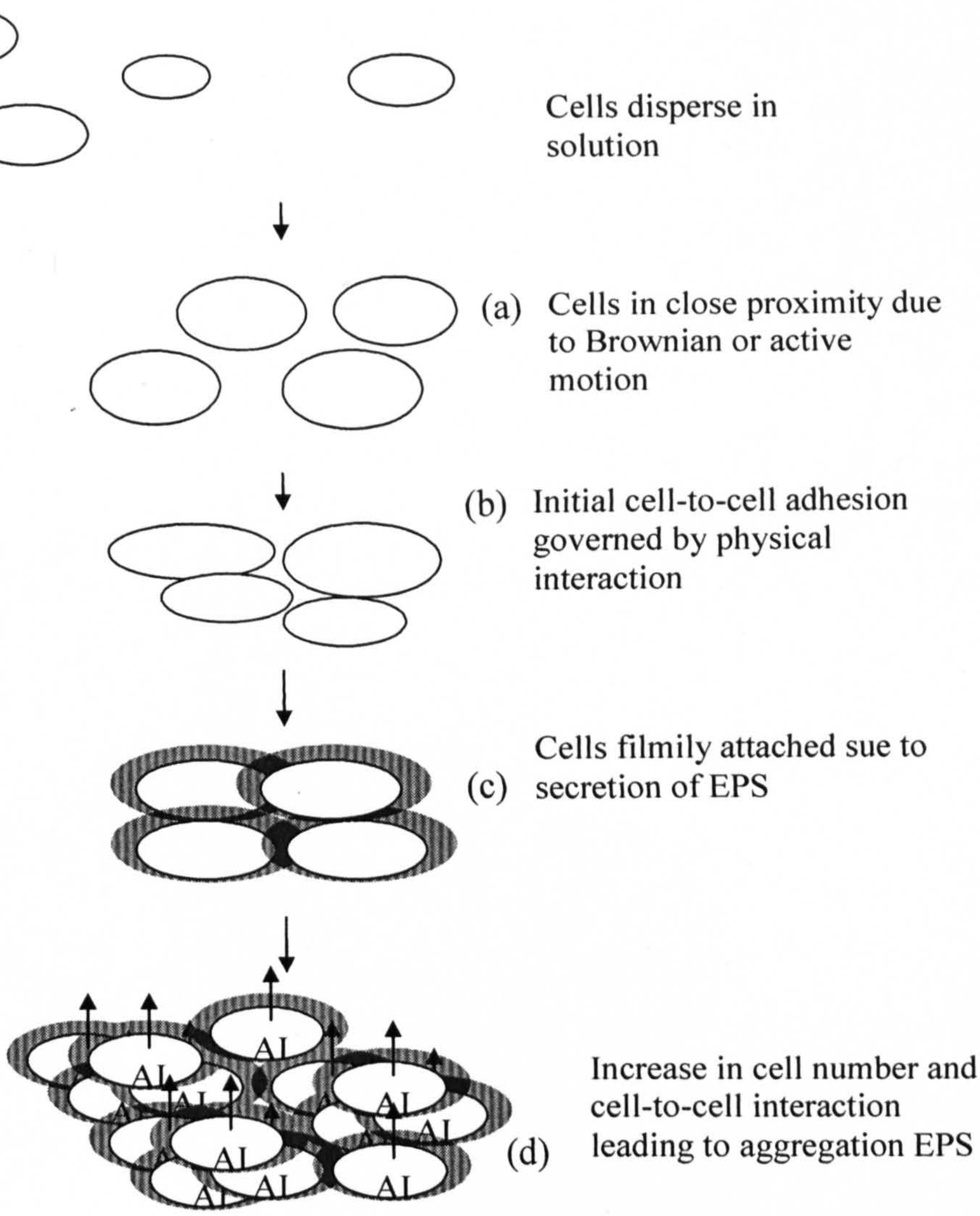

Figure 1.2 Potential model for understanding bacterial aggregation including the different stages of biological aggregation governed by both biological and physical factors

Bacteria exist as aggregates or biofilm in the natural environment and laboratory Bacterial aggregation is not a new discovery, what is new is the molecular, colloidal and imaging techniques, now available, for understanding the important mechanisms that drives the process. These include techniques such as genetic (39, 40), and proteomics analysis (41, 42), which have been used to explain biological processes involved in bacterial aggregation. Potentiometric titration (43), x-ray Photoelectron spectroscopy (44), Infrared spectroscopy (45) and electrophoretic

mobility (46) have also been developed and applied to study the physical properties of bacteria. Although, these techniques have been useful for elucidating the physical factors involved in aggregation, most of the studies have usually been performed under a specific single non-changing biological condition. Hence, our knowledge on the relationships between biological and the physical processes, which control aggregation is limiting. In addition, little is known about how physical properties of bacteria vary as a function of biological factors (e.g. growth conditions, EPS, quorum sensing), which are known to be involved in the aggregation process (33, 47). Unlike non-biological colloids, bacteria are dynamic in nature and their physiology may change as result of aggregation or dispersion. Hence it is paramount to address the effect of different biological factors, as it may provide further insight into the aggregation process.

1.2. Objective Research questions

Although a significant amount of research has been done in the area of bacterial aggregation, our understanding of the aggregation process still remains unclear. This is mainly due to a lack of understanding of the relationships between the physical and biological processes involved in aggregation. In an attempt to increase our understanding of bacterial aggregation, it is paramount to consider together both the physical and the biological processes involved since both can control aggregation. The overall aim of this work is to combine existing colloidal characterization techniques with post genomic methods to develop a deeper understanding of aggregation. Understanding the processes involved in bacterial aggregation is paramount to the development of future engineering and medical solutions to control these processes.

To develop a combined approach, both biological and physical processes involved in aggregation are investigated in order to reveal the fundamental steps that govern the process of aggregation. In so doing, key biological factors that affect bacterial activities including aggregation will be addressed such as growth phase, media composition, extracellular polymeric substances (EPS) and the ability of the bacteria to participate in cell-to-cell communication. The influence of these

biological factors on the physical properties i.e. surface chemistry, of the bacteria will also be measured. This will allow the relationship between the biological and the physical aspects of aggregation to be studied.

1.3. Thesis outline

In order to address the overall aim, the thesis the thesis is structured as follows.

Chapter 2: The aim of this chapter is to review the current literature in the area of bacterial aggregation. The chapter also describes the biological factors that may affect bacterial aggregation, such as, growth phase, media composition, extracellular polymeric substances produced during bacteria growth, quorum sensing. This chapter also gives insight into how these biological factors may influence bacterial aggregation. Physical aspects of bacterial aggregation, as well as suitable techniques for studying aggregation are also discussed here.

Chapter 3: The first major task was to choose suitable model bacteria for this study. *Escherichia coli* strains (AB1157, MG1655, and MG1655 *luxS*⁻) were selected for this purpose. Their growth patterns under different media, and their ability to participate in cell-to-cell communication is presented in this chapter as a precursor to aggregation studies in subsequent chapters.

Chapter 4: In non-biological colloids, the addition of a non-absorbing polymer causes an imbalance in the osmotic pressure, which in turn drives the particles closer together. Thus, a net attractive potential is set up between the particles enhancing the chance of aggregation, a process known as depletion attraction (48, 49). In this chapter, it is hypothesised that bacteria may display a similar phenomena upon addition of non-adsorbing polymer. The effect of non-adsorbing polymer on aggregation capability of *E.coli* AB1157 during growth was investigated and the results are discussed. The changes in the surface properties of *E.coli* as a function of growth were also investigated and correlated with the aggregation pattern of *E.coli*.

Chapter 5: Bacteria produce polymers known as extracellular polymeric substances (EPS) during growth. The focus of this chapter is to elucidate the ability of EPS to induce aggregation in *E.coli* MG1655. The EPS composition produced by *E.coli* MG1655 was determined and characterized using infrared spectroscopy. The effect of EPS extracted at different stages of growth and media on *E.coli* MG1655 aggregation was also investigated.

Chapter 6: In this chapter, further characterisation of the composition of EPS produced by *E.coli* MG1655 is achieved using proteomics. A major component of *E.coli* MG1655 EPS, extracellular proteins, was investigated further here by identifying extracellular proteins as a function of the media type and stages of growth.

Chapter 7: The effect of growth phase and media on the cell surface properties of *E.coli* MG1655 is the main focus of this chapter. This was achieved by identifying and quantifying the functional groups on *E.coli* MG1655 using potentiometric titration and Fourier Transform Infra Red (FTIR) spectroscopy. The variation of the surface functional groups as a function of growth and media was correlated with the aggregation pattern of *E.coli*. The profile of major macromolecules (outer membrane proteins and lipopolysaccharides) was also investigated using FTIR and SDS-PAGE.

Chapter 8: The focus of this chapter is to elucidate the effect of cell-to-cell communication (quorum sensing) on the cell surface properties of *E.coli* MG1655, and how this affects the aggregation ability. This was achieved by comparing the electrokinetic properties of *E.coli* MG1655 with its mutant *E.coli* MG1655 *luxS*, which lacks the ability to participate in quorum sensing.

Chapter 9: This chapter summaries the findings and conclusions generated from this study. Future work is also recommended.

Chapter 2 Literature Review and Research Hypothesis

2.1. Introduction

2.1.1. Outline

This chapter will briefly describe the different definitions and terminology used to describe aggregation before detailing the methods currently available to measure aggregation. Both the physical (i.e. van der Waals and electrostatics due to cell surface properties) and biological factors (growth phase, nutrient, EPS and quorum sensing) which influence aggregation are discussed.

2.1.2. Terminology and Definition

Bacterial aggregation can be defined as the act of clustering microbes to form fairly stable, contiguous, multicellular associations under different physiological conditions. They exist as consortia, enabling them to communicate between themselves and unify their metabolic functions such that they are greater than the sum for each individual organism.

Bacterial aggregation is of great interest to chemists, biologists, and biochemical engineers. Due to this, different scientific disciplines provide varied definitions. In addition to the overall definition given above, different scientific disciplines have defined bacterial aggregation as the gathering together or collection of bacterial cells in intimate contact (7, 50) or more simply, the clustering together of units to make bigger ones. Hence, the later definitions imply that the process of forming microbial aggregates is not only as a result of biological response but may also be due to external physical factors. The first definition appears to be mainly restrictive to biological understanding, whilst the last two attempt to integrate the biological and physical processes involved in microbial aggregation.

Although there has been great interest from different disciplines, one major drawback has been the various terminologies adopted by different disciplines to explain the aggregation process. Common names include flocculation, biofilm, clumping, coagulation, biogranulation, coadhesion, agglomeration and many more. In fact, all the different names can be a hindrance to exchanging information between different research disciplines. For example, the term flocculation is used

instead of aggregation mainly in the bioengineering disciplines to describe the aggregation process observed in the brewery industries and wastewater management (8, 10, 51). The term biogranulation has also been used to describe the microbial aggregation process occurring in wastewater treatment processes (52). Biogranulation was defined as a "cell-to-cell interaction leading to the formation of biogranules" (52, 53). These biogranules can be considered as aggregates since they consist of a mixed community of different bacteria specie. Biofilms are aggregates of cells bound by extracellular polymeric substances, which are attached to a surface (1). Hence biofilm formation can be regarded as an advanced form of the aggregation process. Other forms of aggregation, which have been described, include coaggregation, coadhesion, and autoaggregation. Coaggregation is a type of microbial aggregation involving recognition and adhesion of genetically distinct bacterial partners (54). It was first discovered amongst bacteria isolated from dental plaque (12, 55, 56) but has also been shown in bacteria isolated from other environments such as the water supply system (55). This area has been extensively studied, and has recently been reviewed by Kolenbrander *et al* (56, 57). Autoaggregation involves the recognition and adhesion between microbes of the same strain (58). Coadhesion occurs when microbes aggregate with other genetically distinct microbes that are already attached to a biofilm.

Although the above processes may evolve differently, they all lead to the formation of a cluster of cells, hence they are all forms of aggregation (59). Furthermore, despite the fact that different disciplines have different terminologies to describe the process of aggregation, knowledge obtained from the observation of aggregation in one area, can be transferred to another. This is the overriding concept of this thesis, where knowledge from physical and biological science is combined to further our understanding of bacterial aggregation.

2.2. General methods for observing aggregation

There are many different ways presented in the literature to observe and measure aggregation. The choice of technique mainly depends on the microbial aggregation

system to be investigated. A well-known method is by visual inspection of the aggregates in a transparent flask, or container, over a specific period (60-63). This is a non specific pattern for observing aggregation, where the investigator ascribes their findings by using an arbitrary scoring system of "0" (no aggregation) to "4" (maximum aggregation). Although this method is cheap and fast, it may not be suitable for cases were the aggregation is not significantly pronounced, as it would be difficult to achieve reproducible data. A turbidity method automates the visual scoring method, and has been widely used (5, 60, 63, 64). This method is based on monitoring the sedimentation of aggregates in a transparent container or cuvette over a period of time using a spectrophometer. The difference between the initial and final optical density (OD) of the upper part of the transparent container or cuvette is presented in the form of a percentage of aggregation (Figure 2.1).

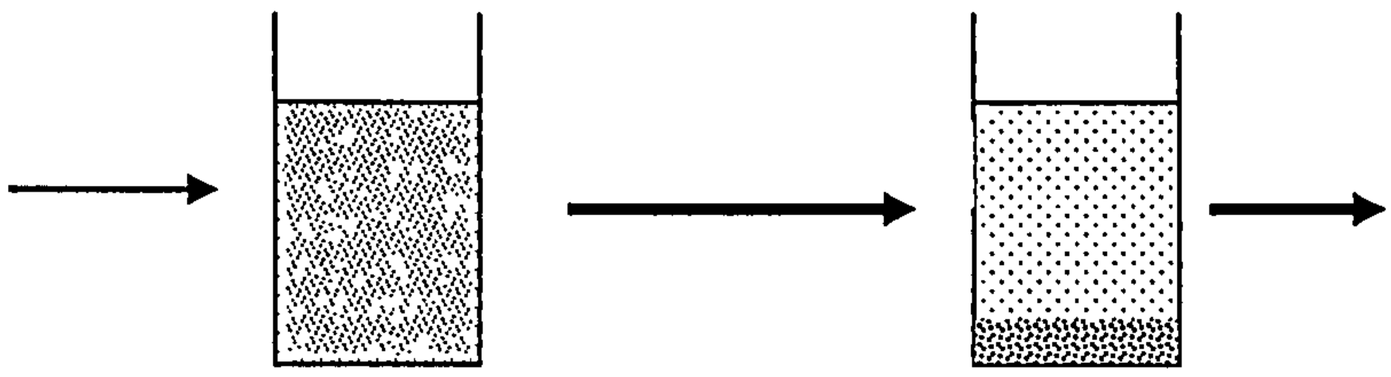

Figure 2.1 Diagram showing the used of turbidity method to measure aggregation

The percentage aggregation is the difference in OD readings taken at time ($O.D_0$) and time ($O.D_t$) divided by the initial OD at time 0 multiply by 100% (Equation 2.1). The rate of aggregation can also be measured by recording the optical density at regular time intervals.

$$\% \quad aggregation \quad = \frac{OD_o - OD_t}{OD_o} \times 100 \qquad \text{Equation 2.1}$$

Another example is the measurement of yeast aggregation, which is generally investigated using the Helm's sedimentation test (65). This involves counting the number of freely dispersed cells in a culture containing aggregates, and then comparing it with the total number of cells. The percentage aggregation or flocculation is then given by

% aggregation = [1-(no. free cells/ total no. of cell)] × 100% Equation 2.2

For oral microbes, aggregation is usually observed by using an aggregation or a coaggregation assay, which is a modified version of the turbidity method described above (66).

Another method for investigating microbial aggregates is the use of imaging and microscopic techniques. Borrego *et al.* (67) used both light and electron microscopy to investigate mycobacterium aggregates under different growth conditions. The authors showed that different nutrients affected the aggregation capability of mycobacterium and the microscopic and turbidity methods were in full agreement. Shen *et al.* (60) compared the coaggregation capability of four bacterial strains obtained from a root surface, using scanning electron microscopy. The authors also observed a good relationship between the microscopy and turbidity method (60). Other microscopy methods such as Atomic Force Microscopy (AFM) (9) and confocal microscopy (13) have been applied.

2.3. Factors affecting bacterial aggregation

2.3.1. Growth conditions and starvation

Bacterial growth is generally defined as the increase in cell number. For prokaryotes, this is achieved by replication through binary fission, where one parent cell splits into two daughter cells (68) (see Figure 2.2). The parent cell first increases in size to about twice the size of the smallest cell, the chromosome and cell mass doubles and this is then followed by the formation of a partition known as septum. An inward growth of the cytoplasmic membrane and cell wall then occurs resulting in the cleavage of two new daughter cells. During binary fission the daughter cells receive the complete chromosome and enough cell constituents for it to survive independently (69). These two daughter cells will at some point divide to form four new cells, and so on. In other words, bacteria increase their numbers by geometric progression (exponential).

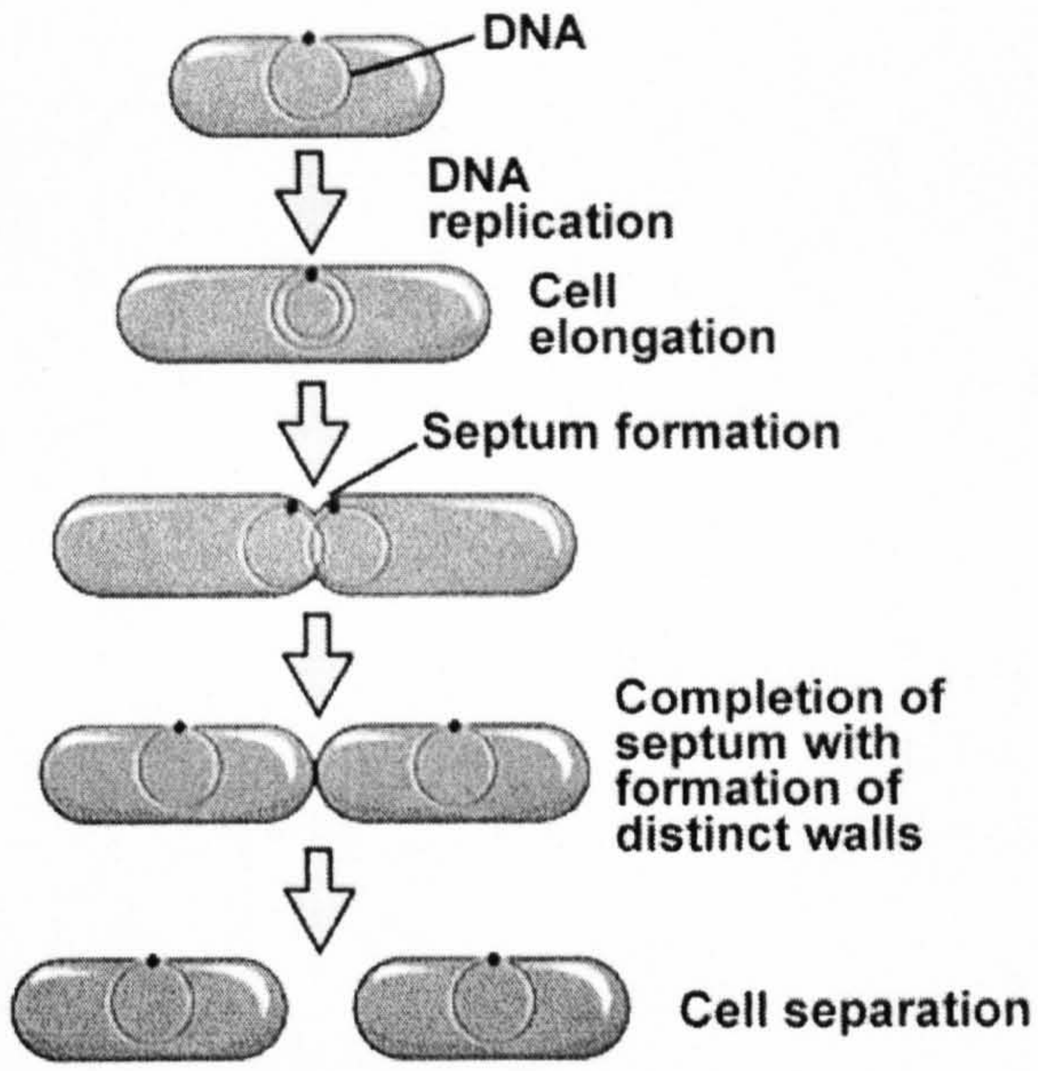

Figure 2.2 The general process of binary fission for cell division of prokaryotes (Reproduced from Madigan et al (70))

The time it takes for a population of bacteria to double is known as the Doubling or Generation time. The generation time widely varies among bacteria. For example, the generation time for *Escherichia coli* at optimum growth conditions is about 20 minutes, while the generation time for some pathogens like *Mycobacterium tuberculosis*, is between 12-24hr (71, 72). The differences in generation time may depend on the method used for the growth measurement, the strain of the bacteria, the growth media or the experimental conditions. A simple equation can be used to express the relationship between the number of cells in a population at a given time and the generation time as given by Equation 2.3.

$$N_t = N_0 \times 2n \qquad \text{Equation 2.3}$$

Where N_t is the number of cells in a population at a given time, N_0, the initial number of cells in the population (N_0), and n the generation time.

The growth of bacteria under batch conditions typically follows four phases; lag, exponential (log), stationary and death phase (70) (see Figure 2.3).

The lag phase occurs immediately after the inoculation of the cells into fresh medium. The lag phase is associated with cells undergoing physiological adaptation to the new environment, before their resumption of binary division. No apparent cell division occurs in this phase although the cells may be growing in volume or mass, synthesizing enzymes, proteins, RNA and increasing in metabolic activity (70).

The log phase is also known as the logarithmic or exponential phase. In this phase, cells are dividing by binary fission and growing by geometric progression. The rate of exponential growth is dependent on the type of medium, growth conditions and types of organism itself. The time taken for a population of cells to double is known as the generation or doubling time. The generation time widely varies among bacteria. For example, the generation time for *Escherichia coli* at optimum growth conditions is about 20 minutes, while the generation time for some pathogens like *Mycobacterium tuberculosis*, is between 12-24hr (71, 72).

The stationary phase occurs when the rate of cell division equals the rate of cell death. There are factors that trigger bacterial growth to progress from the exponential phase to the stationary phase. These include insufficient nutrients, accumulation of inhibitory metabolites or end products, and a lack of "biological" space (70).

Finally the death phase occurs when the number of viable cells decreases geometrically (exponentially). This stage is essentially the reverse of growth during the log phase.

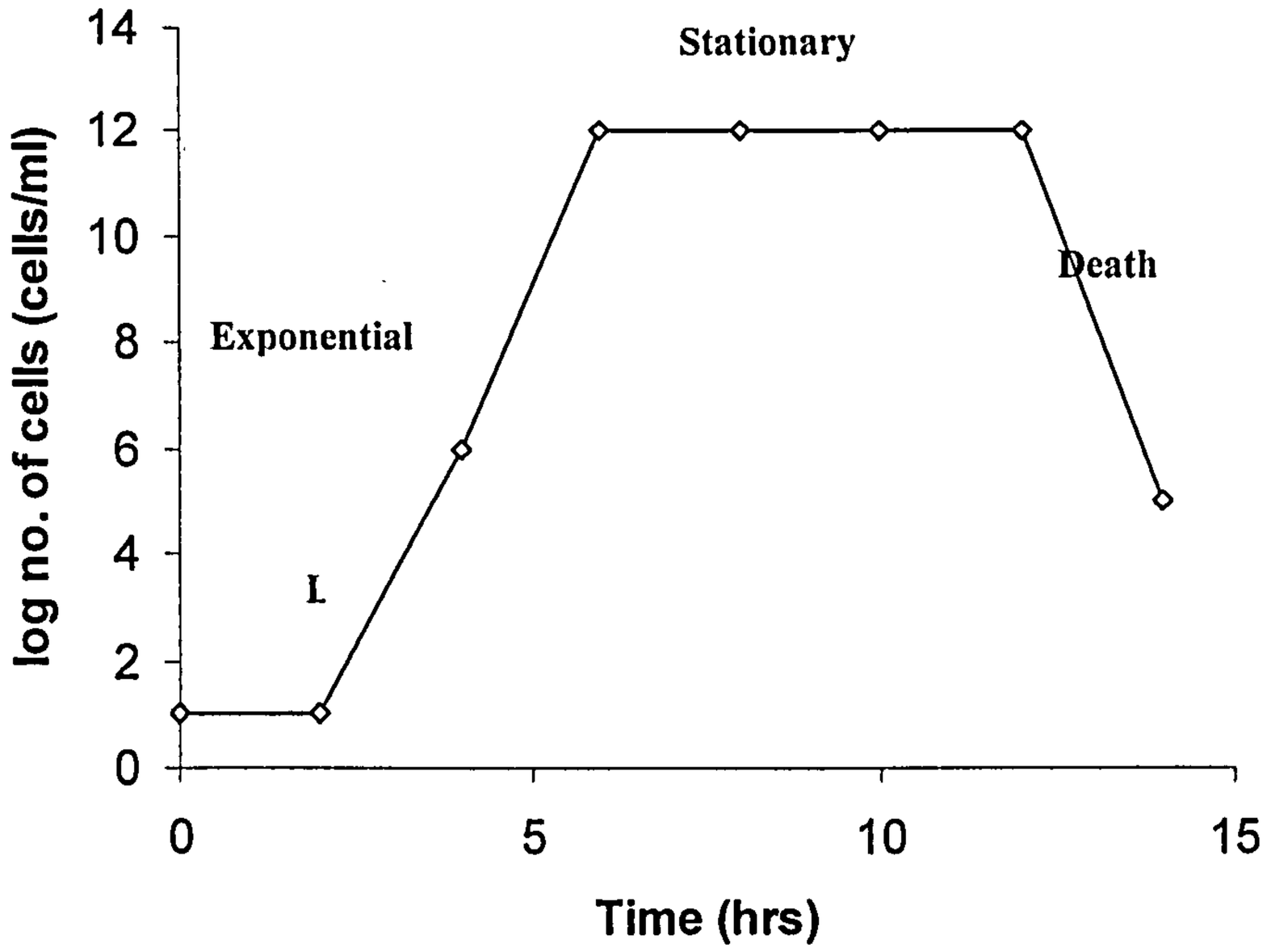

Figure 2.3. A typical batch growth curve

Bacteria are living cells that are able to respond to their environment. Therefore, unlike non-biological colloids, the ability of bacteria to participate in aggregation depends on their physiological status. In response to nutrient depletion (starvation), some bacteria have been suggested to alter the cell surfaces, to promote the aggregation process (24). Limitation of nutrients such as carbon and nitrogen, and the growth stage of bacteria can affect the surface properties through controlling the production of outer membrane macromolecules and extracellular polymeric substances (EPS) (73, 74). Major surface macromolecules, such as lipopolysaccharides and outer membrane proteins, have been shown to vary in response to the growth phase and conditions. The production of EPS in bacteria generally occurs at the onset of the stationary phase, and is controlled by environmental factors such as nutrient availability (75).

As well as nutrient limitation, the nutrient composition can affect the surface properties of bacteria (76). For example, the presence of Mg^{2+} and Ca^{2+} can directly influence biofilm formation in *Pseudomonas fluorescens* by controlling its electrokinetic properties (77). Walker (75), compared the adhesion pattern of

Burkholderia cepacia G4g and ENV435g, when cultivated in nutrient rich Luria broth (LB) and nutrient poor basal salts medium (BSM). Interestingly, the author observed that the adhesion pattern of strains varied when cells were cultivated in the different growth media. Cells cultivated in LB medium displayed a more adhesive capability than cells cultivated in BSM. The author further attributed the differences in adhesive capability to the alteration of electrokinetic and size properties of cells, due to the media used.

The growth phase of bacteria has also been suggested to influence aggregation. Bacteria growth can be simply defined as the increase in cell number. Hayashi *et al.* (78) reported that the cell surface electrokinetic properties of four Gram negative bacteria, *Escherichia coli, Pseudomonas putida*, *Alcaligenes faecalis*, and *Alcaligenes sp.* varied as a function of growth phase. Although they also suggested that these changes may depend on the bacterial strain. Walker *et al.* (79), recently showed that *E.coli* harvested at the stationary growth phase, display a more adhesive capability than cells harvested during the exponential phase. This was due to a difference in the surface properties: the cells displayed a decrease in electrostatic repulsion when harvested at the stationary phase rather than when harvested at the exponential phase. Rickard *et al.* (80) showed that coaggregation abilities among aquatic bacteria were dependent on the growth phase (culture age) with coaggregation ability maximum during the stationary phase. Rickard *et al.* (62) later reported that freshwater biofilm bacteria coaggregate at the onset of the stationary phase.

These findings all indicate that bacteria are able to alter their cell surface properties in response to nutrient availability and/or growth phase which then influences the tendency for bacteria to aggregate.

2.3.2. Extracellular polymeric substances (EPS)

Bacterial aggregates are surrounded by biopolymers which are known as EPS. EPS are mainly responsible for the structural and functional integrity of aggregates and

biofilms as well as playing a key role in the physicochemical properties of these aggregates and biofilms (33). Bacteria naturally produce extracellular polymeric substances during their growth. EPS arises from several metabolic processes such as cell breakage due to cell death, active secretion from various pathways, release of cell surface macromolecules (outer membrane proteins and lipopolysaccharides) and interactions with the environment (81).

The EPS have been found to be composed of polysaccharides, proteins, nucleic acid, lipids and other biological polymers such as humic substances (33). EPS were previously thought to be composed of mainly polysaccharides, and therefore polysaccharides are the most well studied component. This is why the abbreviation "EPS" is mostly used to describe the extracellular polysaccharides or exopolysaccharides (81, 82). However, current studies have shown that significant levels of proteins and nucleic acid are in the EPS extracted from biofilms (83), pure cultures (84) and activated sludge (85, 86).

EPS biosynthesis and compositions vary from one bacteria to another and have been shown to be controlled by several environmental factors such as: growth phase (82), growth media (87), temperature (88), limitation of oxygen (89, 90), nitrogen (91) and cations (e.g. magnesium, calcium and phosphate) deficiency (92). Hence it is not surprising that conflicting reports regarding the compositions of EPS have been given in the literature.

Furthermore, the method used to extract bacterial EPS before analysis can affect the composition reported. Several methods for extracting EPS have been reported, however, it is difficult to compare results due to the lack of a standard protocol. This is a major drawback in analysis of EPS. Zhang *et al* (93) compared five different methods for extraction of EPS for aerobic/sulphate-reducing biofilm, these were regular centrifugation, EDTA extraction, ultracentrifugation, steaming extraction and regular centrifugation with formaldehyde (RCF). RCF and the steaming method gave the highest level of carbohydrate and protein content. Liu and Fang (85), also compared EDTA, cation exchange resin and formaldehyde

extraction methods under various conditions to analysis the EPS content from aerobic, acidogenic and methanogenic sludge. The authors observed that formaldehyde plus NaOH was the most appropriate method for extracting EPS since it released only relatively low levels of nucleic acid. Sheng *et al* (84) recently extracted EPS from *Rhodopseudomonas acidophila* using four different extraction methods (EDTA, NaOH, H_2SO_4, heating/centrifugation). The authors observed that EDTA method was the most effective for extracting EPS, again because it released only relatively low levels of nucleic acid (Table 2.1). The proteins were dominant in the composition of the EPS of *Rhodopseudomonas acidophila* extracted with EDTA, NaOH, and heating/centrifugation.

Table 2.1 Composition of EPS of *R. acidophila* by four extraction methods (reproduced from Sheng et al (84))

Component mg g^{-1} dry cells	**EDTA**	**NaOH**	**H_2SO_4**	**Heating**	**Control (centrifugation)**
Carbohydrate	6.5	7.7	10.6	10.3	4.1
Protein	58.4	126.6	6.2	37.7	6.2
Nucleic acid	5.4	24.9	4.6	23.6	2.6
Total EPS	70.3	159.2	21.4	71.6	12.9
Carbohydrate/protein	0.11	0.06	1.71	0.27	0.66

The EPS synthesized by bacteria exist as tightly bound (capsular EPS or cell-bound-EPS) or loosely attached to the cell surface (free-EPS or slime). The distribution of EPS can be seen in Figure 2.. Bound-EPS are tightly linked to the cell surface either by a covalent bond via phospholipids and glycoprotein, or through noncovalent association via hydroxyl groups of lipopolysaccharides (81, 94). Free-EPS are not directly attached to the cell surface and are usually released in the media. This type of EPS can also be distinguished based on the extraction method used; free-EPS can be separated from a medium by centrifugation with bound-EPS still attached to the cells or aggregates. A further step such as EDTA

extraction, ultracentrifugation or steaming extracted is required to separate the bound-EPS from the cells or aggregates.

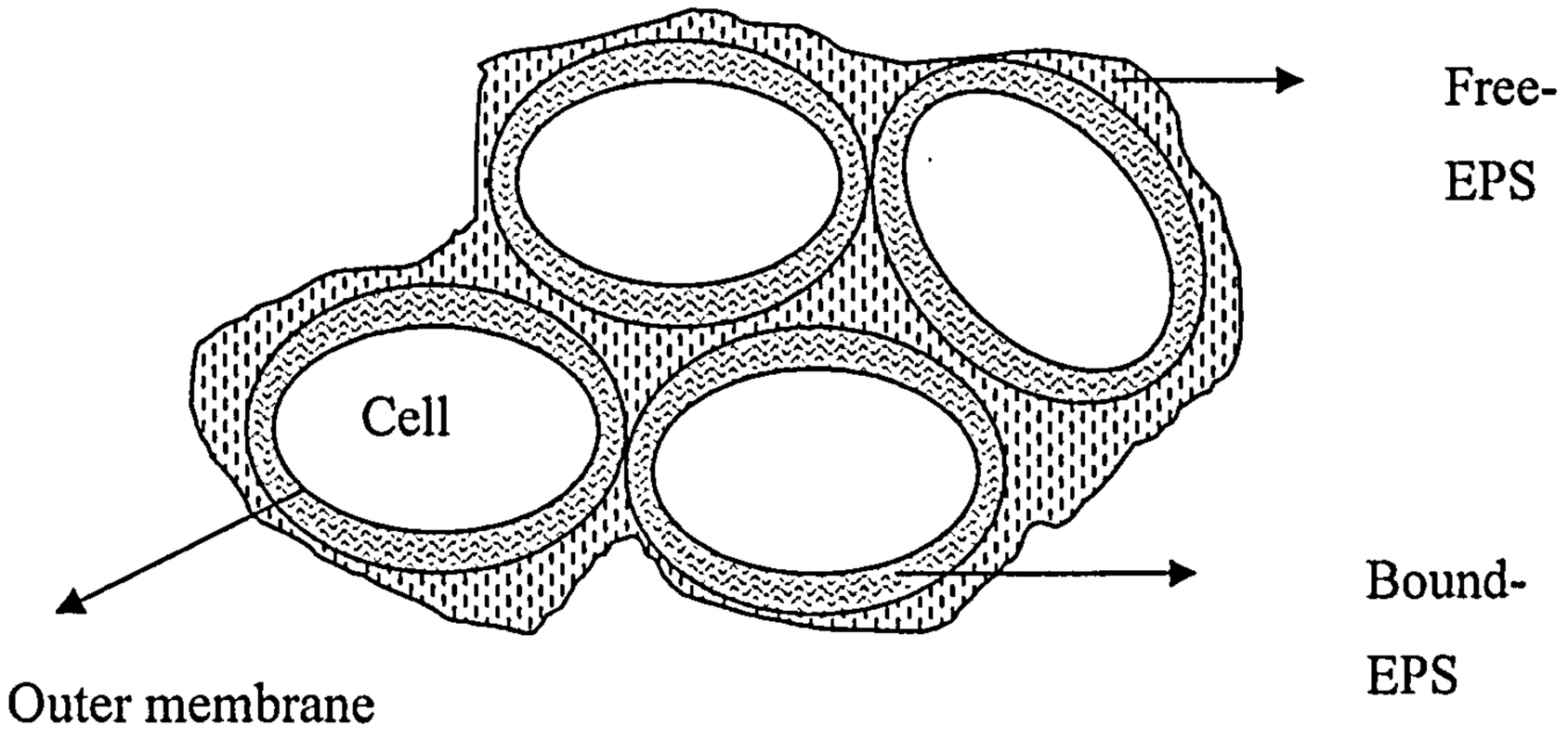

Figure 2.4 Distribution of bound-EPS and free-EPS in bacteria

The major role of EPS has been shown to keep microbial aggregates together (33) by providing a attractive force (33, 95-97), and also in adhesion of aggregates to biotic or aboitic surfaces (in the case of biofilms). This in itself will provide enough stability amongst the cells to withstand any shear force from the environment. Hence cells can easily be attached to surfaces of medical implants and metals, leading to infection or biocorrosion respectively (32, 98). Several recent studies have show that EPS can promote aggregation or biofilm formation by altering the surface chemistry of the cell (26, 99-101). Other functions of EPS have also been proposed and these include; (1) Biofouling, bioleaching and biocorrosion by facilitating the attachment of aggregates on the surface, (2) providing a physical barrier to protect cells from contamination by biocides and antibiotics, (3) response to environmental stress (see reviews (32, 102)).

The conventional way to analyze EPS from aggregates or biofilms is by first removing the cells from the media by centrifugation. Free-EPS can be recovered via precipitation, whilst bound-EPS can be recovered from the cells by several extraction methods. The problem with this approach is that most extraction methods may lead to destruction of the cell surface, and disruption of the EPS changes the original structure of the aggregates or biofilm, hence non-destructive approaches in studying EPS are becoming more fashionable. Such techniques include infrared spectroscopy, environmental scanning electron-microscopy Magnetic resonance spectroscopy and confocal laser scanning spectroscopy (84, 103-105).

2.3.3. Cell-to-cell communication via Quorum sensing

Bacteria are living cells that are able to adapt to their environment. How successful these cells are depends on their ability to sense and respond to the environment. Bacteria have developed several systems that enable them to adapt to changes from the environment through the release and detection of chemicals. One example of this process is a cell density dependent process, known as Quorum sensing. This allows single cells to monitor the microbial community by producing and responding to low molecular mass signal molecules, called autoinducers (AI).

Research into quorum sensing began over 30 years ago on the expression of bioluminescence in the marine bacterium *Vibrio fisheri* and *Vibrio harveyi* (106, 107). At low cell density, *Vibrio fisheri* is non-bioluminescent, but when the concentration increases (high cell density), the organism is bioluminescent. In nature, *Vibrio fisheri* forms a symbiotic relationship with *Eu scolopes*, by growing within the light organ of *Eu scolopes* obtaining nutrients from its host. The bioluminescence of *Vibrio fisheri* is exploited by *Eu scolopes*, to camouflage themselves from predators, a phenomenon knows as counter-illumination.

The molecular basis of quorum sensing in *Vibrio fisheri* has been well studied (108). The gene cluster responsible for light production consists of eight genes (*luxA-E*, *luxG*, *luxI*, and *luxR*) (Figure 2.5) (108). The regulator proteins

responsible for quorum sensing in this organism are proteins encoded by *luxI* and *luxR*. *LuxI* encodes the enzyme autoinducer synthase, which catalyses the reaction involved in the biosynthesis of homoserine lactones (HSLs). *LuxR* encodes the protein which binds to the autoinducer and also to activates *luxA-E* and *luxI* operon. The autoinducer produced by *Vibrio fisheri* has been well studied and found to be N-(3-oxohexanoyl)-L -homoserine lactone (OHHL) (41, 113).

At low concentrations of *Vibrio fisheri* only low levels of the *luxI* gene are expressed and so the levels of OHHL are low (208). As a result, only low levels of light are produced by the organisms (44) because the genes encoding for luciferase are located directly downstream of the *luxI* gene (108). However as the population of cells increases the concentration of OHHL will also increase. Once the concentration OHHL reaches a particular threshold level (1-10 μg/ml) (108) which corresponds to a particular cell density, OHHL binds to *luxR*. This process enables the *luxR* to bind with the *luxA-E* and *I* promoter and activates transcription, resulting in formation of light and OHHL. LuxR contains two domains; the C-terminal which is one-third of LuxR and contains a domain that can interact with the transcription complex and activate the luminescence genes, and the N-terminal region contains conserved residues known to be required for acyl-HSL binding (58). When N-(3-oxohexanoyl)-L -homoserine lactone is abundant in the cells, LuxR repress the transcription of *luxR*.

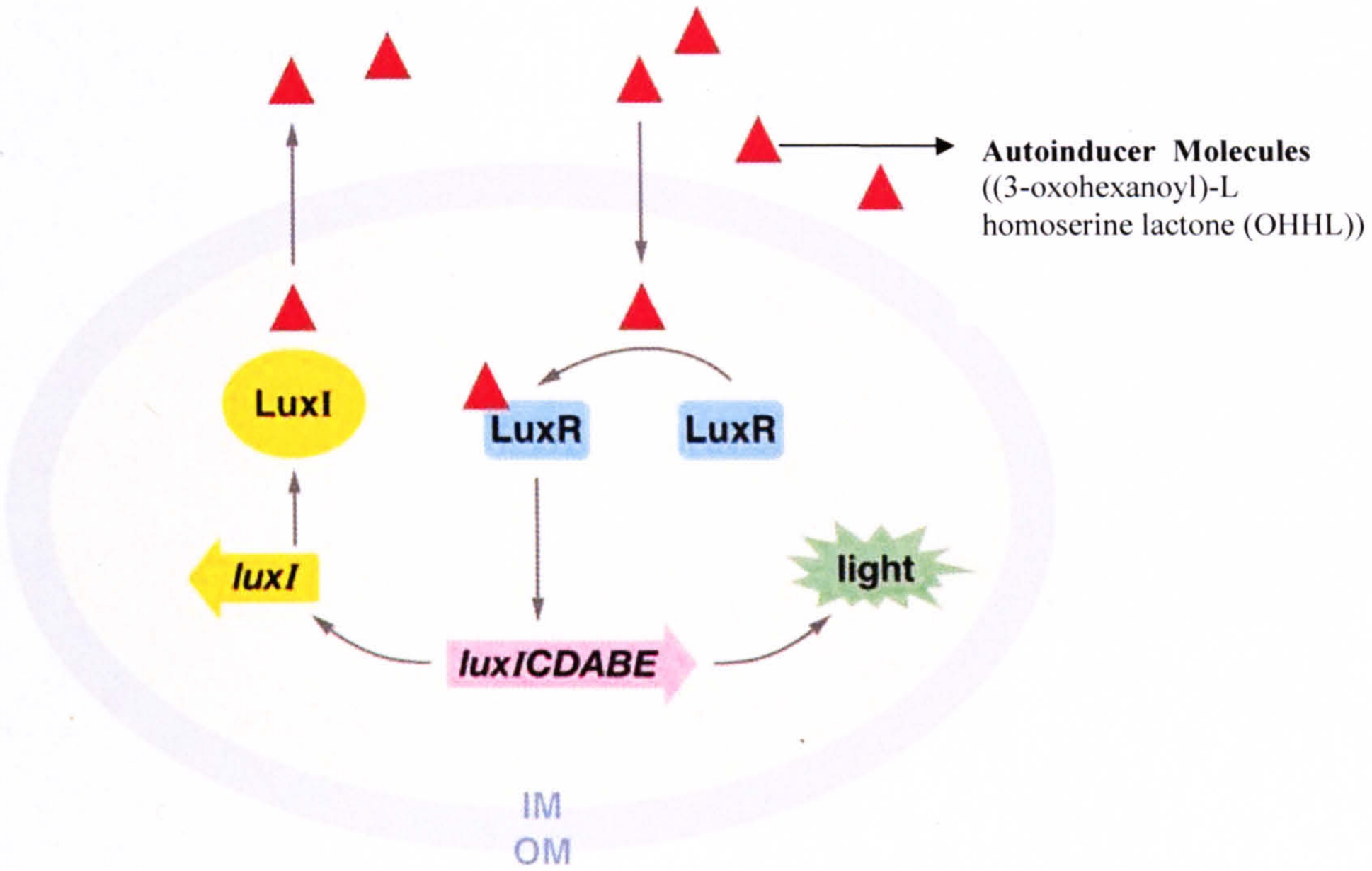

Figure 2.5 Quorum sensing in *Vibrio fischeri*; a *LuxIR* signaling circuit. Red triangles indicate the autoinducer that is produced by *LuxI*. *LuxR* encodes the protein which binds to the autoinducer and also to activate *luxA-E* and luxI operon. OM, outer membrane; IM, inner membrane (reproduced from Waters and Bassler (109)).

Bacteria are collectively able to regulate gene expression via quorum sensing, and therefore regulate their metabolic action. This may not be possible if each bacterium existed in isolation (109). Bacteria use quorum sensing to regulate several physiological processes: Examples of these include, bioluminescence and symbiosis in *Vibrio fisheri* (110-112), antibiotic production in *Photorhabdus luminescences* (113) expression of virulence, formation of biofilms and growth in *Escherichia coli* (39, 114), production of extracellular polymeric substances biosynthesis and pathogenicity in *Erwinia stewartii* (115), and expression of virulence genes *Pseudomonas aeruginosa* (116-118)

Several types of autoinducers (AI) have been identified in bacteria (Figure 2.6). Gram-negative bacteria use N-acyl homoserine lactones (HSLs) as their autoinducer whilst Gram-positive bacteria use amino acids and short peptides (oligopeptide) (36, 119). Each bacterial species also secret their own autoinducers

which are species specific (109, 119). The regulation of *N*-acyl homoserine lactones in Gram negative bacteria follows a *LuxI/LuxR* system described in *Vibrio fischeri.* In *E.coli*, the protein homolog to *LuxR* has been found to be SdiA (120). However, the gene homolog to *luxI*, which code for *N*-acyl homoserine lactones synthase has not yet been identified in the genome of *E.coli*. Hence, quorum sensing via *N*-acyl homoserine lactones has not been reported in *E.coli* since the product may not exist.

Recent studies have shown that *Vibrio fisheri* and *Vibrio harveyi* produce and detect a second autoinducer, AI-2. This have also been found to be produced by many Gram positive and negative bacteria (> 55 bacteria species), and the gene responsible for production of this protein is called *luxS* (121, 122). Unlike AI-1, which may be produced in different forms, AI-2 appears to be similar in all bacteria that have been studied. These findings suggest that AI-2 is a universal signal molecule used in interspecies cell-to-cell communication (121) (Figure 2.6d).

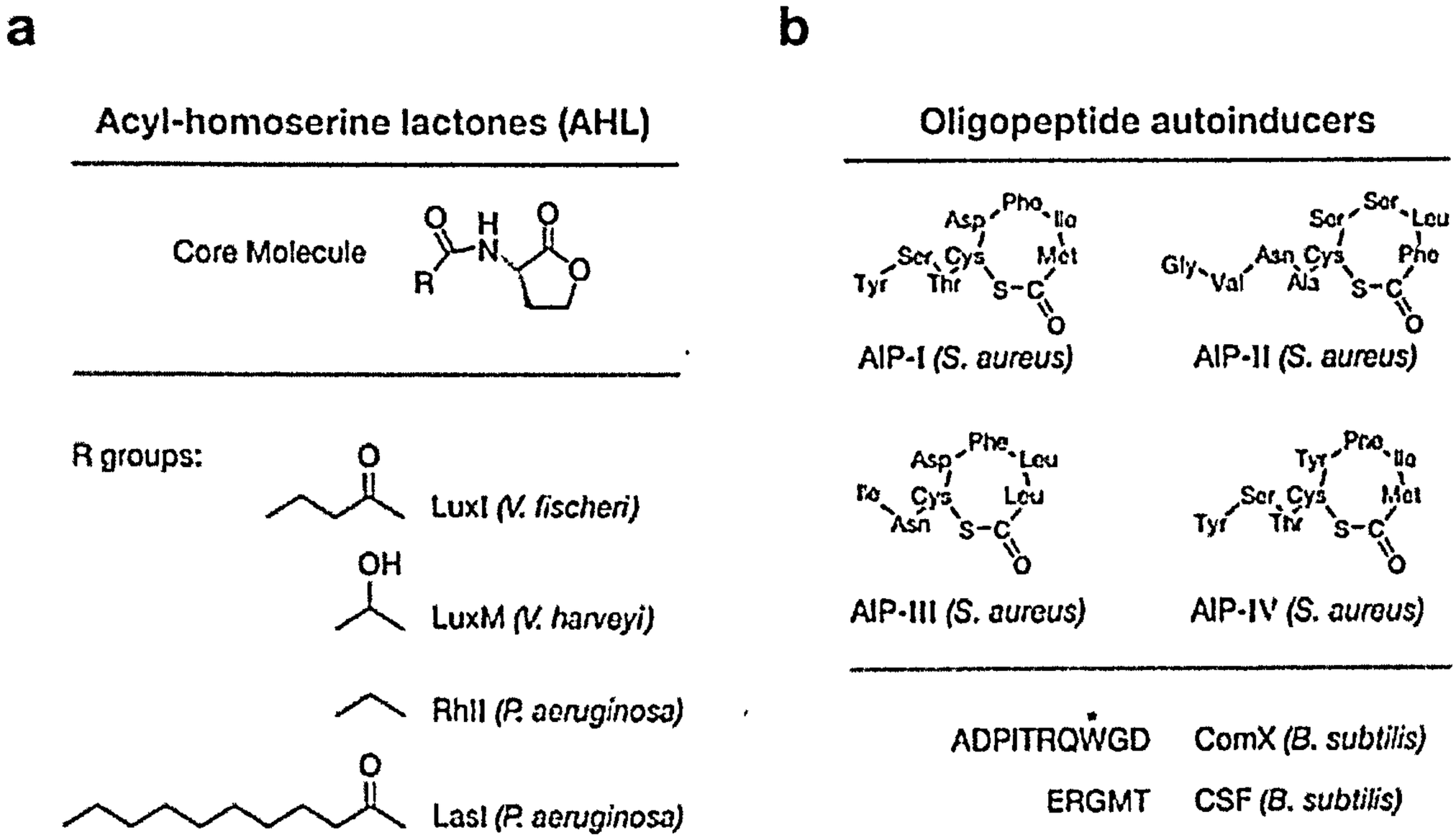

Figure 2.6 Representative bacterial autoinducers. The asterisk above the tryptophan in ComX represents an isoprenyl modification (reproduced from Waters and Bassler (109))

The biosynthesis of AI-2 requires the LuxS protein (123). However, there is still a great debate on whether AI-2 is a signal molecule, since the LuxS protein also plays an important in the recycling of *S*-adenosylhomocysteine (SAH), a very toxic substance (124, 125). Although the biosynthetic pathway for AI-2 is not fully understood, LuxS has been shown to convert *S*-ribosyl-homocysteine into homocysteine and 4,5-dihydroxy-2,3-pentanedione (DPD) (Figure 2.6a). DPD is a very unstable compound which cyclizes and rearranges to form AI-2 upon reaction with water. Chen *at al.* (126) determined the structure of AI-2 in *V. harveyi* by solving the X-ray crystal structure of an AI-2-binding protein, LuxP and found the

structure of AI-2 to be furanosyl-borate-diester (3A-methyl-5,6-dihydro-furo(2,3-d) (1,3,2)dioxaborole-2,2,6,6A-tetraol; *S*-THMF-borate). More recently, Miller *et al.* (127) showed that the structure of AI-2 in *Salmonella typhimurium* was (*2R*,*4S*)-2-methyl-2,3,3,4-tetrahydroxy-tetrahydrofuran (*R*-THMF), which lacks boron. The molecules DPD, *S*-THMF and *R*-THMF are all inter-convertible with each other (Figure 2.7b) and as such AI-2 can be used as a general term for DPD derivatives involved in quorum sensing (122). However, the structure of AI-2 has not been well established in most bacteria known to possess *luxS* (over 55 bacteria). Bacteria with the *luxS* homologue, like *E.coli* and *Salmonella enterica*, have been shown to possess the AI-2-like autoinducer using a *V. harveyi* bioluminescence assay developed by Surette and Bassler (128).

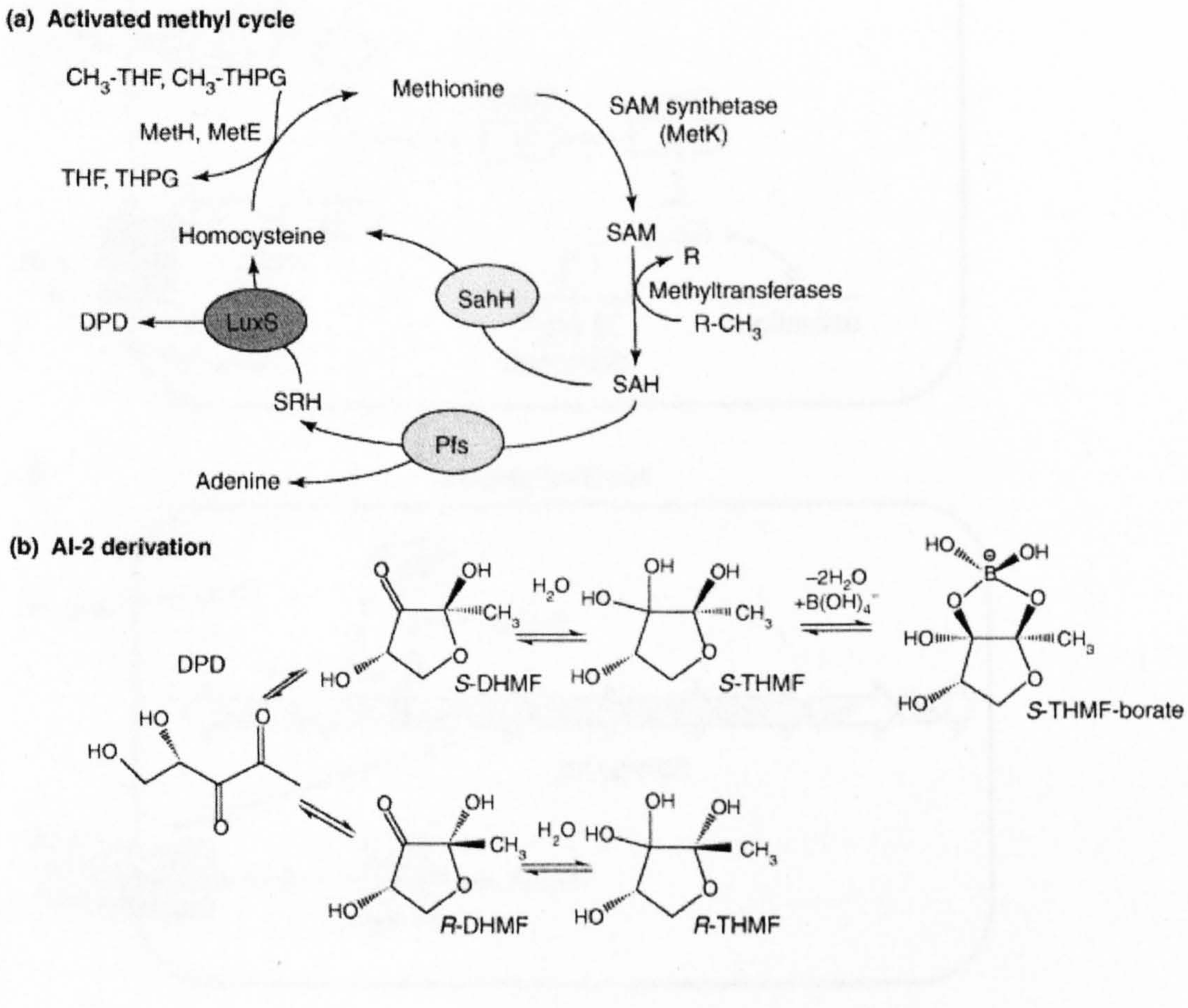

Figure 2.7 Biosynthesis of AI-2 in relation to the activated methyl cycle (reproduced from De Keersmaecker *et al*(122))

Vibrio harveyi, detects and responds to the two types of autoinducer (AI-1 and AI-2), and they are both required for bioluminescence and type III secretion (TTS) of virulence factors (Figure 2.8) (129). In contrast, *E.coli* can only detect, produce or respond to AI-2, which is secreted during the exponential phase and later internalised by the cell at the on set of stationary phase (Figure 2.8b). In the presence of AI-2, AI-2 transporter, Lsr imports AI-2 into the cell and the absence of AI-2, LsrR represses the *lsr* operon (129). During the release of AI-2, LsrK phosphorylates the intracellular AI-2 which then antagonizes LsrR, leading to de-repression of *lsr* expression and causing AI-2 to be a rapidly internalised (130).

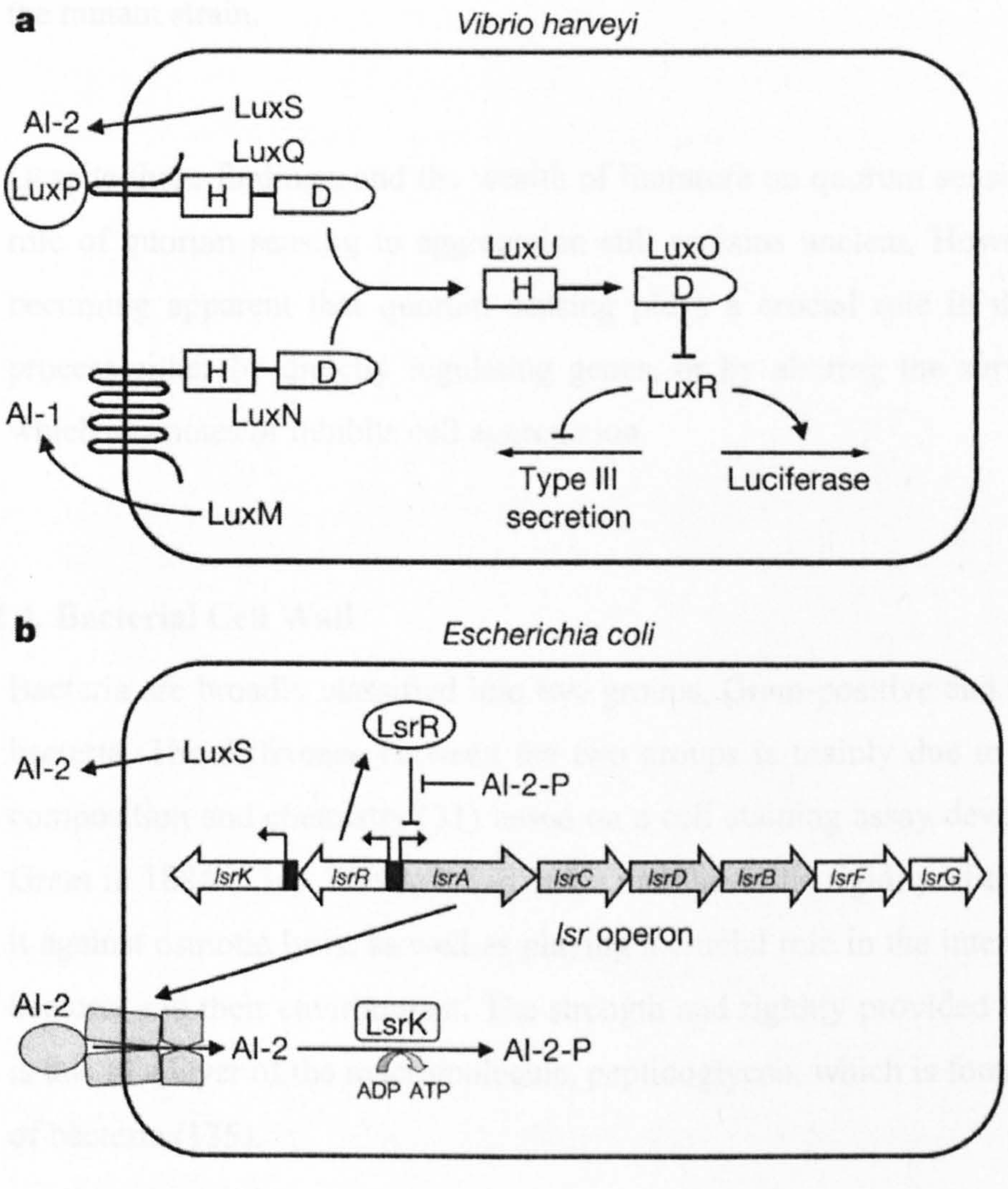

Figure 2.8 **a**, *V. harveyi* quorum sensing. The autoinducers AI-1 and AI-2 are detected by LuxN and LuxPQ, respectively. Information is transduced by phosphorylation. **b**, The *E. coli* Lsr transporter imports AI-2. See the text for details. AI-2-P, phosphorylated AI-2. (Reproduced from Xavier and Bassler (129)).

Puskas *et al.* (47) reported that quorum sensing inhibits *Rhodobacter sphaeroides* aggregation. Mutation of the quorum sensing (homoserine lactone synthase) gene increased the aggregation of *Rhodobacter sphaeroides* in a liquid culture. Atkinson *et al.* (131) reported a similar effect of quorum sensing on aggregation for *Yersinia pseudotuberculosis*. González Barrios *et al.* (132) showed that AI-2 facilitates biofilm formation in *Escherichia coli* by stimulating motility. In contrast, Xu *et al.* (133), recently reported that AI-2 inhibited the biofilm formation in *Staphylococcus epidermidis*. The authors showed that a mutant lacking the AI-2 gene, *luxS* showed increased biofilm formation compared to the wild type. The difference between the strains was attributed to the increase production of EPS in the mutant strain.

Despite these findings, and the wealth of literature on quorum sensing, the precise role of quorum sensing in aggregation still remains unclear. However, it is now becoming apparent that quorum sensing plays a crucial role in the aggregation process either by directly regulating genes, or by altering the surface properties which promotes or inhibits cell aggregation.

2.4. Bacterial Cell Wall

Bacteria are broadly classified into two groups, Gram-positive and Gram-negative bacteria. The difference between the two groups is mainly due to their cell wall composition and chemistry (31) based on a cell staining assay developed by Hans Gram in 1884 (134). The cell wall helps maintains the rigidity of the cells, protect it against osmotic lysis, as well as playing a crucial role in the interaction between bacteria and their environment. The strength and rigidity provided by the cell wall is due to a layer of the macromolecule, peptidoglycan, which is found in both types of bacteria (135).

2.4.1. Membrane of Gram positive bacteria

The cell wall of Gram positive bacteria is mainly composed of peptidoglycan (usually 60-90% of the total cell wall), polysaccharides or teichoic acid (or both),

or lipoteichoic acids (135) (Figure 2.9). Surface proteins are attached to the outer surface of the peptidoglycan, and their function may vary from one strain to another. Peptidoglycan is a polymer composed of sugars and amino acids. The sugar component of the peptidoglycan is made up of repeating units of β-(1,4) linked N-acetylglucosamine and N-acetylmuramic acid residues (136). Amino acids such as L-alanine, D-alanine, D-glutamic acid and lysine or diaminopimelic acid are attached to the N-acetylmuramic acid portion of the peptidoglycan (70).

Teichoic acids extend to the surface of the peptidoglycan and are composed of polymers of glycerol, phosphates, and the sugar alcohol ribitol covalently bond to the N-acetylmuramic acid of the peptidoglycan layer (137). Some teichoic acids are anchored to the plasma membrane via glycolipids, known as lipoteichoic acids. The precise role of teichoic acids remains unclear but the negative charge of teichoic acids has been found to contribute to the overall negative charge of Gram-positive bacteria cell surfaces (70).

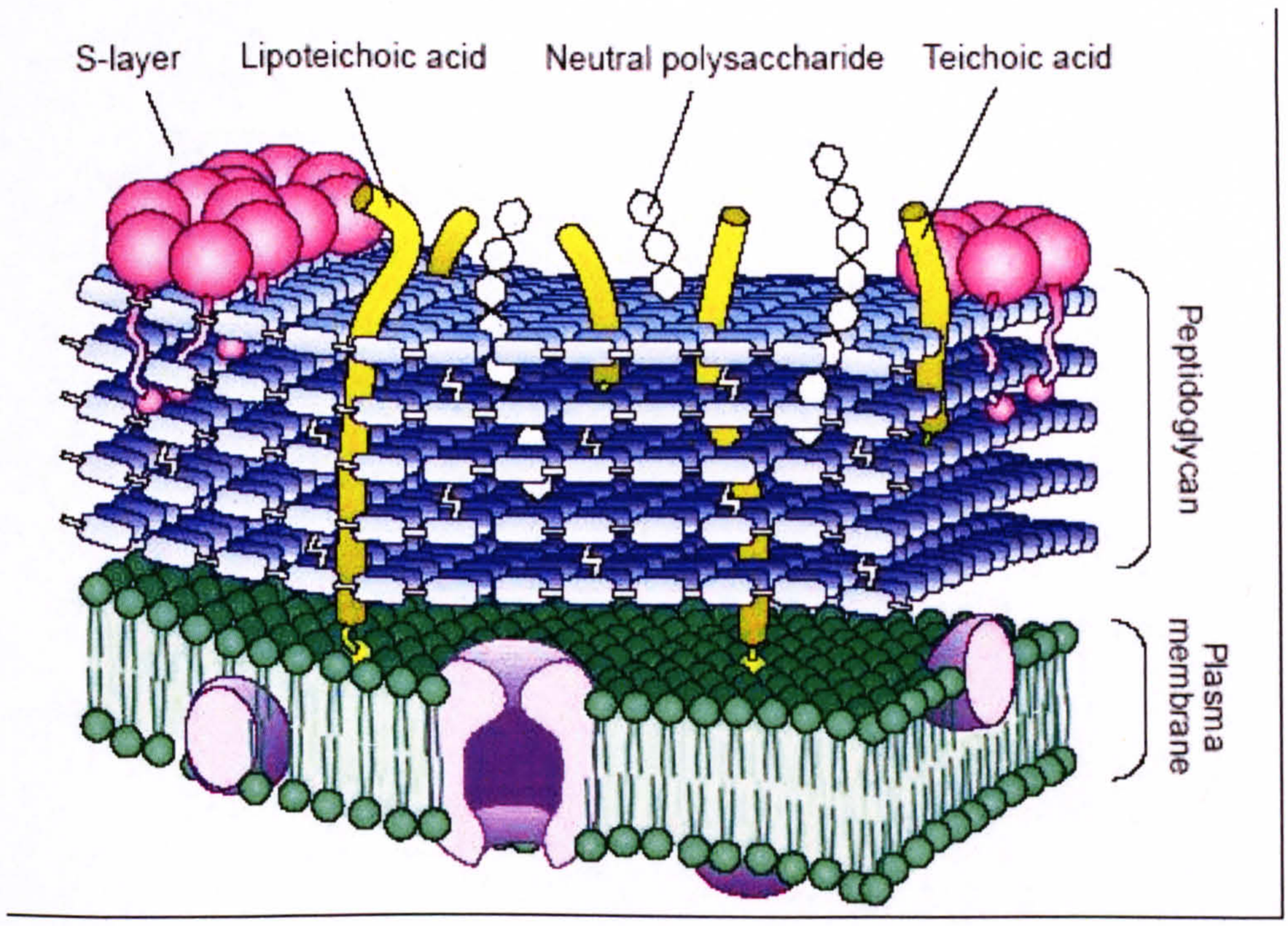

Figure 2.9. The overall general structure of the cell wall of Gram-positive bacteria. (reproduced from Delcour et al (138)).

2.4.2. Outer membrane of Gram negative bacteria

Gram-negative bacteria are surrounded by an envelope which comprised of two membranes (the cytoplasmic or inner membrane (IM) and outer membrane (OM)) separated by a thin peptidoglycan layer, called the periplasm (139) Figure 2.9). The inner membrane is a lipid bilayer which is predominantly composed of phospholipids mainly phosphatidylethanolamine (70–80%), phosphatidylglycerol (15-20%) and cardiolipin (<5%). The inner membrane also contains proteins (IMP) and lipoproteins which are distributed across the IM which serves as a selectively permeable barrier. The periplasmic membrane contains a thin layer of peptidoglycan (less than 10% of the total cell wall) and soluble proteins which mainly provides rigidity for the cell membrane and transportation of small molecules into the inner membrane (140).

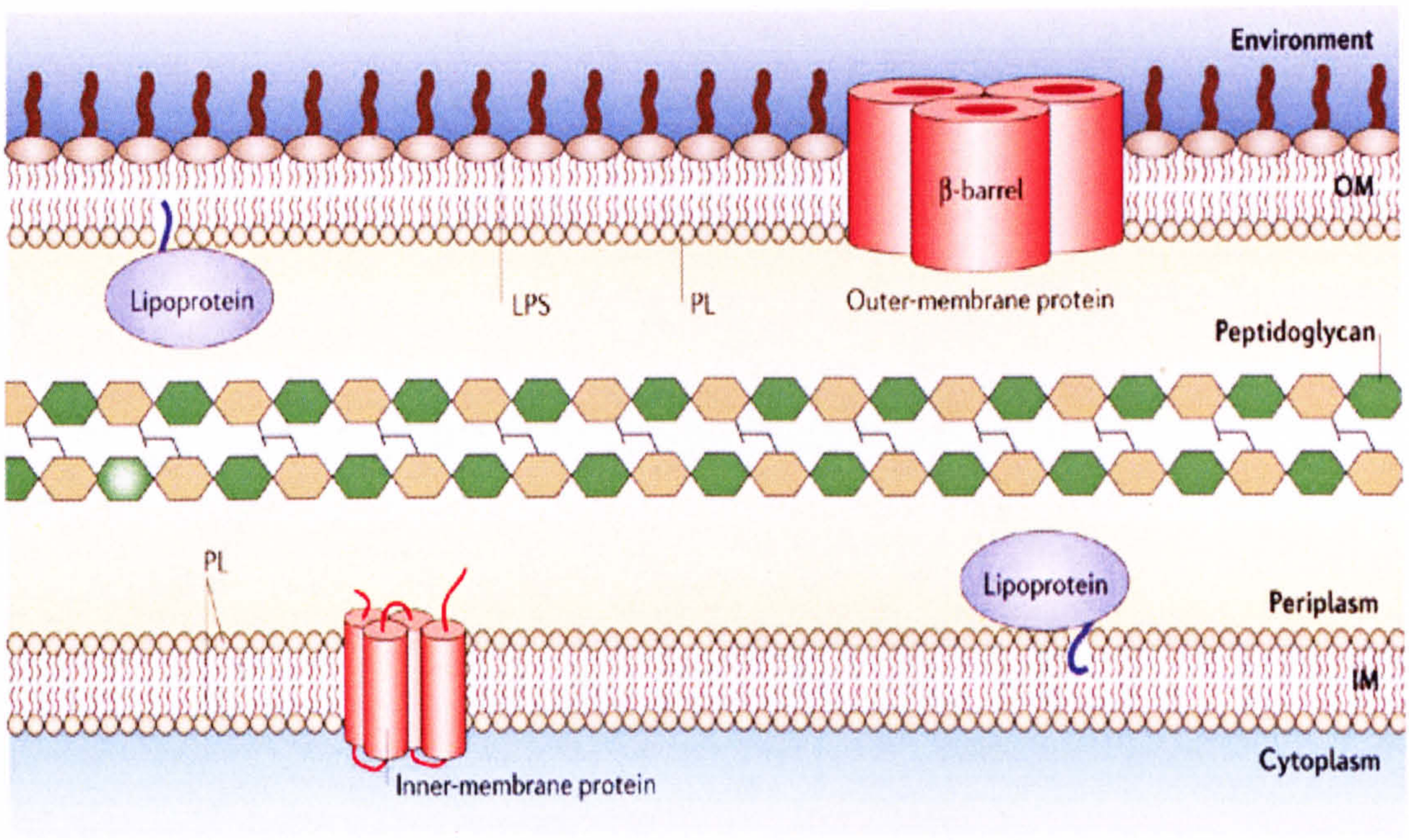

Figure 2.9 General structure of the Gram negative, *Escherichia coli* cell envelope (reproduced from Ruiz *et al* (139))

The outer membrane is the part of the cell which is in contact with the environment. It is composed of lipopolysaccharides (LPS), phospholipids (PL),

outer membrane proteins (OMP) and lipoproteins (LP) (141). The lipopolysaccharides is composed of oligosaccharides (core) and an O antigen, lipid portion (lipid A) which anchors the LPS to the outer membrane. Lipid A consists of a ß-1', 6-linked glucosamine disaccharide backbone, while the core is composed of 3-deoxy-D-manno-octulosonic acid (Kdo) residues. LPS provides a protective barrier for the cell and also contributes to the overall negative charge on the bacteria surface (142).

The phospholipid (PL) component of the outer membrane is mainly phosphatidylethanolamine and phosphatidylglycerol. The enzymes involved in these biosynthesis are located in the inner membrane (139).

Proteins in the outer membrane can be anchored via an N-ternimal N-acyl-diacylglycerylcysteine to the outer membrane (lipoproteins), or are spanned across the outer membrane region (integral outer membrane proteins referred to as outer membrane proteins OMPs). OMPs are composed of amphipathic antiparallel beta-strands folded into a barrel-like cylinder which enables them to channel nutrients into the cell, and excrete toxic waste from the cell (139, 143). Lipoproteins synthesized from the inner membrane are translocated to the outer membrane, while OMP are synthesized in the cytoplasm.

2.4.3. Comparison of Gram negative and Gram positive cell surfaces

The composition of macromolecules present the cell walls are chemically quite different in Gram negative and Gram positive cells (134). Peptidoglycan is the only macromolecule that is common to both types of bacteria. In Gram positive bacteria, their cell wall contains a much thicker peptidoglycan layer than the cell wall of Gram negative bacteria (144). The teichoic and lipoteichoic acids are only found in Gram positive bacteria. A Gram negative bacterium differs from its Gram positive counterpart in that it possesses an addition outer membrane which is of comprised lipopolysaccharides, lipoproteins, outer membrane proteins and phospholipids.

The overall surface charge on of a bacterium originates from the functional groups on the cell surface such as carboxylic, phosphoric, hydroxyl, and amine groups (31). Table 2.2 summarises the active functional groups identified on the different cell surfaces. These functional groups arise from the different macromolecules on the surface of the bacteria, which are also highlighted in Table 2.2. Hence it can be seen that different macromolecules are responsible for the active functional groups of the different cell types and this results in differences in the surface charge of both Gram positive and Gram negative bacteria will differ. For example, Sonohara *et al.* (145) compared surface properties between Gram-negative *Escherichia coli* and the Gram positive bacterium, *Staphylococcus aureus* and demonstrated that Gram-negative bacteria are more negatively charged and have a less soft surface than Gram-positive bacteria.

Table 2.2 Active functional groups from macromolecules of bacterial cell wall*

Active functional groups	Associated bacterial outer membrane macromolecule	
	Gram-positive	Gram-negative
Carboxylic $R\text{-}COOH \leftrightarrow R\text{-}COO^- + H^+$	Peptidoglycan, teichoic acid (glycerophosphate or ribitol phosphate residue)	Lipopolysaccharides, membrane protein e.g. porins,
Phosphate (phosphoric) $R\text{-}PO_4H \leftrightarrow R\text{-}PO_4^- + H^+$ $R\text{-}H_2PO_4 \leftrightarrow R\text{-}HPO_4^- + H^+$ $R\text{-}HPO_4^- \leftrightarrow R\text{-}PO_4^{2-} + H^+$	Teichoic acid, Lipoteichoic acid (teichoic acid covalently bond to lipids)	Lipopolysaccharides, Phospholipids
Amine $R\text{-}NH_3^+ \leftrightarrow R\text{-}NH_2 + H^+$	Peptidoglycan, S-layer	Lipopolysaccharides, membrane proteins
Hydroxyl (phenolic) $R\text{-}OH \leftrightarrow R\text{-}O^- + H^+$	Peptidoglycan, Teichoic acid, Teichuronic acid	Lipopolysaccharides, Phospholipids

*Modified from Hong and Brown, 2006 (31)

Burdman *et al.* (146) showed that OMPs can promote aggregation and flocculation of the cell by interacting with EPS during certain growth conditions. Recent studies have shown that the outer membrane protein, Antigen 43 (Ag43) promotes autoaggregation and flocculation of static cultures of specific *E.coli* strains via an Ag43-Ag43 interaction (64, 147). The outer membrane protein (OmpA) has recently been shown to affect biofilm formation in *E. coli* (41, 148) by inhibiting biofilm formation. An *E.coli* mutant lacking the ability to produce OmpA also showed a significant decrease in biofilm formation.

2.5. Proteomics studies

The term "proteomics" is an analogue of the word "genomics", which involves the study of an organism's entire genome (149). Proteomics can be defined as the study of proteins, which involves qualitative and quantitative comparison of proteins on a large scale under different conditions to further unravel biological processes. The field now also include studies of protein isoforms and modification, interactions, localisation and structure (150). The completion of genome-sequencing projects has aided the development of the field of proteomics. The two major experimental approaches used in the area of proteomics are discussed in the following sub-sections.

2.5.1. Gel-Based technology

This is a well established proteomics approach that involves the combination of two-dimensional gel electrophoresis (2-DE), mass spectrometry and bioinformatics tools. The 2-DE approach involves the separation of proteins based on their isoelectric point (pI) in the first dimension and by molecular weight in the second dimension (151). The 2-DE enables individual proteins to be resolved into spots. The spots are excised from the gel and then subjected to tryptic digestion follow by identification of the proteins using reverse phase liquid chromatography with tandem mass spectrophotometry (LC-MS/MS) (152). Prior to protein identification by LC-MS/MS, the spots are visualised with various stains like Coomassie-blue or silver staining. The differential expression of proteins can then be estimated with the aid of bioinformatic software such as PDQuest (Bio-Rad, UK). This approach has been successfully used to investigate soluble and extracellular proteins (153).

This approach has also been used to some extent to identified bacterial surface proteins (outer membrane proteins and lipoproteins) (154-156). However, surface proteins are more difficult to solubilise and resolve due to their hydrophobicity and as such difficult to analyse using this approach (152). Another major drawback of this approach is that it is laborious and very time consuming (152).

Another gel-based method in proteomics is the combination of SDS-PAGE and mass spectrometry. This method have been recently been shown to be suitable for separating membrane proteins due to the solubilising efficiency of the detergent, SDS (152). In this method, proteins are first separated using SDS-PAGE on a 1D gel based on molecular weight and the protein bands are then excised from the gel. The bands subjected to tryptic digestion followed by identification of the proteins using reverse phase liquid chromatography with tandem mass spectrophotometry (LC-MS/MS). Xiong et al (157) used this method to identify membrane proteins from *Mycobacterium tuberculosis* H37Rv identifying a total of 100 membrane proteins (157).

2.5.2. Shotgun proteomics

In order to address the limitation of the 2-DE approach, non-gel based approaches for the identification of proteins from complex mixtures have been developed, known as shotgun proteomics or multidimensional dimensional protein technology (MudPIT) (158). The approach involves the separation of proteins by two-dimensional liquid chromatography (2-DLC) prior to mass spectrometry. The protein mixture is first subjected to tryptic digestion. The peptide is first separated using a strong cation exchange (SCX) column in the first dimension followed by reverse phase chromatography in the second dimension. The proteins are then identified by subjecting the separated peptides to tandem mass spectrometry (MS/MS). The method is less laborious and time consuming in comparison to gel-based method (152). For quantification purposes the peptide mixture can be labelled with amino acid 'tags' or labels which enable peptide-peak comparisons to be made during mass spectrometry analysis (158). Severin *et al.* (159), recently identified surface associated proteins from *Streptococcus pyogenes* using this approach. A total of 79 surface associated proteins were identified, including 14

proteins containing cell wall-anchoring motifs, 12 lipoproteins, 9 secreted proteins, 22 membrane-associated proteins, 1 bacteriophage-associated protein, and 21 proteins commonly identified as cytoplasmic (159).

2.5.3. Proteomics and aggregation

The rapid development in the field of proteomics as well as genomics have help improved our understanding of microbial processes such as aggregation. De Windt et al (42) recently investigated the aggregation process of *Shewanella oneidensis* by conducting proteomic studies on the surface associated proteins (using the Gel-based method). The authors compared surface proteins of *Shewanella oneidensis* MR-1 with its hyper-aggregating mutant *Shewanella oneidensis* COAG. Their studies revealed that the agglutination protein AggA, associated with the secretion of a putative RTX protein, played a crucial role in the hyper-aggregating properties displayed by *Shewanella oneidensis* COAG (42).

Kalmokoff *et al* (160) conducted proteomic analysis of planktonic (non-aggregated) and biofilm-grown cells (aggregates) of *Campylobacter jejuni*. Their studies showed that proteins involved in the motility complex, including the flagellins (FlaA, FlaB), the filament cap (FliD), the basal body (FlgG, FlgG2), and the chemotactic protein (CheA), displayed higher levels of expression in cells from the biofilm phase than the planktonic phase. In addition, heat shock proteins (GroEL, GroES), oxidative (Tpx, Ahp) stress responses, as well as two known adhesins (Peb1, FlaC) were also observed to displayed higher levels of expression in the biofilm phase (160). The higher expression of these protein further suggest that cell aggregation and biofilm formation may serve as a mechanism for cells to adapted to adverse conditions.

Furthermore, proteomic studies have also been used to investigate factors such as growth conditions, quorum sensing and EPS, which have been suggested to control cell aggregation (161, 162). For example, Cohen *et al* (161) conducted a proteomic analysis of *Lactobacillus plantarum* cells collected during the exponential and stationary phase growth. The authors demonstrated that 29% of surface associated protein with anabolic pathways were at least twofold up-regulated throughout the exponential and early-stationary phases. In the late-stationary phase, six proteins

involved in stress or adaptation were significantly expressed. Kim *et al* (162) recently used a proteomic approach to investigate the role of quorum sensing in *Pseudomonas aeruginosa*. Interestingly, several of the extracellular proteins (AprA, LasB, PrpL) were found to be quorum sensing regulated. Hence it is possible that quorum sensing may regulated extracellular proteins found in the EPS, which is know to be involved in cell aggregation. However further studies are needed to confirm this.

2.6. Physical frameworks available to study bacterial aggregation

Due to the dynamic and complex nature of bacteria, no single theoretical framework has been able to fully explain bacterial aggregation. A common approach is to assume that bacteria are like inert colloids coated with polyelectrolyte such as proteins, polysaccharides or lipids. Traditional theories have been applied to investigate bacterial interaction or bacterial-to–surface interactions. The major theoretical approach that has been adopted to explain the microbial adhesion process is the Derjauin–Landau–Verwey–Overbeek (DLVO) theory (163).

The DLVO theory is a theory used to describe the behaviour of colloid stability in suspension (163, 164). The theory is used to explain the ability of colloids aggregate or remain dispersed (G_{aggr}) in suspension by taking into account the balance between van der Waals (G_{vdW}) attraction and electrostatic (G_{ES}) repulsion (also referred to as the electric double layer). Depending on the relative strength, the interaction between the colloids may be attractive or repulsive. Hence colloid aggregation will occur if the net magnitude of forces is attractive. Conversely, a colloidial dispersion will remain stable if the net magnitude of the energies is repulsive. Both energies contribute to the total Gibbs energy (ΔG_{aggr}), hence the overall cell-to-cell interaction energy can be separated as

$$G_{aggr}(d) = G_{vdW}(d) + G_{ES}(d) \qquad \text{Equation 2.4}$$

The electrostatic repulsion force resulting from the charge ionisable function groups becomes significant when two colloids approach each other and their double layers begin to interfere (165). The electrostatic repulsion is highest when the colloids are almost in contact with each other and lowest outside the double layer region (see Figure 2.11). The Van der Waals force is the attractive intermolecular force in each colloid resulting from fluctuations in the distribution of surface electrons. An attractive energy curve is used to indicate the variation in van der Waals force with distance between the colloids (see Figure 2.10).

When both electrostatic repulsion and van der Waals energy curves are combined together a net energy curve can be deduced (Figure 2.10a). At large distances between colloids, electrostatic repulsion is weakened, resulting in overall attraction with a shallow minimum called the secondary minimum (Figure 2.10b) (165). When the distance between colloids is decreased, a repulsive barrier based on electrostatic repulsion is increased, and as such an energy barrier must be overcome to reach the so-called primary minimum and allow aggregation. The maximum energy is related to the surface potential and the zeta potential, which is discussed in more detail in Section 2.7.

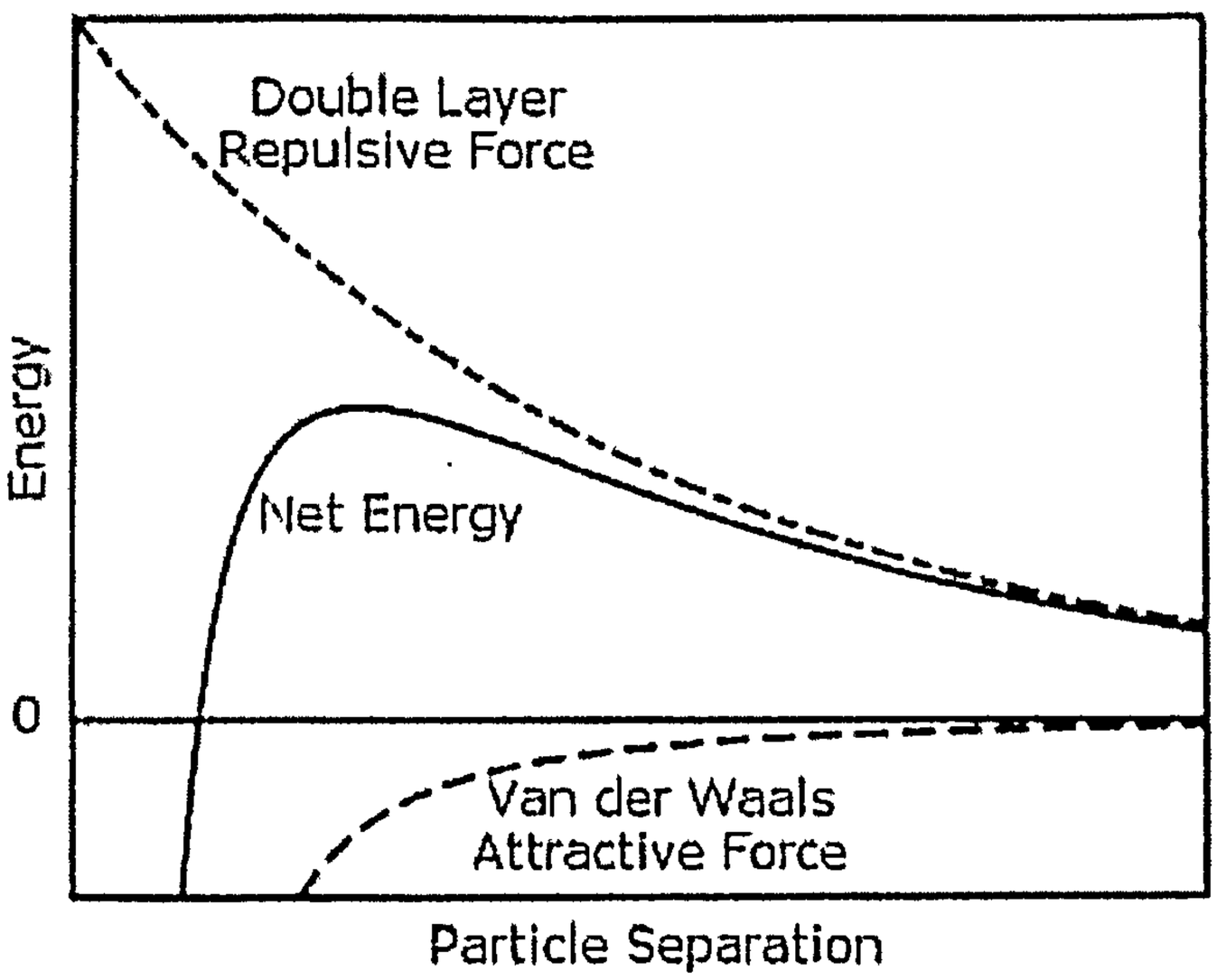

Figure 2.10a Schematic diagram of the variation of free energy with particle separation according to DLVO theory (Reproduced from http://www.malvern.com/LabEng/industry/colloids/dlvo_theory.htm)

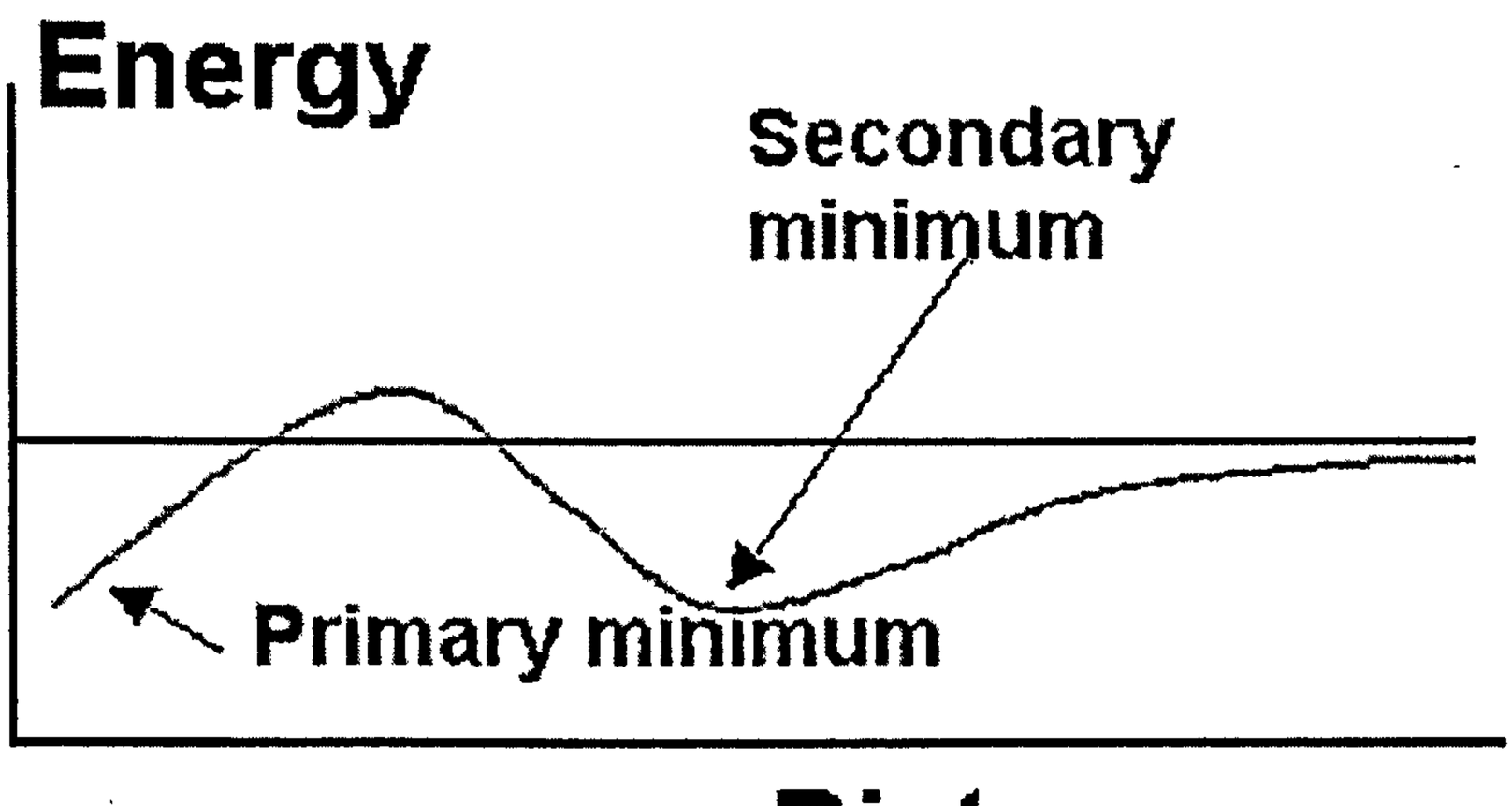

Figure 2.11b.A typical energy/distance curve is shown (reproduced from Vitte *et al.* (165))

The electrostatic repulsion is dominant at low ionic strength because it arises from the electrokinetic properties of the cell surface. However at higher ionic strengths, the electrostatic repulsion becomes less dominant as a result of shielding of the cells surface charge by external electrolyte and steric interactions between outer membrane macromolecules (166). The DLVO approach also assumes that for aggregation to occur the strong electrostatic repulsion among colloids, due to their overall negative charge, will have to be overcome or reduced before aggregation can take place.

Although this theory has been successfully applied for non-biological colloids and in some biological systems (166, 167), the bacterial surface is far more complex than the DLVO theory assumes; as it is semi permeable and allows an influx of nutrient and ions (78). Moreover, bacteria do not have a uniform surface in time or location, as they possess various macromolecules which may vary in response to the environmental changes.

Hence an extension of the standard DLVO approach is required to explain the bacterial aggregation process which considers additional potentials and governing factors. For example, a suspension of non-biological colloidal particles, in the presence of non-adsorbing polymers have been observed to aggregate via a process

known as depletion (48, 49). The interaction is due to an imbalance in osmotic pressure when the non-adsorbing polymers are excluded from the region between particles. Thus, a net attractive potential is set up between the particles enhancing the attractive potential. This approach can be used to describe the cell-to-cell interactions, leading to aggregation, assuming that the extracellular polymers produced by the cells are non-adsorbing. Hence, the approach appears to be more appropriate when considering the interaction of cells in the presence of free-EPS.

2.7. Physical methods for characterization of microbial surfaces

Bacteria can interact with themselves and with the environment. These interactions, whilst biologically initiated, are also controlled by the physiochemical properties of the cell surface. As stated previously, microbial surfaces are composed of macromolecules such as lipopolysaccharides (LPS), phospholipids (PL), outer membrane proteins (OMP) and lipoproteins (LP) (139). These macromolecules possess functional groups, such as carboxyl, phosphate, amino and hydroxyl groups which contribute to the overall physicochemical properties, e.g. surface charge, of the bacterial cells. Measurement of the cell surface is therefore important to determine the chance of aggregation. There are several methods, currently available to measure the surface properties, which will be discussed in the following section.

2.7.1. Potentiometric titration (acid-based titration)

The charge on a microbial cell surface usually arises from the dissociations of the proton active functional groups under in aqueous solution (31) (Figure 2.11).

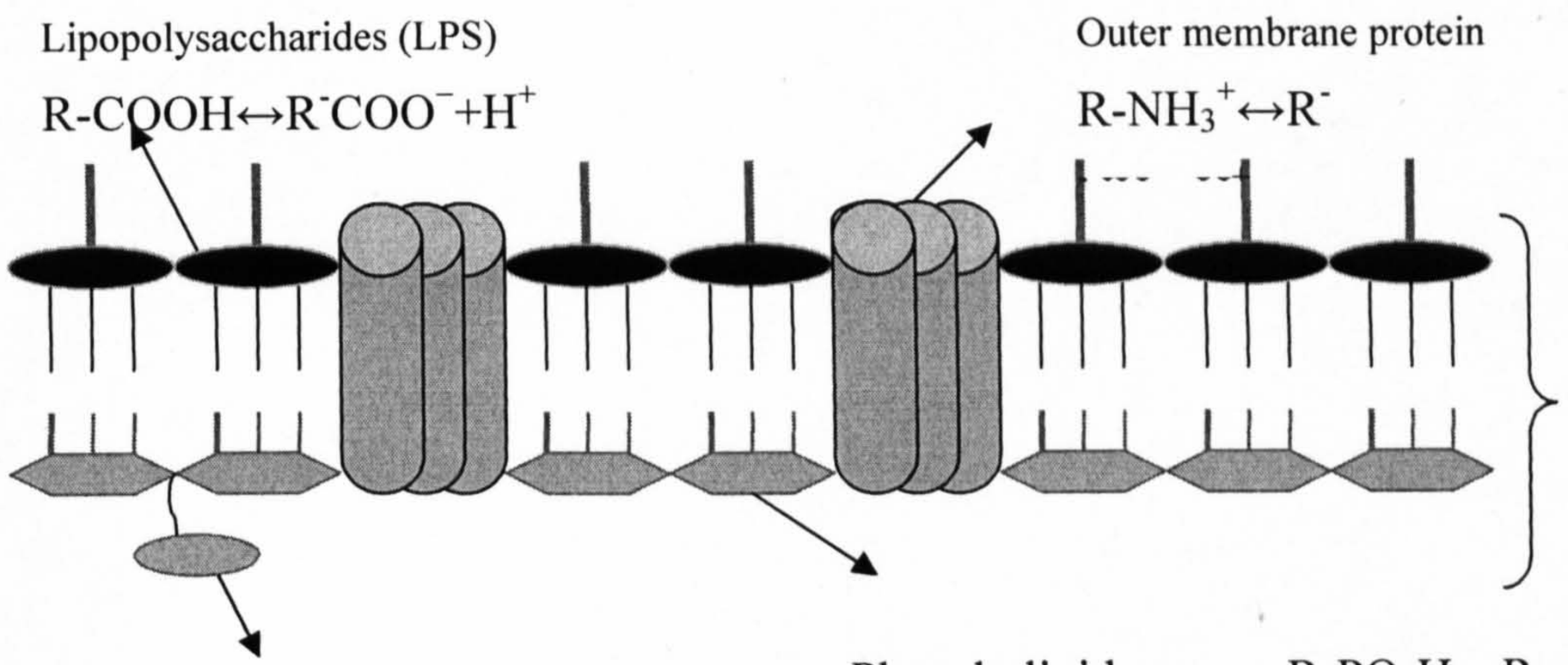

Figure 2.11 Dissociation of proton active functional groups from macromolecules on the surface of Gram negative bacteria.

Potentiometric titration is suitable for investigating the acid-base properties of the microbial surface, and has been found to be successful in elucidating the cell-to-cell and cell to environment interaction (31, 43, 79, 168).

The tendency of a compound to donate a proton is measured by its acid ionization or acid dissociation constant, K_a. These range from 10^{10} for sulphuric acid to 10^{-50} for methane. Deprotonation of proton active functional groups from microbial surfaces is described by

$$RH^0 \Leftrightarrow R^- + H^+ \qquad \text{Equation 2.5}$$

Where R^- is the proton active functional and H^+ is the proton in the suspension. The dissociation constant, K_a of the reaction above is expressed as

$$K_a = \frac{[R^-]a_{H^-}}{[RH^0]} \qquad \text{Equation 2.3}$$

Where $[R^-]$ and $[RH^0]$ is the concentration of deprotonated and protonated sites, respectively and $a_{H.}$ is the activity of the proton in the bulk solution. The pK_a values can then be deduced from

$$pK_a = -\log_{10}(K_a) \qquad \text{Equation 2.4}$$

The pK_a of any reaction can be determined by potentiometric titration and the software often used for this is Protofit (169) or FITEQL (170).

The pKa values for different microorganisms have been published, and the values vary due to differences in both the strain and growth conditions. The calculated pK_a values correspond to carboxyl (pK_1), phosphate (pK_2), and amine (pK_3) groups (Table 2.2), with C_1, C2 and C_3 corresponding to the concentration of the corresponding functional groups (Table 2.3). Walker *et al.* (79) used potentiometric titration to characterize the *E.coli* surface properties at different growth phases. The findings suggested that the potentiometric titration data correlated well with the adhesion capability of the bacteria. Similarly, Hong and Brown 2006 (31) used potentiometric titration to compare the acid-base properties of Gram negative *E.coli* and Gram positive bacteria, *Bacillus brevis* at different growth conditions. Not surprisingly, the acid-base properties of *E.coli* were significantly different from the Gram positive bacteria, *Bacillus brevis,* due to their different cell wall architecture.

Table 2.3 pKa values for different bacterial species as reported in literature

Species	*pK_1	*pK_2	*pK_3	Reference
Synechococcus Green	4.85± 0.31	6.56 ± 0.2	8.76 ± 0.06	(171)
Synechococcus Red	4.98± 0.16	6.69 ± 0.39	8.66 ± 0.21	(171)
Enterobacteriaceae	4.3 ± 0.20	6.9 ± 0.50	8.9 ± 0.5	(172)
S.putrefaciens	5.16± 0.04	7.22 ± 0.15	10.0 ± 0.67	(173)
Calotrix cell	4.7 ± 0.40	6.6 ± 0.20	9.1 ± 0.3	(174)
Calotrix sheath	4.8 ± 0.30	6.5 ± 0.10	8.7 ± 0.2	(174)
Bacillus subtilis	4.8 ± 0.14	6.9 ± 0.50	9.4 ± 0.6	(175)

*pK_1 ≡ carboxyl groups

*pK_2 ≡ phosphate groups

*pK_3 ≡ amine groups

Table 2.4 Surface site concentration values for different bacterial species as reported in literature

Species	Ctot (x 10^{-4} mol/g)	*C_1 (x 10^{-4} mol/g)	*C_2 (x 10^{-4} mol/g)	*C_3 (x 10^{-4} mol/g)	Reference
Synechococcus Green	7.0	2.6 ± 0.4	1.9 ± 0.5	2.5 ± 0.4	(171)
Synechococcus Red	16.6	7.4 ± 1.6	4.4 ± 0.8	4.8 ± 0.8	(171)
Enterobacteriaceae	12.7	5.0 ± 0.7	2.2 ± 0.6	5.5 ± 2.2	(172)
S. putrefaciens	0.78	0.32 ± 0.0	0.09 ± 0.0	0.38 ± 0.0	(173)
Calotrix cell	14.6	3.28 ± 0.3	4.14 ± 0.3	0.92 ± 0.2	(174)
Calotrix sheath	1.83	0.46 ± 0.2	0.45 ± 0.1	0.92 ± 0.2	(174)
Bacillus subtilis	22.6	12 ± 1.0	4.4 ± 0.2	6.2 ± 0.2	(175)

*C_1 ≡ carboxyl groups

*C_2 ≡ phosphate groups

*C_3 ≡ amine groups

2.7.2. Electrophoretic mobility

Interactions leading to aggregation have been shown to be controlled by physical forces such as van der Waals and electrostatic forces (163). The DLVO theory, described previously, considers a combination of these two forces. Electrostatic repulsion forces are determined by the electrokinetic properties of the bacteria due to the presence of macromolecules on their surface, as well as the chemical nature of the solution or environment (such as ionic strength and valency of ions) in which they exist (176). Microbial surface macromolecules such as lipopolysaccharides, lipoproteins, phospholipids and outer membrane proteins possess ionisable functional groups which are dependent on the pH of the environment and they confer the electrokinetic stabilization to the microbial dispersion.

Electrokinetic properties of the bacterial surface are generally elucidated from measuring the Zeta potential, which is the electric potential of the interfacial region between the bacterial surface and the aqueous environment (46). The net surface charge on the microbial surface determines the ion distribution in the surrounding interfacial region, which results in an increased concentration of counter ions (177). An electric double layer exists for each individual cell. The inner region is known as the Stern layer, consisting of the bacterial surface as well as the ions which are strongly bound to the surface. The outer (diffuse) region comprises of less firmly associated ions that extend to the bulk. The outer region contains an inner boundary were ions form a stable association with the cell surface and move with the cells during bacterial motion, while ions beyond this boundary remain in the aqueous environment (177). The potential at this inner boundary (potential at the plane of shear) is known as the Zeta potential (ζ) (Figure 2.12).

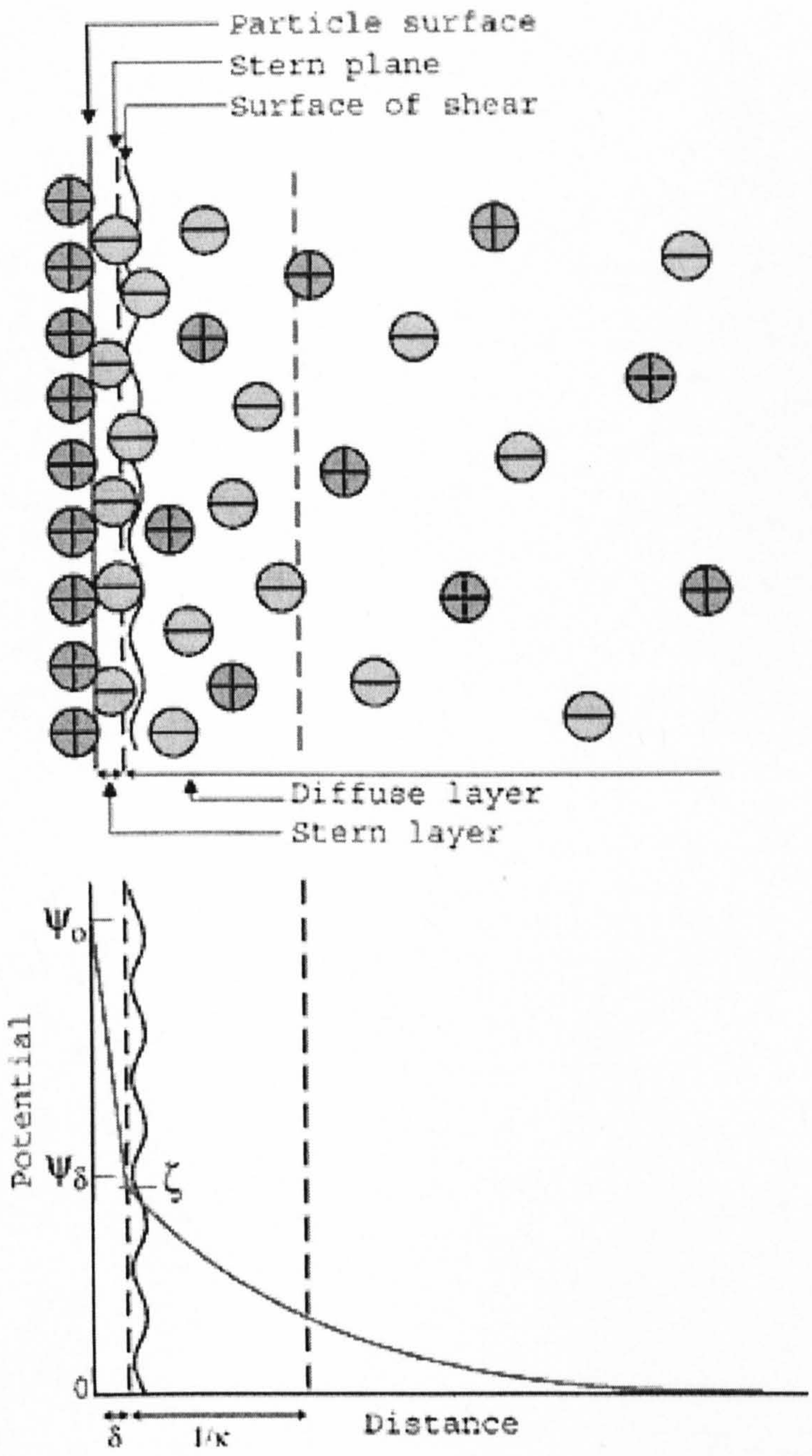

Fugure 2.12 A cross-section representation of the bacterial cell surface, depicting the various solvent layers surrounding the cell (copied from www.colorado.edu/ceae/environmental/ryan/cven6414/lecture02mineralwaterinterface.ppt).

For non-biological colloids the Zeta potential can be obtained by measurement of the electrophoretic mobility (EPM). This is the velocity of a particle in a unit electric field and is dependent on the net charge of the particle. The magnitude of the EPM gives an indication of the overall net charge on the surface of a particle. A

negative EPM value indicates that a particle has a negative charge and vice versa. The electrophoretic mobility is then converted to Zeta potential via Smoluchowski's formula (30, 78, 145, 178, 179). The relationship being

$$\zeta = \frac{\eta\mu}{\varepsilon_0 \varepsilon} \qquad \text{Equation 2.5}$$

Where η is the viscosity of the medium, μ is the mobility, ε_0 is the permittivity of vacuum and ε is the dielectric constant of the medium.

However, equation is not suitable for calculating the Zeta potential for microbial cells due to their surface complexity and non spherical shape (145, 180). Ohshima and Kondo (181-184) have recently developed a formula known as Ohshima's soft-particle electrophoresis theory, which appears to be a more suitable approach to describe bacterial surfaces. The theory assumes the presence of an ion-penetrable layer of finite thickness around a core spherical particle. This approach has been found to be useful in estimating the surface charge of several biological systems (78, 145, 178, 185). Ohshima's soft-particle theory was used by Sonohara *et al.* (145) to compare electrokinetic properties between Gram-negative *Escherichia coli* and Gram positive bacteria, *Staphylococcus aureus*. The work revealed that Gram-negative bacteria are more negatively charged and have a less soft surface than Gram-positive bacteria. This was attributed to the differences in the composition of macromolecules on their cell surface. Skvarla *et al.* (186) investigated the surface properties of *Thiobacillus ferrooxidans* using the soft particle model. They also observed that the application of Ohshima's formula was more suitable for bio-colloids than Smoluchowski's formula. However, Ohshima's soft-particle electrophoresis theory involves the use of several assumptions, such as a spherical shape, which is not the case for all microorganisms. For example, Gram negative bacteria like *E.coli* and *Pseudomonas* are rod-like in shape. Hence, it is not surprising that some researchers prefer to report the measured electrophoretic mobility values rather than Zeta potential (185) since the electrophoretic mobility makes no assumption about shape.

2.7.3. Bacterial adherence to hydrocarbons (BATH) and contact angle

The cell surface hydrophobicity has suggested to be an important factor in bacterial aggregation, attachment and biogranulation (29, 30, 52, 163, 187, 188). An increase in bacterial surface hydrophobicity is usually linked with bacterial aggregation (189, 190). From a thermodynamics point of view, bacterial aggregation is driven by a decrease of free energy. Increasing the cell surface hydrophobicity would cause a corresponding increase in the excess Gibbs energy of the surface. This in turn would promote cell-to-cell interaction. This would further serve as an diving force for cells to aggregate out of the aqueous liquid phase (52).

Two major methods for studying hydrophobic interactions in bacteria include contact angle measurement (29, 167, 191-193) and microbial adhesion to hydrocarbons (MATH) (194-197). Other methods include salt aggregation (193, 198), hydrophobic interaction chromatography (193, 197, 199), hydrophobic microsphere assay (199, 200), and coaggregation with *Fusobacteriumnucleatum* (201). MATH is one of the most commonly used methods to determine microbial cell surface hydrophobicity (202, 203). In MATH, a suspension of cells is repeatedly mixed with a small amount of hydrocarbon for a set period of time, which allows the bacteria to interact with the hydrocarbon phase. The mixture is allowed to stand for a certain period and microbial hydrophobicity is calculated as the percentage of microbial adhesion to the solvent. One of the drawbacks on this method is that MATH is based on adhesion, and does not measure cell surface (202, 204) hydrophobicity alone, but an interplay of hydrophobicity and electrostatic interactions.

Van der Mei *et al.* (205) investigated the surface hydrophobicity of nonencapsulated and encapsulated *Staphylococci* by contact angle measurements. This method has also been used to study the relationship between the hydrophobicity of urogenital isolates of *lactobacilli* and resistance to antibiotics (206). They observed that surface hydrophobicity may be implicated in *lactobacilli* susceptibility to antimicrobial agents. Several studies have suggested that

extracellular polymeric substances are implicated in cell hydrophobicity (207-209). Van der Mei *et al.* (210), observed that a surface layer of protein enhances the cell surface hydrophobicity and facilitates its adhesion to hydrocarbons through hydrophobic interactions.

Although cell hydrophobicity has been recognized as an important driving force in bacteria aggregation, there is still disagreement about the current methods used to measure hydrophobicity. Both the MATH and contact angle method have been compared, and a weak correlation has been observed (193). Furthermore, it is not possible to define the surface hydrophobicity of a bacterium other than on a comparative level between closely related strains (193). Most methods are limited by their inability to measure the actual microbial surface hydrophobicity but rather measure some hydrophobic substratum (190). Ahimou *et al.* (197) investigated the surface hydrophobicity of nine *Bacillus subtilis* strains using microbial adhesion to hydrocarbon (MATH), water contact angle measurements, and hydrophobic interaction chromatography (HIC). Their results revealed that MATH and HIC are influenced by electrostatic interactions whilst the water contact angle seems to be the most suitable method for estimating just the cell surface hydrophobicity.

2.7.4. Fourier transformation infrared spectroscopy (FTIR)

Fourier transform infrared (FTIR) spectroscopy is a rapid non-destructive method which has been applied to many biological systems (45, 211, 212). The technique is based on the principle that atoms in molecules are not held rigidly apart and when subjected to infrared radiation (between 300 and 4000 cm^{-1}), the molecule will absorb the energy and the bond will be subjected to a number of different vibrations (Figure 2.13). The pattern of vibration of the atoms in the molecules depends on the type of binding force and angles of the atoms in the molecules (45). Hence a complex molecule will display several types of vibrations with each arising from different atoms.

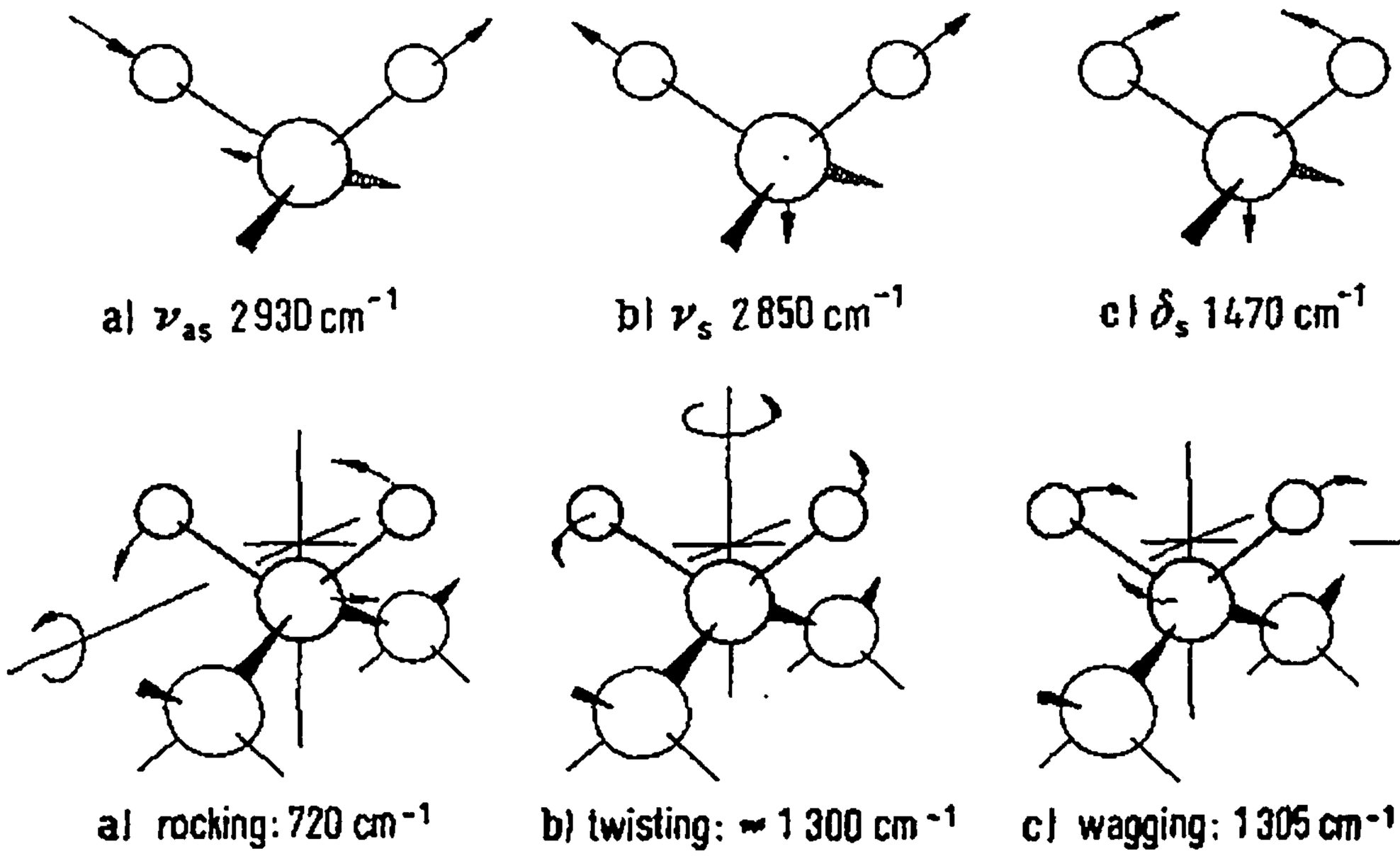

Figure 2.13 Modes of vibration for $>CH_2$ (reproduced from http://www.ir-spektroskopie.de/)

FTIR can be used to identify and characterize microbial cells (212, 213), microbial cell walls (171) and pathogenicity (214, 215) as well as characterization of individual microbial surface macromolecules such as lipopolysaccharides (216), outer membrane proteins (217) and extracellular polymeric substances (84, 218). Despite the success in the use of FTIR in studying microorganisms, the major drawback is that spectra may contain mixed regions of proteins, carbohydrates, lipids and nucleic acids which cannot be individually characterized. Serra *et al.* (219) recently used FTIR to monitor a *Bordetella pertussis* biofilm. They observed changes in the carbohydrate to protein ratio during *Bordetella pertussis* biofilm formation. Furthermore, it is difficult to characterize a bacterial cell surface with FTIR since the spectra may also reveal bands which originate not only from the cell wall but also from the cytoplasm. Hence FTIR should be used in combination with other surface characterization techniques. Dittrich and Sibler (171) recently combined FTIR with Electrophoretic mobility and Potentiometric titration to study picocyanobacteria. The authors reported good correlation between the techniques.

2.8. Conclusions

Based on the literature thus far, it is apparent that bacterial aggregation is strongly influenced by the physiochemical properties of the bacterial surface. A common approach for studying aggregation is to assume that bacteria are inert colloids and hence physical forces such as electrostatic; van der Waals and steric forces govern the bacterial interaction. Although this approach has been successful in explaining colloid interactions, it has limited direct application to bacterial interaction. This is due to the following reasons; (1) The bacterial surface is composed of complex macromolecules such as proteins, lipids and polysaccharides (2) The bacterial surface is not a hard surface since ions and solutes can be transported from the environment into the bacterial cell and (3) Bacteria are dynamic in nature and their surface composition and aggregation ability can vary as a function of their physiological state.

In order to understand bacterial aggregation a combined approach that considers both physical and biological aspects is needed. This is the philosophy behind the approach taken in this thesis. Hence in order to understand bacterial aggregation, it is necessary to consider biological factors that affect bacterial physiology during aggregation, and to determine how this affects the physiochemical properties of the cells. For example, while EPS has been suggested to affect cell bacterial surface properties, it still remains unclear as to how EPS affects bacterial aggregation and its role in this process. In order to achieve this, it is necessary to understand the how changes in bacterial physiology due to different growth phases and nutrients, influences EPS production which in turn influences aggregation. This is the focus of Chapters 3-6.

The bacterial cell surface properties are attributed to the presence of surface macromolecules such as lipopolysaccharides, proteins and phospholipids. These surface macromolecules are controlled by the bacterial physiology due to changes in environmental conditions and as such these changes will control bacterial cell surface properties. Although several studies are available on bacterial cell surface properties, they have mostly focused on a specific biological or environmental

condition. Hence very little is known on how changes in the environmental conditions, such as growth phases or nutrients affect the bacterial cell surface properties. This is addressed in Chapters and 4 and 7.

Furthermore, the ability of bacteria to adapt to changes or to participate in aggregation also depends on their ability to sense and respond to these changes via quorum sensing. Although quorum sensing has been suggested to affect bacterial interactions, its exact role in aggregation still remains unclear. If aggregation is strongly linked with changes in cell surface properties, then it is vital to investigate the link between quorum sensing and changes in bacterial surface properties. This is addressed in Chapters 3 and 8.

Chapter 3 Growth studies and Quorum sensing of *Escherichia coli* AB1157, MG1655 and MG1655 *luxS*$^{-}$

3.1. Abstract

Escherichia coli (AB1157, MG1655 wild and MG1655 *luxS*⁻ (lacking quorum sensing gene for Autoinducer synthase AI-2) were chosen as a model for studying bacterial aggregation. In order to investigate bacterial aggregation it is necessary to characterize the bacteria in terms of growth pattern, nutrient uptake and their ability to participate in quorum sensing. The aim of this chapter was to determine the effect of changes in the growth media to the growth pattern of *Escherichia coli* (*E.coli*) as well as their ability to participate in quorum sensing.

E.coli strains were cultivated in LB (Luria-Bertani) medium or LB supplemented with 0.5% (w/v) glucose (LBG) at 30^0C. The specific growth rate for *E.coli* AB1157, MG1655 and MG1655 *luxS*⁻ were found to be $0.45h^{-1}$, $0.34h^{-1}$ and $0.35h^{-1}$ respectively regardless of the medium used. Neither quorum sensing nor the addition of 0.5 w/v (%) glucose affected the growth pattern of any of the strains. However, the addition of 0.5 w/v (%) glucose to the medium affected the measurable amount of quorum sensing molecule present in the supernatant for *E.coli* AB1157 and MG1655 wild type. The knowledge from this work will lay the foundation for further studies of bacterial aggregation.

3.2. Introduction

The ability of bacterial to participate in aggregation is an index of its physiological state (as discussed in Chapter 2). The physiological status of bacteria has been shown to be controlled by biological factors such as growth phase, nutrients and quorum sensing and as such may affect bacteria aggregation. Therefore, in order to investigate bacterial aggregation, it is necessary to characterize the bacteria in terms of its growth, response to nutrients in the medium and ability to participate in quorum sensing. Each of these factors is discussed in this chapter.

Escherichia coli (*E.coli*) was chosen as the model system to investigate bacterial aggregation, due to its fast growth rate and the fact that the genome has already been sequenced (220). The information from the bacteria genome can be analysed to provide future structural and functional information about unknown genes and proteins that might be implicated in bacteria aggregation.

Three *E.coli* strains are used in this chapter. These are *E.coli* AB1157, MG1655 and MG1655 *luxS*⁻. *E.coli* AB1157 was used in this thesis because it was previously reported by Surette and Bassler (128) to produce and respond to quorum sensing molecules AI-2. Similarly, Hardie *et al.* (221) later showed that *E.coli* MG1655 can also produce and respond to quorum sensing molecules AI-2. *E.coli* MG1655 was also used for further aggregation studies (chapter 5-8) due to the fact that it is one of the most biologically studied *E.coli* strains and its mutant MG1655 *luxS*⁻ had been constructed previously. *LuxS* gene, codes for the enzyme responsible for production of Autoinducer-2 molecule. MG1655 *luxS*⁻ lacks the gene *luxS* and hence the strain is unable to participate in quorum sensing.

The objective of the research presented in this chapter is to quantify the growth pattern of the different *E. coli* strains during different growth conditions, as well as determining their ability to participate in cell-to-cell communication (quorum sensing).

3.3. Materials and methods

All chemicals were purchased from Sigma-Aldrich (Gillingham, Dorset, UK) unless otherwise stated. All experiments were conducted in triplicate (at least), and the average of the results reported. Variation in the experimental results is presented as the average ± standard deviation

3.3.1. Bacterial strain and growth studies

E. coli strains AB1157 (DSM number 9036) was purchased from Deutsche Sammlung von Mikroorganismen und Zellkulturen GmbH (DSMZ), Germany, *E.coli* MG1655 (wild-type) and MG1655 *luxS*$^-$, as well as *Vibrio Harveyi* BB170 (luxN::Tn5, Sensor 1$^-$, sensor 2$^+$) were supplied by Prof Paul Williams, University of Nottingham UK. The *E.coli* MG1655 *luxS*$^-$ mutation is identical to the *E.coli* *luxS*$^-$ mutant that has been previously described in *E.coli* BL21 (126). The mutation was transferred into *E.coli* MG1655 by P1 phage transduction (Winzer, Tavender, and Hardie, personal communication, 2006).

E.coli strains were grown aerobically in Luria-Bertani (LB) medium (tryptone 10.0g/L, yeast extract 5.0g/L, NaCl 10.0g/L (sigma UK), adjusted to pH 7.0) supplemented with or without the addition 0.5w/v (%) glucose at the beginning of growth phase at 30°C. The strains were also grown of LB agar plates at 30°C. LB media supplemented with 0.5 w/v (%) glucose at the beginning of the growth phase is referred to as LBG throughout the thesis. *E.coli* strains were grown at 30°C overnight with aeration in LB or LBG. The culture was then used to inoculate fresh LB or LBG at a 1:100 dilution and grown at 30°C with aeration. The optical density at 600nm was measured using a spectrophotometer (ThermoSpectronic. UK). The growth rate was determined using Equation 3.1. Where μ, is an index of the growth rate and is called the growth rate constant. N_t is the number of cells at any time and N_0 is the initial number of cells.

$$\ln N_t - \ln N_0 = \mu(t - t_0) \qquad \text{Equation 3.1}$$

V.harveyi BB170 were grown aerobically in Autoinducer Bioassay (AB) medium at 30°C (222). AB medium contained 0.3M NaCl, 0.05M $MgSO_4.7H_20$ (Sigma UK), 0.2% Casamino acid (BD Bioscience), 2% glycerol, 1mM L-arginine, 10mM potassium phosphate (pH 7.0). 0.3M NaCl, 0.05M $MgSO_4.7H_20$, 0.2% Casamino acid was dissolved in 1L of distilled water. The pH was adjusted to 7.5 using 0.01 M KOH. It was then sterilized by autoclaving at 121°C for 15 minutes. Finally 1M potassium phosphate (0.1ml), 0.1M L-arginine (0.1ml) and 50% glycerol (0.2ml) were added to 9.6ml AB medium immediately before use. An overnight culture of *V.harveyi* BB170 was inoculated into freshly prepared AB medium at 1:5000 dilutions. The batch growth curve and light production was then determined using a GENios Multi-Detection Microplate Reader (Tecan, UK).

3.3.2. Glucose uptake assay

The amount of glucose present in cell-free cultures was analysed using a glucose assay kit (Kit GAGO-20 Sigma, UK). *E.coli* MG1655 was grown in LBG as previously described. Cell-free culture fluid was obtained during the growth phase by centrifugation of the cells at 15,000 rpm at 4^0C for 10 minutes. The supernatant was filtered through a 0.22µm syringe filter and samples were stored at -20^0C. The amount of glucose present in the culture fluid was then analysed as described by the manufacturer's protocol.

3.3.3. DNA manipulation

The genomic DNA of *E.coli* AB1157, MG1655 (wild type) and mutant were extracted using a GenElute Bacterial Genomic DNA extraction kit NA2100 (Sigma, UK) and extraction was carried out according to the manufacturer's protocol. The *luxS* gene was amplified using the primers *luxS*-F3 (5′-TGCCDTTRTTAGAYAGCTTCA -3′) and *luxS*-R3 (5′-TCCTGCARYTTYTCTTTCGG -3′) designed from Primer3 software (223). Polymerase chain reaction (PCR) kit D4545 (Sigma UK) was used to amplify the *luxS* gene from genomic DNA of *E.coli* strains. PCR reactions (one cycle at 94°C for 2 min, 30 cycles of 95°C for 1 min, 52°C for 1 min, and 72°C for 2 min and finally 72°C for 10 minutes) were carried out using a thermal cycler, GeneAmp PCR system 9700 (Applied BioSystems UK).

3.3.4. Agarose Gel electrophoresis

PCR products were separated by Gel electrophoresis using 1% agarose gel. Agarose gels were prepared by dissolving agarose in 0.5×TBE (Tris-Borate-EDTA) buffer, heated to allow the agarose to dissolve and then stained with ethiduim bromide. 50ml of agarose was then poured into the electrophoretic apparatus. The agarose gel was allowed to cool and solidified for one hour. 0.5×TBE was used as the running buffer. 2µl of DNA loading buffer (0.25% bromophenol blue, 0.25% xylene cyanol, 15% Ficoll Type 400), was mixed with 3µl standard DNA (ladder) and 7µl of each PCR product. The PCR products where then electrophoresed at 75volts for 75 minutes. The PCR products in agarose gels were then visualized under UV light (302nm).

DNA sequences of the PCR products (*luxS*) were determined by MWG-BIOTECH (UK) Ltd. PCR products were directly sequenced using the corresponding PCR primers. The sequence was viewed and edited using Chromas 2.3 software at http://www.technelysium.com.au/chromas.html. Similarity and homology analysis were carried using the FASTA program (www.ebi.ac.uk) and Blast (http://www.ncbi.nlm.nih.gov/BLAST/). Sequence data were aligned using the CLUSTAL W program (www.ebi.ac.uk) (224). Neighbor-joining analysis (225) was performed with the CLUSTAL W program. Phylogenetic trees were visualized with Treeview software (226).

3.3.5. Assay for production of quorum sensing molecules AI-2

The presence of AI-2 secretion in cell-free culture of the *E.coli* strains, were analysed using *V. harveyi* BB170 reporter strain bioassay described by Surette and Bassler (128). *E.coli* cultures were grown to various growth phase in LB and LBG, at 30°C, and cell-free culture fluid was prepared by centrifugation at 14000 rpm for 5mins using a microcentrifuge. The clear culture fluid were passed through 0.22um Millex filter and stored at -20°C if used on the same day, or at -80°C if used after a day. *V. harveyi* BB170 was first grown for 16hr in AB medium, then 180µl of BB170 (diluted 1:5000 in fresh AB medium) was added to 20µl of cell-free culture

fluid. Changes in light production of BB170 as a result of presence of AI-2 were monitored using a GENios Multi-Detection Microplate Reader (Tecan, UK) in luminescence mode. Sterile LB was used as negative control and the experiment was carried out in quadruplicate. Readings were taken every hour.

3.4. Results and Discussion

3.4.1. Growth studies

The increase in cell number over time for *E.coli* AB1157, MG1655 and MG1655 *luxS*$^-$ grown in LB and LBG (i.e. LB supplemented with 0.5 w/v (%) glucose) are shown in Figure 3.1, 3.2 and 3.3 respectively. For all *E.coli* strains, the growth curves represent a typical growth curve under batch conditions with two clearly distinct phases i.e. exponential 2-8hr and onset of stationary phase after 8 hrs. For *E.coli* AB1157 the specific growth rate is 0.45h^{-1} for both LB and LBG. Similarly, the specific growth rate for *E.coli* MG1655 (0.34h^{-1}) and MG1655 *luxS*$^-$ (0.35h^{-1}) were the same in both LB and LBG. Also when comparing MG1655 wild-type and mutant, the ability to produce AI-2 did not have a marked effect on growth. The different between the specific growth rate of *E.coli* AB1157 and MG1655 may be due to strains difference.

The uptake of glucose for *E.coli* MG1655 under batch conditions, for 0.5 w/v (%) glucose, is also shown in Figure 3.2. Over 97% of the 0.5 w/v (%) glucose in the LBG media was taken up by the cells within the first 6hrs of growth, with no glucose remaining after 8 hours.

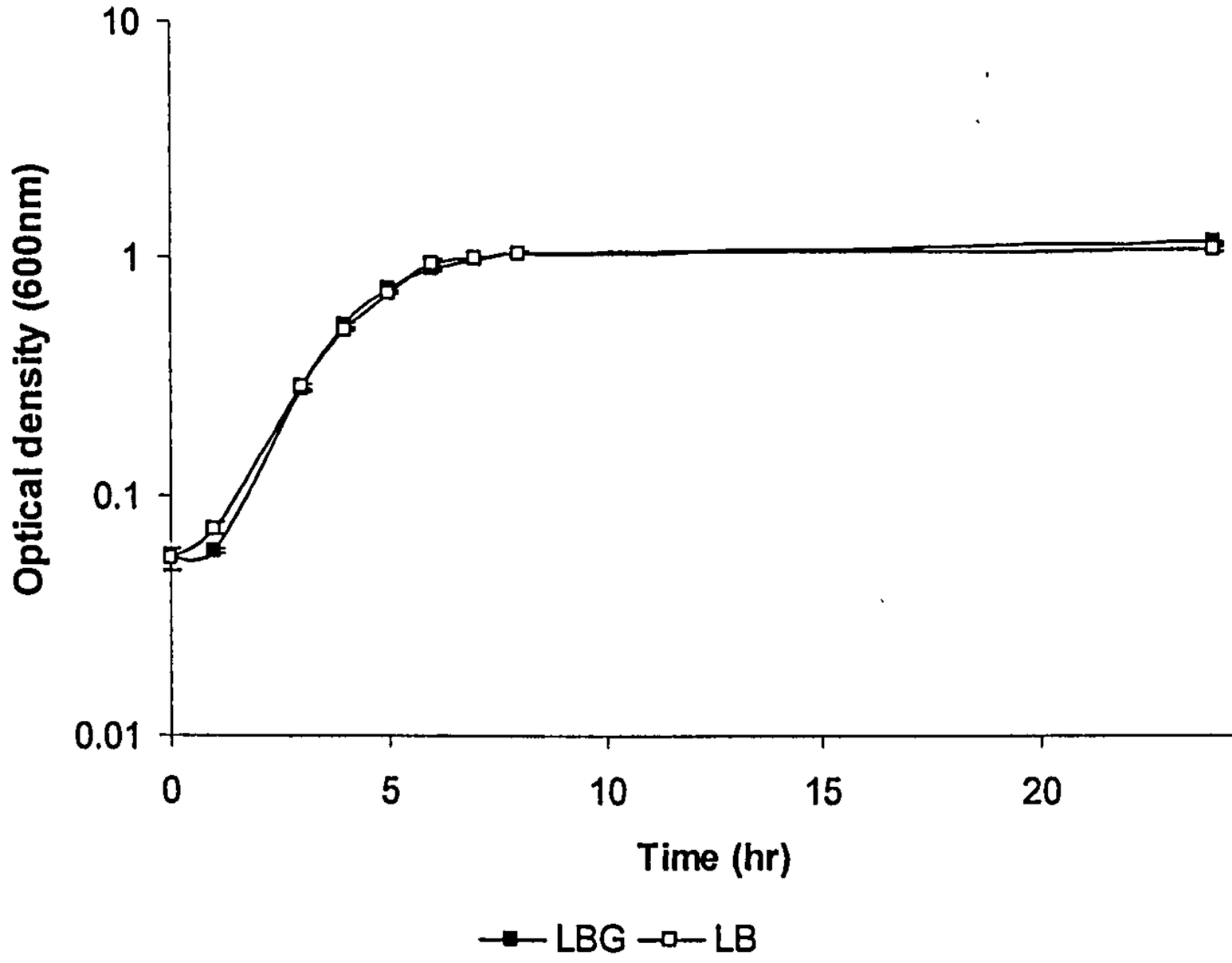

Figure 3.1 Batch growth curve of *E.coli* AB1157 in Luria-Bertani (LB) and Luria-Bertani supplemented with 0.5w/v (%) glucose at the beginning of the growth phase (LBG)

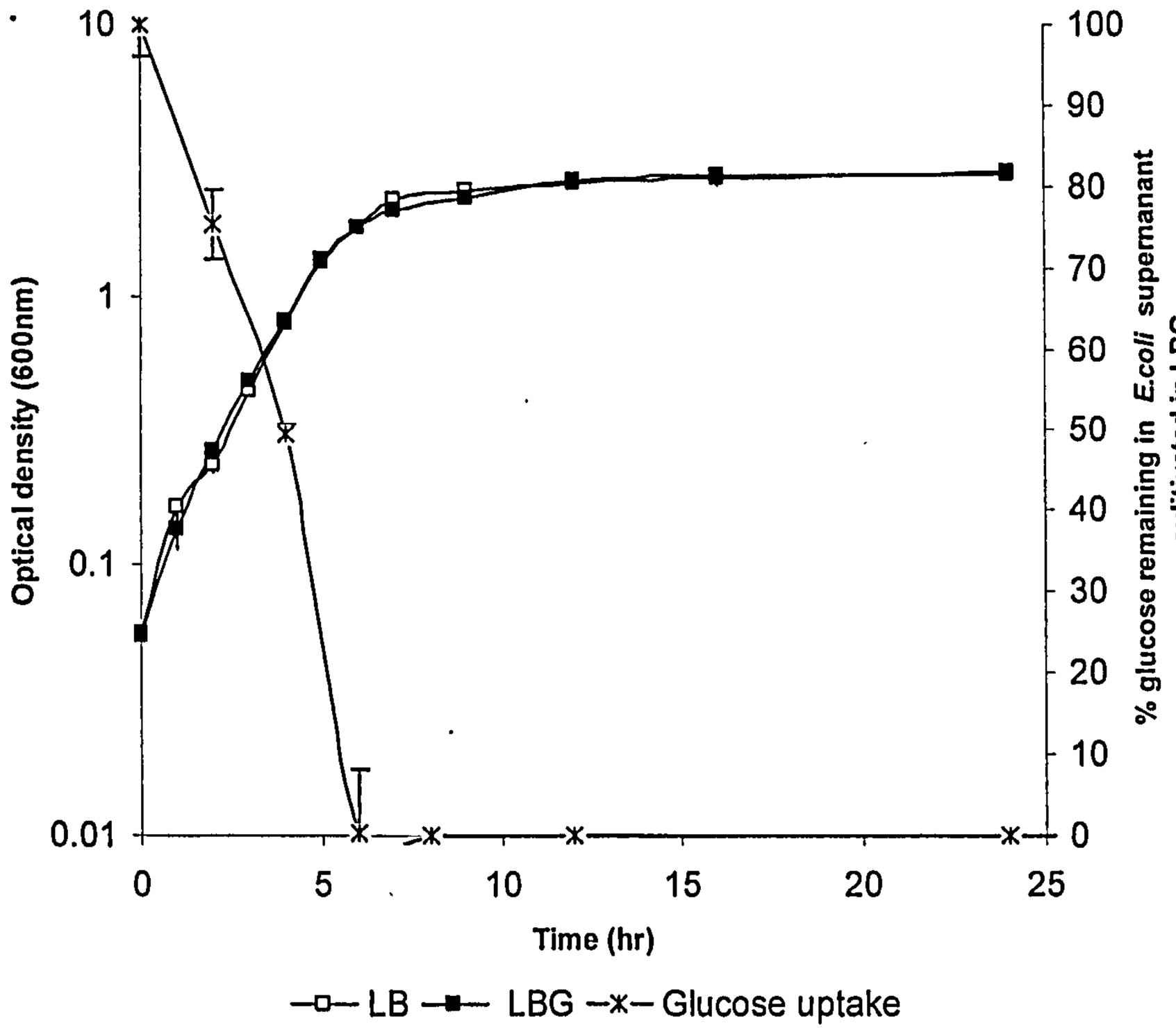

Figure 3.2 Batch growth curve of *E.coli* MG1655 in Luria-Bertani (LB) and Luria-Bertani supplemented with 0.5w/v (%) glucose at the beginning of the growth phase (LBG).

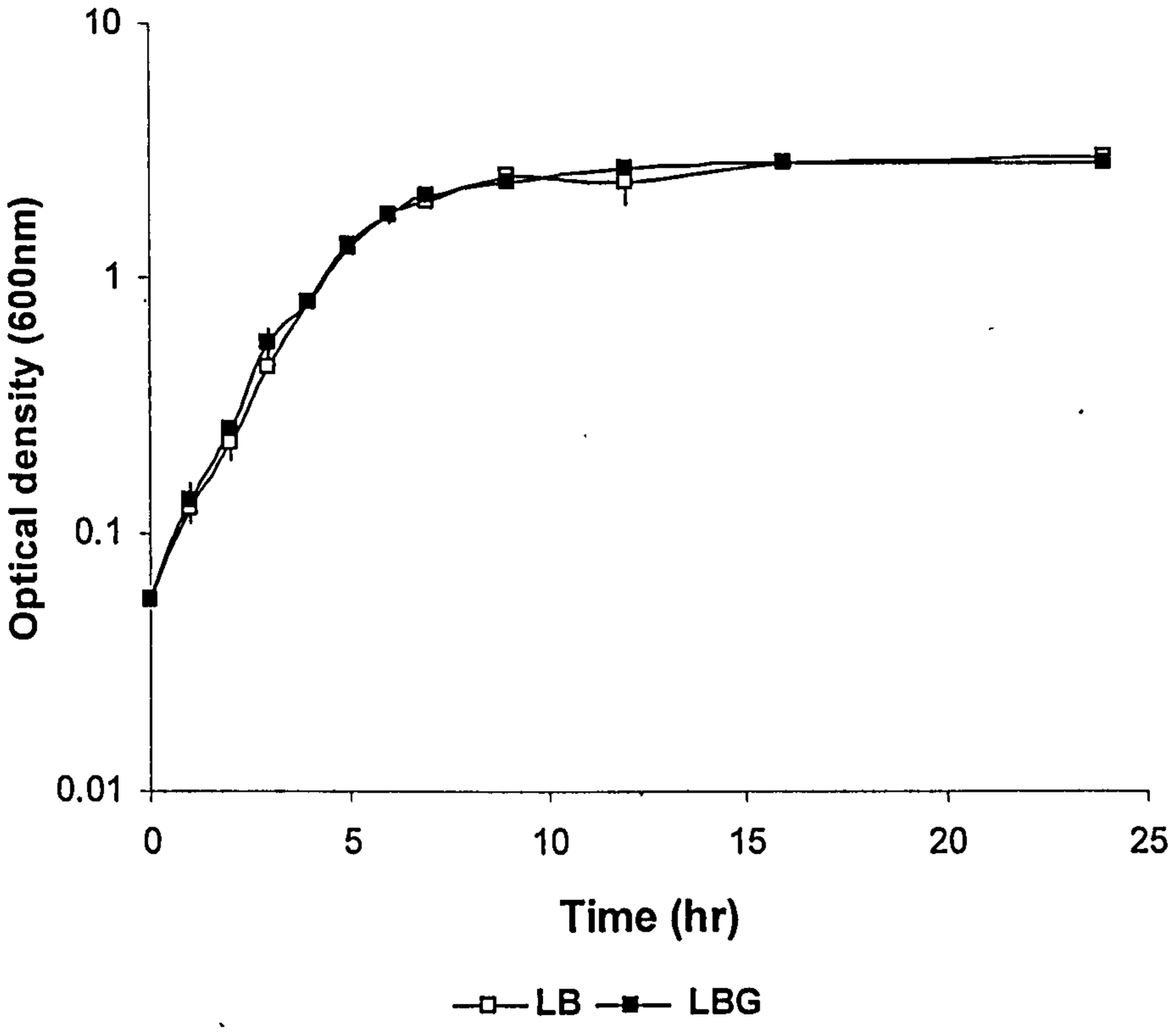

Figure 3.3 Batch growth curve of *E.coli* MG1655 *luxS*⁻ in Luria-Bertani (LB) and Luria-Bertani supplemented with 0.5w/v (%) glucose at the beginning of the growth phase (LBG).

3.4.2. Genetic studies of E.coli strains

The signal molecule for quorum sensing in *Escherichia coli*, AI-2 is produced by the *luxS* gene and has been found to be the universal signal molecule used in interspecies cell-to-cell communication (109, 227). PCR was used to confirm the presence or the absence of *luxS* gene in the *E.coli* strains. Figure 3.4 shows the of PCR products for *luxS* amplified from *E.coli* AB1157. The bands of PCR products amplified from *E.coli* MG1655 wild type and MG1655 *luxS*⁻ (in triplicates) are shown in Figure 3.5. The gels show that a fragment at approximately 500bp was amplified by the PCR reaction in *E.coli* AB1157 and MG1655 wild type (obtained from Lambda which has a ladder of known sizes). As expected, there was no band for the MG1655 mutant. No band was also detected for the negative control (Nucleic acid free water). The 500bp PCR product observed in amplification of *luxS* gene suggests that the gene was successfully amplified and the results were further confirmed by sequencing. The sequences were analysed using several

bioinformatics software such as Blast (http://www.ncbi.nlm.nih.gov/BLAST/), ClustalW and Fasta program (www.ebi.ac.uk).

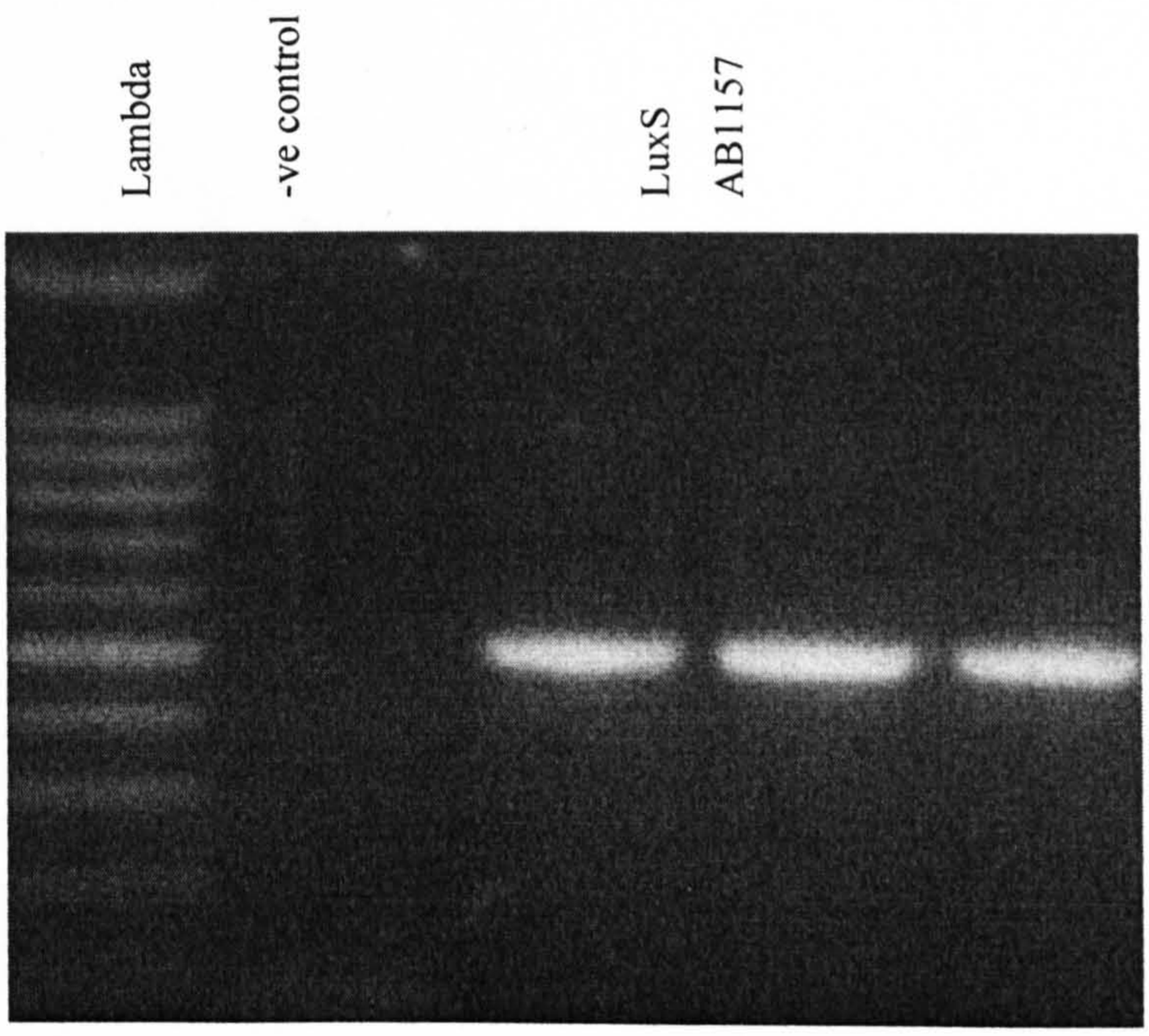

Figure 3.4 Agarose gel showing PCR products with 500bp fragment for *E.coli* AB1157

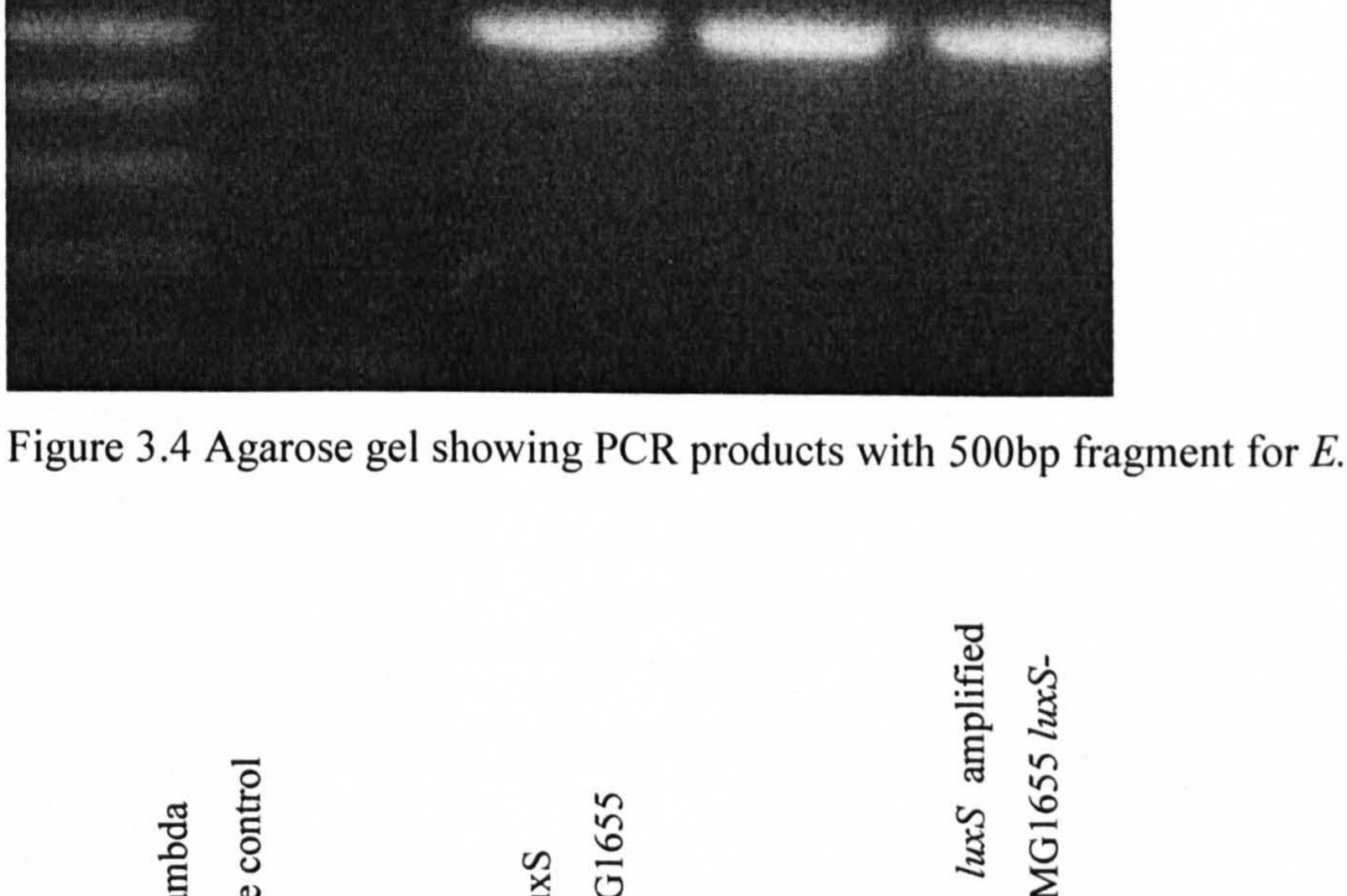

Figure 3.5 Agarose gel showing PCR products with 503bp fragment from *E.coli* MG1655 wild and *luxS*

The autoinducer gene, *luxS* for *E.coli* AB1157 has been submitted to the GenBank database under accession number AJ786260. Figure 3.6 shows a constructed phylogenetic tree based on the *luxS* gene for *E.coli* AB1157 and MG1655. From the phylogenetic tree, the *luxS* gene has over 99% similarities with other *E.coli* K-12 strains. The Autoinder-2-gene, *luxS* was also found to be approximately 90% related to *Salmonella* and about 80% related to *Vibrio harveyi*. These findings confirm the presence of quorum sensing properties in *E.coli* AB1157 and MG1655. Both *E.coli* AB1157 and MG1655 *luxS* gene were found to have the highest similarity with respect to other *E.coli* strains. The results from the phylogenetic tree also suggest an evolutionary link between *Escherichia coli*, *Salmonella spp*, and *Vibrio spp*.

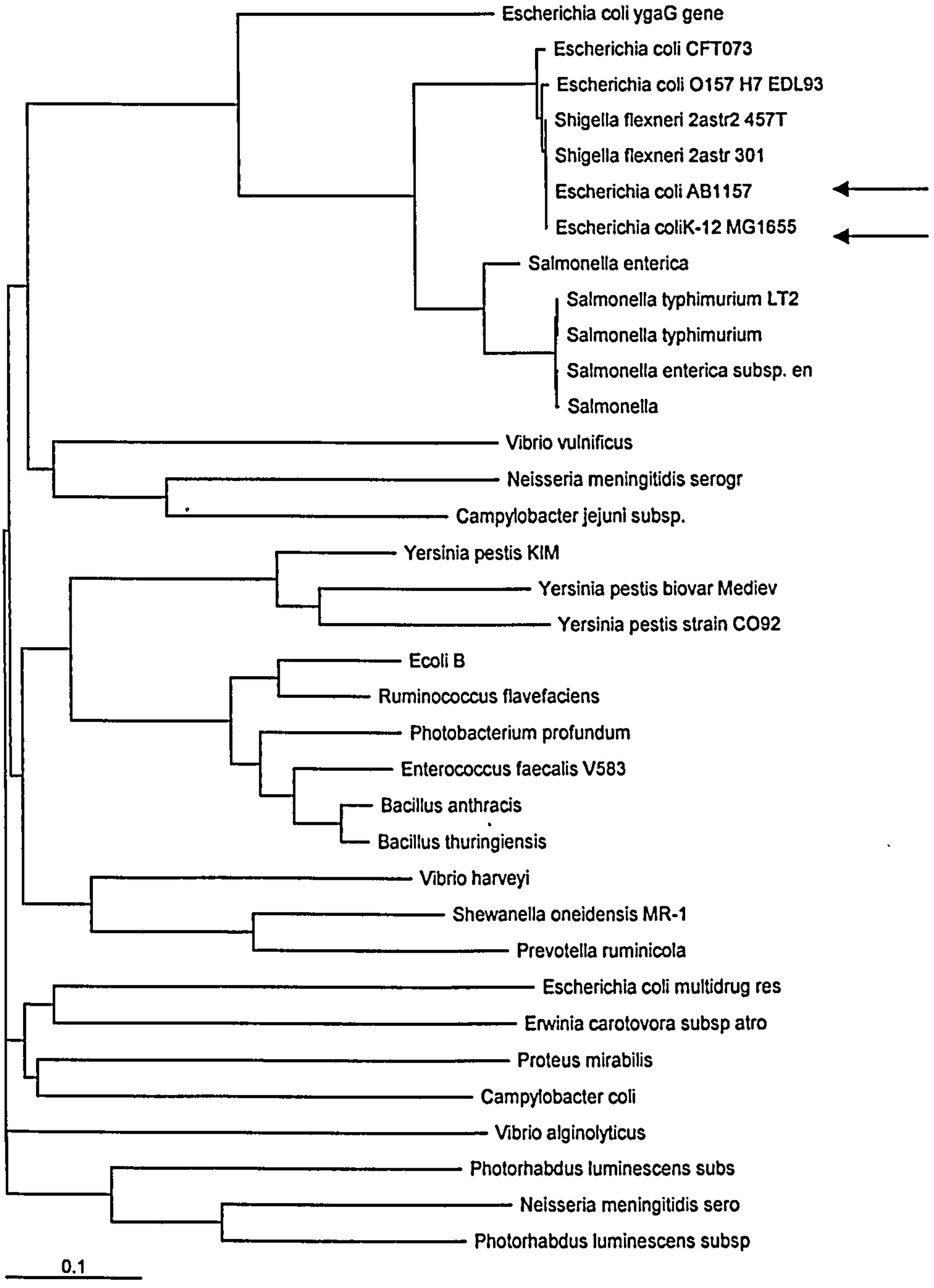

Figure 3.6 Phylogenetic tree of bacteria using *luxS* gene

3.4.3. Autoinduction in Escherichia coli (quorum sensing)

The bioluminescence produced by *Vibrio harveyi* (*V.harveyi*) BB170 during its growth cycle is presented in Figure 3.7. This is consistent with similar responses previously reported (129), with an initial decrease over the first 4 to 5 hours due to inoculation in fresh AB medium, followed by an increase in bioluminescence due to cell growth.

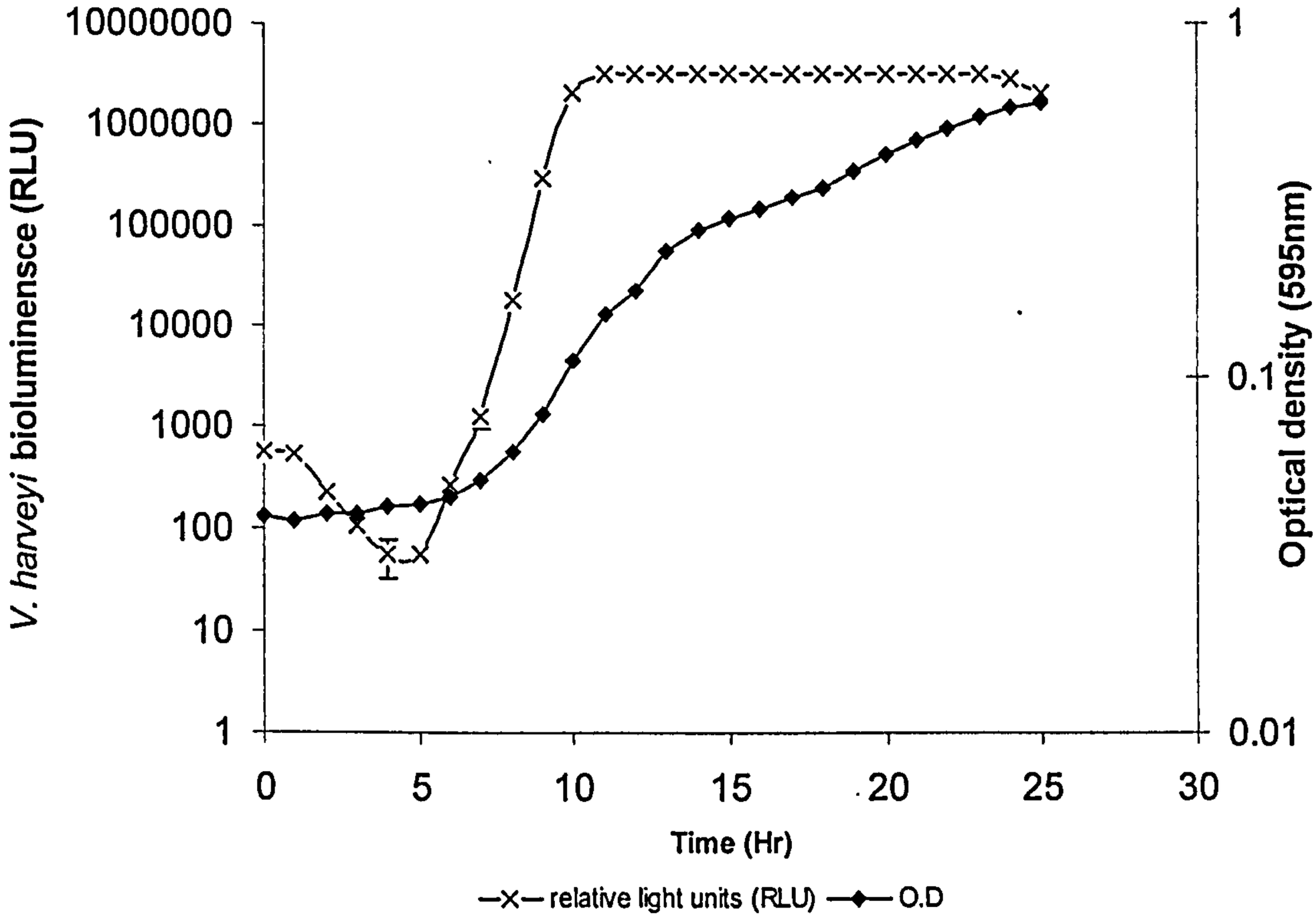

Figure 3.7 Batch growth curve and bioluminescence of *V. harveyi* BB170 at 1:5000 dilutions with AB medium

Figure 3.8 and Figure 3.9 show the fold induction of *E.coli* AB1157 cultivated in LB and LBG as measured during the bioassay respectively. The fold induction of the supernatant collected from *E.coli* MG1655 grown in LB and LBG is also shown in Figure 3.10 and Figure 3.11 respectively, as measured during the *V.harveyi* bioassay. The fold induction is calculated as the light production (measured as relative light units (RLU) of the *V.harveyi* after 4 hours, in cell free culture medium from *E.coli* samples (at different growth phases) divided by the RLU of the *V.harveyi* in LB medium only, again after 4 hours (128). The fold induction directly relates to the level of AI-2 present in the supernatant. The 500bp PCR product observed in amplification of *luxS* gene in *E.coli* AB1157 and MG1655 wild type also confirmed the presence of quorum sensing properties in this strain.

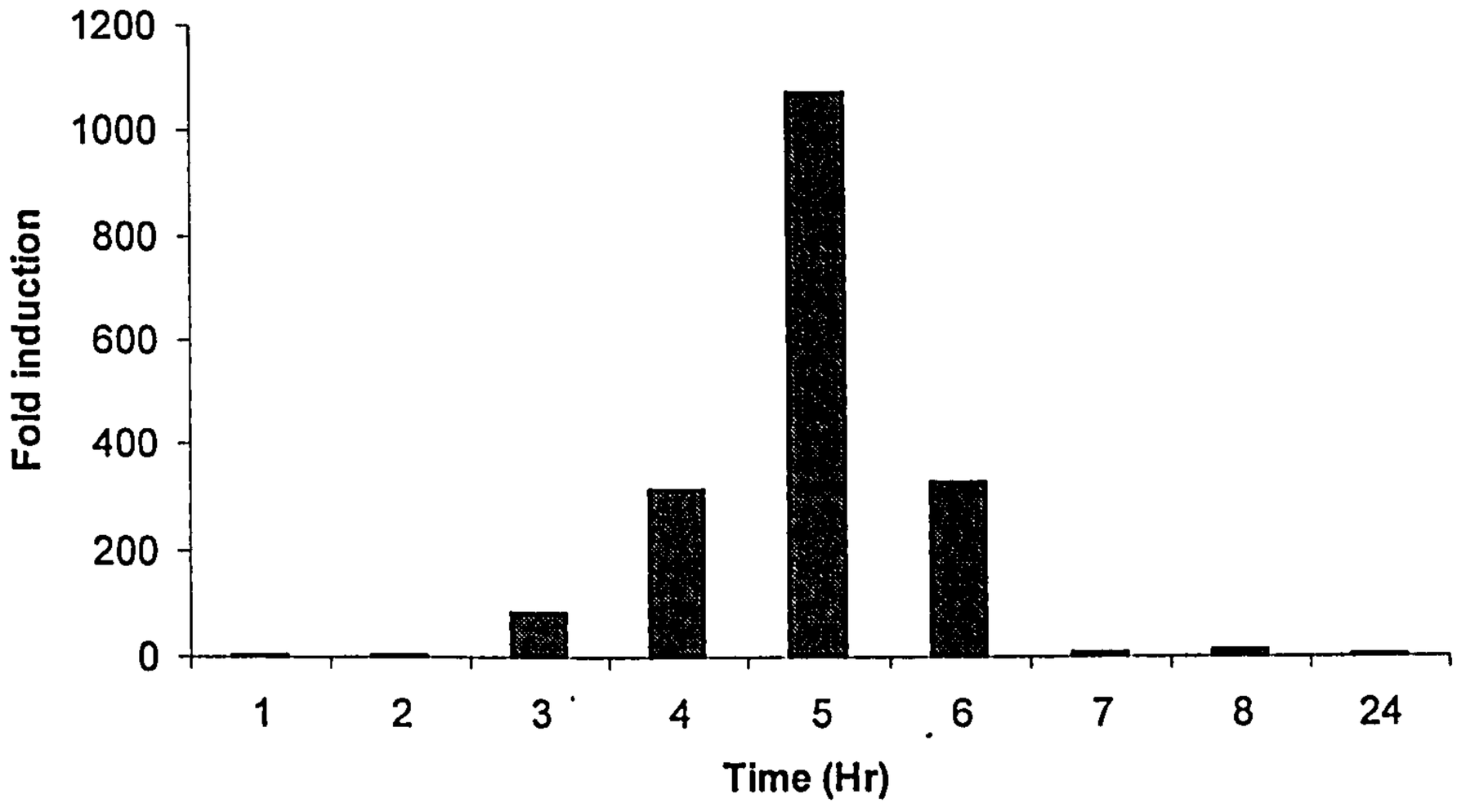

Figure 3.8 The responses of *V. harveyi* reporter strains BB170 (sensor 1-, sensor 2+) to signaling substances (AI-2) present in cell-free culture fluids from *E.coli* AB1157 cultivated in LB.

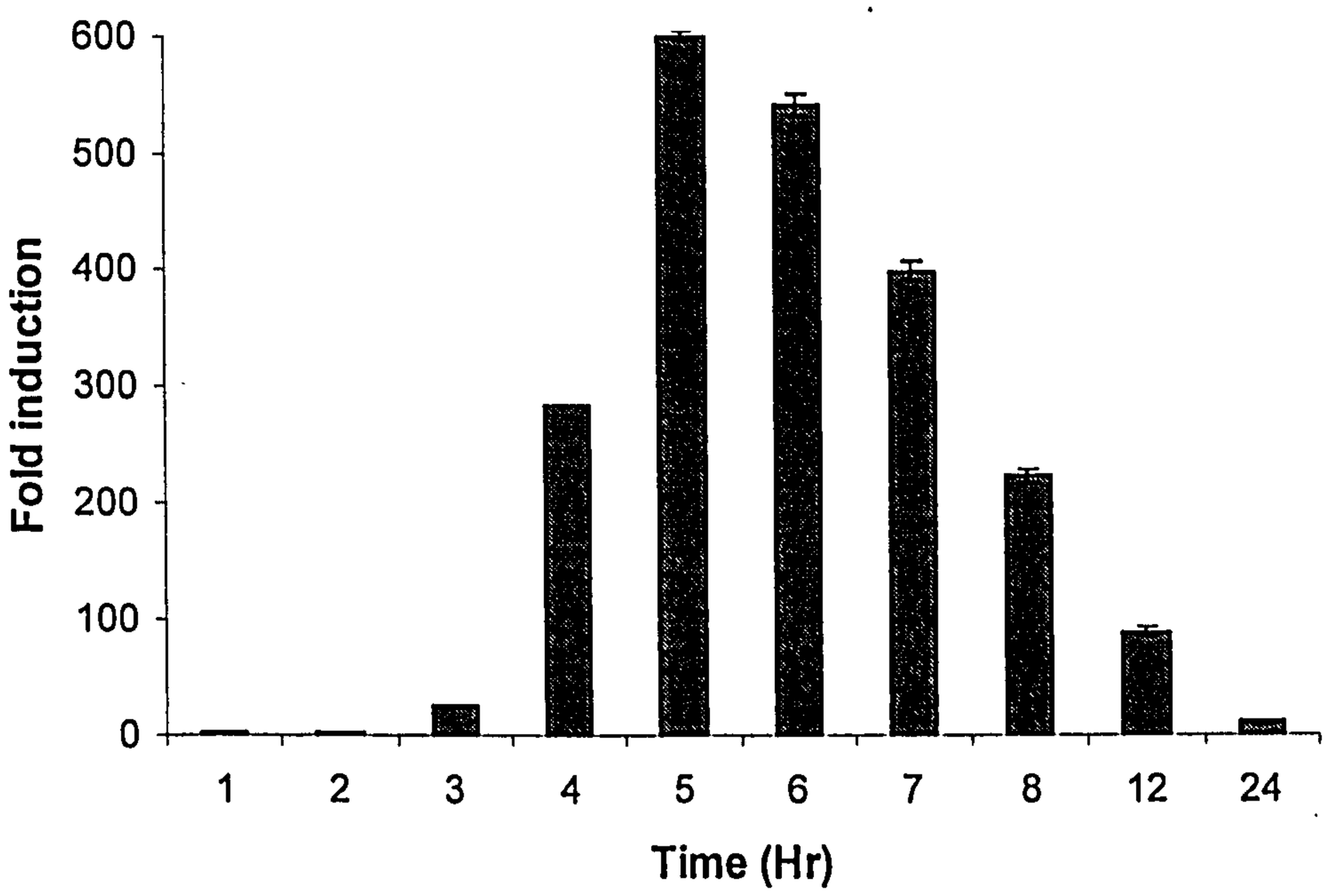

Figure 3.9 The responses of *V. harveyi* reporter strains BB170 (sensor 1-, sensor 2+) to signaling substances (AI-2) present in cell-free culture fluids from *E.coli* AB1157 cultivated in LB with addition of 0.5 w/v (%) glucose at the beginning of growth (LBG).

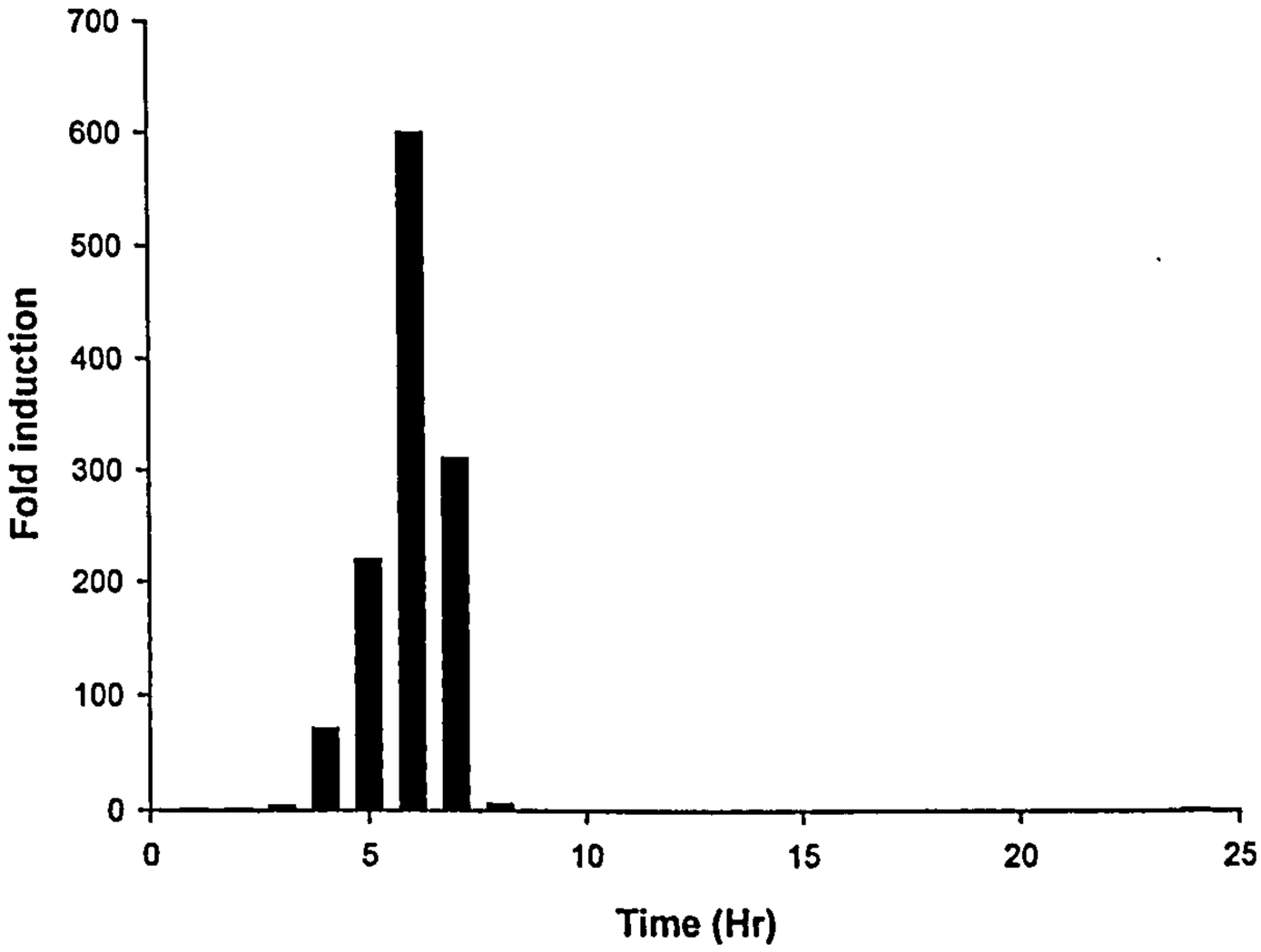

Figure 3.10 The responses of *V. harveyi* reporter strains BB170 (sensor 1-, sensor 2+) to signaling substances (AI-2) present in cell-free culture fluids from *E.coli* MG1655 wild type cultivated in LB.

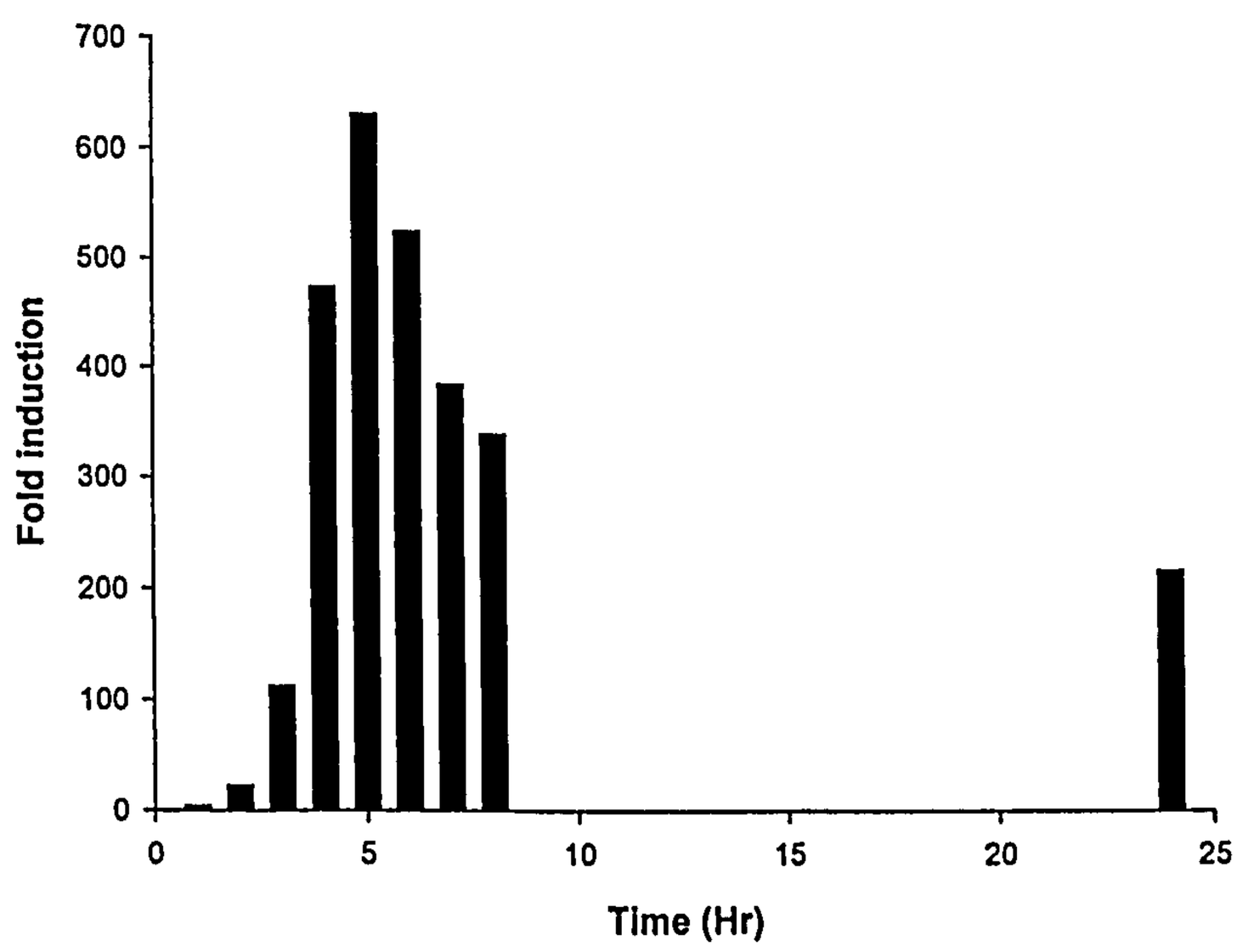

Figure 3.11 The responses of *V. harveyi* reporter strains BB170 (sensor 1-, sensor 2+) to signaling substances (AI-2) present in cell-free culture fluids from *E.coli* MG1655 wild type cultivated in LBG.

Based on Figure 3.8 and Figure 3.10, the fold induction reached a maximum in the mid exponential phase (6hrs) and sharply decreased at the onset of the stationary phase for *E.coli* AB1157 and MG1655 (wild type) when grown on LB. The level of extracellular AI-2 for *E.coli* AB1157 and MG1655 (wild type) grown in LBG, also reached a maximum during the exponential growth phase (6hr) however it still retained a high level of extracellular AI-2 during the stationary phase (24hr) (Figure 3.9 and Figure 3.11). The difference in fold induction in *E.coli* strains cultivated in LB and LBG is consistent with recent findings reporting that the addition of 0.5 w/v (%) glucose prevents the uptake of AI-2 into the cell, hence it accumulates in the supernatant (228). This is due to the fact that glucose decreases cyclic adenosine monophosphate (cAMP) concentration (130) in the cell due to catabolite repression. Once glucose is depleted, cAMP concentration increases and the lsr operon is activated by cAMP, and AI-2 is internalized by the cells (128). Hardie *et al* (221) revealed that glucose affects the amount of measurable AI-2 in cell harvested during stationary phase which is similar to Figure 3.9 and Figure 3.11.

No significant level of AI-2 was detected in the *E.coli* MG1655 *luxS*⁻ grown in LB supplemented with or without glucose using the bioassay. This was to be expected as no PCR product for the *E.coli* MG1655 *luxS*⁻ was found, thus confirming the absence of quorum sensing properties in the mutant strain.

3.5. Conclusion

Escherichia coli is a fast growing Gram negative bacterium and represents a good model for understanding bacterial aggregation since the genome has already been sequenced. Non pathogenic *E.coli* AB1157 and MG1655 (wild type and mutant) were the *E.coli* strains used in this study. Neither quorum sensing nor the addition of 0.5 w/v (%) glucose affected the growth pattern of any of the strains.

The quorum sensing molecule (AI-2) was identified in both *E.coli* AB1157 and MG1655. The signal molecule secretion was found to be dependent on growth phase and media. The addition of 0.5% glucose to LB media suppress the uptake of

the signal molecule by *E.coli*. The findings from this chapter will provide the foundation for future studies to understand aggregation as discussed in next chapters.

Chapter 4 Investigating the Role of Non-Adsorbing Polymers in Microbial Aggregation

(Published in part in Langmuir 2005, Vol. 21, pages 12315-12319)

4.1. Abstract

In non-biological colloids, the addition of a non-adsorbing polymer can cause an imbalance in the osmotic pressure leading to colloid aggregation, a process known as depletion interaction. The objective of this chapter is to determine if similar phenomena can occur in bacteria which may provide an explanation as to how extracellular polymers can contribute to bacterial aggregation.

Depletion aggregation studies were carried out using 0.5 to 2.5 w/v (%) *E.coli* AB1157 harvested at different growth phases, with varying concentrations of a non-adsorbing polymer, sodium polystyrene sulphonate (SPS). Aggregation of *E.coli* was found to be dependent not only on the concentration of SPS added, but also on the growth phase of *E.coli* AB1157. For a constant concentration of cells, more SPS was needed to aggregate cells harvested during the mid exponential phase, than cells harvested in the stationary phase.

The electrophoretic mobility of *E.coli* AB1157 at different growth phases was determined using phase amplitude light scattering. *E.coli* AB1157 was found to be negatively charged and the cell surface properties changed at different growth phases. The electrokinetic results correlated well with the different concentrations of non-adsorbing polymer needed to induce depletion aggregation. This shows that the difference in aggregation properties is due to changes in the bacterial electrokinetic properties during their growth.

4.2. Introduction

Bacterial aggregation is the cell-to-cell adhesion of bacterial species or strains in order to perform a specialized function during certain physiological conditions (7). When aggregated, bacteria are able to communicate between themselves and uniformly perform metabolic functions, which are greater than their planktonic counterparts (1).

Like inert colloids, bacteria can also display pair-wise interactions when in close proximity. This interaction is governed by the surface chemistry of the bacterial surface (some van der Waals forces but mainly electrostatic forces due to the ionic groups on the cell surface) and not surprisingly, as discussed in Chapter 2, their surface properties have been shown to play a significant role in bacterial aggregation (29, 30, 52, 163, 167, 187, 188, 229-231). The electrostatic repulsive potential plays a major role in determining the stability of the cells. In addition, other factors, such as the presence of extracellular polymeric substances (EPS), produced by the bacteria, may affect dispersion stability.

Quantification of the surface electrokinetic properties of bacteria appears to be more difficult to determine in comparison with non-biological colloids as a result of the chemical and structural complexity of bacterial cell surfaces. A well known method for measuring surface electric potentials is the measurement of electrophoretic mobility to obtain the Zeta potential (30, 78, 145, 178, 179). As detailed in Chapter 2, the Zeta potential is usually calculated from the electrophoretic mobility (21). However, this calculation, based on Smoluchowski's formula (Equation 2.7), is not suitable for bacteria due to their surface complexity and non-spherical shape. Despite the advances in Smoluchowski's approach, for example Ohshima's soft-particle electrophoresis theory (181-184), to avoid the application of assumption about the particles shape in this chapter and beyond, the overall surface charge will be reported as electrophoretic mobility only, with no conversion to Zeta potential.

Extracellular polymeric substances (EPS) produced by bacteria have also been shown to be involved in biological aggregation (32, 38, 96, 101, 180, 232, 233). Extracellular polymeric substances (EPS) are biopolymers produced by microorgansims during their growth. The highest production of EPS occurs at the onset of the stationary phase (234, 235). EPS contains polysaccharides, proteins, nucleic acid, lipids and other biological polymers such as humic substances (33). Although, EPS have been shown to keep microbial aggregates together by providing a cohesive force (95-97), its role in aggregation still remains unclear. A detailed knowledge of the bacterial surface electrokinetic properties and the precise role of EPS are still outstanding in an effort to understand bacterial aggregation.

A potential role of EPS in aggregation could be to promote interaction via depletion attraction. From a physical point of view, bacteria can be considered to be a dispersion of colloids surrounded by non-adsorbing polyelectrolyte, EPS. Bacteria are negatively charged (30, 145) and a repulsive bacteria-EPS interaction results in an attractive interaction between bacterial cells commonly referred to as the depletion attraction (48, 49). It is generally accepted that aggregation occurs in a suspension of colloids and non-adsorbing polymers as a result of this depletion interaction (236-238). The role of non-adsorbing polymer in inducing aggregation can be dated as far back as Traube (239), where he was able to demonstrate that the addition of a water soluble polymer to natural rubber resulted in a phase separation. However it was not until 1954, that a satisfactory explanation of this depletion interaction was given by Asakura and Oosawa (48, 49). They postulated that phase separation in a mixture of colloids and non-adsorbing polymers is due to an imbalance in osmotic pressure when the non-adsorbing polymers are excluded from the region between particles. As the particles are drawn closer, the distance between the particles becomes less than the effective diameter of the non-adsorbing polymers. The non-adsorbing polymers are unable to penetrate this region and pushing the particles together leads to an increase in configurational entropy of the system. This leads to an effective attraction between each particle known as the depletion interaction. Vrij (240), developed a model for estimating the depletion attraction potential between two hard spherical particles induced by non-adsorbing polymers. Vincent and co-workers (241), later developed a method

to analyze the depletion interaction of soft spheres (colloids with a layer of adsorbed polymer chains). They analysed this interaction by taking into account the penetration and compression effects between the non-adsorbing polymer and the steric layer on the particles.

Recent developments in colloid science, such as atomic force microscopy (AFM), have allowed the direct measurement of depletion and structural forces (242-246). Milling and Biggs (243), analyzed the depletion forces between silica surfaces and free neutral polymer (poly (dimethylsiloxane)) (243). Yan *et al.* (246), studied the structure and strength of aggregates from latex particles induced by addition of poly(acrylic) acid. Their findings revealed that the concentration of poly (acrylic) acid affects the structural denseness and strength of latex aggregates.

Several non-adsorbing EPS have been shown to induce depletion attractions in oil-in-water emulsions (247) and in dispersions of casein micelles (248, 249). Tuinier *et al.* (249), studied the depletion attraction in a mixture of casein micelles from skim milk and extracellular polysaccharides produced by lactic acid bacteria; *Lactococcus lactis* subsp. cremoris strain NIZO B40. They analysed the depletion attraction between the casein micelles in the presence of polymers using Vrij's depletion model (240). Their findings reveal that upon addition of EPS to casein micelles, depletion attraction occurred. Similarly, phase separation was also found in casein and amylopectin mixtures which was analysed on the basis of Vrij's depletion theory (250).

The laws, kinetics and mechanism of depletion aggregation of inert colloids have been described in the literature (245, 251, 252). However, depletion of non-adsorbing polymer as a mechanism for aggregation in bacterial suspensions has not been well exploited. Only a handful of studies are available on the subject. Therefore, in this study, we seek to understand the role of non-adsorbing polymers, in aggregation of *Escherichia coli* AB1157 as a possible mechanism for understanding the role of EPS.

4.3. Materials and Methods

All chemicals were purchased from Sigma-Aldrich (Gillingham, Dorset, UK) unless otherwise stated. All experiments were conducted in triplicate (at least), and the average of the results reported. Variation in the experimental results is presented as the average ± standard deviation

4.3.1. Bacterial strains and culture conditions

Non-pathogenic, freeze dried *Escherichia coli* (*E.coli*) AB1157 (DSM number 9036) was purchased from Deutsche Sammlung von Mikroorganismen und Zellkulturen GmbH (DSMZ) and re-suspended in Luria-Bertani (LB) media (tryptone 10.0g/L, yeast extract 5.0g/L, NaCl 10.0g/L, adjusted to pH 7.0). *E.coli* was grown at 30°C overnight with aeration in LB broth supplemented with 0.5 w/v (%) glucose at the beginning of the growth phase (LBG). The culture was then used to inoculate fresh LB broth containing 0.5 w/v (%) glucose at a 1:100 dilution and grown at 30°C with aeration. *E.coli* cells were sampled in triplicate at intervals between 0 and 24 hours and harvested by centrifugation at 5000g for 10 minutes. The cell pellets were used in the following experiments.

4.3.2. Electrophoretic mobility measurement

Electrophoretic mobility (EPM) was measured using a phase amplitude light scattering (PALS) zeta potential analyzer (Brookhaven Zeta PALS, U.K) following the technique described by deKerchove and Elimelech (253) and Eboigbodin *et al.* (63). The Brookhaven Zeta PALS instrument employs Phase Analysis Light Scattering (PALS) to determine electrophoretic mobility of charged bacterial cell surfaces. The technique differs from convectional method for measuring EPM such as Laser Doppler Velocimetry (254), as it measures phase changes in frequency spectrum rather than Doppler shift of the frequency. Hence only a slight movement of bacterial cells is required to obtain accurate results, thereby allowing low electrophoretic measurements to be obtained, even as low a 10^{-9} $m^2/V{\cdot}s$. In all cases, the electrophoretic mobility, rather than the Zeta potential is quoted as this gives an unbiased record of the mobility of the cell without assuming a known shape.

Cells were sampled in triplicate at intervals between 0 and 24 hours growth in LB and LBG and harvested by centrifugation at 5000g for 10 minutes. After harvesting, the cell pellets were washed by re-suspending in distilled water followed by centrifugation at 5000g for 10 minutes. This washing step was repeated four times to eliminate residual substrates and extracellular polymers, which were produced by *E.coli* AB1157 during growth. The washed cell suspensions were then dispersed in an ultrasonic bath prior to measurement. Measurements were conducted using an electric field of 2.5Vcm^{-1} at a frequency of 2.0 Hz. The reported values for each EPM represents the average of 10 successive runs carried out in triplicate readings using the Zeta PALS. A typical measurement from the Zeta PALS is shown in Appendix A.

4.3.3. Depletion aggregation measurement

For the depletion aggregation measurements, the cells were harvested at different growth phases; 3.5 hr (early exponential phase), 6 hr (mid- exponential phase), 8 hr (late-exponential phase) 14 hr, 18 hr and 24 hr (stationary phase). The pellet was washed three times and re-suspended in distilled water. This removed loosely bound EPS. Different concentrations of non-adsorbing polymer sodium polystyrene sulphonate (Acros Organics, USA; Average molecular weight 70,000) were added into cuvettes containing 0.5 to 2.5 w/v (%) of *E.coli* AB1157. The cuvettes were visually inspected after 24 hours to determine if the solutions were stable (i.e. no aggregation) or unstable (i.e. aggregation and settling of solution). An aggregation assay was also carried out according to Shen *et al.* (60) which is similar to visual inspection method. The optical density (O.D) of cuvettes containing mixture of cells and SPS (same as visual inspection method) were measured over time. O.D corresponding to the suspension at the upper part of the cuvette was measured, and percentage aggregation was calculated on the difference in OD_{600} readings taken at time 0 to 24hr (Equation 4.1).

$$\%Depletion\ \ aggregation = \frac{OD_o - OD_{24hr}}{OD_o} \times 100 \qquad \text{Equation 4.1}$$

Where OD_0 is the optical density at 600nm of *E.coli* AB1157 immediately after adding the polymer and OD_{24} is the optical density after 24 hours. The percentage aggregation was determined for *E.coli* AB1157 harvested at different growth phases.

4.4. Results and Discussion

The increase in cells over time for *E.coli* AB1157, cultivated in LBG has already been described in Chapter 3 and can be seen in Figure 3.1.

Figure 4.1 shows the effect of the addition of a non-adsorbing polymer sodium polystyrene sulphonate (SPS), to a constant concentration of *E.coli* AB1157 (2.0 w/v (%)), that were harvested during the stationary phase.

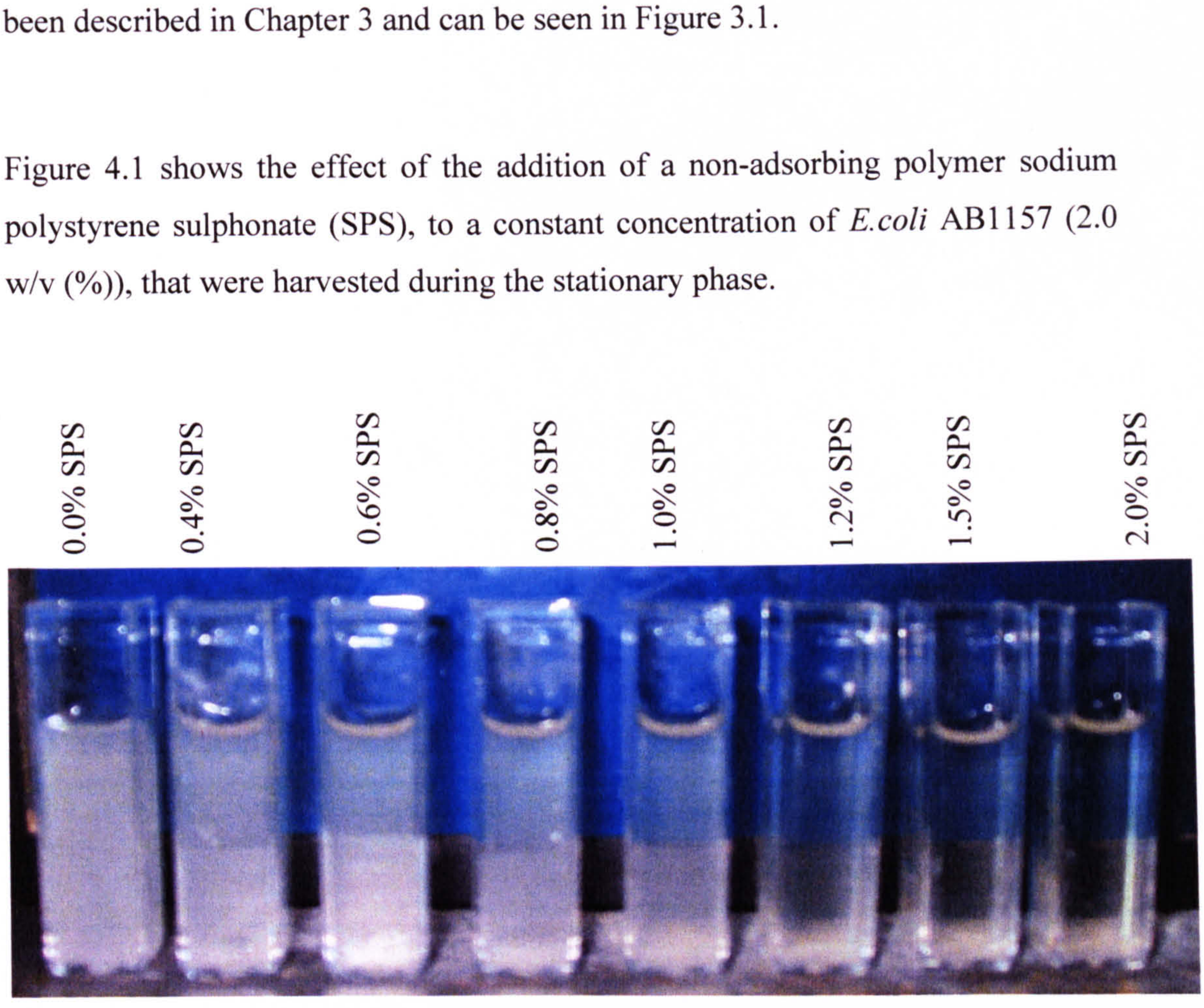

Figure 4.1 Visual inspection of constant *E.coli* AB1157 concentration (2.0 w/v (%) solution) harvested at late stationary phase (24 hr) with 0.0-2.0 w/v (%) sodium polystyrene sulphonate (SPS), after 24hr of SPS addition. Picture clearly shows the difference between stable (un-aggregated (ii-v)) and unstable (aggregated (vi-viii)) solutions. Blank SPS solution in cuvette (i) shows a suspension of *E.coli* in water. The

remaining solutions (cuvettes ii-viii) becoming increasingly clear with increase in SPS due to aggregation and settling of cells at the bottom of the cuvette.

With the addition of no SPS, (Figure 4.1 (i)) the 2.0 w/v (%) *E.coli* solution is turbid and represents a stable (un aggregated) solution. However, the addition of 2.0w/v (%) SPS to the *E.coli* solution, (Figure 4.1(viii)) results in a clear solution with the *E.coli* settled on the bottom of the cuvette. This represents an unstable (aggregated) solution. Therefore from Figure 4.1 it can be seen that as the concentration of SPS increases (from 0 - 2.0w/v (%)) the upper part of the cuvette becomes clearer and the lower phase becomes very turbid. That is, the solution becomes unstable and the *E.coli* settles to the bottom of the cuvette. A sharp interface is evident, which is characteristic of phase separation. The upper phase is rich with SPS while the lower is *E.coli*-rich. The time it takes for phase separation to occur is dependent on the concentration of SPS used. Phase separation is observed after 4-6hrs in a suspension of 2.0w/v (%) *E.coli* and 1.2-2.0 w/v (%) SPS. When a lower concentration of SPS is used, phase separation occurs after approximately 16hrs. However, in irrespective of the amount of SPS used, each phase remains constant after 24hrs. We also investigated whether depletion stabilization reoccurred in an *E.coli* suspension containing higher concentration of SPS, as previously reported for inert colloidal system (255). However, this was not observed for our *E.coli* suspension containing up to 10.0 w/v (%) SPS. The observation is a distinct difference between inert and biological colloids.

Another way of representing the results in Figure 4.1 is shown in Figure 4.2. In this case, the stability of the suspensions of varying concentrations of *E.coli* is determined for different concentrations of SPS. In each case, the cells are harvested during the stationary growth phase. The circles represent a stable solution i.e. no aggregation, while the diamonds indicate an unstable solution, i.e. aggregation. The bold line indicates the progression from stable to unstable solution. From Figure 4.2 it is evident that the degree of depletion aggregation is dependent on the concentration of the non-adsorbing polymers used.

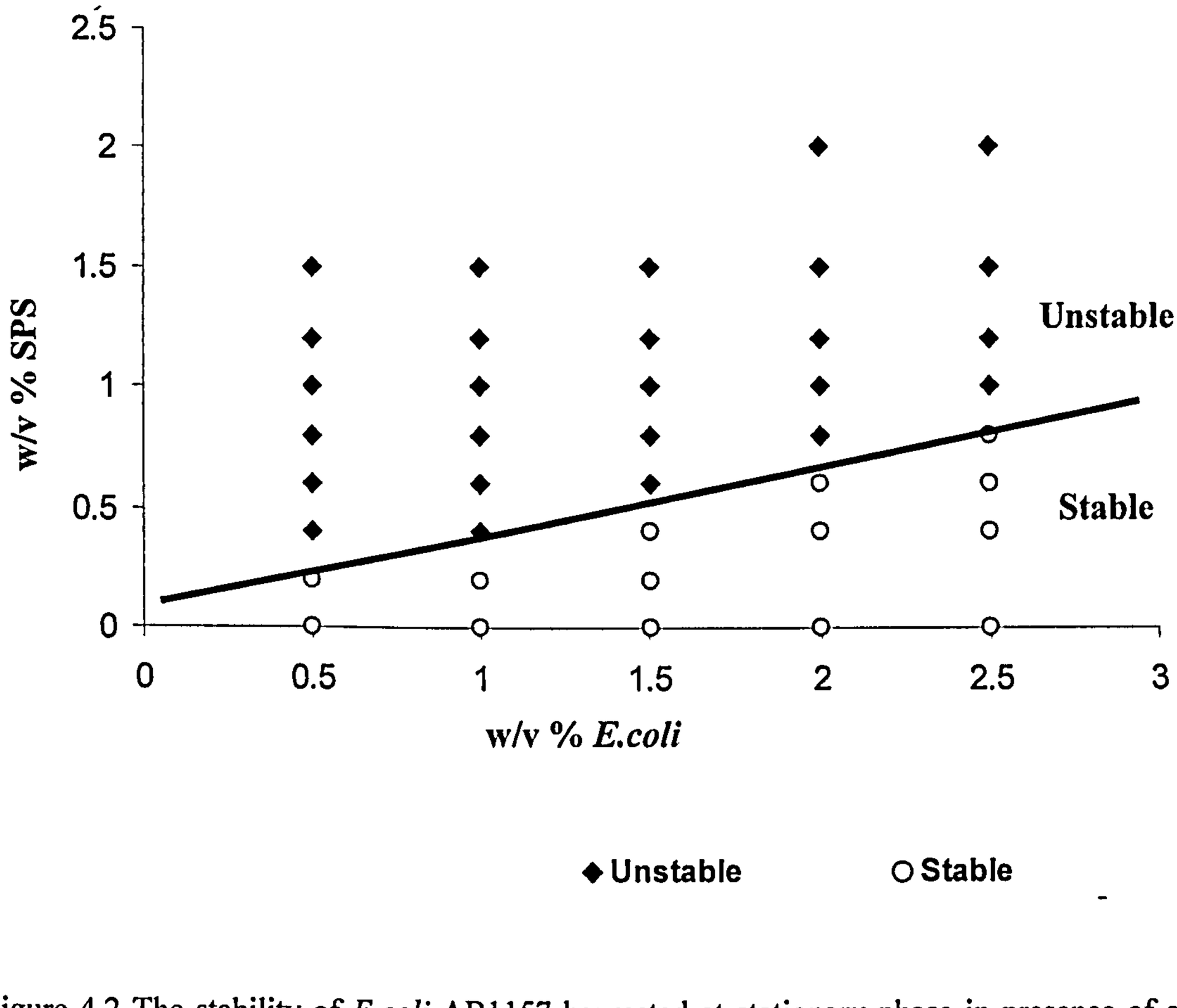

Figure 4.2 The stability of *E.coli* AB1157 harvested at stationary phase in presence of a non–absorbing polymer, Sodium polystyrene sulphonate (SPS). Stable means non-aggregating and unstable means aggregating

The same experiment was repeated for cells harvested at different growth phases to investigate the possible biological interactions that may influence the observed results. The progression line between stable and unstable solution at different growth phases (similar to Figure 4.2) can be seen in Figure 4.3. These results reveal that different amounts of polymer are needed for a constant w/v (%) of *E.coli* to induce aggregation of cells harvested at different growth phases. The least amount of polymer is required for cells harvested during the stationary phase, whilst as the cells move from early to late exponential growth phase, an increase in polymer is needed to create an unstable (i.e. aggregation) solution. Therefore, phase separation due to depletion interaction is dependent on the growth phase of the cells.

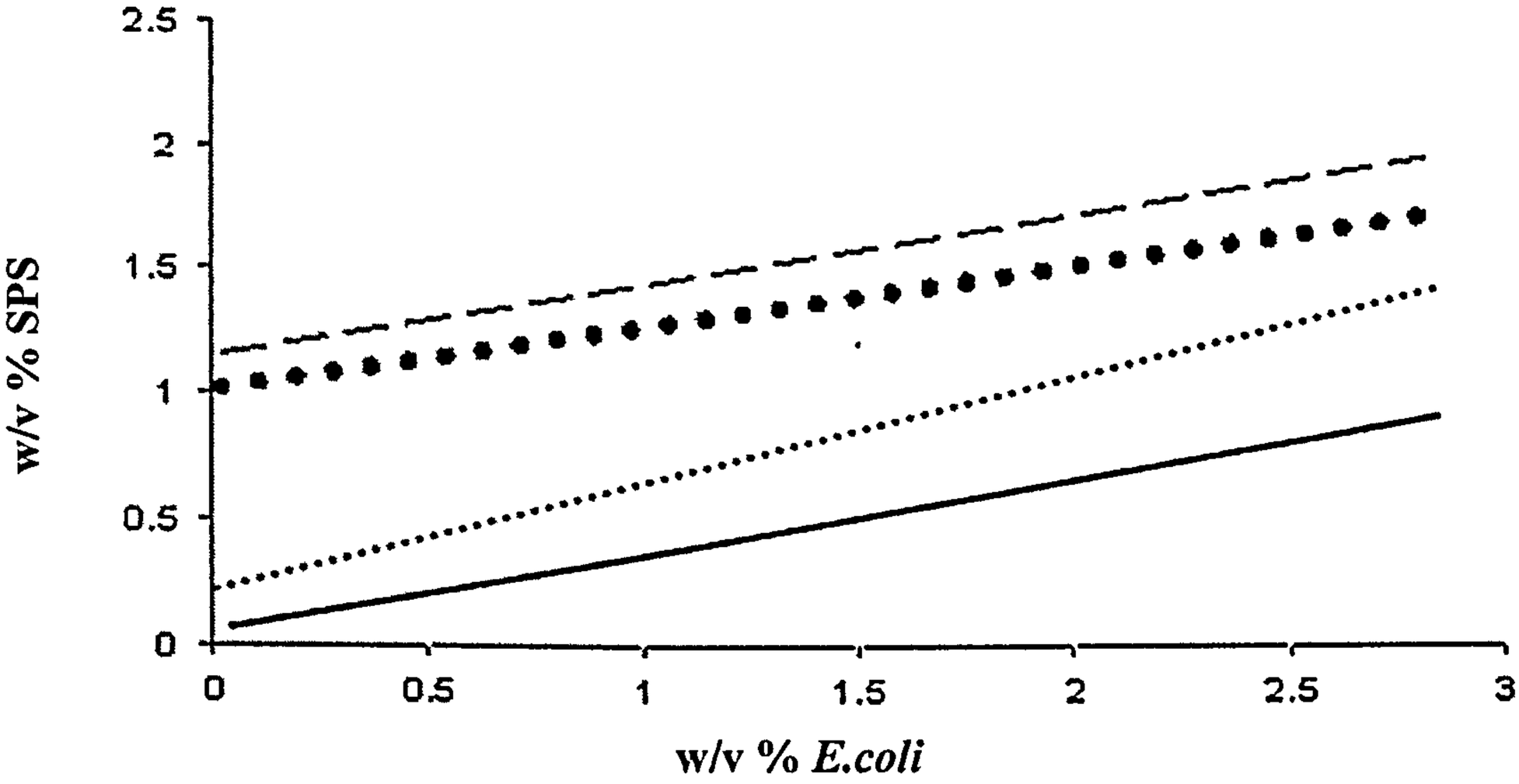

Figure 4.3 The progression from stable to unstable solutions for *E.coli* AB1157 harvested at different growth phases in the presence of a non–absorbing polymer, Sodium polystyrene sulphonate (SPS)

Similarly, as shown in Figure 4.4, the percentage of cells that have aggregated is also dependent on the growth phase of the cells. Figure 4.4 shows the percentage aggregation of *E.coli* at one concentration (i.e. 2w/v (%)) with varying concentrations of SPS. Again, the highest percentage of aggregation occurs for cells harvested during the stationary phase for a constant SPS concentration. These results were also conducted for different concentrations of *E.coli* (0.5 to 2.5 w/v (%)) with the same trend observed, i.e. greater aggregation during the stationary growth phase than the exponential growth phase.

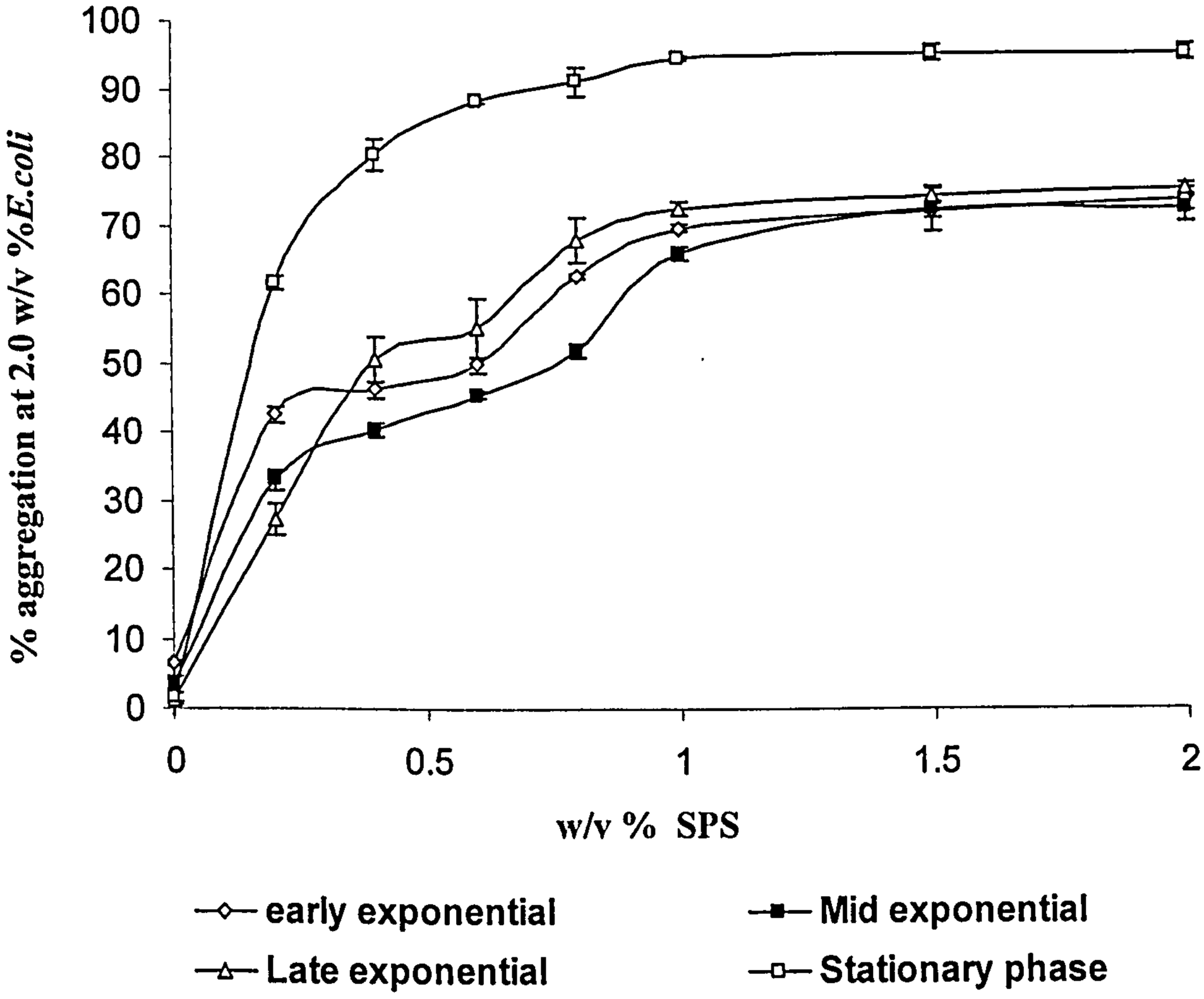

Figure 4.4 Percentage aggregation of 2.0 w/v (%) *E.coli* harvested at different growth phases with varying concentrations of the non-adsorbing polymer sodium polystyrene sulphonate (SPS).

To the authors' knowledge, this is the first time that a colloidal phenomena, such as depletion aggregation, has been shown to be influenced by the cell's growth phase. To investigate this further, Figure 4.5 shows the percentage aggregation at different growth phases, for a constant concentration of *E.coli* AB1157 (2.0 w/v (%)), and a constant concentration of SPS (0.2 w/v (%)). The most marked increase in percentage aggregation occurs during the stationary growth phase (at 18 hours), which supports the results in Figure 4.4. Similar trends were also found for different concentrations of *E.coli* and SPS.

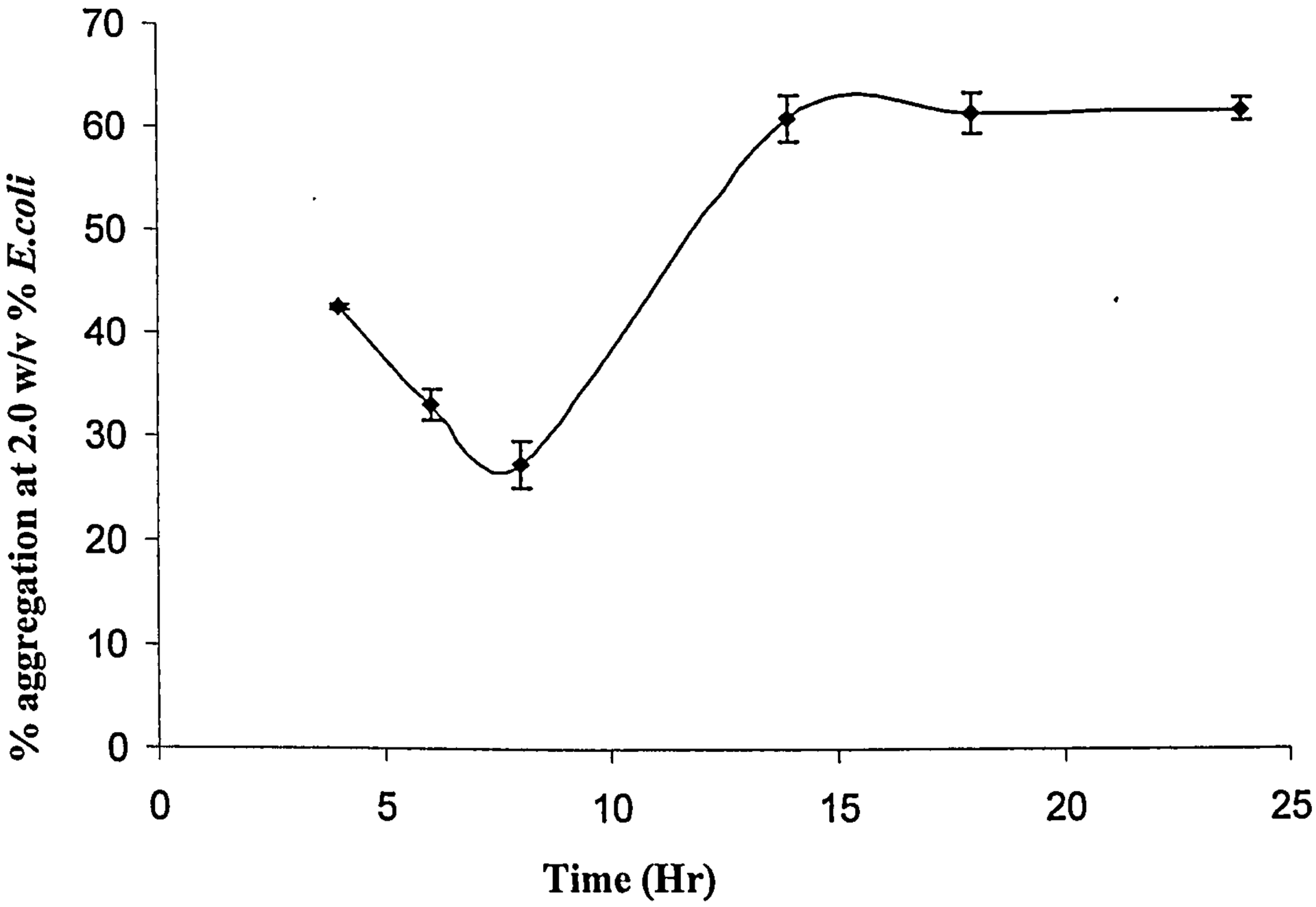

Figure 4.5 Percentage aggregation of *E.coli* AB1157 harvested at different growth phases cultivated in LB supplemented with 0.5 w/v (%) glucose (LBG) with the addition of 0.2 w/v (%) of the non-adsorbing polymer sodium polystyrene sulphonate (SPS).

Based on the results thus far, it is evident that the growth phase of *E.coli* has a significant effect on the percentage aggregation and the amount of polymer necessary to induce this aggregation. Therefore a characteristic of the *E.coli* is changing during the growth phase in order to elicit this response. Figure 4.6 shows the electrophoretic mobility of *E.coli* AB1157 measured using the PALS Zeta potential analyzer (Brookhaven Zeta PALS, U.K) at different growth phases. The *E.coli* AB1157 displays a negative electrophoretic motility value throughout the growth period, suggesting that the cell surface is negatively charged.

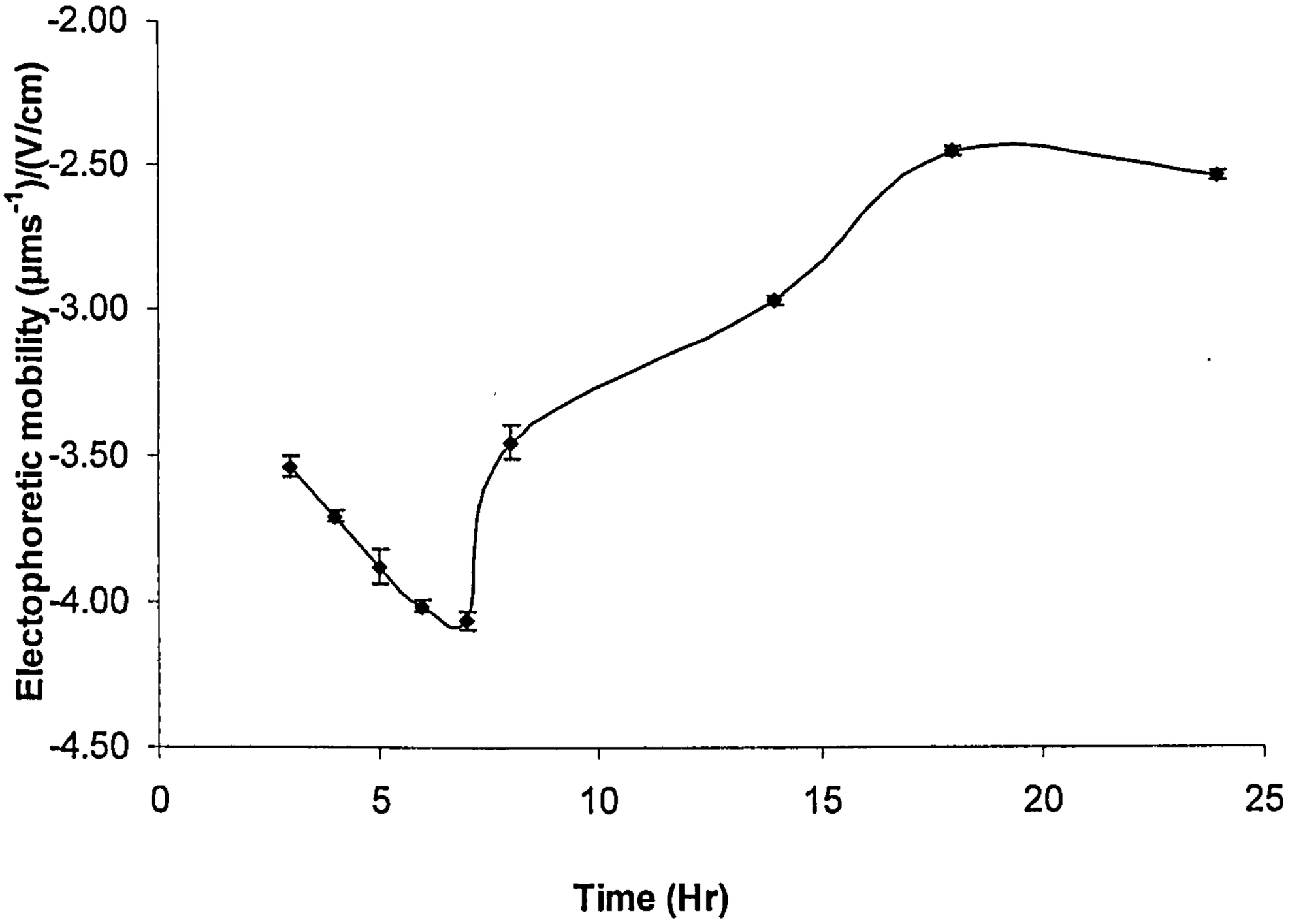

Figure 4.6 Electrophoretic mobility of *E.coli* AB1157 at different growth phases cultivated in LB supplemented with 0.5 w/v (%) glucose (LBG).

A similar negative surface charge was also found by Hayashi *et al.* (78) for Gram negative bacteria. From Figure 4.6, it can be seen that the electrophoretic mobility of the cells steadily increases in magnitude from the early to mid exponential phase and then decreases in magnitude to reach a maximum at -2.5 $(\mu ms^{-1})/(V/cm)$ at 18 hours (stationary phase), and remains relatively constant until the final measurement at 24 hours (again in the stationary phase). This shows that the surface charge of the cells is not constant during the growth phase and that the magnitude of the charge is also dependent on the stage in the growth phase, hence the electrokinetic properties are influenced by the growth phase.

Also, the electrostatic contribution of the bacterial surface predicts the amount of polymer needed to induce depletion attraction and this is dependent on the growth phase. As electrophoretic mobility of the *E.coli* AB1157 decreases, electrostatic

repulsion between the cells will increase, thereby increasing the attraction force needed for depletion aggregation to occur.

These findings are consistent with recent findings by Hayashi *et al.* (78) and suggest that differences in the aggregation properties are due to changes in the electrokinetic properties of bacteria surfaces during their growth. The correlation between high aggregation during the stationary phase (at 18hr in Figure 4.5) and the electrophoretic mobility (Figure 4.6) is also in full agreement with previous findings which state that cellular aggregation or adhesiveness increases as surface charge decreases (178, 180). The strength of induced interaction between cells increases as the concentration of SPS increases. This observation can be related back to the production of EPS by bacteria. As cells progress from the exponential to the stationary phase, the bacteria tend to produce more EPS (235), which are released to its surroundings. When the production EPS gets to a certain threshold, the bacteria and the EPS will come into close proximity which will trigger a depletion attraction between bacterial cells.

4.5. Conclusion

Phase separation occurs in a mixture of bacteria and non-adsorbing polymers, due to a depletion interaction. Different concentrations of non-adsorbing polymer are needed to induce depletion aggregation from cells harvested at different growth phases. Cells tend to aggregate more easily during the stationary phase than in the exponential phase. The magnitude of the electrophoretic mobility of *E.coli* AB1157 decreased from the early incubation phase to the stationary phase and this correlates very closely with differences in aggregation properties during growth. These findings suggest that depletion interactions induced by extracellular polymeric substances are involved in bacterial aggregation. However, unlike non-biological colloids, the depletion aggregation process was also found to be dependent on the bacteria growth phase because of the bacteria altering its surface chemistry.

Chapter 5 Characterization of Extracellular polymeric substances (EPS) from *Escherichia coli*: Role in Bacterial Aggregation

(Published in part in Biomacromolecules 2008, DOI 10.1021/bm701043c)

5.1. Abstract

As seen in Chapter 4, bacteria can be considered to be a dispersion of colloids surrounded by non-adsorbing polymers, which influence aggregation. However bacteria produce polymers known as extracellular polymeric substances (EPS) which are known to play a role in aggregation. Hence, the aim of the study discussed in this chapter, was to investigate the role of free-EPS and bound-EPS on aggregation, and to determine if free-EPS is able to aggregate *E.coli* via the depletion process as observed in Chapter 4 for the non-biological polymer.

EPS was extracted from *E.coli* MG1655 at different growth phase and media composition. The EPS extracted from *E.coli* MG1655 was quantified and characterized using FTIR spectroscopy. *E.coli* MG1655 was found to produce significantly low amount of bound-EPS and did not contribute to aggregation of *E.coli.* The protein content of free-EPS significantly increased as the cells progressed from the exponential to stationary phase, while the carbohydrate content remained relatively constant. FTIR reveals the variation of different functional groups such as amines, carboxyl and phosphoryl groups for free-EPS extracted at the different growth conditions.

The re-addition of free-EPS to *E.coli* resulted in aggregation of the cells in all growth conditions. Free-EPS extracted from the 24 hour *E.coli* MG1655 cultures cultivated in LB had the greatest effect on the aggregation ability of the cells.

5.2. Introduction

A major player in microbial aggregation or biofilm formation is the ability of cells to produce biopolymers, often called extracellular polymeric substances (EPS), during their growth (26). Polysaccharides were the most well studied biopolymers which may account for why the abbreviation "EPS" has been used to describe exopolysaccharides or extracellular polysaccharides (81, 82). In this thesis, the

term EPS refers to polysaccharides, proteins, nucleic acid and other biopolymers situated outside the cell. EPS are complex heterogeneous substances and their composition and location may be due to several metabolic processes such as growth phase, cell breakage due to cell death, active secretion, release of cell surface macromolecules (outer membrane proteins and lipopolysaccharides) and interaction with the environment (81).

EPS can be classified by its relative proximity to the cell surface. EPS tightly linked via a covalent or noncovalent association are known as capsular EPS (or cell-bound EPS) while EPS which are not directly attached to the cells surface, are known as Slime (free-EPS). The type of EPS can also be distinguished based on the extraction method used; free-EPS can be separated from a medium by centrifugation with bound-EPS still attached to the cells or aggregates (see Figure 2.). A further step is required to separate the bound-EPS from cells or aggregates. Previous findings have revealed that EPS also contribute to the surface properties of microoorgansims. The interaction between EPS and the solid surfaces can be attractive or repulsive depending on the constituents of the EPS or a variation in the affinity of the EPS for the solid surface or aqueous phase (256, 257). The role of EPS in cell-to-cell interaction leading to aggregation may follow a similar manner as cell-to-solid surface. However, this interaction may only be valid for bound-EPS since free-EPS is not directly linked to the cell surface. The interaction between the free-EPS and the cells may vary due to the changes in the compositions of EPS or the cell surface chemistry of the bacteria (63).

From a physiochemical point of view, bacteria can be considered to be a negatively colloidal 'particles' (30, 145) surrounded by non-adsorbing polyelectrolyte, i.e. free-EPS. As discussed in Chapter 4, non adsorbing polymers can promote particles to aggregate via a process known as depletion attraction (48, 49, 240). In Chapter 4 it was reported that depletion interactions occur in *E.coli* by using a non-adsorbing polymer sodium polystyrene sulphonate (SPS) and that the level of interaction was dependent on the both the electrokinetic properties on the surface dictated by the growth phase, and the concentration of polymer (258).

Here we hypothesize that free-EPS promotes aggregation in a similar depletion interaction approach. In this chapter, the bound and the free-EPS from *E.coli* is harvested at different growth phase and characterized using FTIR. The contribution of bound and free-EPS to aggregation is then quantified.

5.3. Materials and methods

All chemicals were purchased from Sigma-Aldrich (Gillingham, Dorset, UK) unless otherwise stated. All experiments were conducted in (at least) triplicate, and the average of the results reported. Variation in the experimental results is presented as the average ± standard deviation.

5.3.1. Bacterial strains and Growth studies

Escherichia coli MG1655 was used in this study and cultivated with aeration at 30°C in Luria-Bertani (LB) medium supplemented with or without 0.5 w/v (%) of glucose as previously described in Chapter 3. LB media supplemented with 0.5 w/v (%) glucose is referred to as LBG throughout the Chapter. Overnight culture (~16hrs) of *Escherichia coli* MG1655 was then used to inoculate fresh LB or LBG at a 1:100 dilution and grown at 30°C with aeration. The optical density at 595nm was measured using a spectrophotometer (ThermoSpectronic, UK). Viability tests for the *E.coli* cells, under same conditions used for the aggregation assay and surface characterization techniques, were performed using a Live/Dead BacLight kit (Molecular Probes, UK) following the manufacturer's protocol. Cells were viewed with Axioplan II imaging fluorescence microscope equipped with a DF10 filter (Carl Zeiss Ltd, UK).

5.3.2. Extracellular polymeric substances (EPS) extraction

Cells were harvested by centrifugation at 5000 rpm for 15 minutes at 4^0C. Cell pellets and supernatant were used for bound-EPS and free-EPS extractions respectively. Bound-EPS was extracted from the cell pellet using the EDTA method as described by Sheng *et al.* (84) with some modifications. Cells were washed twice with 0.9 % NaCl to remove any traces of the media. The washed cells were re-suspended in 1:1 volume of solution 0.9% NaCl and 2% EDTA then incubated for 60 minutes at 4^0C. The supernatant containing bound-EPS was then

harvested by centrifugation at 10000g at 4^0C for 60 minutes and then filtered through a nitrocellulose membrane (Fisher Scientific, UK).

Free-EPS was extracted from the supernatant using the method described by Omoike and Chorover (218). The supernatant was re-centrifuged at 10000g for 30 mins at 4^0C to remove residual cells and then the supernatant, containing free-EPS was precipitated with 1:3 volume ethanol and the suspension stored at -20^0C for 18hrs. Free-EPS were then removed by centrifugation at 10000g for 15 mins at 4^0C. The extract was re-suspended in ultra pure water and dialyzed against ultra pure water to removed ethanol using 2000 MWCO Spectrum DispoDialyzer (Medicell, UK).

Both bound and free-EPS were stored at -20^0C until needed for further analysis. The EPS was then analysed for total proteins using the Lowry method with bovine serum albumin (BSA) as a standard (259). The total carbohydrate content was also analysed using the Anthrone method (260) with glucose as the standard.

5.3.3. Fourier transformation infrared spectroscopy (FTIR)

The various functional groups in the free-EPS were characterized using FTIR spectroscopy using a Perkin Elmer Spectrum One Fourier Transformation Infrared Spectrophotometer (PerkinElmer, UK). Twenty microlitres of EPS was allowed to dry at room temperature for 45 minutes on a demountable liquid-cell kit (Sigma, UK) with CaF_2 windows. At least 100 scans, with a resolution of 4cm^{-1}, were collected for all samples between 4000cm^{-1} and 900cm^{-1}.

5.3.4. Aggregation studies

5.3.4.1 Role of Bound-EPS

The role of bound-EPS in aggregation was observed by carrying out an aggregation assay on *E.coli* MG1655 cells before and after bound-EPS extraction. The aggregation assay was previously described in Chapter 4 with some minor modifications. Cells were harvested and washed twice with 0.9% NaCl (pH 7.0).

The cell pellet was re-suspended in 0.9 % NaCl and the optical density (O.D) was adjusted to ~0.6 prior to measurement to ensure standardization across the tests. 1 ml of cells was then transferred into cuvettes. O.D corresponding to cells at the upper part of the cuvette was measured and percentage aggregation was calculated as the difference in OD_{600} readings taken at time 0 to 5hr according to Equation 2.1. The OD reading was taken between times 0 to 5hr rather than 0 to 24hrs (as seen in chapter 4) due to the fact that percentage aggregation of *E.coli* remains relatively constant between 5 and 24hrs. 0.9% NaCl was used rather than distilled water in this assay, to prevent any pH effect on *E.coli* aggregation.

5.3.4.2 Role of Free-EPS

A depletion aggregation assay was used to observe the role of free-EPS in *E.coli* MG1655 aggregation. The procedure for carrying out depletion aggregation assay is the same as the aggregation assay above apart from the fact that 0.1ml of the extracted free-EPS (~0.5mg or 0.05mg) was transferred into cuvettes containing 0.9ml of cells (~0.5mg).

5.4. Result and discussion

5.4.1. Characterisation of Extracellular polymeric substances

The growth studies of *E.coli* MG1655 cultivated in LB and LBG have previously been reported in section 3.4.1 with no significant difference in growth rate between cells cultivated in LB or LBG (261). The uptake of 0.5 w/v (%) glucose during batch cultivation of cells was also shown in Chapter 3, with over 97% of glucose taken up by the cells after 6hrs. Viability of cells was found to be approximately 83 and 81% for cells at exponential (6 hrs) and stationary (24 hrs) phase respectively, in both types of media.

Table 5.1 shows the protein and carbohydrate content of both bound and free-EPS produced at different growth phases in LB and LBG. The carbohydrate content of bound-EPS extracted from cells cultivated in both LB and LBG remains relatively constant as cells progressed from exponential phase (6hr) to stationary phase (24hr). However, the protein content of bound-EPS extracted from the cells

cultivated in LB decreased as the cells proceeded from the exponential (6hr) to the stationary (24hr) phase. A similar, although, less pronounced decreased in protein content was also observed for cells grown in LBG between exponential and stationary growth phase. The comparison of protein content at the same growth phase but different media (LB vs. LBG) showed very little difference.

The low values observed from bound-EPS (protein and carbohydrate) suggest that *E.coli* MG1655 produces very little EPS, in the growth phases for which the experiment was conducted. The amount of EPS (protein and carbohydrate) produced by this strain, is very low when compared to previously reported work (e.g. the protein and carbohydrate content of EPS from *Pseudomonas putida* in batch cultures was 214 and 54 mg/g respectively (83)). This suggests that *E.coli* MG1655 produces very little EPS is consistent with previous reports of *E.coli* strains which show little or no EPS (79, 262).

Table 5.1 EPS content of *E.coli* MG1655 at different growth phases, cultivated in Luria-Bertani (LB) and LB with 0.5w/v (%) glucose (LBG).

	Carbohydrate (mg/g dry cells)	Protein (mg/g dry cells)	Carbohydrate/ protein ratio
Bound EPS			
E.coli LB 6hr	3.53 ± 1.91	1.43 ± 0.43	2.47
E.coli LB 24hr	1.34 ± 0.03	0.42 ± 0.25	3.19
E.coli LBG 6hr	1.89 ± 0.07	0.88± 0.07	2.15
E.coli LBG 24hr	2.27 ± 1.07	0.54 ± 0.25	4.20
Free-EPS			
E.coli LB 6hr	14.26 ± 0.02	9.79 ± 1.03	1.46
E.coli LB 24hr.	7.00 ± 0.44	25.66 ± 2.26	0.27
E.coli LBG 6hr	10.61 ± 0.21	7.98 ± 1.44	1.33
E.coli LBG 24hr	20.51 ± 0.79	17.17 ± 1.38	1.19

E.coli MG1655 produces relatively higher amount of free-EPS compared to bound-EPS under the same growth conditions (Table 5.1). The carbohydrate content of free-EPS decreased as the cells progressed from the exponential to stationary phase, for cells cultivated in LB. However, for cells cultivated in LBG, the carbohydrate concentration increased as the cells progressed from exponential to stationary phase. The protein content of the free-EPS from cells cultivated in both LB and LBG increased as they progress from the exponential to stationary phase. The increase in the protein content is consistent with previous findings suggesting that *E.coli* cells shed their outer membrane or periplasmic proteins during growth phase (263). The increase in protein may also be due to an increase in shedding of membrane macromolecules during cell growth (263). Since the amount of carbohydrate and protein concentration varied, due to a change in media (LB and LBG) and the growth phase, it stands to reason that their physiochemical characteristics may also differ.

Bound and free-EPS extracted from *E.coli* MG1655 at different growth phases and growth media were further characterized using FTIR spectroscopy. Each spectrum contains information about the functional groups arising from predominantly carbohydrate, proteins, nucleic acid as listed in Table 5.2. This provides a list of absorption band assignments corresponding to functional groups of these macromolecules in the region between 1800 and 900cm^{-1}, and is based on observations of the vibration patterns, previously reported for bacteria (45, 171, 264, 265).

Table 5.2 List of band assignments from FT-IR analysis of EPS

Wave Number (cm^{-1})	**Functional Groups**
~ 3400	stretching vibrations O–H of water
~ 2960	Asymmetric stretch C–H of methyl groups
~ 1740	ν>C=O of ester functional group mainly from membrane lipids and fatty acids
~ 1650	νC=O stretching vibrations of amides associated with proteins. Usually known as Amide I band
~ 1550	δN–H bending of amides associated with proteins. Usually known as Amide II band
~ 1455	$\delta_{ac}CH_2/\delta_{ac}CH_3$ Asymmetric deformation of CH_3 and CH_2 of proteins
~ 1398	$\delta_{ac}CH_2/\delta_{ac}CH_3$ and ν_sC-O .Symmetric deformation of CH_3 and CH_2 of proteins, and symmetric stretch of carboxylic acids groups (C–O of COO^- groups)
~ 1240	ν_{as}P=O Asymmetric stretch of phosphodiester backbone of nucleic acids
~ 1200-900	νC–O–C of polysaccharides
~ 1080	ν_{as}P=O Symmetric stretch of the phoshodiester backbone of nucleic acids

Data adopted from Dittrich and Sibler (171); Lin *et al*. (264); Maquelin *et al*.(265); and Schmitt and Flemming (45).

The spectra of bound-EPS extracted from *E.coli* MG1655 cultivated in LB at exponential (6hr) and stationary (24hr) phase is shown in Figure 5.1. The effect of a change in media (LBG) on bound-EPS content of *E.coli* MG1655 harvested at exponential and stationary phase is also analysed using FTIR analysis spectroscopy (Figure 5.2).

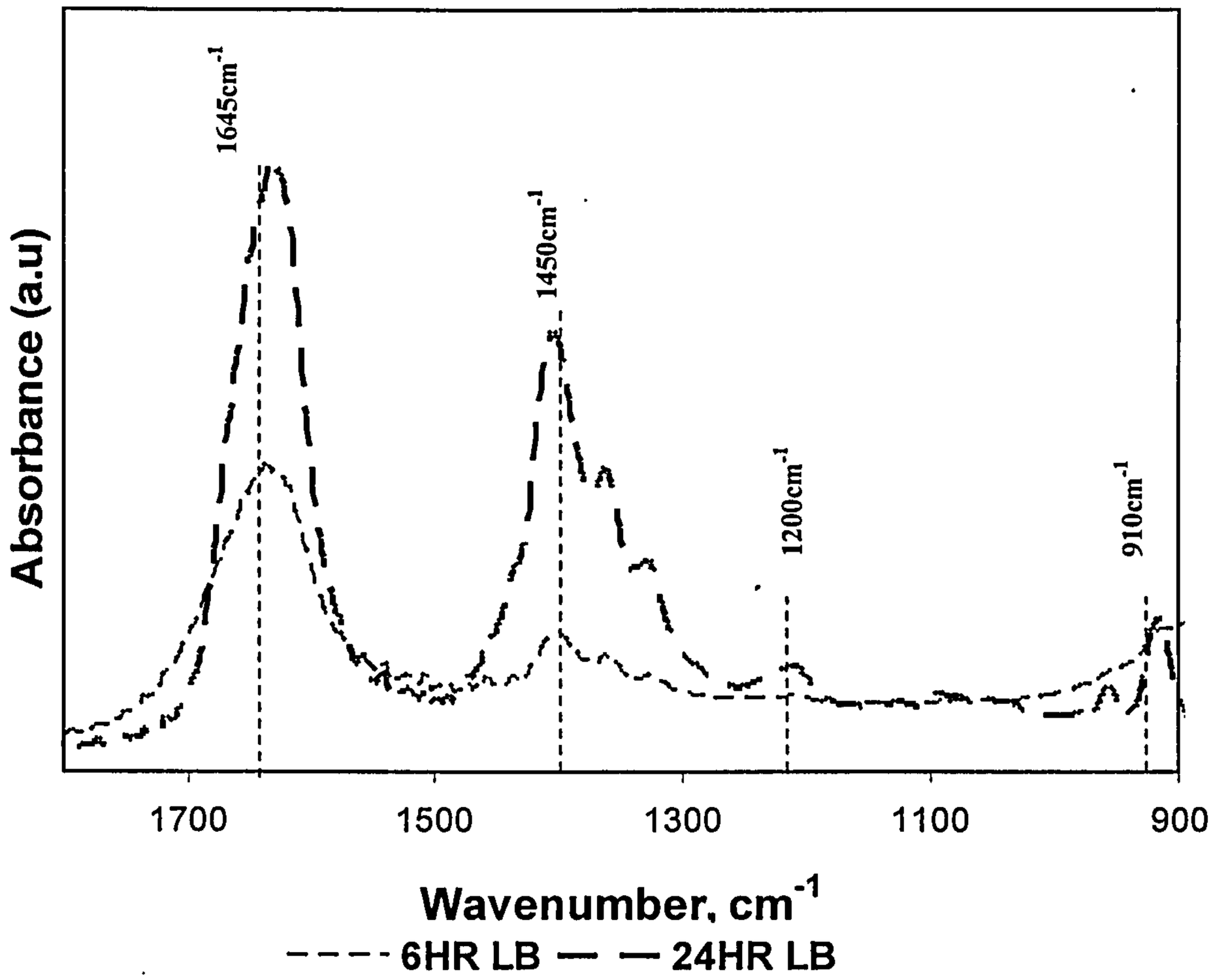

Figure 5.1 FTIR spectra of bound-EPS extracted from *E.coli* MG1655 cultivated with LB and extracted during exponential (6hr) and stationary phase (24hr)

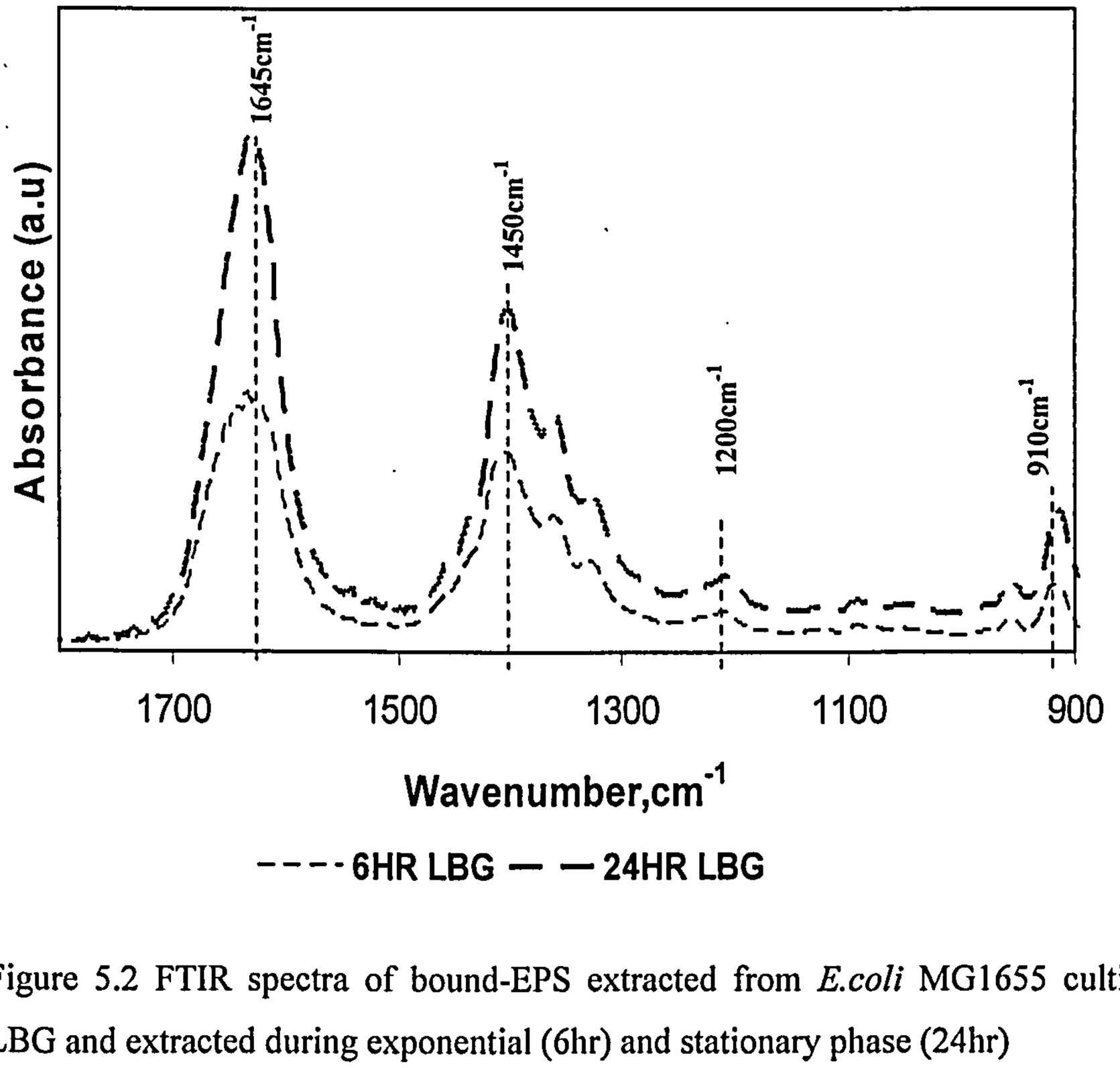

Figure 5.2 FTIR spectra of bound-EPS extracted from *E.coli* MG1655 cultivated with LBG and extracted during exponential (6hr) and stationary phase (24hr)

In Figure 5.1 and Figure 5.2 the band at the approximate 1645cm^{-1} region corresponds to the amine I which are characteristics of functional groups C=O stretching vibrations of proteins. The peak at 1450 cm^{-1} corresponds to bending of CH_3 and CH_2 groups from proteins (δCH_2, δCH_3) may also have a contribution from an amine III band. The peak at ~1400 cm^{-1} arises from to the stretching C-O ($\nu_{C\text{-}O}$) of carboxylic groups which overlap with the amide III band making it difficult to distinguish. The bands between 1200 and 950 cm^{-1} are attributed to the vibrations of C-O-P and C-O-C stretching of diverse polysaccharide groups, and the bands at 1260 and 1080 cm^{-1} exhibit the stretching of P=O ($\nu_{P=O}$) of phosphoryl and phoshodiester groups from phosphorilated proteins, polyphosphate products and nucleic acids.

Differences in spectra were observed for bound-EPS extracted from cells harvested at different growth phase and media (Figure 5.1 and Figure 5.2). The bands between 1200 and 950 cm^{-1} correspond to polysaccharide groups for bound-EPS

extracted from cells cultivated in LB at 6hr is relatively low as compared to bound-EPS extracted from cells cultivated in LB at 24hr (Figure 5.1). Amide I and II bands arising mainly from proteins were also relatively low for bound-EPS extracted from cells cultivated in LB and harvested at the exponential phase, when compared to its stationary phase counterpart. Interestingly, spectra of bound-EPS from cells cultivated with LBG (Figure 5.2), displayed significantly different patterns to those cultivated in LB (Figure 5.1). The spectra of bound-EPS from exponential and stationary phase cells cultivated in LBG appeared to not significantly change in contrasts with those cells cultivated in LB. These finding suggest that both changes in growth phase and media affect the composition of bound-EPS in *E.coli* MG1655.

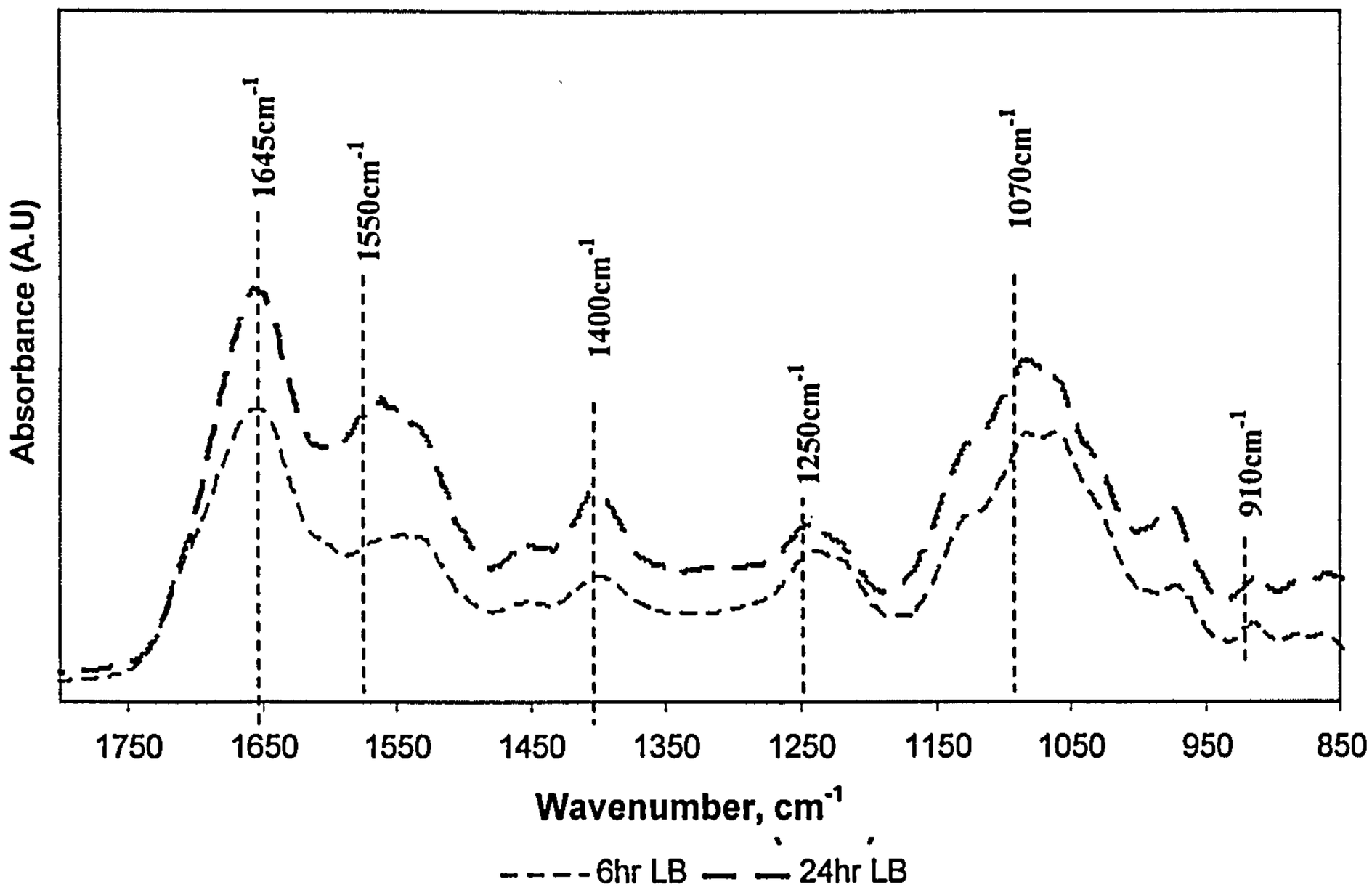

Figure 5.3 FTIR spectra of free-EPS extracted from *E.coli* MG1655 cultivated with LB and extracted during exponential (6hr) and stationary phase (24hr)

Figure 5.3 shows the spectra of free-EPS extracted from *E.coli* MG1655 cultivated in LB at exponential (6hr) and stationary (24hr) phase. The relative absorbance of the bands between 1650 and 900 cm^{-1} increased as cells progress from the exponential to stationary phase, which accounts for difference in carbohydrate to proteins ratio observed at different growth phase in Table 5.1. Figure 5.4 shows the

spectra of free-EPS extracted from *E.coli* MG1655 cultivated in LBG at different growth phases. The relative intensity of the peaks in the proteins and polysaccharides region also increased with increasing growth phases. The ratio of amine I and II was also varied between free-EPS extracted from *E.coli* cultivated in LBG at different growth phases suggesting that the quantity and types of proteins differs which is in agreement with the changes in ratio of carbohydrate to protein observed in Table 5.1.

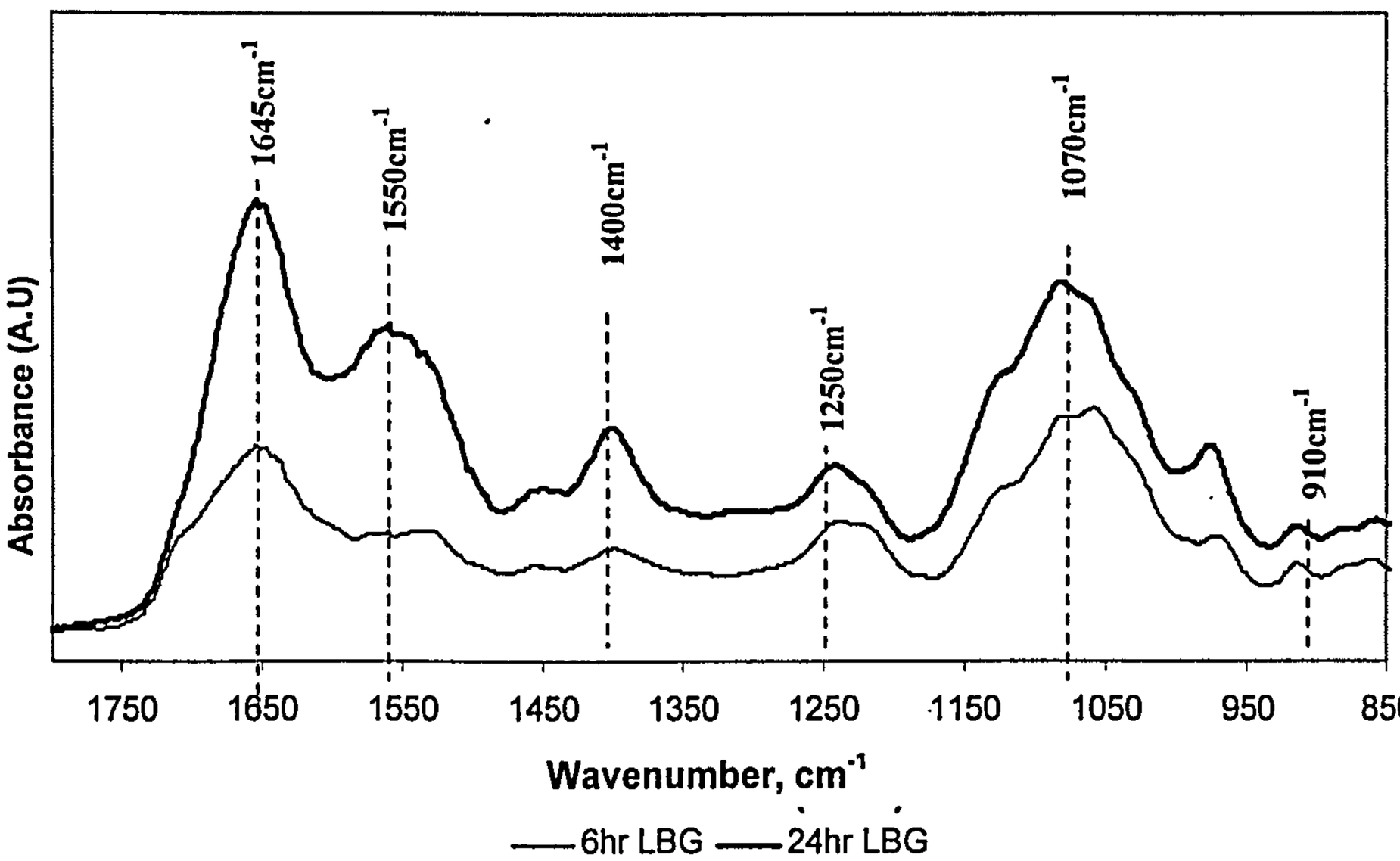

Figure 5.4 FTIR spectra of free-EPS extracted from *E.coli* MG1655 cultivated with LBG and extracted during exponential (6hr) and stationary phase (24hr)

One major difference between bound and free-EPS is the presence or absence of a peak at ~1545cm^{-1} corresponding to the bending of N–H amides. This peak is predominately low or absent in bound-EPS in contrast to free-EPS. The band at ~1240cm^{-1}, corresponding to the asymmetric stretching P=O of phoshodiester backbone of nucleic acids is present in all spectra of free-EPS (Figure 5.3 and Figure 5.4) but is absent in spectra from bound-EPS (Figure 5.1 and Figure 5.1). These findings suggest that the content of bound-EPS is predominantly dominated by proteins and carbohydrate. However, free-EPS are also dominated by proteins

and carbohydrates but a significant level of nucleic acid is also present, which may be due to cell lysis and nucleic acid excretion.

5.4.2. Effect of bound-EPS on aggregation capability of E.coli MG1655

The role of bound-EPS on the aggregation ability of *E.coli* MG1655 was investigated by carrying out the aggregation assay on *E.coli* MG1655 before and after bound-EPS extraction. The percentage aggregation of *E.coli* MG1655 cultivated in LB and LBG harvested at the exponential and stationary phase before and after bound-EPS extraction is shown in Figure 5.5.

The results revealed that the presence or absence of bound-EPS did not affect the autoaggregation ability of *E.coli* MG1655 irrespective of growth phase or change in media. This may be due to the very low amount of bound-EPS produced during the conditions of the experiments. It is also important to note here that no free-EPS was present. Furthermore the primary role of bound-EPS may not be in initial cell-to-cell adhesion but in holding cells together after adhesion (266). The difference in aggregation capability of *E.coli* MG1655 harvested at different growth phase and media is discussed in more detail in Chapter 7.

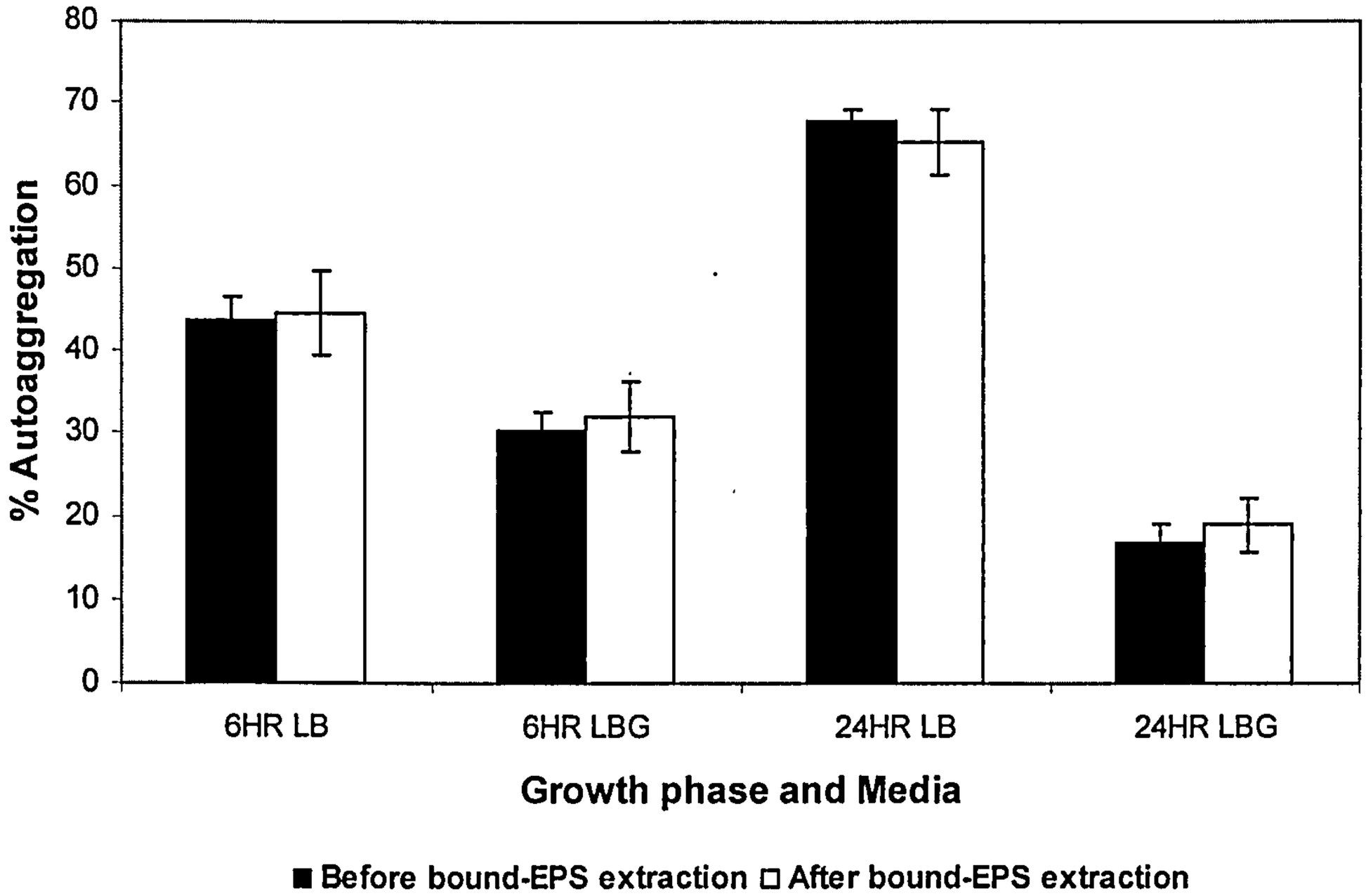

Figure 5.5 Percentage aggregation of *E.coli* MG1655 cultivated in LB and LBG harvested at exponential (6hr) and stationary phase (24hr) before and after bound-EPS extraction.

5.4.3. Depletion Aggregation in E.coli MG1655 by free-EPS

The effect of non-adsorbing polymers on the aggregation of *E.coli* AB1157 via a phenomenon known as depletion interactions is reported in Chapter 4. In this case, *E.coli* AB1157 displayed a similar attraction as previously reported for colloids upon addition of an inert, non-adsorbing polymer (Sodium Polystyrene Sulphonate (SPS)), suggesting that bacterial aggregation can be induced by non-adsorbing polymers. Hence, we investigated this work further to show if the free-EPS produced by *E.coli* MG1655 can also induce depletion interaction in cells which will further explain the function of free-EPS in bacterial aggregation.

The depletion aggregation ability of *E.coli* MG1655 cultivated in LB, harvested at mid-exponential phase (6hr) and stationary phase (24hr) is shown in Figure 5.6 as

a % change in optical density. The results reveal that EPS triggers the aggregation capability of *E.coli* MG1655 harvested at different growth phases.

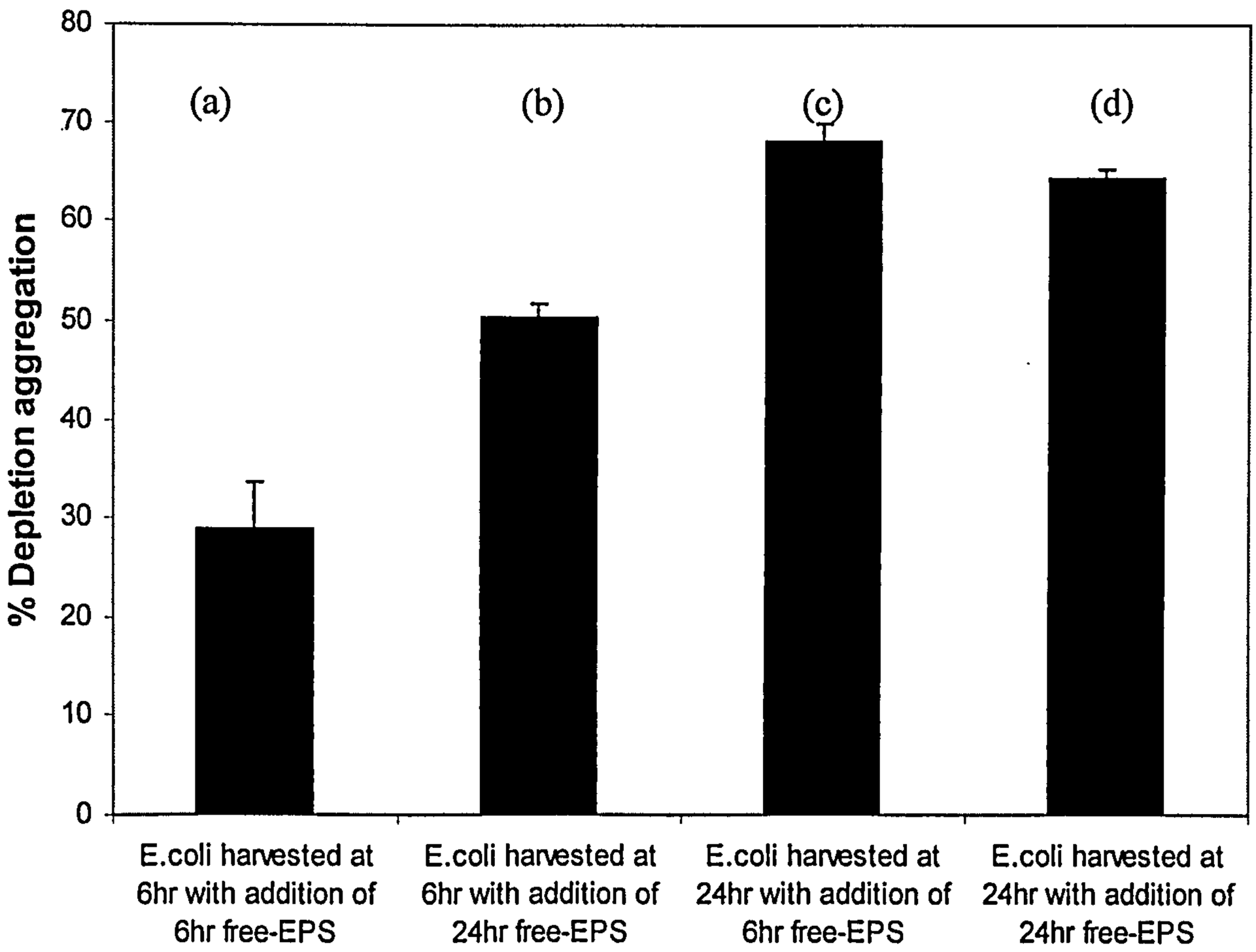

Figure 5.6 Depletion aggregation of *E.coli* MG1655 cultivated in LB at different growth phase, with the addition of free-EPS extracted from cells cultivated in LB at different growth phases.

The addition of free-EPS extracted from cells at exponential growth phase (6hr) or stationary phase (24hr) to *E.coli* MG1655 harvested at the stationary phase display similar aggregation ability (Figure 5.6 (c) and (d)). However, the addition of free-EPS extracted from cells at exponential growth phase (6hr) or stationary phase (24hr) to exponential phase cells displayed different aggregation ability (Figure 5.6 (a) and (b)). Cells harvested at exponential phase were found to display an increase in aggregation ability when free-EPS, harvested at stationary phase was added (Figure 5.6 (b)), relative to the addition of free-EPS extracted at 6 hrs (Figure 5.6

(a)). However it should be noted that cells harvested at stationary phase (24 hours) displays a higher autoaggregation capability (i.e. without addition of free-EPS) at all times, than cells harvested after the exponential phase (6 hours), Figure 5.5. This may account for the lesser effect of free-EPS on cells harvested at stationary phase.

The depletion aggregation ability of *E.coli* MG1655 cultivated in LBG harvested at mid-exponential phase (6hr) and stationary phase (24hr) is shown in Figure 5.7 as a % change in optical density. The addition of free-EPS harvested in the exponential phase (6hr) from cells grown in LBG had a significant effect on aggregation ability of cells at exponential phase (Figure 5.7 (a)) compared to stationary phase (Figure 5.7 (c)). A similar effect was seen for free-EPS harvested at 24hrs when added to cells at the exponential and stationary phase (Figure 5.7 (b) and (d)). However, it should also be noted that cells harvested at exponential phase (6 hours) displays a higher autoaggregation capability (i.e. without addition of free-EPS) at all times, than cells harvested after the stationary phase (24 hours) (Figure 5.5) and as such may also account for the lesser effect of free-EPS on cells harvested at stationary phase.

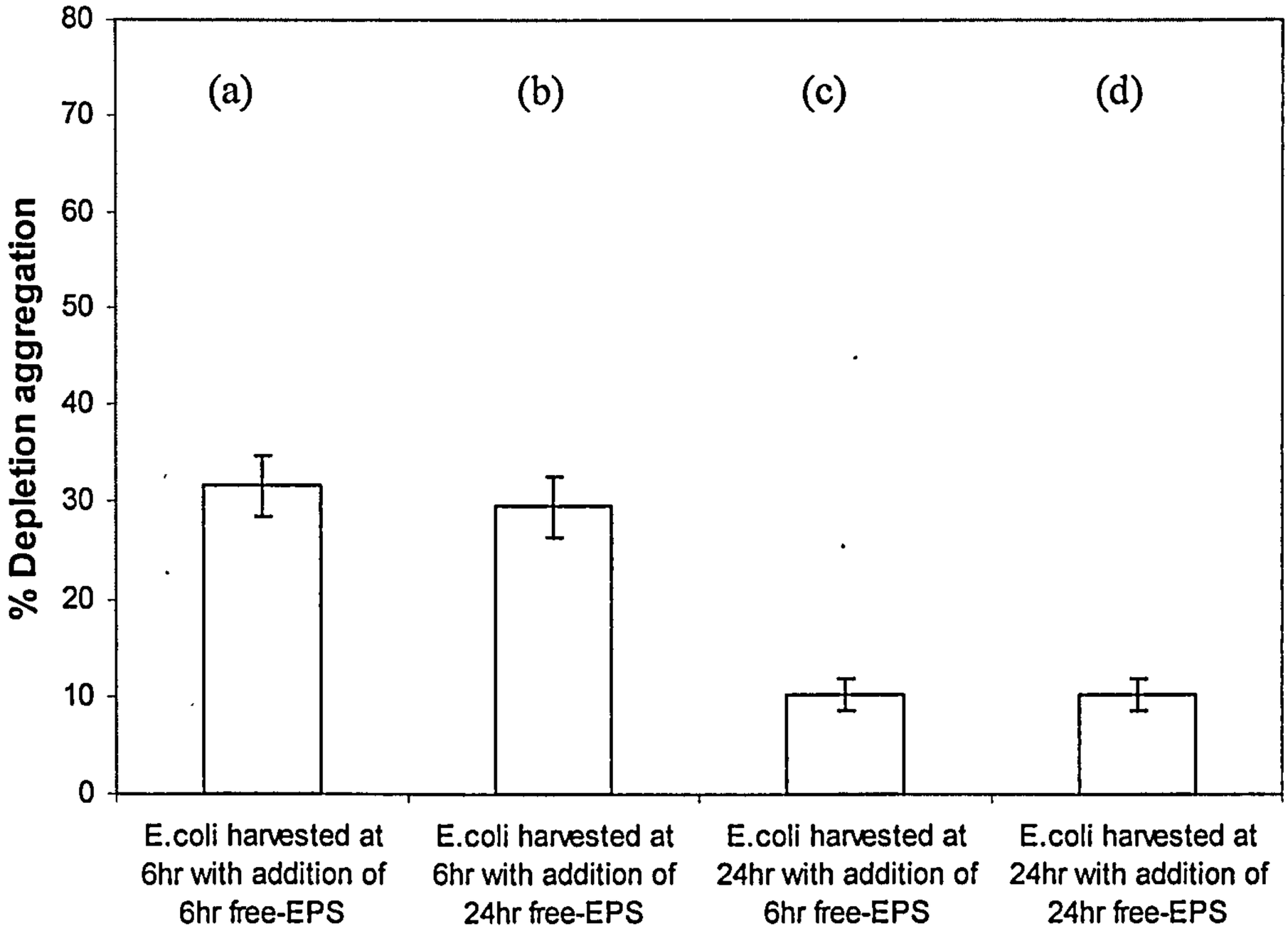

Figure 5.7 Depletion aggregation of *E.coli* MG1655 cultivated in LBG with free-EPS from LBG

The results thus far shows that free-EPS extracted from *E.coli* MG1655 cultivated in LB and harvested at stationary growth phase displayed the highest ability to induce aggregation. This was investigated further by the addition of free-EPS extracted from cells at the stationary growth phase (24hr) cultivated in LB, to cells cultivated in LBG at both exponential and stationary phase (Figure 5.8). Interestingly, the aggregation ability of cells cultivated in LBG for both exponential and stationary growth phase relatively (compared with Figure 5.7) increased by about 30% when free-EPS extracted from *E.coli* cells cultivated in LB at stationary growth phase (24hr LB) was added.

These findings suggest that free-EPS may induce cell aggregation via depletion interaction, as observed for inert polymers. The composition of free-EPS determines its ability to induce aggregation in *E.coli* which in itself is controlled by the growth phase and media. EPS extracted from cultures at different growth phases, have a varying capacity to induce aggregation. Hence it is possible to force aggregation of *E.coli* cells with both inert and biologically produced polymers.

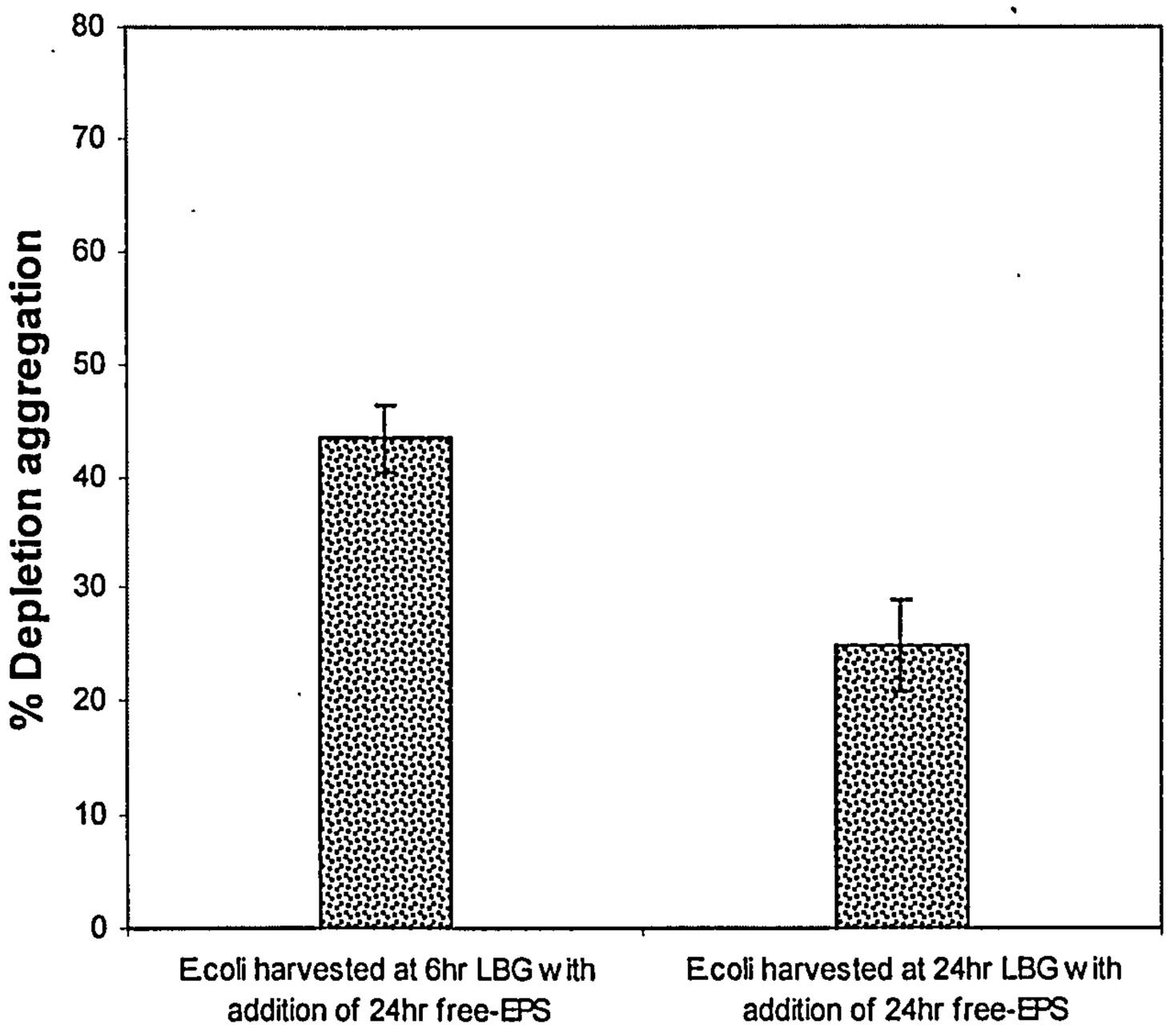

Figure 5.8 Depletion aggregation of *E.coli* MG1655 cultivated in LBG with free-EPS from 24hr LB

5.5. Conclusion

E.coli MG1655 was found to produce a small amount of bound-EPS and a relatively large amount of free-EPS under the condition used for this study. The protein content of free-EPS was found to significantly increase as *E.coli* MG1655 cells progress from exponential to stationary phase. The composition and aggregation capacity of free-EPS extracted from a biological system is dependent on the growth phase and medium of the cells. The role of free-EPS in biological aggregation follows the process of depletion attraction, as observed for inert polymers (i.e. SPS, Chapter 4). Cells harvested at exponential phase were found to display an increase in aggregation ability when free-EPS, harvested at stationary phase was added. Hence it is possible to manipulate bacterial aggregation with inert polymers and biologically produced polymers.

Chapter 6 Proteomic Analysis of Extracellular Proteins from *Escherichia coli* MG1655

(Published in part in Biomacromolecules 2008, DOI 10.1021/bm701043c)

6.1. Abstract

Studies in extracellular polymeric substances (EPS) have focused mainly on extracellular polysaccharides, since it's was previously thought to be the major macromolecule in EPS. However, extracellular proteins have recently been observed in significant amounts and are thought to be the major macromolecule in EPS from cell culture, aggregate or biofilms. The extracellular proteome of *E.coli* MG1655 in response to changes in environmental conditions was identified using a proteomic approach (SDS-PAGE and QStar XL Hybrid ESI Quadrupole TOF tandem mass spectrometer). The hydrophobicity of proteins identified was determined by the grand average hydropathy (GRAVY) index using the ProtParam. Localization of the proteins identified was also predicted using the program PSORTb v.2.0 and LipoP v1.0 software

The number of extracellular proteins identified increased as cells progressed from exponential to stationary phase for a certain growth media. A total of 79, 117, 132 and 175 extracellular proteins were identified for *E.coli* cells cultivated in 6hrLB, 6hrLBG, 24hrLB and 24hrLBG respectively. Some of the extracellular proteins identified were common or unique to various growth condition used in this study.

6.2. Introduction

Extracellular polymeric substances (EPS) have been shown to play a key role in aggregation and biofilm formation in microorganisms (267). Early investigations on EPS suggested that extracellular polysaccharides were the most abundant component (268), hence researchers in EPS have mainly focused on the polysaccharide component of EPS. However EPS have now been found to contain significant amounts of extracellular proteins as well as nucleic acids (86, 269), and in some cases they have been found to be the dominant component of EPS found in cell culture, aggregates or biofilms (269, 270). Extracellular proteins (ECP) are the protein content of free-EPS, which arise from the active secretion during growth of microorganisms and then translocated to the environment, or may also rise due to cell lysis as a result of cell death.

Microorgansims possess several pathways for extracellular translocation of proteins across the membrane to the environment or growth medium. These include the signal sequence independent pathway (type I), the main terminal branch of the general secretion pathway (type II), the contact-dependent pathway (type III), the type IV pathway, the filamentous hemagglutinin secretion pathway and the autotransporter pathway (271). In *E.coli*, transportation of extracellular proteins is thought to be via the general secretory pathway (GSP), which involves the translocation of precursor across the cytoplasmic membrane via the signal peptide-dependent Sec pathway (272).

The role of extracellular proteins in aggregation appears to be limiting in the literature, and this may be due to the fact that researchers have historically paid more attention to the polysaccharide content of EPS. Moreover, previous studies on proteins have mainly focused on identification or expression analysis of intracellular proteins or single extracellular proteins (273). Extracellular proteins (ECP) have also been suggested to play a crucial role in the virulence properties of microorgansims. The physiology and metabolism of microorganisms are affected by changes in environmental conditions, and as such the composition of extracellular proteins is expected to vary. Hence, understanding the variation of extracellular proteins may provide information of bacterial physiological state, such as their aggregation capability.

Proteomics is a powerful tool for identification of proteins, as well as changes in the expression of proteins due to variations in environmental conditions (274). However, this technique has mainly been used for identification and expression analysis of cytosolic proteins. More recently, proteomic analysis have been employed in studying extracellular proteins (153, 275). Chapter 5 showed that a variation in free-EPS due to changes in growth phase and media can contribute to difference in the aggregation capability of *E.coli*. The protein content of free-EPS (i.e. extracellular proteins, ECP) was observed to significantly vary during changes in growth phase and media. Hence, the objective of this study is to identify ECP of *E.coli,* at the same conditions in which the variation of aggregation properties was

observed, to investigate the possibility of trends in the protein expression during aggregation.

6.3. Materials and methods

6.3.1. Extraction of extracellular proteins

Free-EPS was extracted from cells cultivated in LB and LBG at different growth phases according to the method described in 5.3.3. Extracellular proteins were extracted from free-EPS by extracting with 1:5 ice-cold acetone and stored in -20^{0}C for 18hrs. The solution was then centrifuged at 15000g for 10 minutes and the supernatant was discarded. Acetone precipitation was repeated for the pellets containing proteins and then stored for further analysis. The concentration of ECP was then analysed using the Lowry method with bovine serum albumin (BSA) as a standard (259).

6.3.2. Sodium dodecyl sulfate polyacrylamide gel electrophoresis (SDS-PAGE)

SDS-PAGE was performed on extracellular proteins of *E.coli* MG1655 using a 10 % (w/v) polyacrylamide gel following the method previously described by Laemmli, U. K. (276). Protein extract (100µg/ml protein) was dissolved in ultra pure water and then electrophoresed at constant voltage (120V) until the bromophenol blue tracking dye front reached the bottom of the gel. Low-molecular-weight protein markers (New England Biolabs, UK) were used as protein standards and the protein bands were stained with Bio-Safe Coomassie blue stain (Bio-Rad, UK).

6.3.3. In Gel Digestion

Gels obtained from SDS-PAGE containing extracellular proteins were rinsed with deionized water, cut into smaller pieces and then subjected to Tryptic digestion as previously described by Gan *et al.* (277). Gel pieces were then destained twice with 200µl of 200mM Ammonium Bicarbonate in 40% Acetonitrile (ACN) and then vacuum dried for approximately 15 to 30 min. The gel pieces were then subjected to reduction and alkylation using 200µl 10mM Dithiothreitol (DTT) and 200µl 55mM Iodoacetamide (IAA) respectively. Reduction and alkylation buffers were discarded and gel pieces were washed twice with 200µl 50mM Ammonium

Bicarbonate and then once with 200µl 50mM Ammonium Bicarbonate in 50% Acetonitrile. All liquid from the gel pieces were discarded after centrifugation at 13,000g for 10sec and then vacuum dried for approximately 20mins. 20µl of trypsin solution (0.4µg) and 50µl of 40mM Ammonium Bicarbonate in 9% Acetonitrile (ACN) were added to the gel pieces and then incubated overnight (16hrs) at 37^0C. Peptides were then extracted separately with 50mM Ammonium Bicarbonate, Acetonitrile, 5% Formic Acid (FA), and 5% Formic Acid in 50% Acetonitrile. The solution from all extraction was combined and vacuum dried for 20 mins and stored at -20^0C prior to mass spectrometric analysis.

6.3.4. Nanoliquid chromatography electrospray ionization-tandem mass spectrometry

Dried samples were re-suspended in 7.5µl of buffer (0.1% formic acid and 3% ACN) and sonicated for 5mins. Samples were analysed using a QStar XL Hybrid ESI Quadrupole TOF tandem mass spectrometer, ESI qQ TOF-MS/MS (Applied BioSystems, Framingham, MA, USA; MDS-Sciex, Concord, Ontario, Canada), coupled with a nanoLC system comprising a combination of an LC Packings Ultimate Pump, Switchos pump, and Famos Auto sampler (Dionex/LC Packings) as previously described (277). The peptide mixture was separated on a 75 µm Pepmap capillary column. Data acquisition on the mass spectrometer was set to perform data acquisition in the positive ion mode, with a selected mass range of 300-2000m/z. Peptide with 2^+ and 3^+ charge states were selected for fragmentation.

6.3.5. Database searching

Mass spectra obtained were searched against the mass spectra of protein sequences in the NCBI Database using Mascot 1.6b.16 (www.matrixscience.com). Search parameters were set at peptide tolerance of up to 0.2 Da and an MS/MS tolerance of up to 0.2 Da; oxidation of methionine and carbamidomethyl modification of cysteine; one missed cleavage of trypsin. MOWSE scores greater than 50 were considered as significant.

The hydrophobicity of proteins identified were determined by the grand average hydropathy (GRAVY) index (278) using the ProtParam tool (279) at http://us.expasy.org/tools/protparam.html. The GRAVY value for a protein is derived from the sum of hydropathy values for each amino acid residue, divided by the length of residues in the sequence. Proteins with GRAVY values greater than +0.3 were used as an indicator of hydrophobic proteins.

Localization of the proteins identified was also predicted using the programme PSORTb v.2.0 (280) at http://psort.org/psortb/index.html. However, PSORTb v.2.0 program can not predict lipoproteins, and hence, LipoP v1.0 software (281) was also used, which predicts lipoproteins by differentiating between lipoprotein signal peptides from other signal peptides.

6.4. Results and Discussions

The growth studies of *E.coli* MG1655 cultivated in LB and LBG was not significantly different (as seen in Figure 3.2).

The production of extracellular proteins (ECP) in *E.coli* MG1655 cultivated in LB and LBG during growth can be seen in Figure 6.1. The production of ECP increased as cells progressed from the exponential (6hr) to stationary phase (24hr) in both LB and LBG. ECP production during the exponential phase for *E.coli* cells did not significantly change when cultivated in LB and LBG. However during the stationary growth phase, ECP production was significantly higher for MG1655 cultivated in LB then in LBG. The result revealed that ECP production in *E.coli* MG1655 is affected by both changes in growth phase and media at the stationary phase. Hence we investigated this further by subjecting the ECP from all conditions (i.e. 6hr LB, 6hr LBG, 24hrLB and 4hr LBG) to SDS-PAGE.

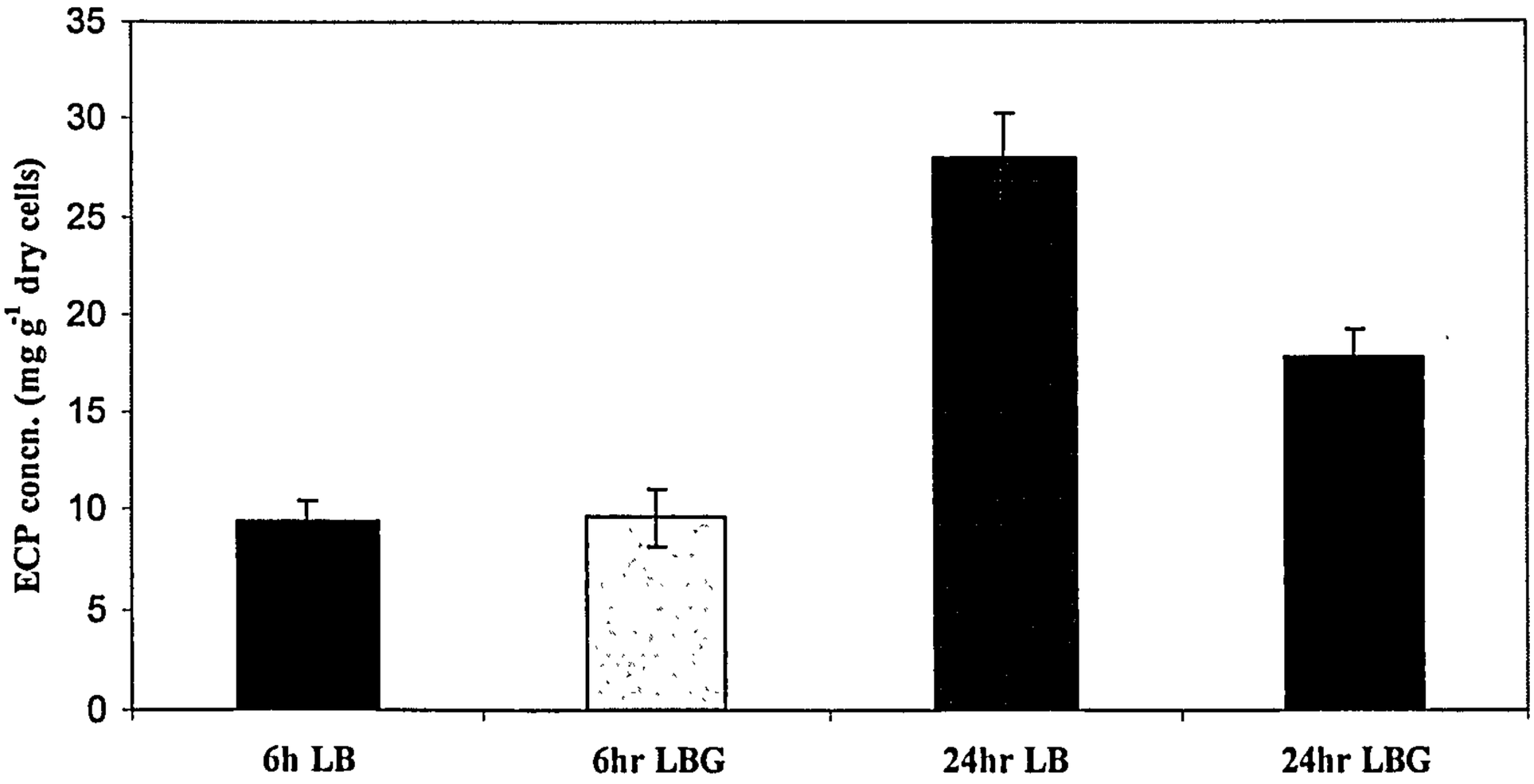

Figure 6.1 Production of Extracellular proteins in *E.coli* MG1655 cultivated in LB and LBG during growth.

Figure 6.2 shows the SDS-PAGE profiles of proteins present in free-EPS from *E.coli* MG1655. Proteins were found to be distributed over a wide range of molecular weight (10-70kDa). SDS-PAGE revealed differences in the protein profiles from free-EPS harvested at different growth phases and from media. This techniques correlates well with the major differences in protein patterns already observed using the FTIR (Figure 5.3 and Figure 5.4). More distinct protein bands were observed in free-EPS extracted from stationary phase cells, cultivated in LB compared with free-EPS from exponential phase in LB, and from free-EPS from both growth phases in LBG.

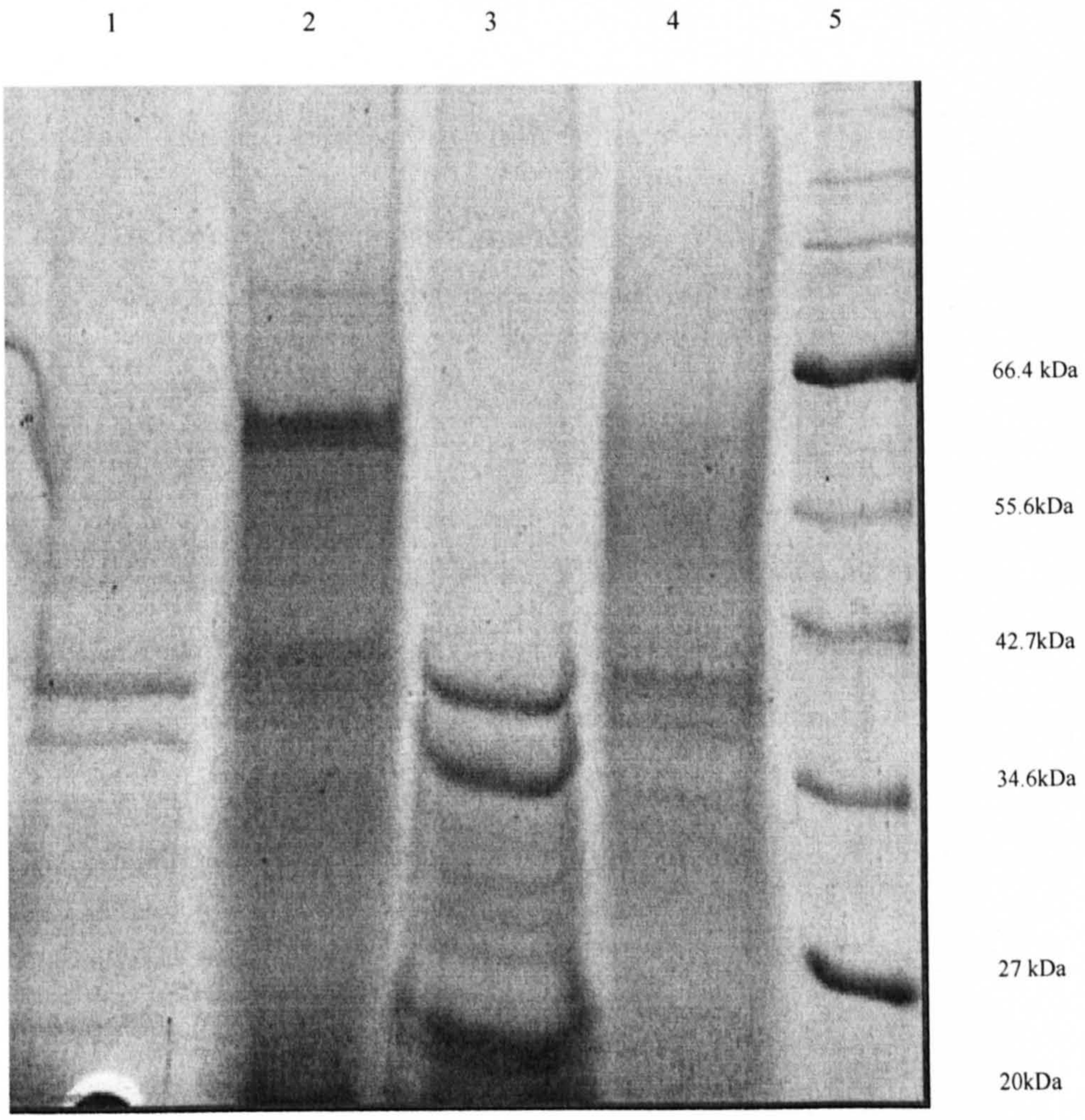

Figure 6.2 One dimensional SDS-PAGE gel of proteins from the free-EPS extracted from cells harvested at different growth phases, in LB and LB with 0.5% (w/v) glucose (LBG)

Lane 1 – Proteins from free-EPS extract from cells grown in LB, harvested at 6hrs

Lane 2 - Proteins from free-EPS extract from cells grown in LBG, harvested at 6hrs

Lane 3 - Proteins from free-EPS extract from cells grown in LB, harvested at 24hrs

Lane 4 – Proteins from free-EPS extract from cells grown in LBG, harvested at 24hrs

Lane 5 – MW protein marker

The master list of *E.coli* extracellular proteins identified at all growth conditions is available in Appendix C. Based on the mass spectrometry data and analysis, a total 503 extracellular proteins were identified across all cells cultivated in 6hrLB, 6hrLBG, 24hrLB and 24hrLBG. However, 40 of these ECP were produced in all growth conditions (Appendix B). A total of 79 and 175 extracellular proteins were identified from the free-EPS of cells harvested during the cells at exponential (6hr) and stationary phase (24hr), cultivated in LB respectively (Figure 6.3a). For *E.coli* cells cultivated in LBG, a total of 117 and 132 extracellular proteins were identified from free-EPS harvested from cells at exponential (6hr) and stationary phase (24hr) cultivated in LBG respectively (Figure 6.3b). The result suggests that extracellular proteins are differentially secreted during changes in growth phase of *E.coli* MG1655.

58 of the proteins identified in free-EPS from cells cultivated in LB were found to be common across the growth phases, with 21 and 117 proteins unique to cells harvested at the exponential (6hr) and stationary phase (24hr) respectively (Figure 6.3(a)). Likewise, 77 extracellular proteins were found to be common to free-EPS cultivated in LBG with 40 and 55 proteins unique to cells harvested at exponential (6hr) and stationary phase (24hr) respectively (Figure 6.3(b)). The differences observed are as a result of differences in the growth phase of *E.coli* MG1655.

Figure 6.4 represents the common and unique proteins for proteins identified in free-EPS of cells harvested at the same growth phase, but cultivated in different growth media. Figure 6.5a shows that 66 extracellular proteins were found to be common to free-EPS cultivated in LB and LBG and harvested at the exponential phase (6hr) with 13 and 51 unique to cells cultivated in LB and LBG respectively (Figure 6.4(a)). Similarly, 105 extracellular proteins were found to be common to free-EPS is cultivated in LB and LBG harvested at stationary phase (24hr) with 70 and 27 unique to cells cultivated in LB and LBG respectively (Figure 6.4(b)). The differences observed is due to the changes in the media (supplementing LB with 0.5% glucose, LBG) used for cultivating *E.coli* MG1655.

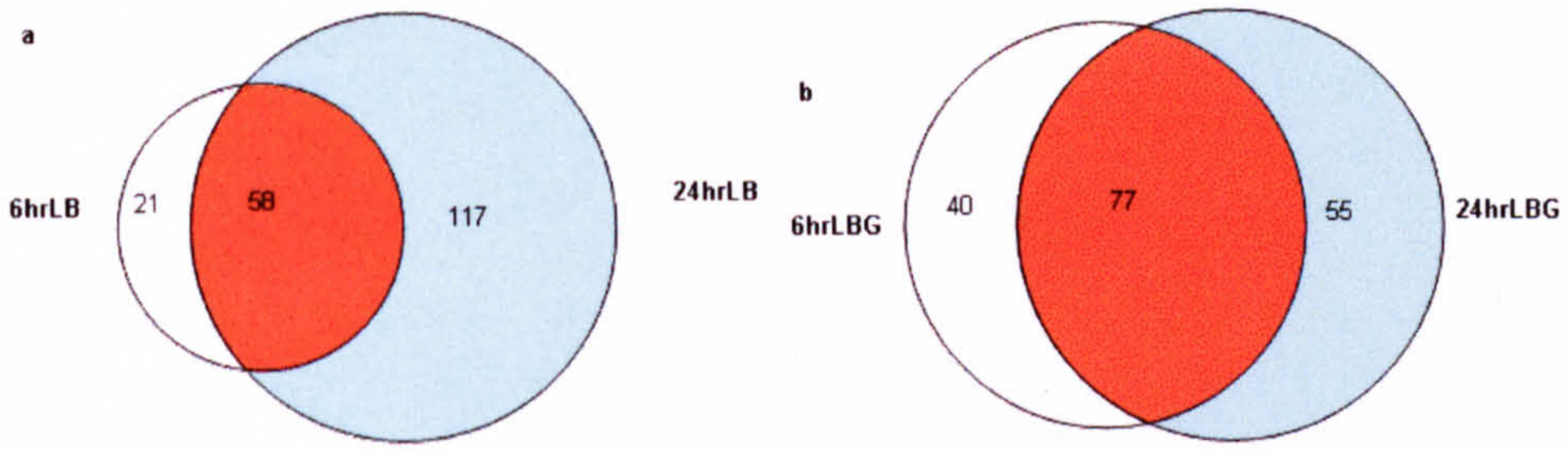

Figure 6.3 Number of extracellular protein identified as unique or common in the free-EPS of *E.coli* MG1655 cultivated at different growth phase in the same medium (a) cultivated in LB (b) cultivated in LBG.

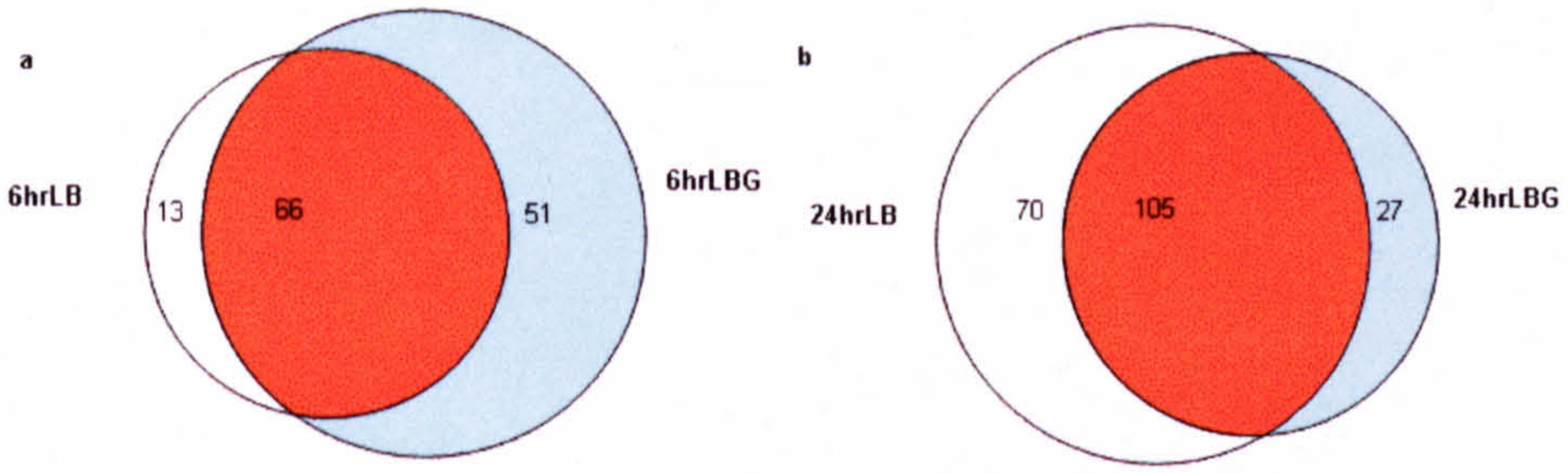

Figure 6.4 Number of extracellular proteins identified as unique or common in free-EPS of *E.coli* MG1655 harvested at (a) exponential phase (6hr) (b) stationary phase (24hr), cultivated in LB and LBG.

E.coli extracellular proteins identified in all growth conditions were categorized according to their functionality using the Encyclopedia of *Escherichia coli* K-12 Genes and Metabolism (http://ecocyc.org/) and the InterPro (http://www.ebi.ac.uk/interpro/index.html) databases (Figure 6.5). Extracellular proteins with functionality related to amino acid metabolism, carbohydrate metabolism, cell wall and membrane, cellular processes, and translation, were among the highest proteins identified from *E.coli* MG1655 under all growth and media conditions. Other extracellular proteins identified include proteins involved

in energy production, hypothetical proteins, lipid metabolism, nucleotide and nucleoside metabolism, transport and secretion, transcription. 19, 18, 22 and 25% of extracellular proteins identified were related to carbohydrate metabolism for *E.coli* MG1655 harvested at 6hr LB, 6hr LBG, and 24hr LB and 24hr LBG respectively. 6, 13, 9 and 8 % of extracellular proteins identified were related to Amino acid metabolism for *E.coli* MG1655 harvested at 6hr LB, 6hr LBG, and 24hr LB and 24hr LBG respectively.

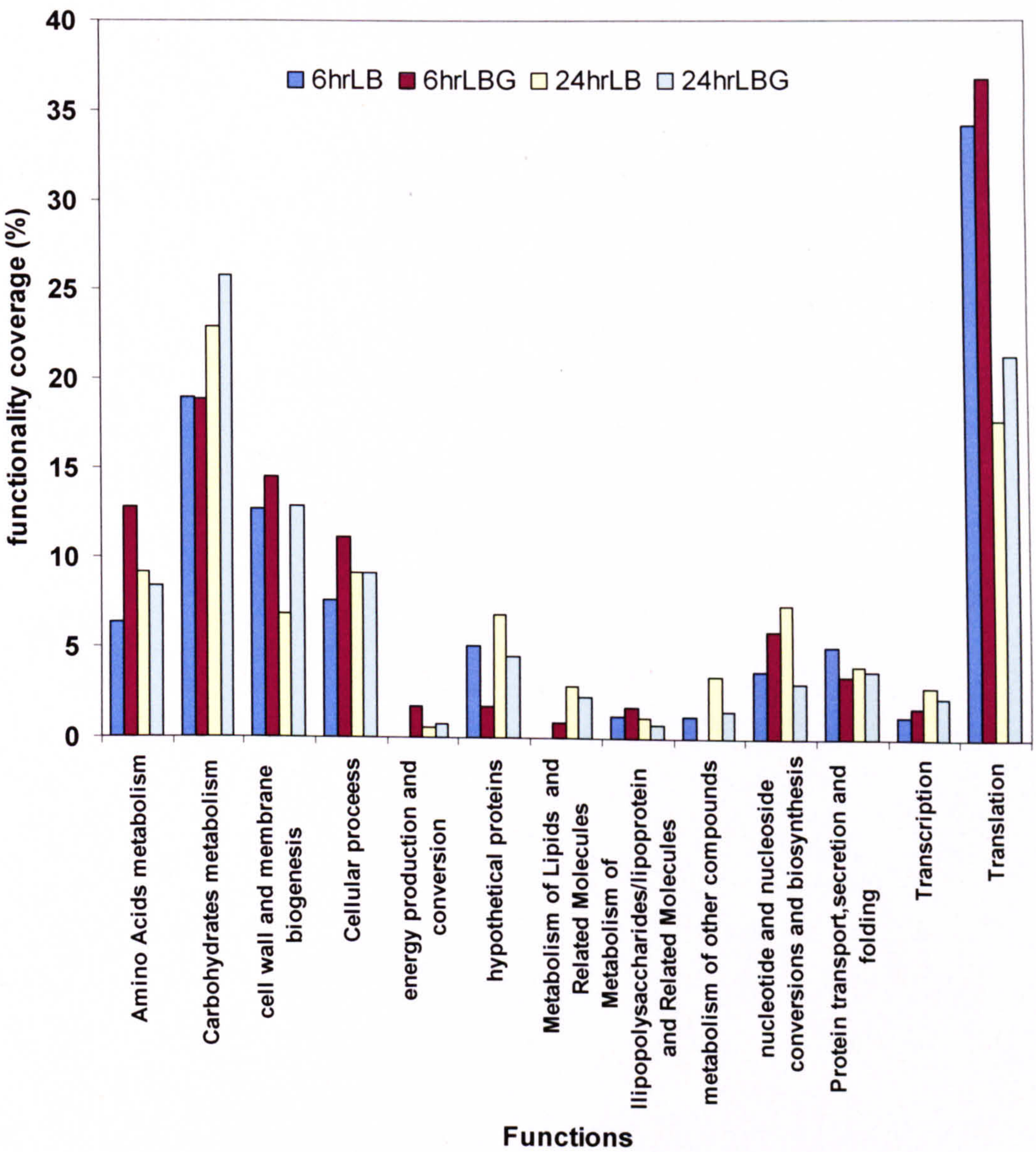

Figure 6.5 Distribution of *E.coli* MG1655 extracellular proteins identified according to their functionality groups

Several enzymes involved in glycolytic, pentose phosphate, gluconeogenesis pathways, which are involved in carbohydrate metabolism were found in the extracellular proteome of *E.coli* MG1655 cultivated in all growth phases and media. Enzymes involved in glycolytic pathway include, glyceraldehyde-3-phosphate dehydrogenase, phosphoglycerate kinase, Triosephosphate Isomerase, Phosphofructokinase, phosphoglyceromutase, phosphopyruvate hydratase (enolase) were found. Enzymes involved in amino acid metabolism such as aspartate Aminotransferase and L-threonine 3-dehydrogenase were also identified. Ribosomal Proteins involved in protein synthesis such as 30S and 50S ribosomal protein were also produced in *E.coli* ECP under all conditions.

As anticipated, the present outer membrane proteins and related proteins were also found in dominate in *E.coli* MG1655 extracellular proteome. These include outer membrane Porin protein A (OmpA), Outer Membrane Protein X (OmpX), Outer Membrane Protein W (Ompw) and outer membrane porin protein C (OmpC), which were all detected in all growth phases and media. The presence, of outer membrane proteins in the extracellular proteome of *E.coli* have been suggested to be either due to cell lysis (263, 275) or shedding of membrane macromolecules during cell growth (263). Outer membrane porin proteins are involved in transport of sugars and other solutes and ions in and out of the membrane and as such, changes in environmental condition may lead to the expression of different outer membrane proteins (140). Hence the varied number outer membrane proteins were identified in all growth conditions used in this study is not surprising. The number of outer membrane proteins and related macromolecules were higher for cells cultivated in LBG than LB regardless of the growth phase. This may be due to the expression of addition outer membrane porins required for glucose transport.

Proteins involved in various cellular processes such as adaptation of specific conditions, cell protection, motility and cell-to-cell communication were also identified in all growth conditions. The DNA protection protein (DPS), which binds to DNA to protect it from oxidative damage, was also identified under all condition of study. DPS have been reported to be hyper expressed during biofilm

formation, prolonged starvation and stationary phase (282). Proteins involved in maintaining protein folding before they are transported across the cytoplasm were also identified; these include Heat shock proteins Hsp90, chaperone Hsp60, molecular chaperone Hsp70 and Trigger Factor. The proteins, chaperone Hsp60, molecular chaperone Hsp70 and Trigger Factor were identified from all condition of study while Heat shock proteins Hsp90 was only identified in stationary growth phase (both in 24hrLB and 24hrLBG). Flagella hook-associated protein (flgK) was only found in the extracellular proteome for stationary phase *E.coli* cells cultivated in LB.

In *E.coli*, one of the mechanisms of translocation of proteins produced in cytoplasm to the outer membrane or extracellular environment is a via the general secretory (SecB) pathway. SecB, which also acts to prevent misfolding of proteins, binds to the N-terminal signal sequence of newly synthesized precursor polypeptides(preproteins) to be translocated and targets these proteins to the Sec apparatus (144, 283). A major protein involved in the general secretory pathway, molecular chaperone SecB was identified in the extracellular proteome of free-EPS from *E.coli* MG1655 in all growth conditions. Recent findings by Baars *et al* (284) have shown that SecB is involved in exporting outer membrane protein receptors for ferrichrome (FhuA), peptidyl-prolyl cis-trans Isomerase (FkpA), OmpT, OmpX, OppA, Tol-Pal system protein B (TolB) and Tol-Pal system protein C (TolC). SecB has also been linked to the export of some predicted periplasmic proteins (YbgF, YcgK, YgiW, and YncE) (284). Oligopeptide transporter protein (oppA) which facilitates the transport of oligopeptide into and out *E.coli* cells or between *E.coli* cells was also identified in the extracellular proteome under all condition of study.

It is well known that cell-to-cell communication via a quorum sensing in bacteria regulates several genes during cell growth and plays an important role in biofilm formation (109, 133). In this study, the quorum sensing protein (Autoinducer-2, LuxS) was identified in only the proteome of the exponential phase of free-EPS from *E.coli* MG1655 cultivated in LBG (6hrLBG). *E.coli* secretes quorum sensing

molecules (AI-2) into the media during exponential phase growth, and it is internalized by the cells immediately after the exponential phase, when the cells are cultivated in LB. However, in *E.coli* cells cultivated in LB supplemented with glucose, AI-2 remains in the media even after the exponential phase (see Chapter 3). This is due to the fact that glucose inhibits the uptake of AI-2 quorum sensing autoinducer (AI-2) via a decrease of cyclic adenosine monophosphate (cAMP) concentration (130). Once the glucose in the media diminishes, AI-2 can then be internalized by the cell. Hence this may account for why AI-2 was only identified in the extracellular proteome of *E.coli* 6hrLBG.

Other key extracellular proteins in *E.coli* were also identified, most of which were not unique to all growth conditions used in this study (Appendix C). For example the protein involved in flagella biosynthesis, hook-filament junction protein 1, was only identified from the extracellular proteome of *E.coli* MG1655 cultivated in LB which was harvested at the stationary phase (24hr LBG).

Extracellular proteins identified from free-EPS extracted from *E.coli* MG1655 were further characterized based on their location and hydrophobicities.

Table 6.1 shows the location of proteins identified determined by PSORTb as well the indication of the protein hydrophobicities determined from the GRAVY index. Only one extracellular protein, oxaloacetate decarboxylase was found to have a GRAVY index above or equal to +0.3 (0.322) and regarded as hydrophobic. The extracellular protein, oxaloacetate decarboxylase was only identified in the extracellular proteome of *E.coli* MG1655 harvested at the exponential phase (6hr), cultivated in either LB or LBG. All other extracellular proteins identified were found to be below the + 0.3 GRAVY index value.

PSORTb program was used to predict the cellular location of identified extracellular proteins under the different growth conditions used in this study. The extracellular proteins identified were predominantly cytoplasmic proteins with

percentages of 50.6, 59.0, 65.7 and 52.3 % for cells harvested at 6hrLB, 6hrLBG, 24hrLB, 24hrLBG respectively. A higher percentage of outer membrane proteins was seen in the extracellular proteome of *E.coli* MG1655 cultivated in LBG (12.8% and 10.6% for 6hr LBG and 24hrLBG respectively) than in the extracellular proteome of *E.coli* MG1655 cultivated in LB (8.9% and 5.7% for 6hr LB and 24hrLB respectively). The increase in outer membrane proteins observed for cells cultivated in LBG may be due to the presence of outer membrane proteins required for glucose transport. Furthermore, the percentage of periplasmic proteins was found to be higher in the extracellular proteome of *E.coli* MG1655 cultivated in LBG, harvested at the stationary phase (6.1%) then in cells harvested at the exponential phase (1.7%) in the same growth medium. Conversely, the percentage of periplasmic proteins was found to be higher the extracellular proteome of *E.coli* MG1655 cultivated in LB, remaining relatively constant in both the exponential and stationary phases (3.8% and 3.4% for 6hrLB and 24hrLB). The percentage of protein located in the cytoplasmic membrane was found to be slightly higher in the extracellular proteome of *E.coli* MG1655 cultivated in LB, than in LBG (1.3, 0.9, 1.7 and 0.8 % for cells harvested at 6hrLB, 6hrLBG, 24hrLB, 24hrLBG respectively). However, the PSORTb program is unable to predict the locations of some proteins, hence a significant percentage of the proteins in the extracellular proteome of *E.coli* MG1655 were designated as unknown (35.4, 25.6, 23.4 and 30.3 % for cells harvested at 6hrLB, 6hrLBG, 24hrLB, 24hrLBG respectively). Another drawback of the PSORTb program is that it is unable to detect membrane lipoproteins. Therefore the program LipoP v1.0 was used to address this limitation. The number of lipoproteins identified in the extracellular proteome of *E.coli* MG1655 was found to be 4, 4, 2 and 3 for cells harvested at 6hrLB, 6hrLBG, 24hrLB, 24hrLBG respectively.

Table 6.1 Comparison of extracellular proteins identified according localization and hydrophobicity

	6hrLB	6hrLBG	24hrLB	24hrLBG
LOCATION[a]	**% of total**[b]	**% of total**[b]	**% of total**[b]	**% of total**[b]
Cytoplasmic	50.6	59.0	65.7	52.3
Cytoplasmic Membrane	1.3	0.9	1.7	0.8
Extracellular	0.0	0.0	0.0	0.0
Outer Membrane	8.9	12.8	5.7	10.6
Periplasmic	3.8	1.7	3.4	6.1
Unknown	35.4	25.6	23.4	30.3
GRAVY[c] **≥+0.3**	1	1	0	0
Lipoproteins[d]	4[d]	4[d]	2[d]	3[d]
pI[e]	4.6-11.5	4.2-11.5	4.3-11.5	4.3-11.5
MW (kDa)[f]	57-100	57-104	57-151	57-151

[a]Cellular location was predicted using PSORTb v.2.0 software (http://www.psort.org/psortb/).

[b]Percentage of total proteins observed

[c]Grand average hydropathy (GRAVY) values were calculated using the ProtParam tool at http://us.expasy.org/tools/protparam.html

[d]Lipoprotein signals were obtained using the LipoP tool at www.cbs.dtu.dk/services/LipoP/.

[e]The pI range

[f]The MW range

6.5. Concluding remarks

The extracellular proteome of *E.coli* MG1655 in response to different growth and media conditions was determined using proteomic analysis. Changes in the environmental conditions such as and media and growth phase had an effect on the extracellular proteome of *E.coli* MG1655. A total of 79 and 175 extracellular proteins were identified from the free-EPS of cells harvested during the cells at exponential (6hr) and stationary phase (24hr), cultivated in LB respectively. While for *E.coli* cells cultivated in LBG, a total of 117 and 132 extracellular proteins were identified from free-EPS harvested from cells at exponential (6hr) and stationary phase (24hr) cultivated in LBG respectively. A total of 40 of these proteins were produced in all growth conditions. The quorum sensing protein (Autoinducer-2, LuxS) was identified the proteome of the exponential phase of

free-EPS from *E.coli* MG1655 cultivated in LBG (6hrLBG). Hence the information provided by the extracellular proteome may give an insight into the response of *E.coli* physiology to changes in environmental conditions.

Chapter 7 Investigating the surface properties of *Escherichia coli* under glucose controlled conditions and its effect on aggregation.

(Published in part in Langmuir 2007, 23:6691-6697)

7.1. Abstract

The hypothesis that is tested in this chapter is that the relative presence of glucose in the media, at the beginning of the growth phase, influences the surface chemistry of the cell which as a consequence reduces the tendency for the cells to interact and form aggregates. In this chapter, we used *Escherichia coli* MG1655 as a model organism, and measured the change in surface chemistry of cells harvested at different growth phases, which had been cultured in Luria-Bertani media with and without the addition of glucose, using potentiometric titration and infrared spectroscopy. Cells, cultivated with the additional supplement of glucose at the beginning of the growth phase, displayed a higher concentration of surface functional groups and a variation in outer membrane proteins. As a consequence, the tendency for cell-to-cell attachment was significantly reduced. Our findings reveal that glucose limits aggregation in *Escherichia coli* MG1655 by altering the concentration of functional groups from macromolecules present on the bacterial surface.

7.2. Introduction

This thesis has so far shown that free-EPS will induce aggregation; however EPS is not the only factor that contributes to bacterial aggregation. Like inert colloids, cell surface properties can also play a key role.

Several environmental factors, such as nutrient availability and growth phase, pH, temperature and oxygen, have all been suggested to influence aggregation (24, 25, 73), and these factors have also been shown to alter the surface properties of bacteria (63, 73, 261). Glucose has been linked to biofilm (i.e. cell to surface) formation, where supplementing the media with glucose can limit biofilm formation of *Escherichia coli* MG1655 (285). This inhibitory effect of biofilm formation of *E.coli* was attributed to catabolite repression via cyclic adenosine monophosphate ($_{C}$AMP) and $_{C}$AMP receptor proteins due to the presence of glucose. In addition, current findings have also revealed that outer membrane macromolecules are also regulated during the growth phase, and under different nutrient conditions, such as glucose or nitrogen limited conditions (73, 286-288) which have been shown to promote aggregation and biofilm formation.

Whilst the biological effect of nutrients on aggregation and biofilm formation has received great attention, physical characteristics, such as macromolecules present on the bacterial surface, including extracellular polymeric substances, flagella and pili, have also been shown to facilitate biofilm formation and aggregation (289-292). From a physiochemical perspective, however, cell-to-cell interactions leading to attachment are governed by physical laws (some van der Waals forces, but mainly electrostatic forces due to the ionisable functional groups of macromolecules on the cell surface) which relate to the diffuse layer potential of the cells, and hence have an influence on aggregation (163, 229).

Generally, bacteria cell walls possess a variety of functional groups that provide binding sites, such as, hydroxyl, phosphoryl, amines and carboxylate groups. These functional groups, arising from macromolecules on the bacterial cell wall and

extracellular polymer substances in the cell wall, can protonate or deprotonate when interacting with their immediate surroundings, and as a result, cell walls develop a net pH dependent charge (293). For Gram-negative organisms the macromolecules present on the outer membrane predominantly consist of lipopolysaccharides, phospholipids and proteins, while for Gram-positive bacteria, the macromolecules present predominantly consist of peptidoglycan and teichoic acid (31).

The outer membrane of *E.coli* serves mainly as a selective barrier for permeability and also provides strength to the cell. The outer membrane is comprised of phospholipids, lipopolysaccharides and lipoproteins and proteins which may vary from strain to strain. These macromolecules on the outer membrane possess active functional groups which include carboxyl, amino, as well as phosphate groups (Table 2.2) and play a significant role in the interaction of the cell with the environment (31) such as cell-to-cell adhesion or cells-to-solid surfaces attachment (e.g. biofilm) (294, 295) and adsorption of aqueous metal cations (296, 297). Hence, the variation in the characteristics and concentration of these macromolecules will affect cell-cell interactions. The architecture and content of these macromolecules have been shown to vary in response to changes in the environmental conditions, such as growth phase and nutrients (73, 298). However, little is known about the variation of these active functional groups on the bacteria cell wall and their implication in aggregation, especially under different conditions such as nutrient limitation and growth phase.

Hence, in this chapter, we hypothesize that those changes in the relative presence of glucose in the media, at the start of growth, influence aggregation in *Escherichia coli* MG1655 by altering the surface properties of the cell. For *E.coli* MG1655, we investigate the effect of glucose addition, with particular reference to variation in cell surface properties, in an attempt to describe aggregation in terms of the surface properties of the cell. This is achieved by carrying out aggregation studies on cells grown in media supplemented with or without glucose and elucidating their surface properties using potentiometric titration and infrared spectroscopy.

7.3. Materials and methods

All chemicals were purchased from Sigma-Aldrich (Gillingham, Dorset, UK) unless otherwise stated. All experiments were conducted in triplicate (at least), and the average of the results reported. Variation in the experimental results is presented as the average ± standard deviation.

7.3.1. Bacterial strains and Growth studies

For all aggregation and surface analysis experiments, *Escherichia coli* MG1655 was cultivated aerobically at 30°C in two different media (1) Luria-Bertani (tryptone 10.0g/L, yeast extract 5.0g/L, NaCl 10.0g/L, adjusted to pH 7.0) medium only, referred to as LB and (2) Luria-Bertani medium with the addition of 0.5w/v (%) glucose, at the beginning of the growth phase, referred to as LBG throughout the paper (as seen in Chapter 3). *E. coli* strains were grown at 30°C overnight with aeration in LB or LBG. The culture was then used to inoculate fresh LB or LBG at a 1:100 dilution and grown at 30°C with aeration. The optical density (OD) at 600nm was measured using a spectrophotometer (ThermoSpectronic, UK).

7.3.2. Glucose uptake assay

The amount of glucose present in cell-free cultures was analysed using a glucose assay kit (Kit GAGO-20 Sigma, UK). Briefly, *E.coli* MG1655 was grown in LBG as previously described. Cell-free culture fluid was obtained during the growth phase by centrifugation of the cells at 15,000rpm at 4^0C for 10 minutes. The supernatant was filtered through a 0.22μm syringe filter and samples were stored at -20^0C. The amount of glucose present in the culture fluid was then analysed as described by the manufacturer's protocol.

7.3.3. Aggregation studies

The auto-aggregation properties of *E.coli* MG1655 grown in LB and LBG, harvested at exponential (6hr) and stationary phase (24hr) were measured using the method described in Chapter 4. Cells were harvested and washed twice with 0.9%

NaCl (pH 7.0) solution. The cell pellet was then re-suspended in 0.9 % NaCl solution to an adjusted optical density (OD) of 0.6 (equivalent to ~10^8 cells/mL), prior to measurement. This ensured standardization across all aggregation tests. 1 ml of suspended cells was transferred into cuvettes and the OD corresponding to cells at the upper part of the cuvette was measured. As the cells aggregated, they settle to the bottom of the cuvette and the percentage aggregation was calculated from equation 2.1 as the difference in OD_{600} measurements between the initial measurement (time = 0 hours) and subsequent time intervals (0 to 5 hours).

7.3.4. Biofilm studies

The biofilm assay was conducted, following the crystal violet (CV) assay previously described by O'Toole and Kolter (299). Briefly, an overnight culture of cells, cultivated in LB, supplemented with or without different concentrations of glucose, was inoculated with 1:100 dilutions in fresh media (of the same concentration of glucose) in a 96-well plate (200µl). Cells were then grown for 6, 24 and 48 hours without shaking. The wells were then stained with 180µl of 0.5% CV, rinsed three times, and then solubilized by the addition of 200µl of 95% ethanol. The $O.D_{595}$ was then determined using GENios Multi-Detection Microplate Reader (Tecan, UK).

7.3.5. Extraction of outer membrane proteins (OMP)

Outer membrane proteins (OMP) were extracted from cells grown in LB and LBG, after 6 and 24 hours, following the method recently described by Kim *et al* (217). For each of the four conditions, cells were harvested and then re-suspended in 50ml of 10mmol^{-1} Tris-HCl (pH 7.5), adjusted to the same OD (~2). Cells were then washed twice and re-suspended in 5ml of same buffer. The cells was disrupted in an ice bath four times for 60s using a ultrasonic cell disruptor (Branson 450, UK) and unbroken cells were removed by centrifugation at 5000g for 10mins at 4^0C. The supernatant was then centrifuged at 21000g for 60mins and pellet (containing the cell envelope) was re-suspended in 5ml of same buffer and N-Lauroylsarcosine sodium salt (Sigma, UK) was added was added to a final concentration of 1.5% (v/v) to solubilized the inner membrane proteins (300). The

suspension was incubated at room temperature 20 min, the outer membranes were collected by centrifugation at 20000g for 90 min and suspended in sample buffer and stored at -20^{0}c used for further analysis.

7.3.6. Sodium dodecyl sulfate-poly acrylamide gel electrophoresis (SDS-PAGE)

Sodium Dodecyl Sulfate Polyacrylamide Gel Electrophoresis (SDS-PAGE) was performed on the OMP extract from *E.coli* MG1655 cells grown in LB and LBG, harvested at different growth phases, using a 12% (w/v) polyacrylamide gel (276). OMP extracts (75-80µg per lane) were electrophoresed at a constant voltage (120V) until the bromophenol blue tracking dye front reached the bottom of the gel. Low-molecular-weight protein markers (New England Biolabs, UK) were used as protein standards and the protein bands were visualized with Bio-Safe Coomassie blue stain (Bio-Rad, UK).

7.3.7. Extraction of lipopolysaccharides (LPS)

LPS was extracted from *E.coli* MG1655 using an LPS extraction kit (Molecular solutions Europe, UK). Extraction was performed according to the manufacturer's protocol. This method for extracting LPS have also been recently used to study *Salmonella enterica* serotypes (216).

7.3.8. Potentiometric titration

Potentiometric titration was carried out to determine the different types of functional groups on the bacterial surface (43). All titrations were made in a vessel with a lid as part of a Metrohm Titrino 718 STAT automatic titrator (Metrohm, UK) at 20^{0}C. Temperature was kept constant and continuously monitored during the titration. *E.coli* harvested at different growth phases from different medium (LB and LBG); equivalent to constant 75mg dry weight of biomass for all cases (washed four times with $NaClO_4$), was suspended in a vessel with 25 mL of $NaClO_4$, and then purged with N_2 for 1h to remove CO_2. The same OD was then used for each experiment, following the methods of Burnett *et al.* (168) and Banerjee *et al.* (301).

A positive pressure was maintained during the titration by allowing a gentle flow of N_2 on the headspace of the vessel. The suspension was titrated with 0.1 M HCl until pH=3.5 and then with 0.1 M NaOH until pH=10. In order to test reversibility of the protonation-deprotonation behavior, the suspension was back titrated with 0.1 M HCl from pH 10 to 3.5. In order to calculate the acidity constants (pK_a), and the corresponding total concentration of the binding site, data from each titration curve were fit using the programme Protofit 2.1 (169). A student paired t-test was used to determine any statistical differences between the active site concentration of cells cultivated in LB and LBG at a 95% confidence level ($P<0.05$).

7.3.9. Fourier transformation infrared spectroscopy (FTIR)

Fourier transformation infrared spectroscopy (FTIR) spectroscopy was conducted using a Perkin Elmer Spectrum One Fourier Transformation Infrared Spectrophotometer (PerkinElmer, UK), in order to characterize the various functional groups present on the cell surface and the extracted OMP. At least 100 scans, with resolution of $4cm^{-1}$, were collected for all samples. Cells were harvested as described above and washed twice with 0.9% NaCl. Bacterial suspensions in 0.9% NaCl were scanned using a demountable liquid-cell kit (Sigma, UK) with CaF_2 windows. The spectra of 0.9% NaCl were used as a background and the baseline shift of the spectra was corrected using the Spectrum One software. This was carried out for cells grown in LB and LBG at different growth phases. To study the OMP and LPS 20µL (~3.5 mg/ml) of OMP extracts were placed on a CaF_2 slide and allowed to dry at room temperature for 45 minutes. The spectra for each sample were then collected as detailed above.

7.4. Results and Discussion

7.4.1. Auto-aggregation at different growth phases and biofilm studies.

The increase in cell number over time for *E.coli* MG1655 grown in LB and LB supplemented with 0.5 w/v% glucose is shown in Chapter 3. The graph represents a typical growth curve under batch conditions with three clearly distinct phases i.e. lag phase 0-1hrs, exponential 2-8hr (3hr, 6hr and 8hr represent early, mid and late exponential phase respectively) and onset of stationary phase after 8 hrs. The specific growth rate was found to be the same ($0.34h^{-1}$) for *E.coli* MG1655 grown in LB or LBG (as previously described in Chapter 3). The uptake of glucose, under batch conditions, for 0.5% glucose, is also shown in Figure 3.2. Over 97% of the 0.5% glucose in the LB media was taken up in the cells within 6hrs of growth, with no glucose remaining after 8 hours. Viability of cells was found to be approximately 83 and 81% for cells at exponential (6hrs) and stationary (24hrs) phase respectively in both media.

Figure 7.1 and Figure 7.2 show the auto-aggregation ability of *E.coli* MG1655 cultivated in LB and LBG (i.e. LB with 0.5% glucose) harvested at mid-exponential phase (6hr) and stationary phase (24hr) respectively. For cells harvested during the exponential phase, the initial aggregation capability of the cells cultivated in LB and LBG is similar. However, after 2.5hrs of aggregation, the cells grown in LB displayed a slightly greater aggregation potential than cells cultivated in LBG Figure 7.2). After 5 hours, the percentage of cells aggregated was more than 40% for cells grown in LB compared to 30% for cells grown in LBG.

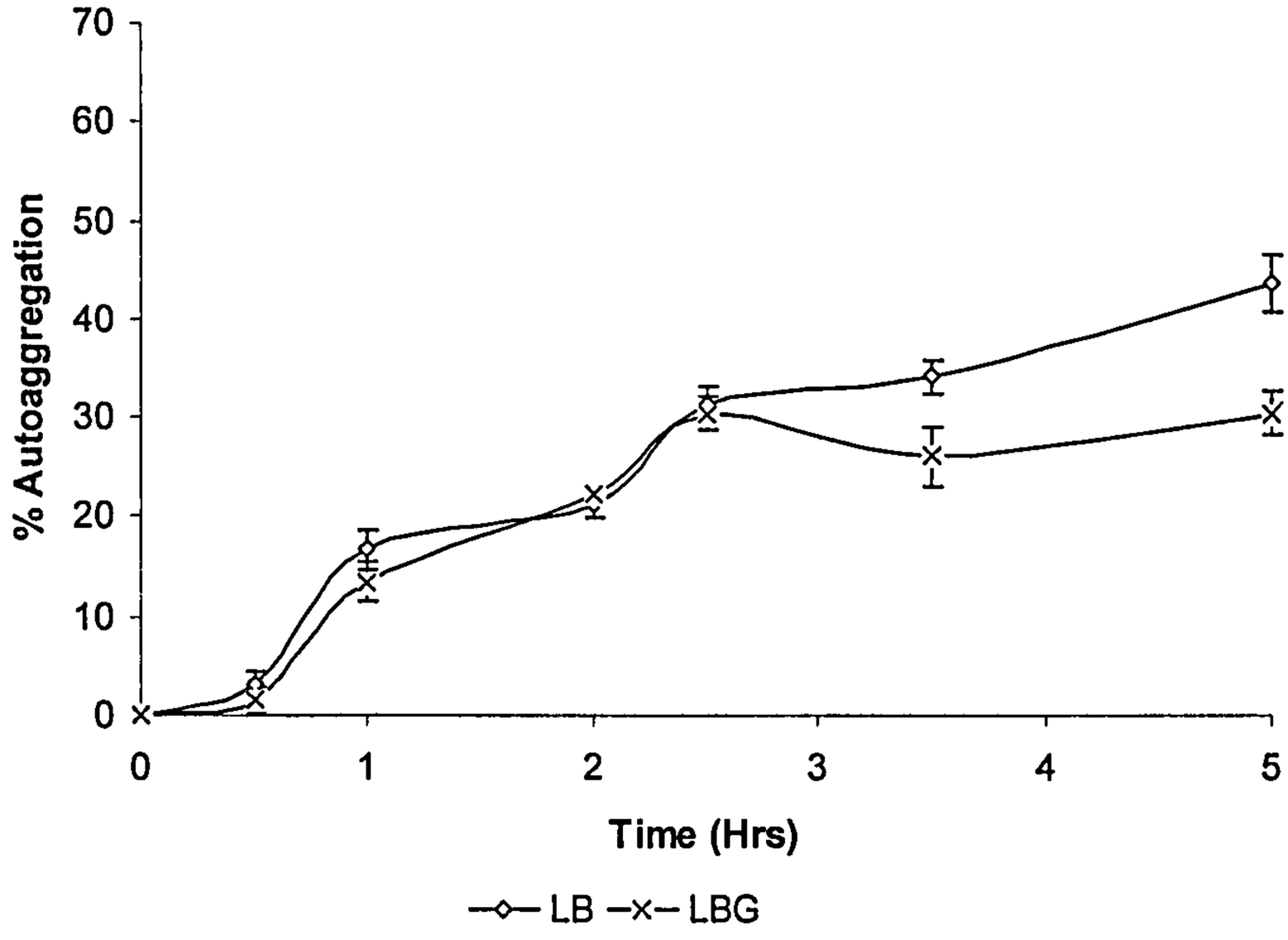

Figure 7.1 Percentage auto-aggregation of *E.coli* MG1655 cultivated in LB and LBG (LB with 0.5% glucose) harvested at during the mid-exponential growth phase (6 hours).

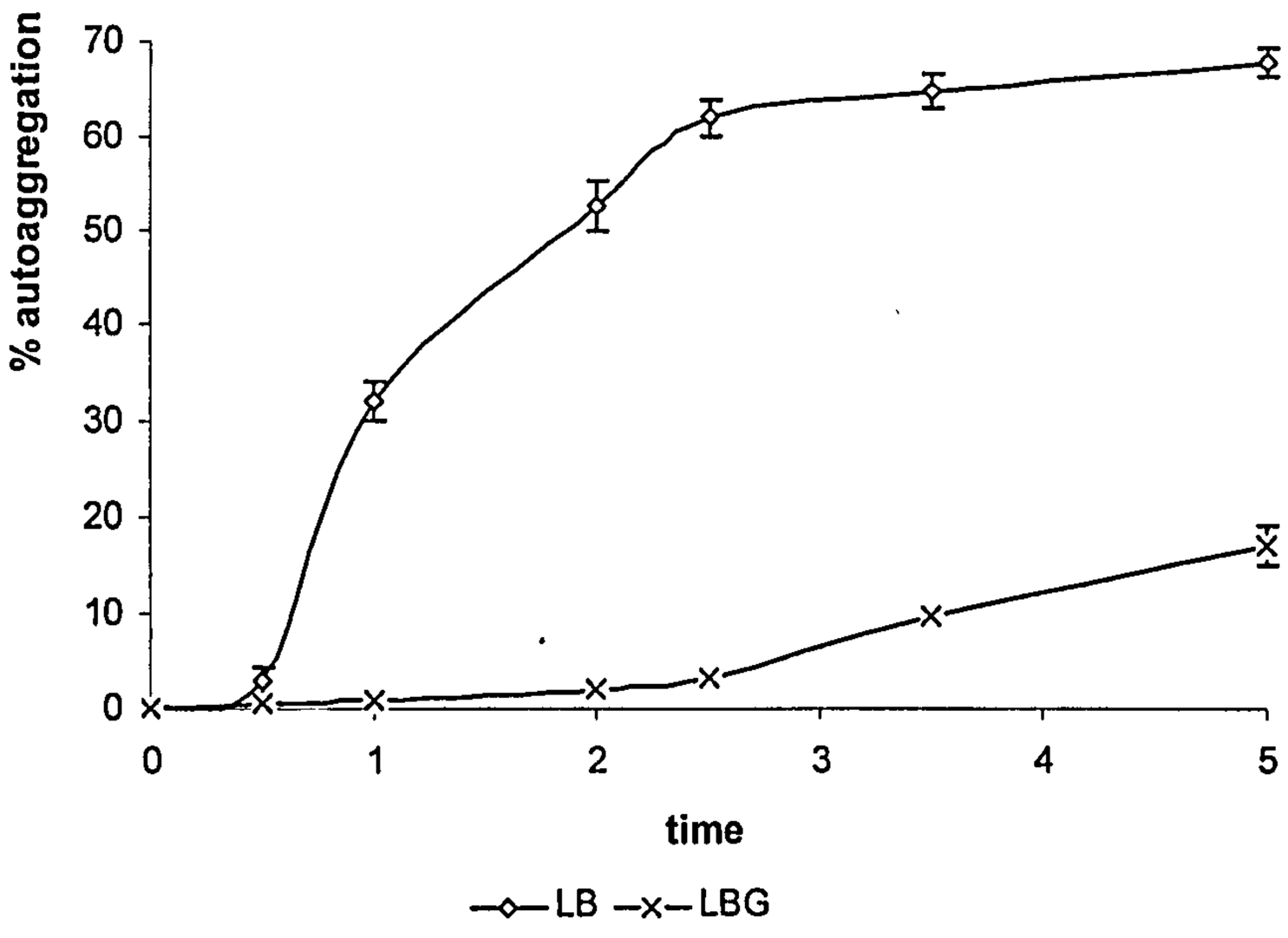

Figure 7.2 Percentage auto-aggregation of *E.coli* MG1655 cultivated in LB and LBG (LB with 0.5% glucose) harvested during the stationary growth phase (24 hours).

For cells harvested during the stationary phase, the tendency to aggregate increased dramatically for cells cultivated in LB, where the percentage of cells aggregated increased to 65% after 2.5hrs and remained relatively constant for the remainder of the test (Figure 7.2). The increase in aggregation ability of cells cultivated in LB, from exponential to stationary phase, is consistent with results from previous studies where they also found that the aggregation and the adhesion properties of cells increased in the stationary phase (63, 79). In contrast, stationary phase cells, cultivated in LBG, showed low aggregation properties. The aggregation potential of cells cultivated in LBG was low and relatively constant for the first 2 hours, with only a gradual increase to approximately 10% aggregation after 5hrs. Even though most of the glucose in the media was consumed during the exponential growth phase (see Figure 3.2), the addition of glucose to the media, resulted in a greater than 6 fold decrease in aggregation ability for cells cultivated in LBG compared to cells cultivated in LB, both harvested during the stationary phase. Hence, based on these results, glucose reduces the tendency for of *E.coli* MG1655 in the stationary growth phase to form aggregates.

Visual observation of the effect of glucose on aggregation can be seen in Figure 7.3 1mL of *E.coli* cells (OD = 0.65), harvested at the stationary phase, were rinsed in 0.9% NaCl and re-suspended in 0.9% NaCl and left undisturbed for 5 hours. The cells that were grown in LB and harvested during the stationary phase aggregated, and therefore settled to the bottom of the cuvette, leaving a clear solution (Figure 7.3 (i-iii)). In contrast, the solution containing cells grown in LBG remained fairly turbid as a majority of cells were still in solution (Figure 7.3 (iv-vi)). The formation of aggregates, in LB is further demonstrated using Epifluorescence microscopy (Figure 7.4), where more aggregates were found in cells cultivated in LB than in LBG (Figure 7.5).

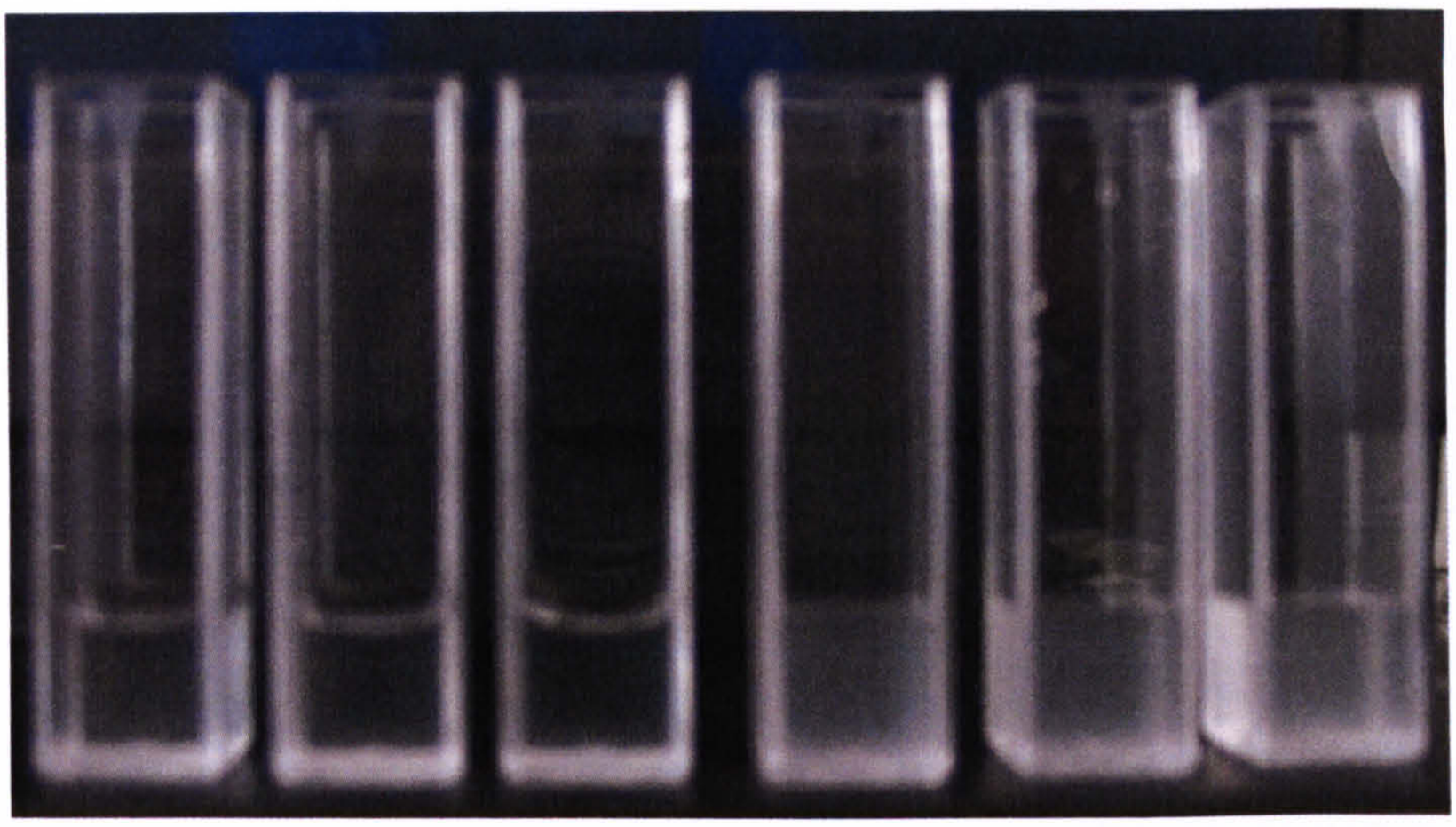

(i) (ii) (iii) (iv) (v) (vi)

Figure 7.3 Visual inspection of the auto-aggregation of *E.coli* MG1655 grown in LB (i-iii) and LBG (LB with 0.5% glucose) (iv-vi), harvested at stationary growth phase (24 hr). Picture was taken after 5 hours

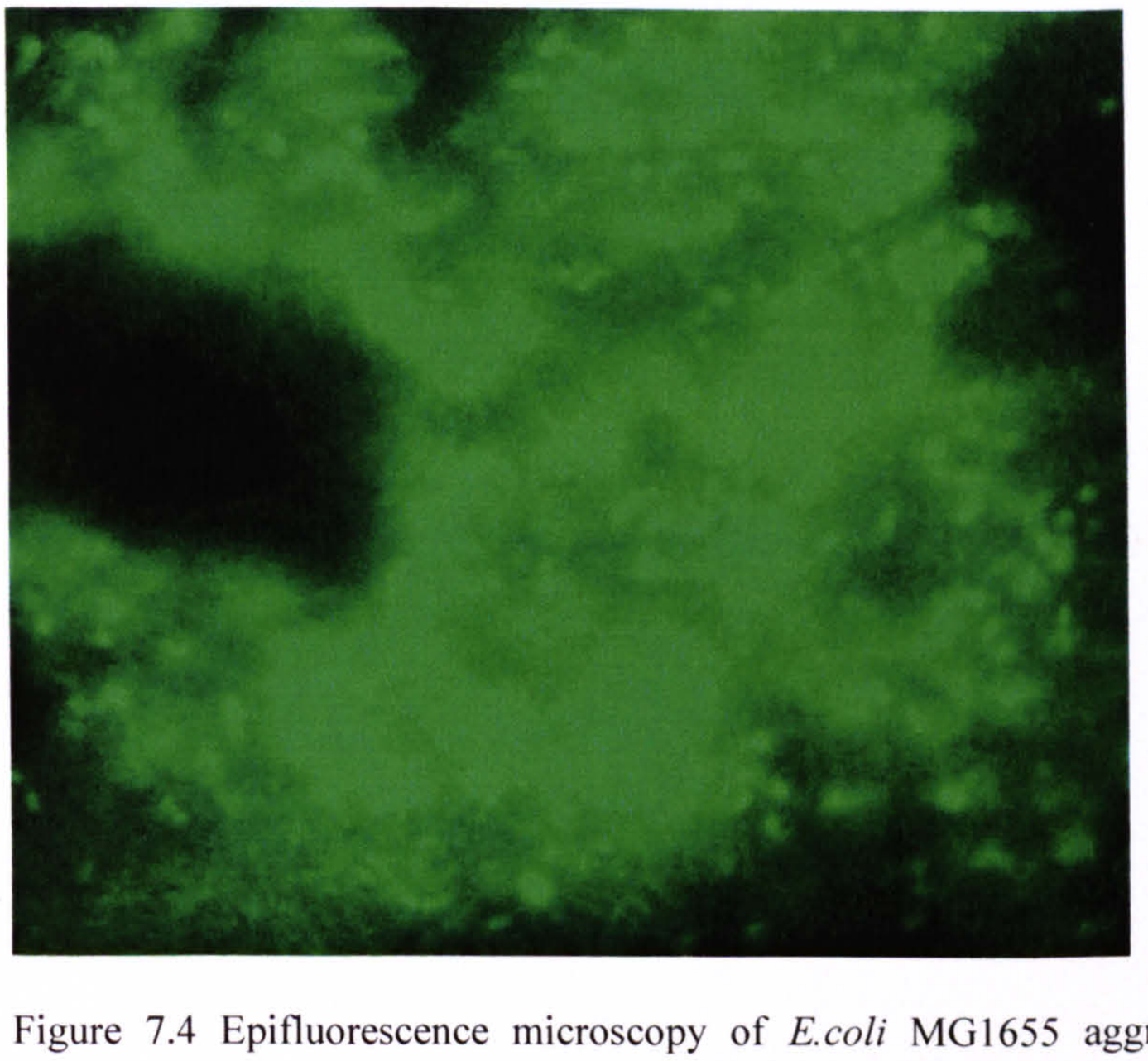

Figure 7.4 Epifluorescence microscopy of *E.coli* MG1655 aggregates formed in LB harvested after 24 hours. Cells were stained with SYTO 9 (Invitrogen, UK) and imaging was performed using an Axioplan II imaging fluorescence microscope equipped with DF10 filter (Carl Zeiss Ltd, UK) and 63× magnification.

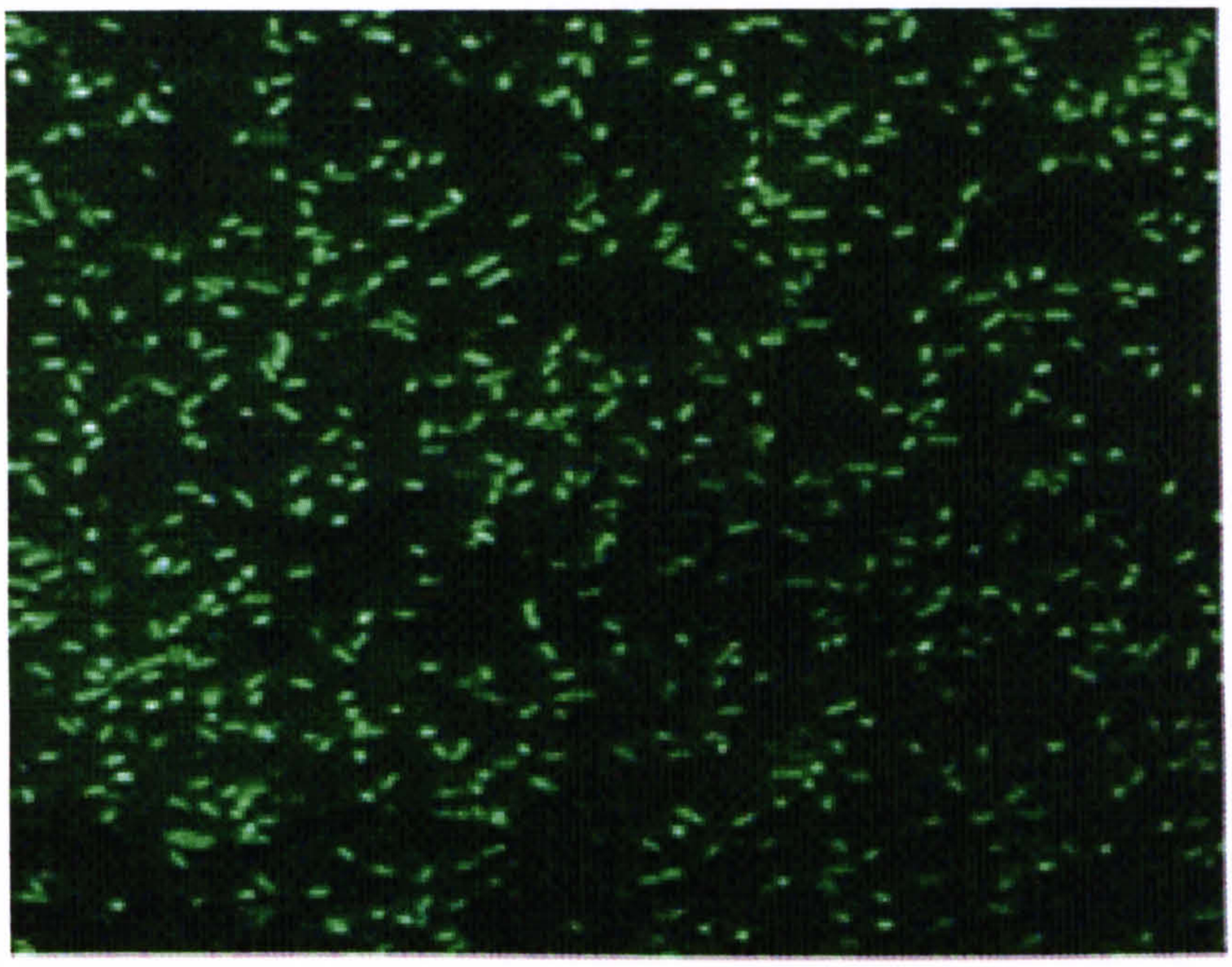

Figure 7.5 Epifluorescence microscopy of *E.coli* MG1655 single cells found in LBG (LB with 0.5% glucose), both harvested after 24 hours. Cells were stained with SYTO 9 (Invitrogen, UK) and imaging was performed using an Axioplan II imaging fluorescence microscope equipped with DF10 filter (Carl Zeiss Ltd, UK) and 63× magnification.

Whilst, the focus of this thesis is not specifically on biofilm formation, biofilm studies were conducted here for comparison. The effect of glucose in biofilm formation of *E.coli* MG1655 after 6, 24 and 48hr of biofilm growth can be seen in Figure 7.6. We anticipated that glucose may also affect biofilm formation (cell to surface) in *E.coli* since it was found to affect aggregation (cell to cell) as shown in Figure 7.1 and Figure 7.2. No significant difference in biofilm formation was found for cells cultivated in LB and LB supplemented with all concentrations of glucose, after 6 hours growth. This compares with a similar aggregation potential of cells, harvested in the exponential phase, from both LB and LBG, as shown in Figure 7.1. For cells, cultivated in LB and LB with 0.1% glucose, after 24 hours growth, a higher biofilm formation capacity was found than for cells cultivated in the same medium, but after 6 hours growth. The opposite effect was seen for cells grown in 0.5% and 1% glucose, where a decrease in biofilm formation was found after 24 hours of biofilm growth, compared with 6 hours.

For cells cultivated in LB and LB with 0.1% glucose, an increase in biofilm formation was found after 48 hours, compared to biofilm formation after 6 and 24 hours. Cells cultivated in LB and LB with 0.1% glucose, after 48 hours, also had a similar biofilm formation capacity, which demonstrates that addition of 0.1% glucose did not significantly inhibit biofilm formation. However, cells cultivated in LB and LB with 0.1% glucose, after 48 hours, had a greater biofilm formation capacity that cells cultivated in LB with 0.5 and 1% glucose, at the same growth phase. This therefore demonstrates that beyond 6 hours, increasing the glucose concentration beyond 0.1% glucose inhibits biofilm formation for a constant growth phase, suggesting that glucose repression of biofilm in *E.coli* is concentration dependent.

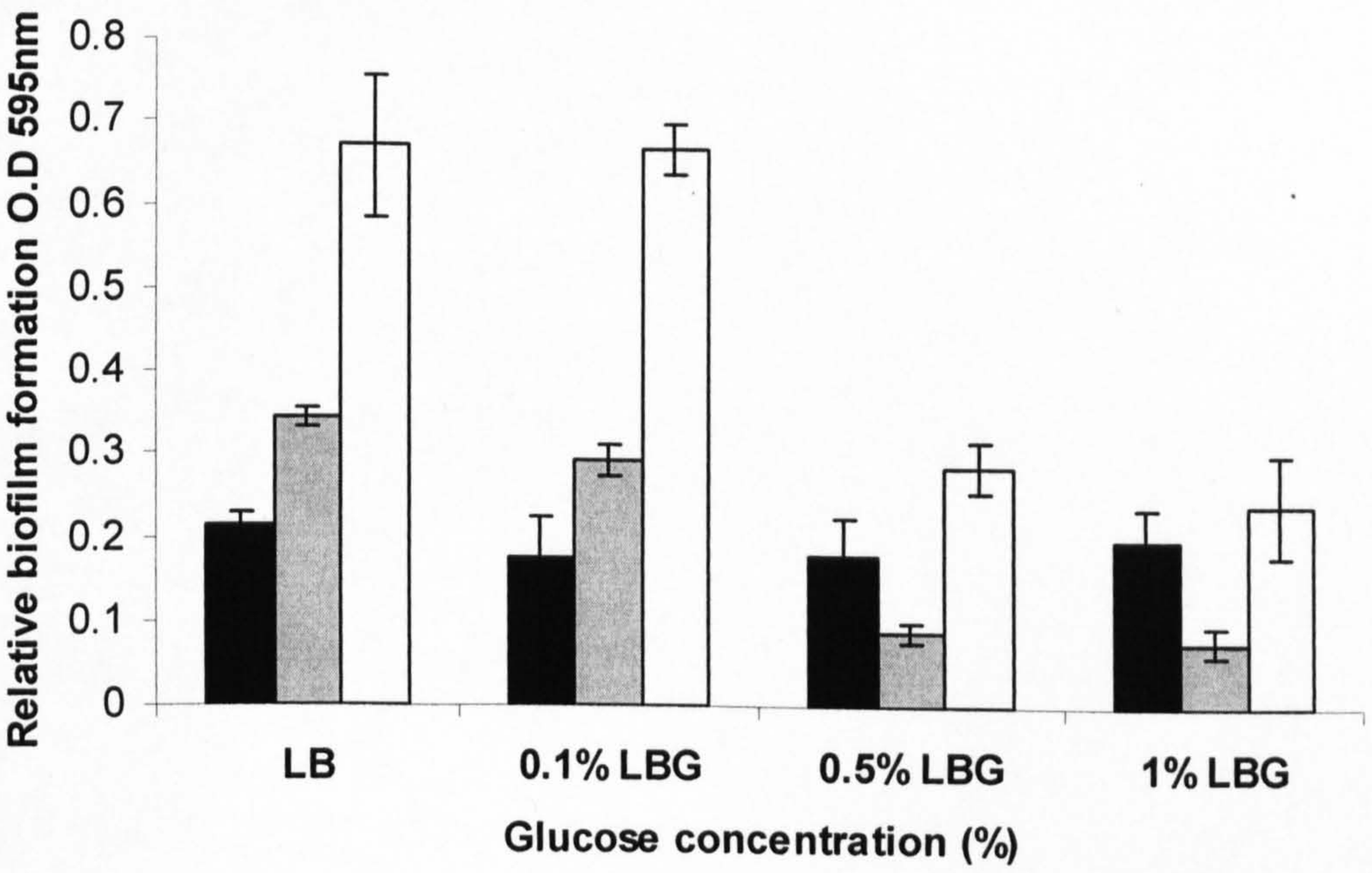

Figure 7.6 A comparison of biofilm formation capacity of the *E. coli* MG1655 cultivated in LB and LB supplemented with 0-1% glucose after 48, 24 and 6hrs growth

The effect of glucose on aggregation (Figure 7.1 to Figure 7.5), rather than biofilm formation (Figure 7.6), of this particular bacterial strain has not yet been reported,

but similar effects of glucose on biofilm formation, as seen here, has been previously reported for several species of Enterobacteriaceae (285). Jackson *et al.* (285) added 0.2 (w/v) % of glucose to *E.coli* MG1655 at different times of growth, and observed the inhibition of biofilm formation at 24 hours. The inhibition was linked to catabolite repression via cyclic AMP ($_{C}$AMP) and $_{C}$AMP receptor proteins (285). Interestingly, their findings revealed that the glucose/biofilm inhibition effect did not return already formed biofilm back to a planktonic state. Hence, glucose may only affect the initial cell adhesion process.

In this current study, 0.1 to 1 (w/v) % of glucose was added only once to the inoculated culture, and the amount of biofilm formed was monitored during the bacteria growth cycle. This approach allows the effect of glucose concentration, uptake, depletion and growth phase on biofilm formation in *E.coli* MG1655 to be taken into account. As a result, the inhibition effect of glucose on biofilm formation was found to be dependent on the bacterial growth phase as well as the glucose concentration (Figure 7.6). This finding correlates well with recent findings by Stanley *et al.* (302), revealing that 0.1% glucose did not inhibit biofilm in *Bacillus subtilis* but the addition of 1% glucose did. Stanley *et al.* (302) also revealed that major macromolecules presence on the *Bacillus subtilis* cell wall, including proteins, lipoproteins, teichoic acid, teichuronic acids were differentially expressed, adding to the glucose inhibitory effect.

Furthermore, media supplemented with glucose have also been showed to inhibit the uptake of AI-2 quorum sensing autoinducer (AI-2) via a decrease of cyclic adenosine monophosphate (cAMP) concentration (130) in the cell due to catabolite repression. Once glucose is depleted cAMP concentration increases and the lsr operon is activated by cAMP, and AI-2 is internalized by the cells (128). Recently, AI-2 was found to alter the cell surface charge during growth of this *E. coli* MG1655 strain cultivated in both LB and LBG (261). It was also observed that a mutant lacking the gene (AI-2) for quorum sensing in *E.coli* MG1655 displayed a lesser negative charge than the wild type suggesting that AI-2 may play a role in altering surface characteristics. It is not surprising therefore that AI-2 has been

showed to control biofilm formation in *E. coli* by controlling the genes involved in the regulation of membrane proteins (303, 304). as well as activities such as motility (132).

Based on the observed limitation of aggregation, due to the relative presence of glucose in the media, it is hypothesized that this may be due to the differential expression of surface macromolecules present on the cell wall of *E.coli* MG1655, which alters the cell surface chemistry and presence of these active functional groups. In order to gain further understanding on the interaction responsible for aggregation in *E.coli*, the active functional groups of the cells were quantified and characterized using potentiometric titration and infrared spectroscopy (43, 171).

7.4.2. Titration studies

The potentiometric titration curves of *E.coli* MG1655 grown in LB and LBG at different growth phase is presented in

Figure 7.7 and Figure 7.8 respectively. The concentration of deprotonated sites is standardized per mass of dry bacteria (mol/g), and calculated as follows:

$$[H^+]_{consumed/released} = (C_a - C_b - [H^+] + [OH^-]) / m_b \qquad \text{Equation 7.1}$$

Where m_b is the dry weight of the bacteria in suspension concentration (g/L), C_a and C_b are the concentrations of acid and base added at each titration step and $[H^+]$ and $[OH^-]$ represent molar species concentrations of H^+ or OH^-, and suspension concentration (g/L).

All acid-base titration curves of *E.coli* cultivated with different media and at different growth phases displayed protonation or deprotonation throughout the titrated pH range (3.5-10). For all titration curves the proton adsorption/desorption reactions were essentially reversible. During the whole titration, no evidence of

saturation was observed with respect to proton adsorption. A comparison of the shapes of the titration curves for *E.coli* MG1655 and the electrolyte without bacteria (blank) showed that that the bacteria provided enough buffering capacity to the solution over the selected pH range. The absence of this behavior would have caused the slope of the bacterial suspension titration curve to match with the one corresponding to the blank. This buffering capacity is due to functional groups on the bacterial surface consuming the added base by losing protons or the added acid by accepting protons (43).

Figure 7.7 shows the titration curve of *E.coli* MG1665 at different growth phases cultivated in LB. Each curve represents the average of replicate samples, taken at different growth phases and standardized against the cell mass. A degree of variability can be seen in Figure 7.7 but these differences may not be significant due to the heterogenic nature of bacteria surfaces. More important, are the differences in titration curves observed when cells were grown in LBG (Figure 7.8) compared to LB. Titration curves of cells grown in LBG at different growth phases were found to have a steeper slope than cells grown in LB. This indicates that the bacteria grown in LBG provided higher buffering capacity to the solution over the selected pH range, due to the functional groups on the bacterial surface consuming the added base (by losing protons), or the added acid (by accepting protons).

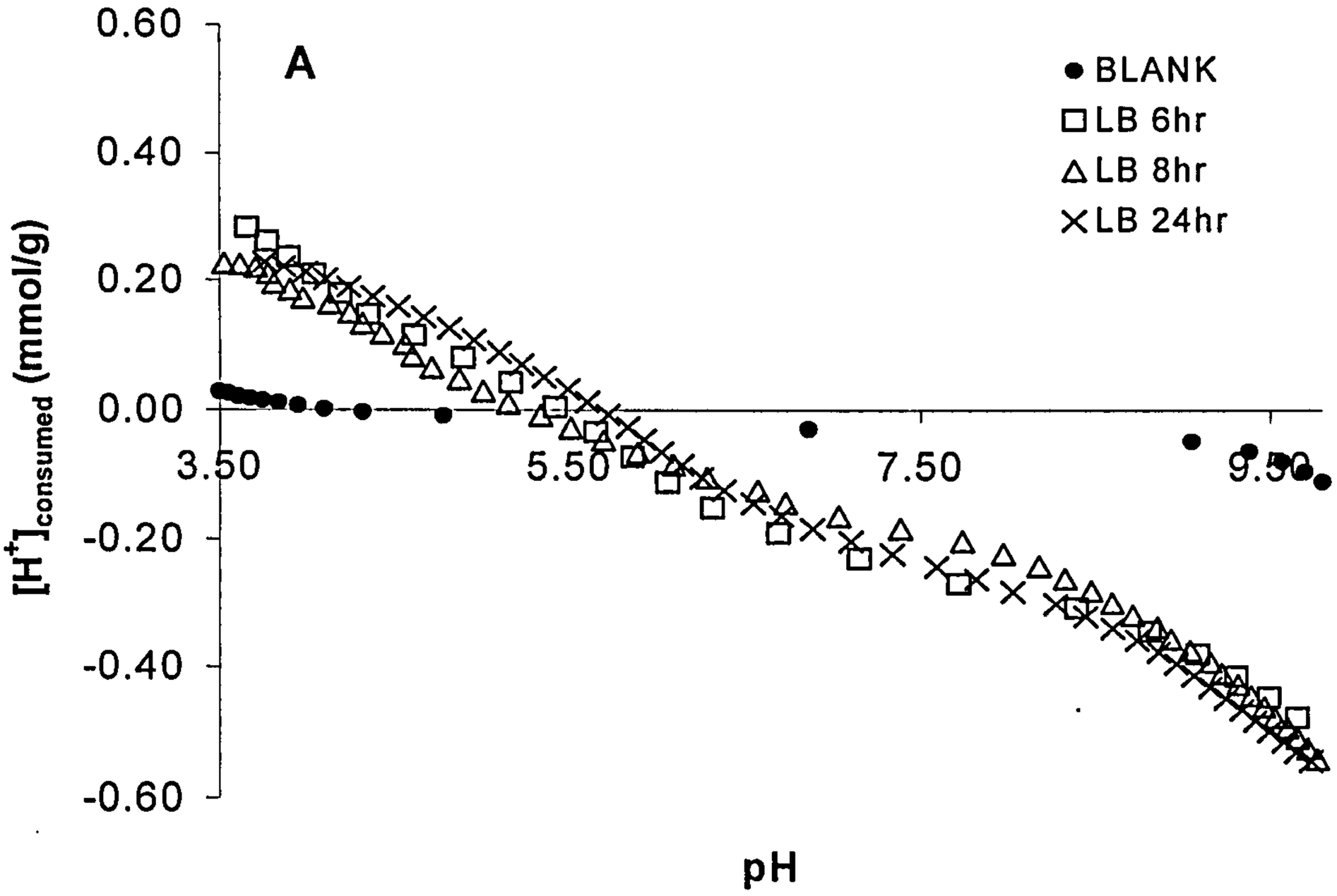

Figure 7.7 Potentiometric titration curve of *E.coli* MG1655 harvested at cultivated in LB

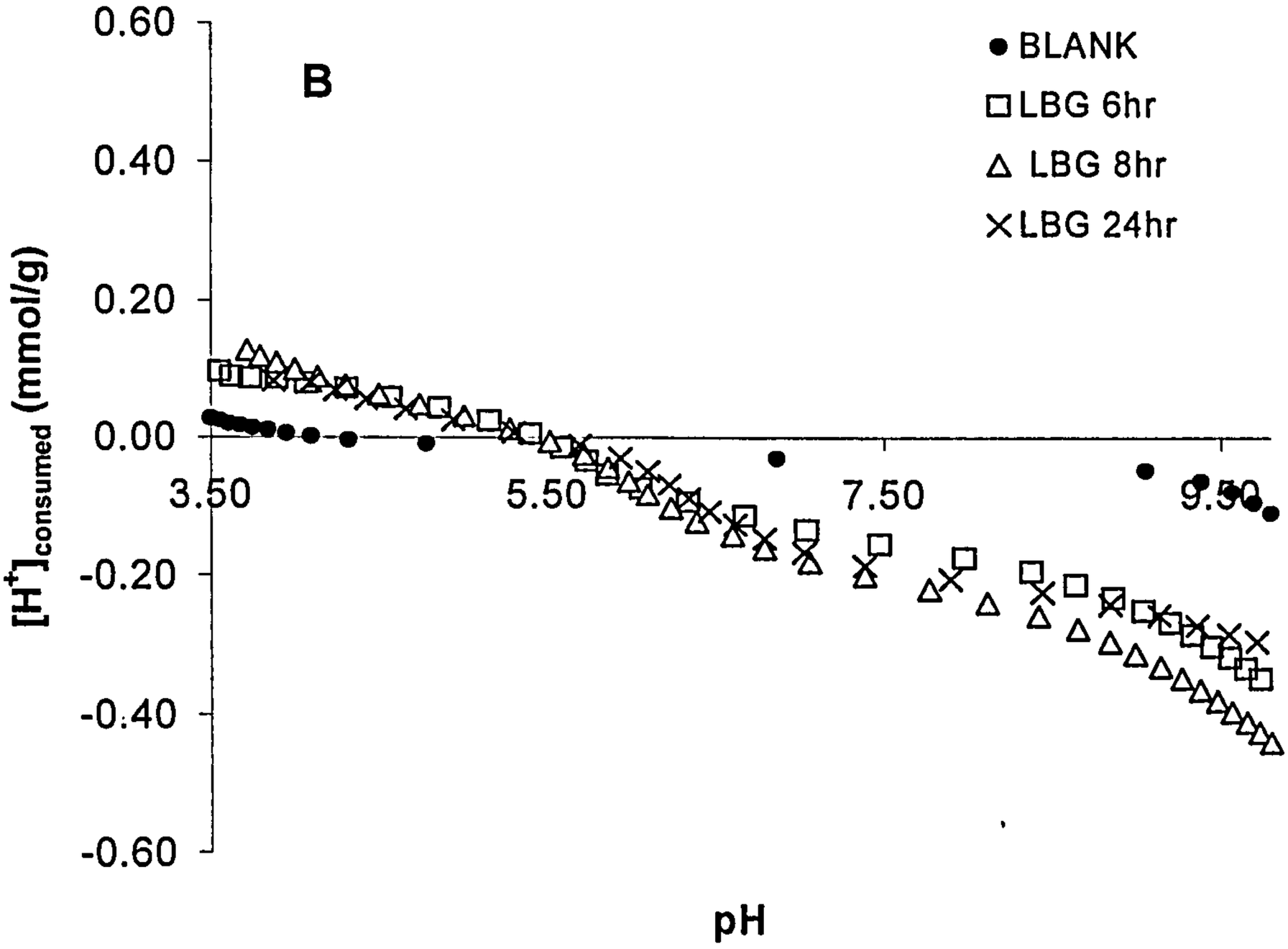

Figure 7.8 Potentiometric titration curve of *E.coli* MG1655 harvested at cultivated in LB

In order to calculate the acidity constants (pK_a), data from each titration curve was fit using Protofit 2.1. A three-site model was applied to the titration curves to predict the active functional groups on the *E.coli* surface. A three-site model was found to be the best fit model for predicting the active functional groups, rather than a two-site or four-site model. The three site model has also been found to be useful in elucidating the deprotonation constants in previous studies in both Gram positive and Gram negative bacteria (31, 43, 74, 174). Table 7.1 shows that the pK_a values for *E.coli* MG1655 range from 3.4 ± 0.4 to 4.4 ± 0.2 for pK_1, 5.6 ± 0.5 to 6.9 ± 2.4 for pK_2, and 9.9 ± 0.6 to 11.1 ± 0.2 for pK_3. The calculated pK_a values could be tentatively assigned to carboxyl (pK_1), phosphate (pK_2), and amine (pK_3) groups. These values are consistent with previously published work on biological systems (74), however, the pK_a values for *E.coli* MG1655 at different growth phases and media were not dramatically different. This suggests that all active functional groups are present on the *E.coli* surface, even when the growth phase and media changes and that the types of the macromolecules present on the surface remains the same.

The average pH of zero proton charge (pH_{zpc}) for *E.coli* MG1655, as predicted by Protofit 2.1, was found to be 4.9 ± 0.4 for cells cultivated in LB or LBG, across all the growth phases. This is in agreement with the pH_{ZPC} value reported for a different strain of *E.coli, i.e. E.coli* AB264 (pH_{ZPC} = 5.7 ± 0.2) (305).

The surface site concentrations obtained using Protofit 2.1 (normalized to the dry mass of bacteria) for different growth phases and media can also be seen in Table 7.1. The values vary from one condition to another with the total concentration of active sites varying from 11.4 ± 0.3 × 10^{-4} mol/g to 24.1 ± 1.7 × 10^{-4} mol/g. A similar range was found by Hong and Brown (31) who reported the total concentration of active functional groups for *E.coli* ATCC 29181 to be between 7.1 × 10^{-4} mol/g and 39.8 × 10^{-4} mol/g. Borrok *et al.* (297) report values of 2.52 × 10^{-4} mol/ wet g for *E.coli* AW607, which is lower than the results reported here

and by Hong and Brown (31). However it is difficult to compare the results as the basis of wet versus dry weight is different.

For *E.coli* MG1655 grown in LB, the C_{tot} value (again normalized against cell mass) was found to decrease slightly from $12.6 \pm 1.4 \times 10^{-4}$ mol/g to $11.4 \pm 0.3 \times 10^{-4}$ mol/g as the cells moved from the exponential to the stationary phase. A reverse trend was observed for cells cultivated in LBG, with the C_{tot} increasing from $12.3 \pm 0.8 \times 10^{-4}$ mol/g to $20.0 \pm 0.6 \times 10^{-4}$ mol/g as cells move from the exponential to the stationary phase. Cells harvested at 8hr and 24hr (late-exponential and stationary phase) exhibited a dramatic increase in C_{tot} over that at 6hr, which may be due to an increase in membrane protein and lipopolysaccharides (LPS) as a result of depletion of glucose in the media (306). These findings suggest that although the types of macromolecules present on the *E.coli* surface remain the same, their concentration varies dramatically when cells are supplemented with glucose during growth, and this is responsible for the differences in their surface chemistry.

Table 7.1 Deprotonation constants and surface site concentration for *E.coli* MG1655 grown in LB and LBG (LB with 0.5% glucose) at different growth phases calculated by Protofit 2.1.* Variation in the replicates are reported as the average ± SD. Student paired t-test was used to assess the active site concentration of cells cultivated in LB and LBG were statistical different at 95% confidence level ($P<0.05$)

Deprotonation Constants				
	pK_1	pK_2	pK_3	pH_{ZPC}
E.coli LB 6hr	3.4 ± 0.4	5.6 ± 0.5	10.3 ± 0.3	4.5
E.coli LB 8hr	4.4 ± 0.8	6.9 ± 2.4	10.3 ± 0.1	5.5
E.coli LB 24hr	4.2 ± 0.1	5.8 ± 0.3	9.9 ± 0.6	5.0
E.coli LBG 6hr	4.4 ± 0.2	6.1 ± 0.1	10.6 ± 0.1	5.1
E.coli LBG 8hr	3.9 ± 0.1	6.2 ± 0.1	11.1 ± 0.2	4.9
E.coli LBG 24hr	4.1 ± 0.1	5.9 ± 0.5	10.8 ± 0.4	4.5

Surface Site Concentration				
	C_1 ($\times 10^{-4}$ mol/g)	C_2 ($\times 10^{-4}$ mol/g)	C_3 ($\times 10^{-4}$ mol/g)	C_{tot} ($\times 10^{-4}$ mol/g)
E.coli LB 6hr	3.1 ± 0.9*	3.7 ± 0.9*	5.8 ± 0.7*	12.6 ± 1.4
E.coli LB 8hr	1.3 ± 1.2	2.8 ± 0.8*	7.9 ± 1.2*	12.5 ± 1.9
E.coli LB 24hr	2.1 ± 0.1	3.5 ± 0.3*	5.9 ± 0.1*	11.4 ± 0.3
E.coli LBG 6hr	1.1 ± 0.8*	2.1 ± 0.1*	9.1 ± 0.2*	12.3 ± 0.8
E.coli LBG 8hr	1.4 ± 0.2	2.5 ± 0.1*	20.2 ± 1.6*	24.1 ± 1.7
E.coli LBG 24hr	1.4 ± 0.1	3.8 ± 0.3*	14.8 ± 0.5*	20.0 ± 0.6

Cells which were harvested at 24hr in LBG displayed a higher total concentration of active functional groups than cells harvested at the same time from LB media. The major increase in active functional groups occurred in C_3 which corresponds to amine and hydroxyl groups predominantly from membrane proteins, suggesting that glucose induces the expression of membrane proteins. The variations of the active functional groups, displayed as a result of differences in growth phase and medium helps predict the electrostatic interaction which governs cell-to-cell or cell-to-surface interaction. The increase in the concentration of active functional groups (C_{tot}) in LBG implies a much higher charge density on the bacteria surface, which could contribute to an increase in electrostatic repulsion between the cells and hence the observed decrease in aggregation in *E.coli* MG1655 in cells cultivated in LBG at 24hr (Figure 7.1 and Figure 7.2). Furthermore, at 6hr growth, cells cultivated in LB did not reveal any dramatic differences when compared to cells harvested after 24hr in the amount of aggregates formed. This correlates well with the similar values for the concentration of functional groups on the cell surface, regardless of the growth phase, indicating similar electrostatic repulsion effects were displayed for cells cultivated in LB. This finding suggests that the effect of glucose on aggregation occurs when glucose is depleted in the media.

7.4.3. Infrared spectroscopy

The infrared spectra of *E.coli* MG1655 cultivated in LB and LBG at different growth phases can the seen in Figures 7.9 and 7.10 respectively. Each spectrum contains information about the functional groups arising from macromolecules, such as carbohydrates, proteins, lipids and nucleic acid, as listed in Table 5.2. Table 5.2 provides a list of absorption band assignments corresponding to functional groups of these macromolecules in the region between 2000 and 1000 cm^{-1}, and is based on observations of the vibration patterns, previously reported for bacteria (45, 171, 264, 265).

Figure 7.9 shows the spectra of *E.coli* MG1655 cultivated in LB at different growth phases. The region corresponding to the amine I and II bands can be observed at 1645 and 1545 cm^{-1} respectively, and the peak at 1450 cm^{-1} exhibits

contributions from the amine III band and bending of CH_3 and CH_2 groups from proteins (δCH_2, δCH_3). The region between 1470 and 1300 cm^{-1} corresponds to the bending vibrations of CH_3, CH_2 and CH groups. However, the peak appearing at ~1400 cm^{-1} can also overlap contributions due to the stretching C-O (ν_{C-O}) of carboxylic groups. The bands between 1200 and 950 cm^{-1} are attributed to the vibrations of C-O-P and C-O-C stretching of diverse polysaccharide groups, and the bands at 1260 and 1080 cm^{-1} exhibit the stretching of P=O ($\nu_{P=O}$) of phosphoryl and phoshodiester groups from phosphorilated proteins, polyphosphate products and nucleic acids. The peak at approximately 1740 cm^{-1} (attributed to the vibrational stretching C=O ($\nu_{C=O}$) of ester functional groups from lipids and fatty acids, and also contributions from carboxylic acids) was observed at 24hr growth (stationary phase) but not observed in 3, 6 and 8hr growth. The relative absorbance of the bands between 1650 and 900 cm^{-1} also increased with increasing growth phases for cells cultivated in LB.

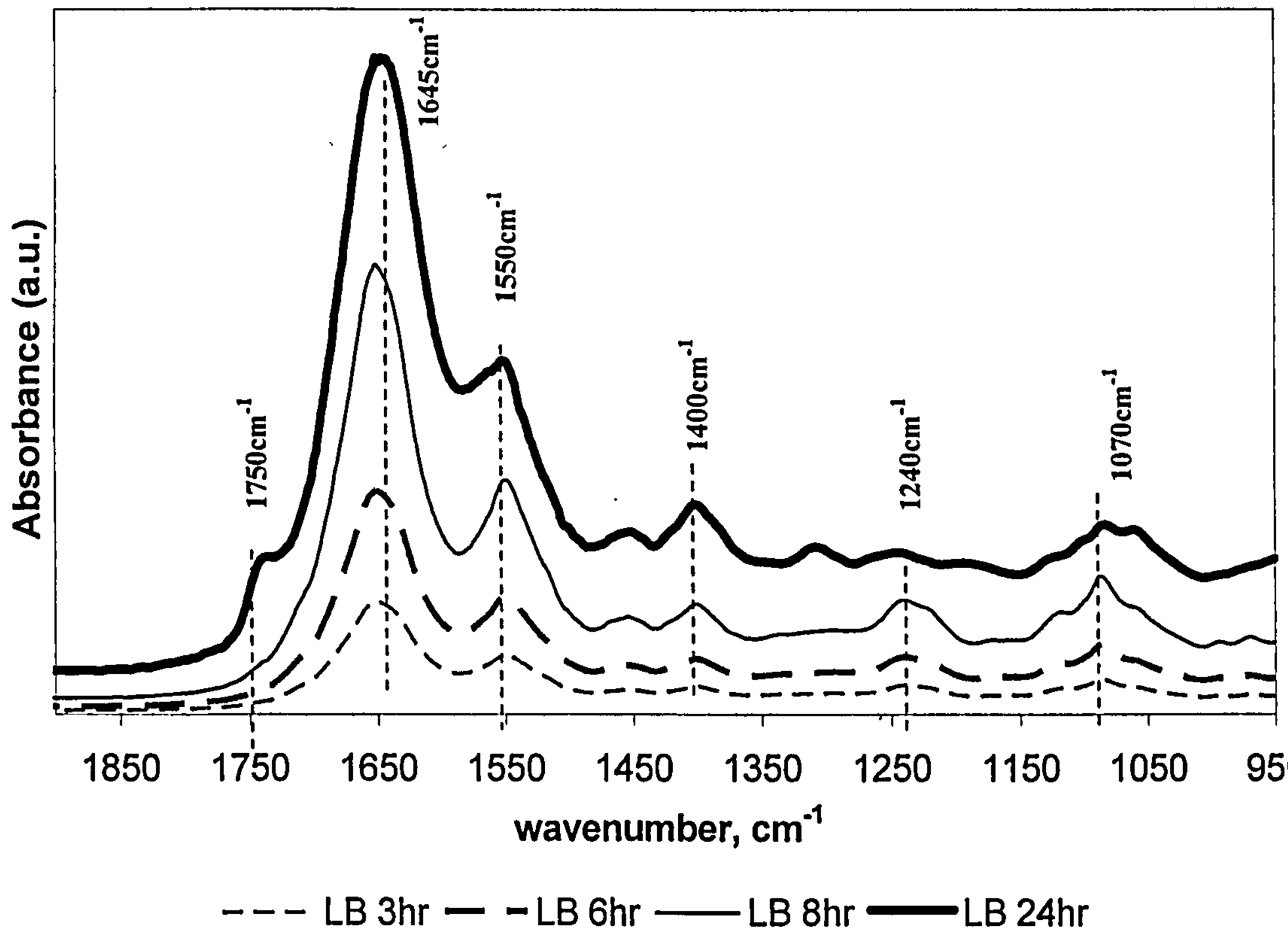

Figure 7.9 FTIR spectra of *E.coli* MG1655 harvested at different growth phases cultivated in LB. The spectra reported here are based on the average of a minimum of 100 scans per replicate, for each growth phase with and without the addition of glucose.

Figure 7.10 shows the spectra of *E.coli* MG1655 cultivated in LBG at different growth phases. The peak at approximately 1740 cm^{-1} ($\nu_{C=O}$ of ester functional groups from lipids and fatty acids) was observed in 6, 8 and 24hr growth, although the relative intensity was lower at 6hr growth. The relative intensity of peaks in the proteins and polysaccharides region also increased as cells progress from exponential to stationary phase. When comparing the spectra of *E.coli* MG1655 grown in LB and LBG, significant differences with regard to the peaks and their intensities can be seen. The peak at approximately 1740 cm^{-1}, which was only found in *E.coli* at 24hr growth phase in LB, was observed in *E.coli* cultivated in LBG at 6, 8 and 24hr growth indicating a possible effect of the glucose in the concentration of carbonyl groups. The intensity of the peak at 1740 cm^{-1} at 24hr growth was also higher in cells cultivated in LBG than LB. Although the band corresponding to this signal is almost certain to be esters, a contribution due to the C=O stretching of protonated carboxylic acids is also possible, however, the results obtained with the potentiometric titrations did not show a significant increase in the concentration of carboxylic groups, suggesting that the C=O stretching band detected by FTIR is not from carboxylic acids and hence do not protonate/deprotonate during the titration experiments, or the carboxylic groups responsible for this absorption are not surface related. The bands between 1650 and 1000 cm^{-1} were also found to vary with growth medium. However, it is important to note that it is currently not possible to distinguish between *E.coli* surfaces and the inner cell contents, as these spectra were taken using a liquid flow cell in transmittance mode. Hence, at this stage, the FTIR results should be used in conjunction with other surface chemistry techniques such as the potentiometric titration and study of the outer membrane molecules, such as proteins. By combining the information obtained with the FTIR spectra and potentiometric titrations, the identity of functional groups can be confirmed. Hence, the presence of carboxylic groups (pKa ranges from 3.4 to 4.4), phosphoryl groups (pKa ranges from 5.8 to 6.9) and hydroxyl/amine groups (pKa ranges from 9.9 to 11.1) in *E. coli* at different growth phases and media was verified.

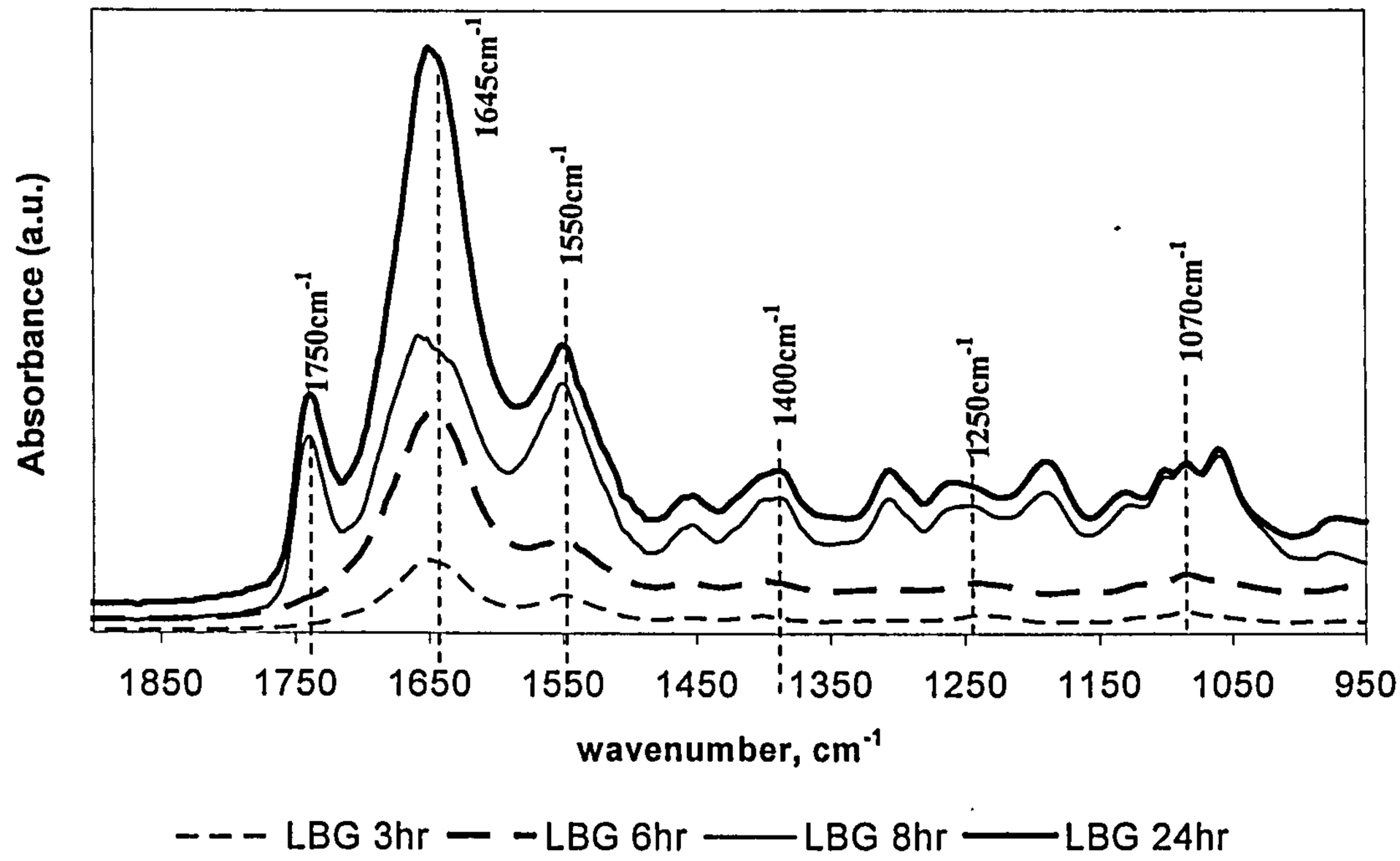

Figure 7.10 FTIR spectra of *E.coli* MG1655 harvested at different growth phases cultivated in LBG (LB with 0.5% glucose). The spectra reported here are based on the average of a minimum of 100 scans per replicate, for each growth phase with and without the addition of glucose.

We characterized the outer membrane protein (OMP) of cells cultivated in LB and LBG, at different growth phases, using FTIR and SDS-PAGE. The OMP extract was scanned (average 100 scans) within 1800-1200cm^{-1}, providing information about the conformation and secondary structure of OMP (307). Figure 7.11 shows the spectra of *E.coli* MG1655 OMP cultivated in LB and LBG, at different growth phases. The spectra revealed differences in peak appearance, as well as the relative intensity, of the OMP extracted (and therefore expressed) under different growth phases and media conditions. The peak at approximately 1740 cm^{-1} may account for the lipids that anchors lipoproteins to the outer membrane via N-terminally attached lipids (139). The ratio of amide I (1650cm^{-1}) to amide II (1550 cm^{-1}) bands predominantly associated with proteins varied dramatically with changes in growth and media, indicating variability in OMP with different structural and functional integrity during these conditions.

It can be seen from the FTIR spectra in Figure 7.11 that the OMP extracted from *E.coli* MG1655 cultivated for 24h in LBG show three absorption bands at 1740 cm^{-1}, 1640 cm^{-1} and 1550 cm^{-1} attributable to $\nu_{C=O}$ of esther functional groups from membrane lipids, $\nu_{C=O}$ of amides associated with proteins and δ_{N-H} of amides from proteins, respectively, whereas the spectrum corresponding to the OMP from *E.coli* MG1655 cultivated for 24h in LB show the absorption bands corresponding to amides (usually known as the amide I and II bands), but the peak corresponding to carbonyl groups from esters was not detected. The presence of the band at 1740 cm^{-1} might suggest that the OMP from *E. coli* cultivated for 24h in LBG medium could be covalently linked to lipids, forming lipoproteins, however, further analysis needs to be done to make a conclusion. The band at 1740 cm^{-1} is also absent in the spectra corresponding to 6h in both LB and LBG medium. The amide II band (1550 cm^{-1}) is very weak in the OMP at 6h in both LB and LBG, however, the amide I band (1640 cm^{-1}) can be clearly seen in all samples, and the intensity is higher as cells progress from exponential to stationary phase. Although the FTIR analysis from these OMP cannot give indication of a particular protein, these results indicate that the OMP extracted from *E. coli* varies due to differences in growth phases and media (LB or LBG).

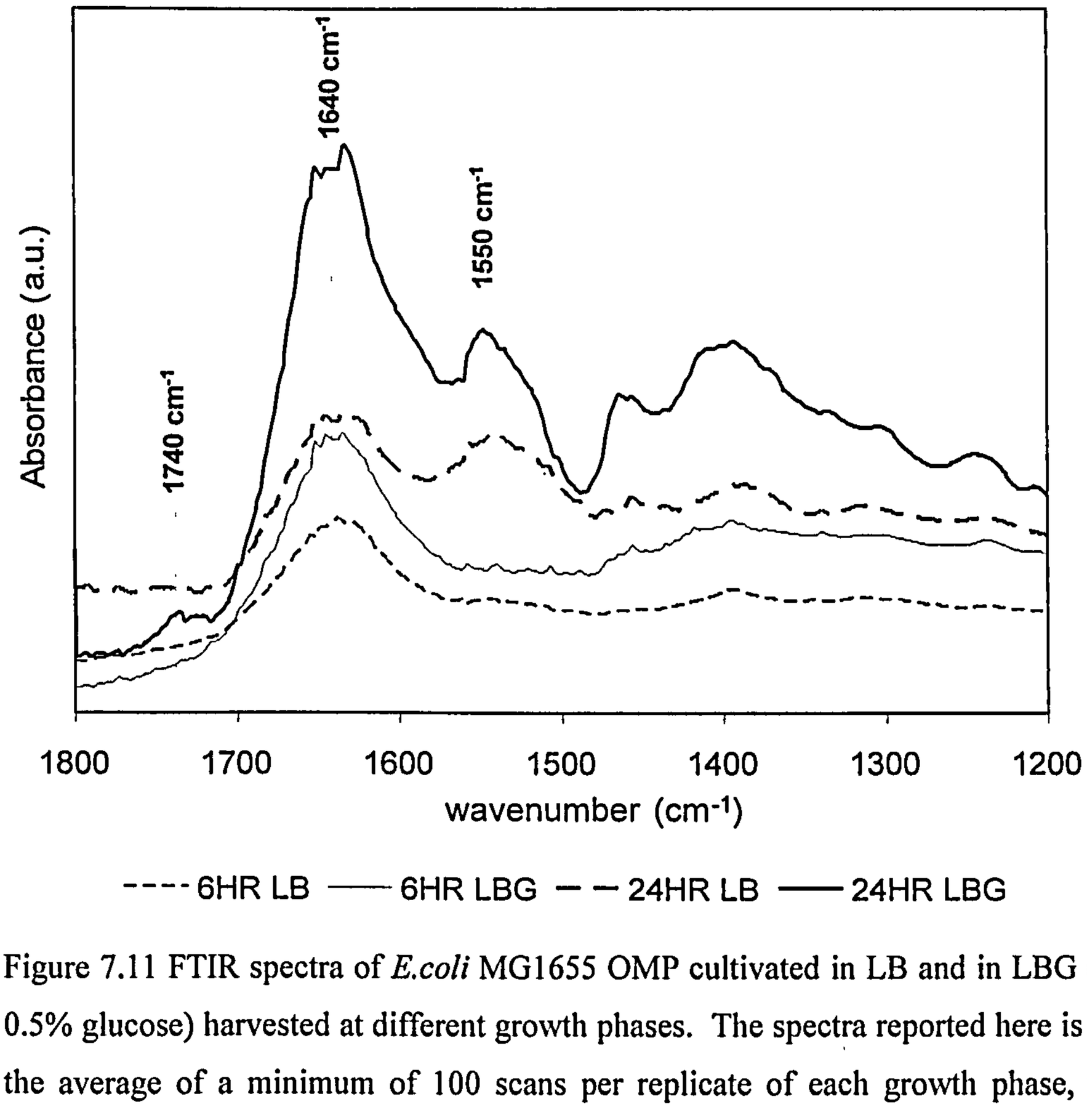

Figure 7.11 FTIR spectra of *E.coli* MG1655 OMP cultivated in LB and in LBG (LB with 0.5% glucose) harvested at different growth phases. The spectra reported here is based on the average of a minimum of 100 scans per replicate of each growth phase, with and without the addition of glucose

SDS-PAGE of OMP extracted from *E.coli* MG1655 cultivated in LB and LBG at different growth phases is presented in Figure 7.12. Again this technique correlates well with the major differences in protein patterns already observed using the FTIR (Figure 7.11). Further analysis is needed to identify the specific proteins, however, based on previous studies, the two protein bands between 30-35kDa, present in all conditions, may correspond to the major outer membrane proteins, porins (OmpA, OmpC, ompF, LamB) which facilitate transportation of low molecular weight from the environment into the cell (140). OmpA has been recently shown to affect biofilm formation in *E. coli* (41, 148) by decreasing biofilm mass. The protein band of approximately 20kDa is present in cells cultivated in LB (with greater stain intensity for 24hours growth compared to 6 hours) and not in cells cultivated in LBG irrespectively of the growth phase. The protein band of approximately 22kDa is observed from cells harvested at 24hrs in both LB and LBG and may

arise from outer membrane lipoprotein (Slp), which is usually induced during carbon starvation or retarded growth (308). Proteins found below 15kDa were mainly observed in cells cultivated in LBG after 24 hours, and may be attributed to outer membrane lipoproteins(309, 310) which also account for the lipid region at the 1740cm^{-1} region observed from the FTIR spectra. Hence, both the FTIR and qualitative SDS Page show changes in the OMP due to the presence of glucose in the media, and growth phase. This suggests that the OMP contribute to the interaction properties between cells.

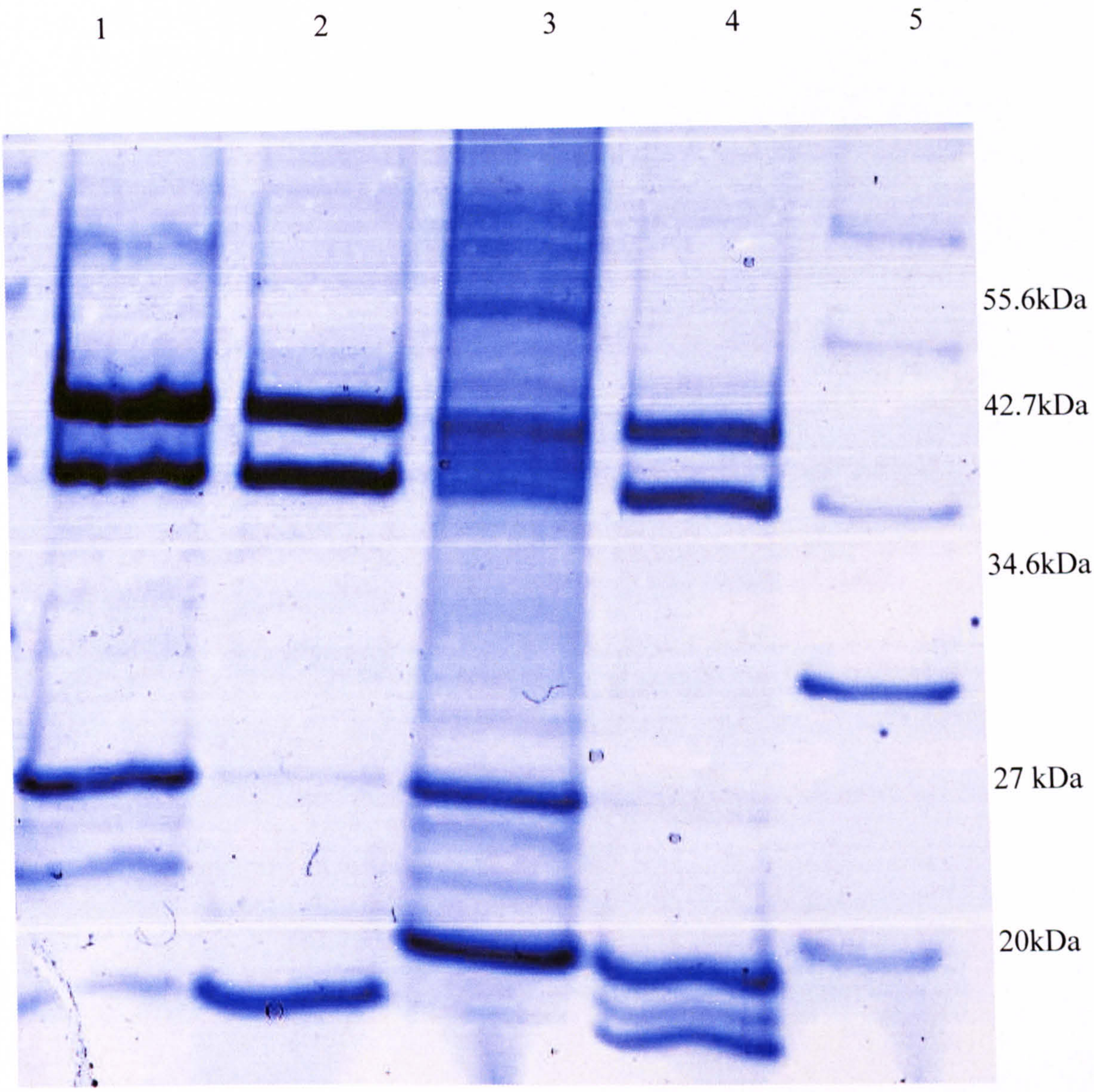

Figure 7.12 One dimensional SDS-PAGE gel of OMP extracted from cells harvested at different group phases, with and without the addition of glucose.

Lane 1 – OMP extract from cells grown in LB, harvested at 6hrs

Lane 2 - OMP extract from cells grown in LBG, harvested at 6hrs

Lane 3 - OMP extract from cells grown in LB, harvested at 24hrs

Lane 4 – OMP extract from cells grown in LBG, harvested at 24hrs

Lane 5 – MW protein marker

.

The lipopolysaccharides (LPS) is also a major macromolecule present in the outer membrane of *E.coli* cell surface and have been recently been shown to contribute to initial cell-to-cell adhesion (142). Hence LPS of *E.coli* MG1655 was also characterised using FTIR spectroscopy within 1800-900cm^{-1}. Figure 7.13 shows the spectra of *E.coli* MG1655 LPS cultivated in LB and LBG, at different growth phases. The peak at approximately 1650 cm^{-1} corresponds to C=O stretching vibration arises from the lipid A region of lipopolysaccharides(311). The weak band in the region approximately 1550 cm^{-1} arises from bending vibration of N–H which is also are arises from the lipid A backbone of Lipopolysaccharides. The bands between 1200 and 900cm^{-1} are attributed to the vibrations of C-O-P and C-O-C stretching of diverse polysaccharide groups of lipopolysaccharides. The spectra revealed no major differences in peak appearance, and a light variation in the relative intensity of the LPS observed under different growth phases and media conditions. The FTIR spectra suggest that the LPS might remain relatively constant as compared to the OMP of *E.coli* MG1655 under these conditions of studies

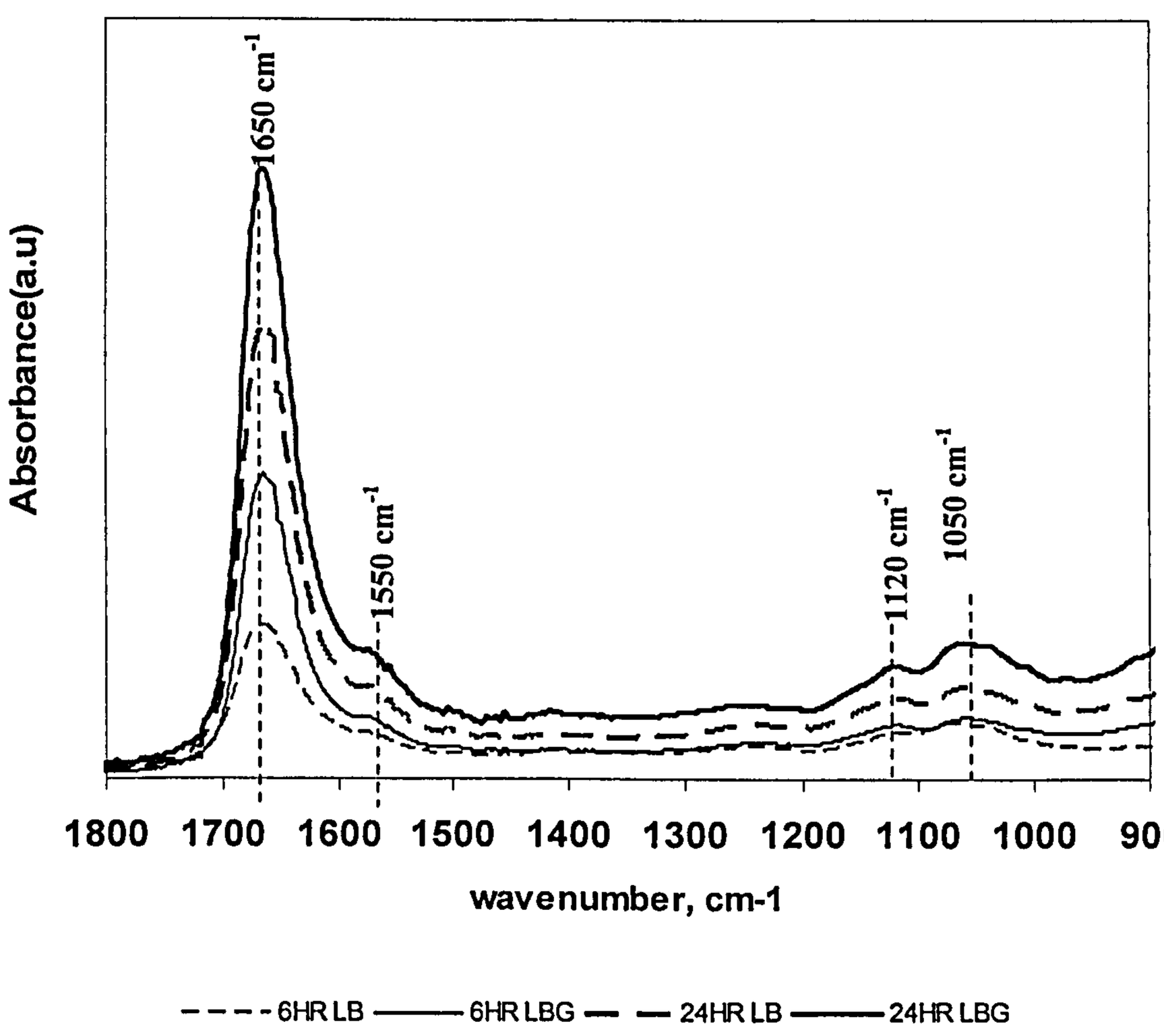

Figure 7.13 FTIR spectra of *E.coli* MG1655 LPS cultivated in LB and in LBG (LB with 0.5% glucose) harvested at different growth phases.

7.5. Conclusion

A combination of potentiometric titration and FTIR spectroscopy enabled the variation in concentration and characteristic of functional groups on the cell surface and extracted outer membrane proteins during growth and in different media to be observed. Mainly differences were found due to changes in the media (i.e. LB versus LBG), where the addition of glucose resulted in the predominant increase in concentration of amine and hydroxyl groups on the cell surface, leading to an reduction in cell to cell interactions, as shown in the reduction of aggregation capacity. FTIR further confirms the presence of active functional groups (carboxyl, phosphate, and amine), which was surmised from the pKa values from the titration studies, and demonstrated that the relative intensity of these functional groups varies. The dramatic increase in the relative absorbance of the peaks for cells cultivated in LBG, as they move from exponential to stationary growth phase, indicates an increase in the concentration of active functional groups due to the differential expression of proteins and lipopolysaccharides on the bacteria surface. The high concentration of active functional groups displayed by cells cultured in LBG after 24hrs is thought to be due to depletion of glucose in the medium which triggers the expression of macromolecules like lipopolysaccharides, membrane proteins and phospholipids on the outer membrane of *E.coli*.

Chapter 8 Characterization of Bacterial Quorum Sensing and the potential Influence on Cell Surface Electrokinetic Properties

(Published in part in Applied Microbiology and Biotechnology, **73**:669-675.)

8.1. Abstract

Previous chapters in this thesis have shown that changes in growth phase and addition of glucose to LB media alter EPS composition and cell surface chemistry and hence aggregation. The addition of glucose to the media has also been shown to prevent the uptake of the quorum sensing signal molecule in *E.coli,* which is involved in the regulation of several genes. Hence this chapter tested the hypothesis that quorum sensing may also influence the aggregation process via altering the microbial surface properties. *Escherichia coli* MG1655 and MG1655 *luxS*$^-$ (lacking quorum sensing gene for Autoinducer synthase AI-2) were used for this study. AI-2 production (or lack of) in both strains was analyzed using the *Vibrio harveyi* bioassay. The levels of extracellular AI-2 with and without the addition of glucose in the growth medium were consistent with previously published work. The surface electrokinetic properties were determined for each strain of *E.coli* MG1655 by measuring the electrophoretic mobility using a phase amplitude light scattering (PALS) Zeta potential analyzer. The findings show that the surface charge of the cells is dependent upon the stage in the growth phase as well as the ability to participate in quorum sensing. In addition, significant differences in the electrophoretic mobility were observed between both strains of *E.coli*. These findings suggest that quorum sensing plays a significant role in the surface chemistry of bacteria during their growth.

8.2. Introduction

Bacterial cell surface properties have been shown to play a crucial role in bacterial aggregation, adhesion, interaction, formation of biofilm and the cells stability in a suspension (7, 312) and previous chapters. This is due to the presence of charged macromolecules on the bacterial outer membrane, lipopolysaccharides (i.e. the carboxyl group carries a net negative charge), sialic acids and/or membrane proteins (293). Hayashi *et al.* (78) and Eboigbodin *et al.* (63) (In chapter 4) were able to demonstrate that the growth phase of different bacteria dictates their cell surface properties as measured by electrophoretic mobility. In both cases, a maximum in electrophoretic mobility occurred during the early stationary phase. Sonohara *et al.* (1995) also used electrophoretic mobility to detect differences in surface properties between Gram-negative and Gram-positive bacteria. Their findings revealed that Gram-negative bacteria are more negatively charged and have a less soft surface than Gram-positive bacteria.

Therefore, despite the chemical and structural complexity of bacterial cell surfaces, compared with non-biological colloids, measurement of the electrophoretic mobility has been successful in being able to compare and characterize the electrokinetic surface properties of a variety of different bacterial strains (30). However, whilst it is possible to quantify the changes in cell surface electrokinetic properties using a colloidal approach as demonstrated previously, it is also important to address key biological factors that may govern the charge in cell surface properties which will inhibit or promote adhesion. In Chapter 7, the influence of glucose was considered. In this chapter, the role of quorum sensing in investigated.

There is evidence suggesting that cell-to-cell communication via quorum sensing, may influence bacteria cell surface properties, and cell aggregation, with differences in colony surface morphology and aggregation ability observed for cells which have lost their ability to produce quorum sensing molecules (27, 28, 313). Cell-to-cell communication via quorum sensing has been well studied in several biological systems (for reviews see (109, 121)). Bacteria are able to

monitor the microbial community via quorum sensing by producing, detecting and responding to low molecular weight signal molecules, called autoinducers (AI). Recent findings have shown that most bacteria produce, detect and respond to an autoinducer AI-2, suggesting that it may be used in interspecies cell-to-cell communication (109, 123).

AI-2 has been shown to play a crucial role in biofilm formation of *Streptococcus mutans* by the regulation of glucosyltransferase genes (314, 315). Park *et al.* (28) observed differences in aggregation properties between *Escherichia coli* strains lacking the ability to produce AI-2 (deleted LuxS gene) and the wild type strains. More recently, AI-2 has been show to control biofilm formation in *Escherichia coli* by controlling the genes involved in the motility (132) and the regulation of outer membrane proteins (316). González Barrios *et al.* (132) recently demonstrated that a dramatic change in biofilm formation was observed on the addition of AI-2 by intensifying motility. Wizner *et al.* (316) showed that quorum sensing also regulates outer membrane proteins such as lectins, which in some bacteria are involved in cell-to-cell adhesion. These findings suggest that the outer surface of bacteria, and hence the electrokinetic properties, will be altered if quorum sensing regulates these outer membrane macromolecules. DeLisa *et al.* (304) used DNA microarray analysis to identify genes which are regulated by AI-2 in *Escherichia coli* and found that, ompG (an outer membrane porin protein) rfaY (biosynthesis of core lipopolysaccharides), flip (Flagellar biosynthesis), rfaj (UDP-D-glucose :(galactosyl) lipopolysaccharides glucosyltransferase) and b1502 (putative adhesin) were all regulated by AI-2.

Although there is strong evidence suggesting that quorum sensing alters the outer membrane polymers, quantification of the change in cell surface electrokinetic properties, still remains unclear. From a bio-engineering point of view, the cell surface electrokinetic properties are a major factor that governs bacterial adhesion and aggregation. The reason is that as the cells are brought into close proximity, an attractive interaction potential must be present to promote cell-cell aggregation and it is the cell surface structure that will dictate the strength and type of this interaction (78). The studies in previous chapters suggest that quorum sensing may

be involved in the regulation of macromolecules in the bacterial cells surface and as such will influence aggregation process. The results presented in Chapter 3 show that quorum sensing molecules are produced during the exponential growth phase and then internalised by the cells at the on-set of stationary growth. This finding can be correlated with studies presented in Chapter 4 showing that the surface chemistry changes as cells progress from the exponential to the stationary growth phase. Hence there could be a link between quorum sensing and the cell surface chemistry. This hypothesis is further strengthened by the findings in Chapter 7, which show that the addition of glucose to the beginning of the growth experiment, altered the cell surface chemistry of *E.coli*. The addition of glucose also changed the ability of *E.coli* to internalise quorum sensing molecules (as shown in Chapter 7). The link between quorum sensing and glucose is thought to be governed by a decreasing cyclic adenosine monophosphate (cAMP) concentration (130) in the cell due to catabolite repression. Once glucose is depleted, the cAMP concentration increases. The *lsr* operon is activated by cAMP, and this leads to the internalisation of AI-2 by the cells (128) and Figure 2.6b).

Hence, in this Chapter we seek to quantify the influence of quorum sensing (AI-2) on the cell surface electrokinetic properties and how it may also influence the aggregation process. The hypothesis that we are testing, based on results generated earlier in this thesis, is shown in Figure 8.1. *E.coli* produces the autoinducer AI-2 during their growth via *luxS* expression. Once the concentration of AI-2 reaches a particular threshold, AI-2 will bind to *luxR*. We hypothesise that this process may then enable *luxR* to bind with promoters involved in the regulation of surface macromolecules (Figure 8.1)

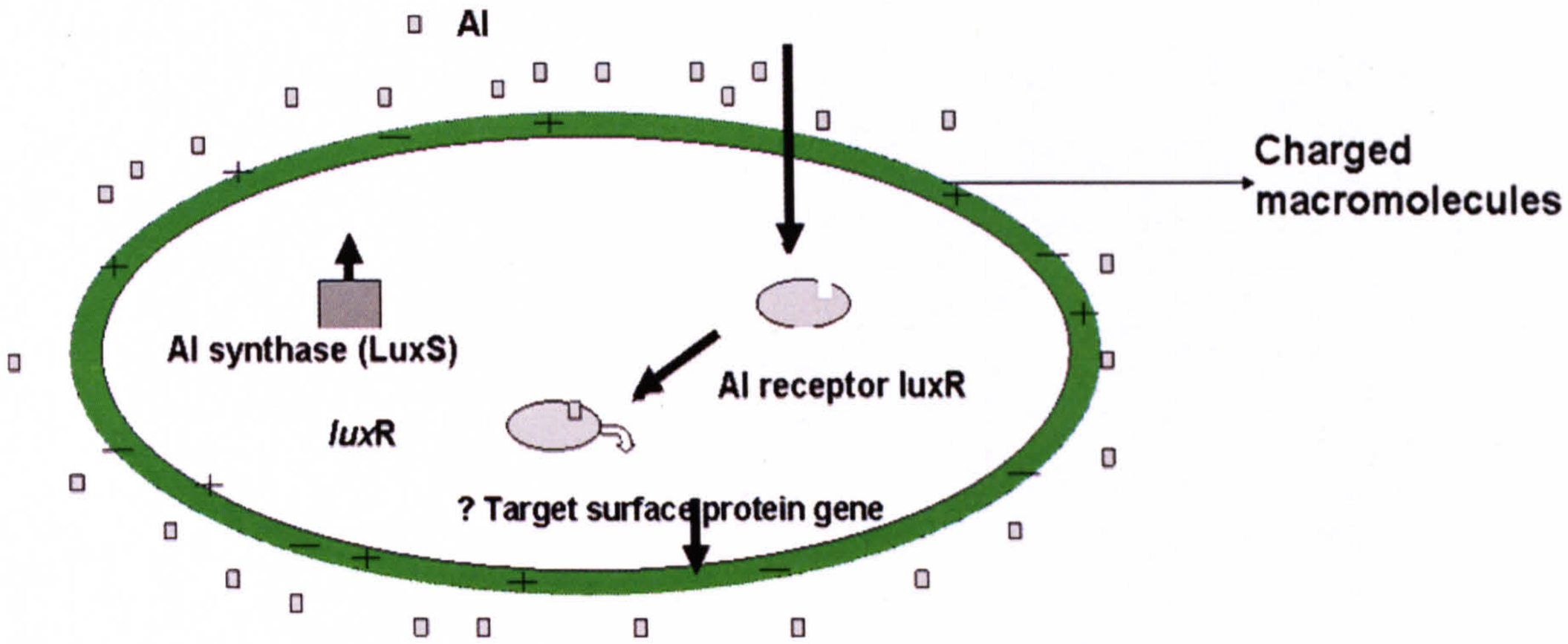

Figure 8.1 Hypothetical role of quorum sensing on surface charge of Bacteria

The link between quorum sensing and cell surface chemistry during growth phase is investigated in this chapter using the electrophoretic mobility techniques demonstrated in Chapter 4. These findings are then correlated with the aggregation ability of cells with and without the ability to produce AI2 during the same growth phases as discussed in Chapters 5 and 7.

8.3. Materials and methods

8.3.1. Bacterial strains

E. coli strains MG1655 (wild-type) and MG1655 *luxS*⁻ as well as *Vibrio Harveyi BB170* (luxN::Tn5, Sensor 1-, sensor 2+) were used in this study (supplied by Prof Paul William, University of Nottingham UK). The *E.coli* MG1655 *luxS*⁻ mutation is identical to the *E.coli luxS*⁻ mutant that has been previously described in *E.coli* BL21 (126). The mutation was transferred into *E.coli* MG1655 by P1 phage transduction. (Winzer, Tavender, and Hardie from the Institute of Infections and Immunity, University of Nottingham, personal communication, 2006). The *E.coli luxS*⁻ contained a deletion of *luxS* over a 500bp range and this was confirmed using PCR analysis as described in Chapter 3.

8.3.2. Growth Studies

E.coli strains were grown aerobically in Luria-Bertani (LB) medium (tryptone 10.0g/L, yeast extract 5.0g/L, NaCl 10.0g/L (sigma UK), adjusted to pH 7.0) supplemented with or without 0.5w/v (%) glucose, and on LB agar plates at 30°C. LB media supplemented with 0.5 w/v (%) glucose is referred to as LBG

throughout the chapter. *E.coli* strains were grown at 30°C overnight with aeration in LB or LBG. The culture was then used to inoculate fresh LB or LBG at a 1:100 dilution and grown at 30°C with aeration. *V.harveyi* BB170 were grown aerobically in Autoinducer Bioassay (AB) medium at 30°C (222). AB medium contained 0.3M NaCl, 0.05M $MgSO_4.7H_20$ (Sigma UK), 0.2% Casamino acid (BD Bioscience), 2% glycerol, 1mM L-arginine, 10mM potassium phosphate (pH 7.0). 0.3M NaCl, 0.05M $MgSO_4.7H_20$, 0.2% Casamino acid was dissolved in 1L of distilled water. The batch growth curve and light production was then determined using a GENios Multi-Detection Microplate Reader (Tecan, UK) (A detailed method is already be described in Chapter 3).

8.3.3. Assay for production of AI-2

The presence of AI-2 secretion in *E.coli* cell-free culture were analysed using *V. harveyi* BB170 reporter strain bioassay described by Surette and Bassler (1998) (as described in Chapter 3). *V. harveyi* BB170 was first grown for 16hr in AB medium, then 180µl of BB170 (diluted 1:5000 in fresh AB medium) was added to 20µl of cell-free culture fluid. Changes in light production of BB170 as a result of presence of AI-2 were monitored using a GENios Multi-Detection Microplate Reader (Tecan, UK) in luminescence mode. Sterile LB was used as negative control and the experiment was carried out in quadruplicate.

8.3.4. Electrophoretic mobility measurement (EPM)

Electrophoretic mobility (EPM) was measured using a phase amplitude light scattering (PALS) zeta potential analyzer (Brookhaven Zeta PALS, U.K) following the technique described in Chapter 4. Cells were sampled in triplicate at intervals between 0 and 24 hours growth in LB and LBG and harvested by centrifugation at 5000g for 10 minutes. After harvesting, the cell pellets were washed by re-suspending in 10mM potassium chloride (KCl) followed by centrifugation at 5000g for 10 minutes. This washing step was repeated four times to eliminate residual substrates and extracellular polymers, which were produced by *E.coli* strains during growth. Measurements were conducted using an electric field of

$2.5Vcm^{-1}$ at a frequency of 2.0 Hz. The reported values for each EPM represents the average of 10 successive runs carried out in triplicate readings using the Zeta PALS. For EPM of cells at different ionic strength, cells were suspended in different ionic strength from 5-100mM KCl (no pH adjustment, 5.6-5.8).

8.3.5. Autoaggregation assay

The auto-aggregation properties of *E.coli* MG1655 and MG1655 *luxS*⁻ mutant grown in LB and LBG, harvested at exponential (6hr) and stationary phase (24hr) was measured using the method previously described in Chapter 7.

8.4. Result and Discussion

The bioluminescence produced by *V.harveyi* BB170 during its growth cycle followed similar responses reported by Xavier and Bassler (129) with an initial decrease over the first 4 to 5 hours, due to inoculation in fresh AB medium, followed by an increase in bioluminescence due to cell growth (as seen in Chapter 3). The batch growth curves of *E.coli* MG1655 in LB and LBG are also represented in Chapter 3 to show how the fold induction varied during the growth phase and correlates well with results obtained from other previously studied bacteria (221, 317, 318). When *E.coli* is grown in LB supplemented with glucose, the glucose prevents the uptake of AI-2 into the cell, hence it accumulates in the supernatant (228). Similar results have been observed by Hardie *et al*. (221) Their findings revealed that glucose affects the amount of measurable AI-2 in cell harvested during stationary phase.

Figure 8.2 shows the change in electrophoretic mobility (EPM) of both *E.coli* strains as a function of ionic strength (KCl) for a constant stage in the growth phase. The cells were harvested after 6 hours, in the mid exponential growth phase. From Figure 8.2, it can be seen that for all ionic strengths, both *E.coli* strains display a negative EPM, and that the magnitude of the EPM decreases with increasing external electrolyte. The change in EPM with ionic strength for each *E.coli* strain is very similar but the *E.coli* wild-type exhibited larger (more negative) EPM

values than the *E.coli* MG1655 *luxS*. The addition of the electrolyte to the system brings about a change in the magnitude of the EPM but does not promote a change in the sign of the EPM. This suggests that the electrolyte is not significantly adsorbing to the surface of the cells. It is interesting to note, that the significant difference in the magnitude of the EPM between the two strains is observed for all ionic strengths.

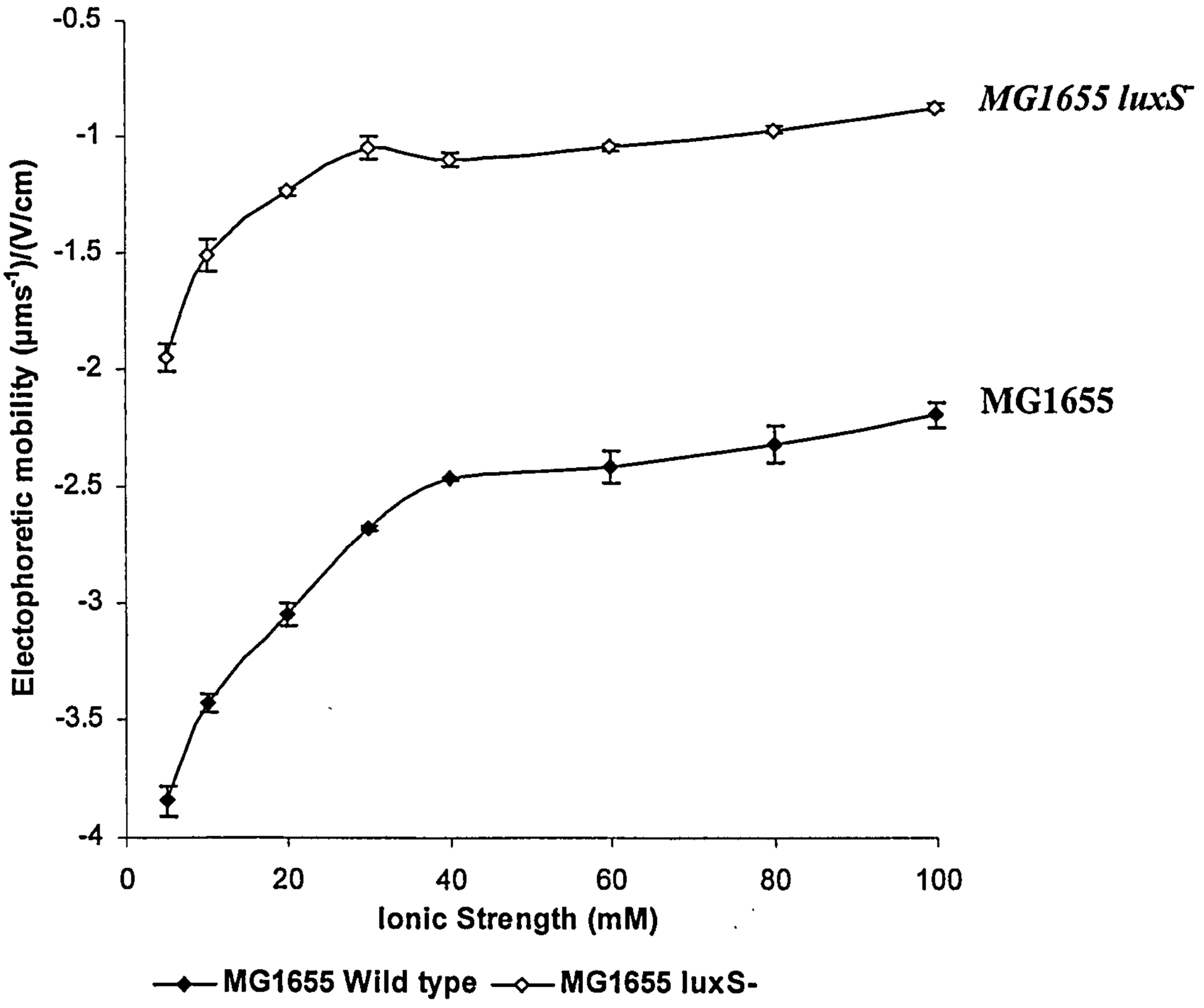

Figure 8.2 Electrophoretic mobility (EPM) vs. ionic strength (KCl) for the *E.coli* MG1655 wild type and *E.coli* MG1655 *luxS* mutant harvested at 6hrs cultivated in LB.

This difference in surface charge is demonstrated in Figure 8.3 and Figure 8.4, which show the electrophoretic mobility of *E.coli* MG1655 wild type and *E.coli* MG1655 *luxS*, at different growth phases, in different media, respectively. Again both *E.coli* strains display a negative EPM value throughout the growth period, in both LB and LBG. For *E.coli* MG1655 wild-type (Figure 8.3), the electrophoretic

mobility of the cells steadily increases in magnitude from the early to mid exponential phase and then remains relatively constant until the final measurement at 24 hours. The EPM of *E.coli* MG1655 wild-type grown in LBG also varies considerably across the growth phase with a lower negative EPM value at 8hr than cells cultivated in LB.

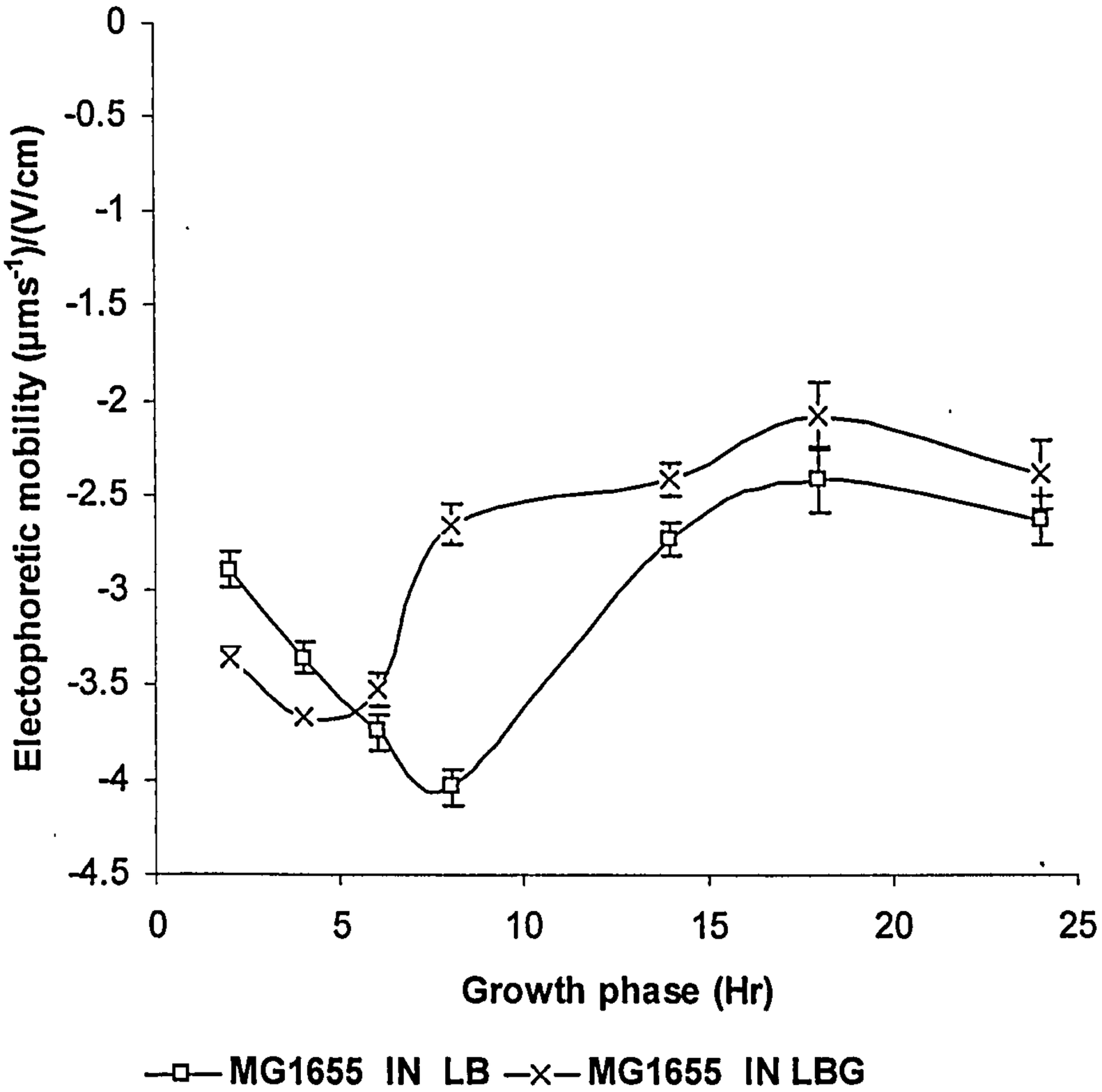

Figure 8.3 Electrophoretic mobility of *E.coli* MG1655 wild type grown in LB and LB supplemented with 0.5 w/v (%) glucose (LBG)

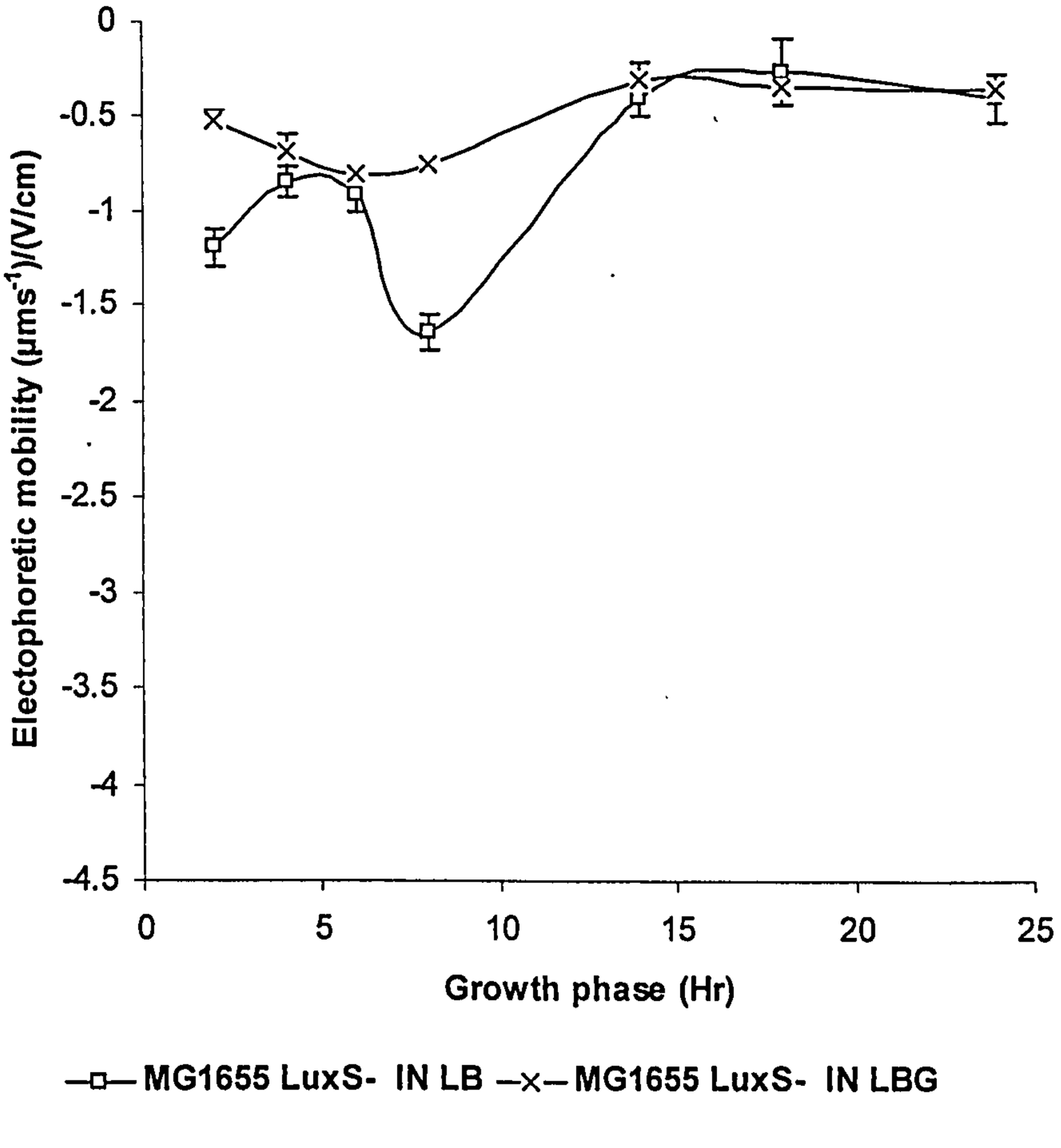

Figure 8.4 Electrophoretic mobility of *E.coli* MG1655 *luxS* grown in LB and LB supplemented with 0.5 w/v (%) glucose (LBG)

However, in comparison, the EPM of *E.coli* MG1655 *luxS* remains relatively constant throughout the growth phase without a dramatic change in the EPM during the exponential phase. *E.coli* MG1655 wild-type grown in LBG again displayed a lower negative EPM value at 8hr than cells cultivated in LB. Therefore not only is the absolute value of the EPM different between the two strains (as observed in Figure 8.2 and comparison between Figure 8.3 and Figure 8.4) but so too is the change in EPM as a consequence of growth phase

In Figure 8.5, it can be seen that once the mutant strain is grown in a medium containing AI-2, the magnitude of the EPM changes dramatically and the change in EPM over growth phase mimics that of the wild-type. The effect on the surface charge of the mutant strain grown in the presence of AI-2 is more pronounced than the small changes seen in EPM due to growth media as shown in Figure 8.4

The electrophoretic mobility of the *E.coli* strains was found to be dependent on the growth phase and quorum sensing ability of the cells as well as the ionic strength of the media and to a lesser extent growth media. Gram negative, non-pathogenic *Escherichia coli* strains were chosen as the model system due to their fast growth rate, and that quorum sensing, via the signal molecule AI-2, in *Escherichia coli* has been well studied and shown to influence several physiological responses (1, 20).

The dependence of electrophoretic mobility of the *E.coli* strains on ionic strength is consistent with previous work on bacteria (78, 79, 319). The magnitude of the electrophoretic mobility decreased with increasing external electrolyte due to shielding of the bacterial surface (319). However, even with 100mM KCl the EPM still displayed a negative value without showing a tendency to approach a zero value, indicating that the bacteria are discrete entities and respond differently to inert particles. For inert particles, the electrophoretic mobility values continue to decrease with increasing electrolyte concentration, approaching a zero value at higher electrolyte concentration (320). The bacteria cell surface differs from inert particle because they possess an ion-penetrable membrane layer in which the functional groups are located. Moreover, the van der Waals attraction is significantly weakened in these systems by the large water content of the cells. Extracellular polymers, attached to the cell surface, also provide a degree of steric stabilization. Hence the bacterial electrokinetic properties differ from their non-biological colloid counterpart due to the functional group heterogeneity on bacterial surfaces. The measurement of electrophoretic mobility is directly related to the surface charge. Whilst this electrostatic interaction has been the main interaction studied to date (78, 178), manipulation and control over the weak van der Waals attraction and any external protein induced interaction (63) is needed in order to fully understand and eventually control the cellular interaction process. Hence, the cell surface chemistry will dictate the strength and type of cell-cell interaction. However, it is important to note that the electrophoretic mobility measurements can be influenced by *E.coli* size and shape. Therefore it is important to combine other surface characterization techniques such as FTIR and Potentiometric titration (Chapter 7).

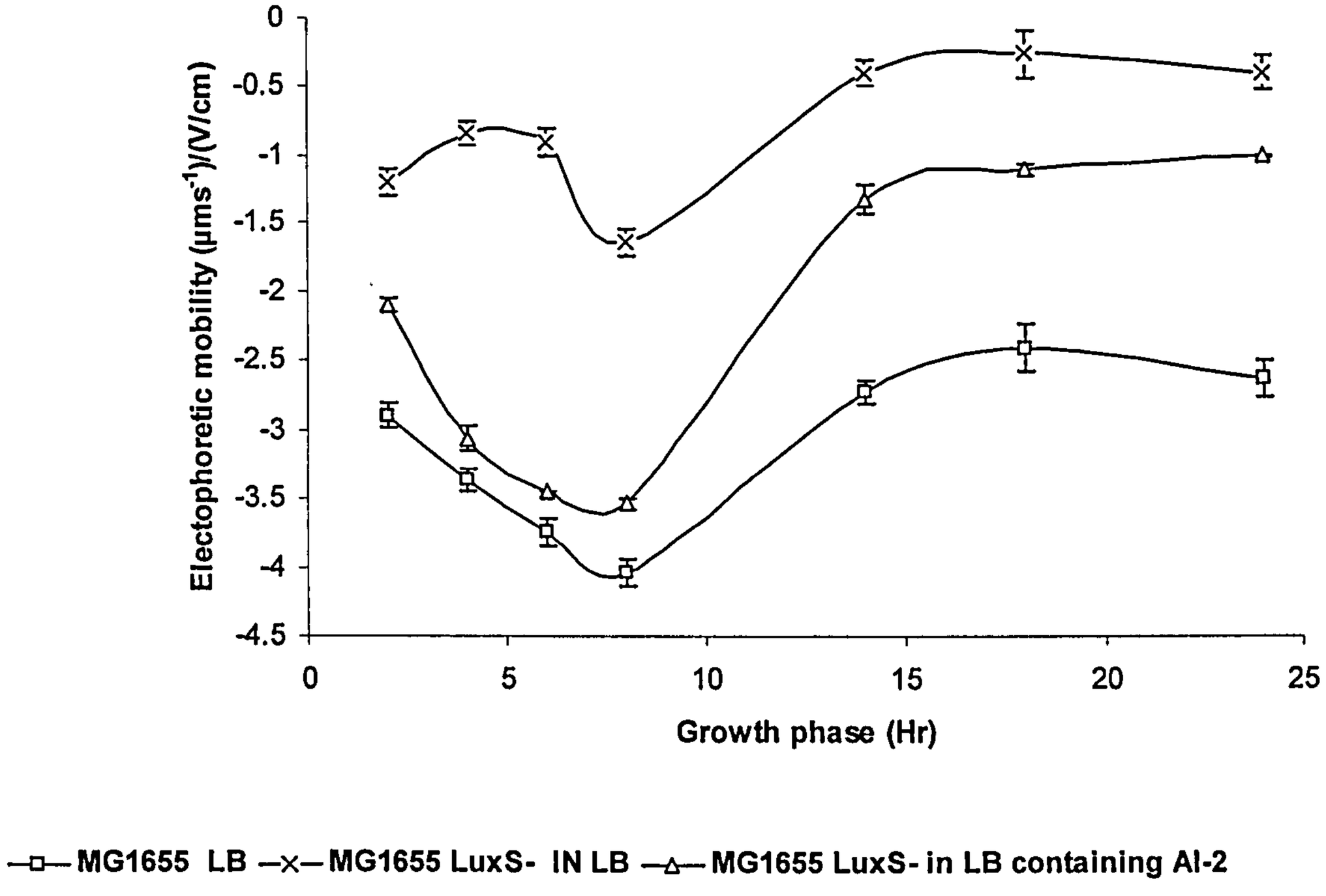

Figure 8.5 Electrophoretic mobility of *E.coli* MG1655 *luxS*⁻ mutant grown in LB containing AI-2 from the supernatant of *E.coli* MG1655 wild type, compared with the electrophoretic mobility of *E.coli* MG1655 wild type and *E.coli* MG1655 *luxS*⁻ both grown in LB.

However, both *E.coli* strains were found to be negatively charged throughout their growth phase (Figure 8.3 and Figure 8.4) and at different ionic strengths (Figure 8.2). A similar negative surface charge was also found for Gram-negative bacteria (78, 145, 319) and was also observed by Eboigbodin *et al.* (63) and Chapter 4, for a different *E.coli* strain (AB1157). Changes in the surface charge may be due to the changes in major components of the outer membrane proteins, and lipopolysaccharides proteins such as porins during growth (140, 293) (Chapter 4 and 7) . It is also important to note, that the lowest EPM value for MG1655 (wild-type), corresponds to the highest fold induction, as shown in Chapter 3, which is during the exponential growth phase.

The observed differences in EPM values between the *E.coli* strains is hypothesized to be due to changes in the composition of functional groups presence in the outer membrane macromolecules induced by AI-2 production. Recent studies, using DNA microarray analysis, showed that the expression of surface macromolecules such as lipopolysaccharides and porins present in the outer membrane are induced by the presence of AI-2 (304). Hence, if AI-2 controls the induction of major outer membrane macromolecules, then it is to be expected that the MG1655 (*luxS*⁻ mutant), that is not able to produce AI-2, will have a different EPM to the wild type. This is shown in Figure 8.5.

To test this further, cell free culture fluid taken from *E.coli* MG1655 (wild type) after 6 hours (i.e. when the autoinducer level was at its highest) was used to grow the MG1655 *luxS*⁻. The EPM of the mutant, grown in the wild type supernatant, was then measured at different growth phases (see figure 8.5). Surprisingly, the EPM values changed dramatically from the original EPM for the mutant and were now similar to the wild-type strains grown on LB. It is possible, however, to change the EPM response of the *E.coli* MG1655 *luxS*⁻, by supplementing the media of the mutant strain with the supernatant (containing AI-2) of the wild-type. This observation implies that the presence of autoinducer (AI-2) directly influences the surface charge of the cell surface.

The alteration of cell surface properties by AI-2 may also contribute to aggregation processes in *E.coli* MG1655. Hence an aggregation assay on *E.coli* MG1655 wild and *luxS*⁻ was conducted and the result can been seen in Figure 8.6. The percentage auto-aggregation of *E.coli* MG1655 wild type cultivated in LB and LBG has previously been reported and described in Chapter 7. There was no significant difference in the aggregation capability of *E.coli* MG1655 *luxS*⁻ and *E.coli* MG1655 wild type when cultivated in LB at exponential phase (6hr). However *E.coli* MG1655 *luxS*⁻ has a least negative EPM value than its *E.coli* MG1655 wild counterpart. Again, there was no difference between the aggregation capability of *E.coli* MG1655 *luxS*⁻ and *E.coli* MG1655 wild type cultivated in LB harvested at stationary phase (24hr) even though there EPM values are different. These finding

suggest that the surface charge alone, cannot accurately be used to understand the aggregation capability of bacteria. Other factors such as EPS, surface heterogeneity and other biological factors may contribute to the aggregation capability of the bacteria. Similarly when cultivated in LBG, *E.coli* MG1655 *luxS*⁻ showed no significant changes in aggregation capability with *E.coli* MG1655 wild type harvested at exponential phase (6hr). Interestingly, when cultivated in LBG, *E.coli* MG1655 *luxS*⁻ showed a significant increase in aggregation capability than *E.coli* MG1655 wild type harvested at stationary phase (24hr) even though their EPM values were similar. The results show that *E.coli* MG1655 *luxS*⁻ aggregation ability is higher than *E.coli* MG1655 wild type when cultivated in LBG harvested at stationary phase, suggesting that AI-2 may also contributes to the aggregation process.

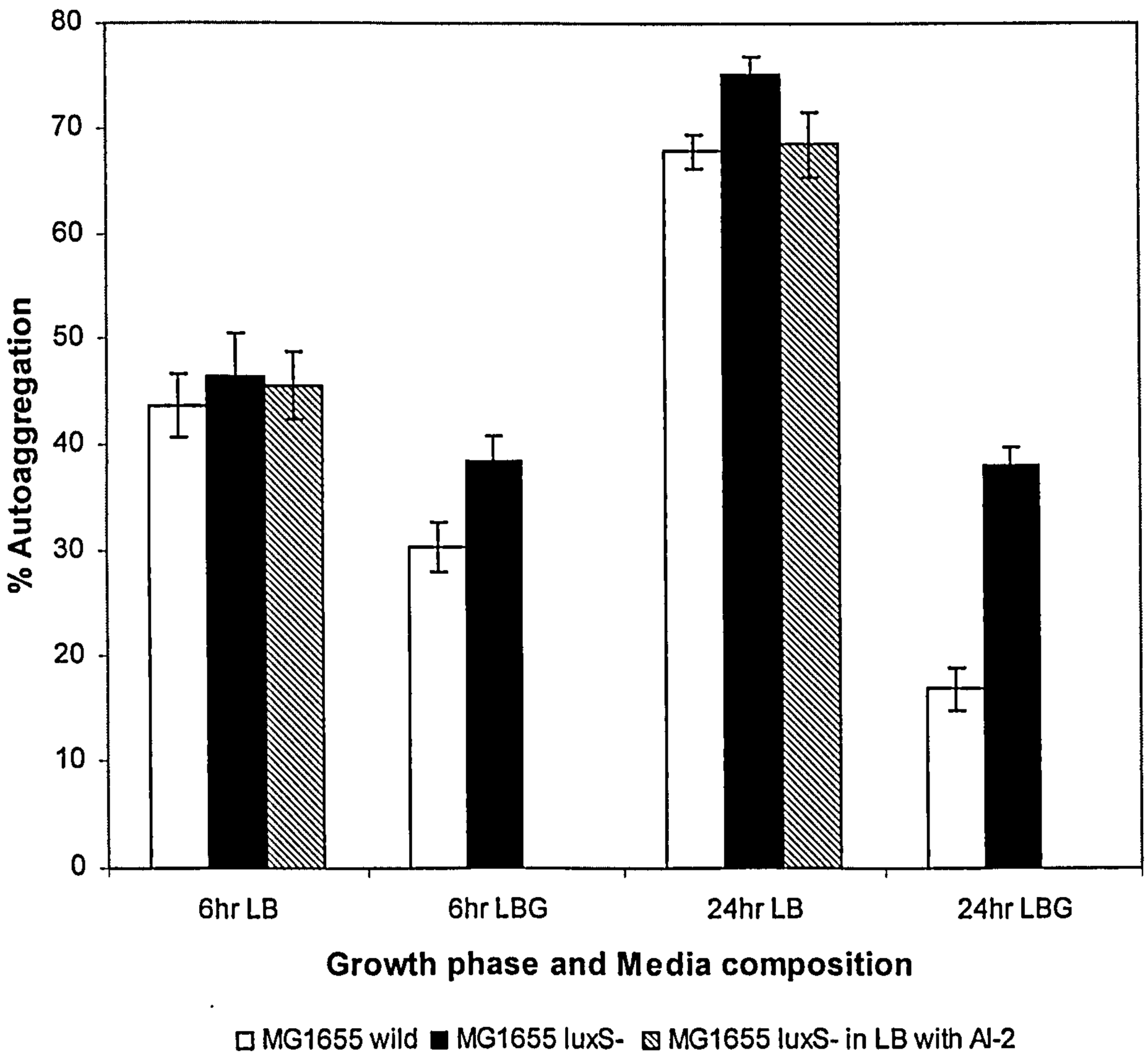

Figure 8.6 Percent auto aggregation of *E.coli* MG1655 wild and *luxS*⁻ cultivated in LB and LBG

To test this further, an autoaggregation assay was carried out again for MG1655 *luxS*⁻ grow in cell free culture fluid taken from *E.coli* MG1655 (wild type) after 6 hours (contains the highest AI-2 activity Chapter 3). The results suggest that the growth of *E.coli* MG1655 *luxS*⁻ in LB in the presence of AI-2 slightly reduces the aggregation capability of cells harvested at stationary phase but not at exponential phase. The effect of AI-2 on *E.coli* aggregation is similar to Acyl-HSL effect on Rhodobacter sphaeroides previously reported by Puskas *et al.* (47). The slight differences in aggregation ability of *E.coli* MG1655 wild and mutant *luxS*⁻ correlates well the difference in their EPM values. Cells cultivated in 24hrLBG have a less negative EPM values that cells cultivated in 24hrLB. Hence the electrostatic repulsion among cells cultivated in 24hr LBG is reduced due to the absence of AI-2 and hence the tendency to aggregate increases. This suggests that quorum sensing plays a role in dispersion of cells rather than promoting aggregation.

8.5. Conclusions

The results show that the surface charge of the cells is not constant during the growth phase and that the magnitude of the charge is dependent on the stage in the growth phase. In addition, significant differences in the electrophoretic mobility between *E.coli* MG1655 wild type and MG1655 *luxS*⁻ show that quorum sensing allows bacteria to alter their surface properties in response to their environment. The aggregation ability of MG1655 *luxS*⁻ was higher than *E.coli* MG1655 wild type among cells harvested at the stationary phase cultivated in LBG. These findings suggest that quorum sensing influences aggregation by altering the surface chemistry of bacteria during their growth.

Chapter 9 Conclusions and Recommendations

9.1. Introduction

This thesis focused on understanding the key biological factors that may have an effect on the aggregation process of *Escherichia coli*. A bio-physical approach was used, where the role of *E.coli* physiology as well the physical characteristics mainly the cell surface chemistry, were investigated in relation to aggregation. Like inert colloids, bacteria exhibit similar properties to non-biological colloids and a display pair-wise attraction when in close proximity. Hence, interactions leading to aggregation are thought to be governed by the surface chemistry. However, unlike inert colloids, *E.coli* like other bacteria is dynamic in nature. Therefore, key biological factors such as growth phase, nutrients, extracellular polymeric substances as well as the ability of *E.coli* to participate in cell-to-cell communication (quorum sensing) dictate the physiological state and as such affects its aggregation capability. Hence it may be anticipated that such biological factor may also affect the cell surface chemistry of *E.coli*.

The influence of extracellular polymeric substances produced by bacteria, and quorum sensing on *E.coli* aggregation as well as their changes in growth phase and media were addressed in this thesis. These changes were also correlated with changes in cell surface chemistry.

In non biological systems (inert colloids) the addition of a non-adsorbing polymer (SPS) leads to an imbalance in osmotic pressure, which in turn causes an attraction between particles which brings them closer together (48, 49), and as such facilitates particle aggregation, a phenomenon known as depletion attraction. This theory was applied to elucidate the role of free-EPS in the aggregation of *E.coli* (strains AB1157 and MG1655) (Chapter 4). Interestingly, *E.coli* displayed similar properties to non- biological colloids upon addition of an inert, non-adsorbing polymer, Sodium Polystyrene Sulphonate (SPS). However unlike non-biological colloids, the growth phase, and the composition of EPS influenced the aggregation ability of *E.coli*. The composition of EPS, mainly the protein content from *E.coli*, was found to be dependent on the growth phase and nutrient in the media. A higher concentration of SPS was needed to induce aggregation in cells harvested at the exponential phase, than cells harvested in the stationary phase. The variation was

attributed to the changes of cell surface chemistry during growth phase. Hence aggregation in *E.coli* can be induced by using an inert non absorbing polymer.

E.coli produces EPS which are mainly composed of polysaccharides and proteins. These are known to play a role in aggregation. Both the composition of bound and free-EPS were determined as a function of growth phase and media (Chapter 5). However *E.coli* produced relatively low amount of bound-EPS compared with free-EPS under the conditions of study. The protein content of free-EPS increased at cells progressed from the exponential to the stationary phase. Apart from the increase in protein content, the type of protein produced changed as a function of growth phase and media was examined in Chapter 6.

The bound and free-EPS extracted from *E.coli* at the exponential and stationary phase cultivated in different media (LB and LBG) were further characterized using FTIR spectroscopy (Chapter 5). The FTIR spectra revealed the presence of different functional groups, which is due to changes in growth phase and media. The role of bound-EPS in *E.coli* aggregation was observed by comparing the aggregation properties of cells before and after bound-EPS extraction. However, it was found that this did not affect aggregation of *E.coli* which was attributed to the low levels of bound-EPS produced.

To test whether free-EPS is able to induce aggregation in *E.coli* via the depletion process. Free-EPS extracted from *E.coli* harvested at different growth phases and media was added to *E.coli* cells. The addition of free-EPS led to aggregation of *E.coli* cells, in all growth conditions used. The addition of free-EPS extracted from cells harvested at the stationary phase displayed a much higher effect on the aggregation ability of the cells, than the addition of free-EPS extracted from cells at the exponential phase. This effect was attributed to differences in the composition of free-EPS as a result of changes in growth phase and media. This study showed that the role of free-EPS in *E.coli* aggregation complies with the depletion attraction process exhibited by inert polymers and hence it is possible to also induce aggregation in *E.coli* by using biopolymers.

Although both inert polymers and EPS were found to play an important role in aggregation of *E.coli*, the aggregation capability was also found to be dependent on the growth phase and the media used. It was anticipated that this effect may be due to changes in the cell surface chemistry. Hence the cell surface chemistry of *E.coli* cells were investigated using three different surface characterization techniques; electrophoretic mobility (EPM) (Chapter 4), potentiometric titration (Chapter 7) and infrared spectroscopy (Chapter 7). The magnitude of the EPM gives an indication of the overall net charge on the *E.coli* cell surface. The *E.coli* cells surface, displayed a negative EPM value under the conditions studied suggesting that *E.coli* is negatively charged. Cell harvested at the exponential phase were found to be more negatively charged than cells harvested at the stationary phase. This explains the differences in the amount of SPS needed to induce aggregation in cells harvested at the exponential and stationary phases (Chapter 4).

Without the addition of non-biological polymers or EPS, *E.coli* still displays variations in their aggregation ability, as a function of growth or nutrient composition (media). This thesis hypothesized that changes in the growth phase and media affect the surface chemistry of the cells, which as a consequence affects the tendency for the cells to interact and form aggregates. From potentiometric titration studies, functional groups (carboxyl, phosphate, and amine groups deduced from pKa values) present of the *E.coli* surface did not change as a function of growth phase and media. However the, concentration of these functional groups changed with respect to group phase and media and correlated well with the changes in aggregation capability of *E.coli*. FTIR spectroscopy was using to complement the results obtained from potentiometric titration studies, and confirmed the presence of functional groups. Changes in the functional groups on the *E.coli* surface as a function of growth phase and media was also confirmed by FTIR spectroscopy.

Aggregation in bacteria serves an adaptive process in response to adverse changes in environmental conditions. Hence the ability of cells to aggregate will also depend on their ability to sense and respond to these changes in environmental conditions. In *E.coli* the ability to sense and respond to these changes is via a cell density dependent process known as quorum sensing (109). In addition, depletion

attractions increase the proximity of bacteria to each other and hence may promote the quorum sensing, since it is a cell density dependent process. Therefore, it was paramount to address the role of quorum sensing in the aggregation of *E.coli*. This was achieved by comparing the surface chemistry and aggregation capability of *E.coli* cells which have the ability to participate in quorum sensing (*E.coli* MG1655) and *E.coli* cells which lack the quorum sensing ability (*E.coli* MG1655 *luxS*⁻) (chapter 8). Interestingly, *E.coli* cells which had the ability to participate in the quorum sensing displayed a higher negative charge that cells lacking quorum sensing ability. However, only *E.coli* cells which lacked quorum sensing cultivated in LBG and harvested at the stationary growth phase, displayed a higher aggregation capability.

9.2. *Concluding remarks*

As *E.coli* cells progressed from the exponential to stationary phase, the production of EPS increased (as shown Chapter 5 and 6) and the quorum sensing molecule (AI-2) produced during the exponential growth phase was internalised by the cells when cultivated in LB (Chapter 3). The tendency of cells to aggregate also increased due to changes in the surface chemistry as cells progress from the exponential to the stationary phase. The changes in surface chemistry observed during growth phase may be due to the influence of quorum sensing as seen in Chapter 8. Further evidence can be seen in Chapter 7, where glucose was added to *E.coli* cultivated in LB. The glucose prevented the internalization of quorum sensing molecule (AI-2) and as such the surface chemistry at stationary for cells cultivated in LB and LBG differed, which accounted for the differences in the aggregation ability. Furthermore the free-EPS produce by cells at stationary phase had the higher capability to induce aggregation than that in stationary phase. The amount of free-EPS as well as its composition also varied upon addition of glucose to LB (i.e LBG) (Chapter 5). Hence it is possible that quorum sensing may also regulate EPS production. However this study further demonstrated that free-EPS only significantly induce aggregation in cells with low aggregation capability. The free-EPS is not required in situation were the cell surface property favors aggregation process. However, when cell surface properties due not promote the aggregation process, the free-EPS becomes a key factors. Hence, this thesis

suggest that the cell surface chemistry and free-EPS may both be controlled by quorum sensing and hence aggregation process. However further studies are needed in order to confirm this. These are discussed in the next section.

9.3. Recommendations

This thesis addressed the role of key biological factors such as growth phase, nutrient, EPS and quorum sensing as well as physical factors such as surface chemistry which are involved in bacterial aggregation. Although this thesis revealed significant findings in understanding bacterial aggregation, it still remains in its infancy in fully understanding the entire process involved in bacterial aggregation. As such there is the need to investigate several areas further, as detailed below.

This thesis demonstrated that it is possible to induce aggregation in bacteria by the addition of synthetic or EPS to bacterial suspensions. The ability of these polymers to induce aggregation is dependent on the composition as well as the surface chemistry of the cell. However, it still remains unclear as to the exact component of EPS that are involved in aggregation process. Although the carbohydrate content of EPS have been suggested to be the most abundant component, this thesis shows that the protein content dominates in EPS and changes during different growth condition. Proteins were identified, although their changes in expression as an index of growth phase and media was beyond the scope of this thesis and is recommended to be considered in future research. Hence further analysis should be carried out on the expression of extracellular proteins during cell aggregation. Using a quantitative proteomic approach (e.g. iTRAQ (158)) it would be possible to identify and quantify the extracellular proteins which are up- or down- regulated during the aggregation process. This will provide further insight to the key component of EPS involved in aggregation.

Likewise, this thesis has shown that quorum sensing influences the aggregation process in *E.coli* by altering the cell surface properties. However, the techniques used in this thesis (electrophoretic mobility, FTIR, potentiometric titration and SDS-PAGE) to elucidate surface chemistry; can only provide an indication of the

extent of cell surface alteration. They do not provide information about which surface macromolecules are regulated during the aggregation process. Therefore, the specific surface macromolecules which are regulated by quorum sensing still remains unknown. Hence it will be interesting to investigate the role of quorum sensing in the production of cell surface macromolecules such as lipopolysaccharides and outer membrane proteins using a proteomic or genomic approach. For example, proteomic studies of outer membrane proteins can be conducted on *E.coli* and its *luxS*- mutant (lacking the ability to participate in quorum sensing). Findings from these studies will reveal macromolecules which are regulated by quorum sensing.

Furthermore, it is possible that quorum sensing may also affect EPS production in bacteria and as such alter the cell surface chemistry and aggregation process. To best of the knowledge of the author this has not yet been investigated. Hence it is recommended that the role of quorum sensing on EPS production should be a focus of future research. This could be conducted by comparing the amount of EPS produced from a bacterium which posseses the ability to participate in quorum sensing and a mutant (lacking quorum sensing ability). Comparison of EPS production and composition (as demonstrated in Chapter 6) should be compared across the conditions investigated in Chapter 5, 7 and 8, to provide the link between quorum sensing, EPS production and aggregation ability.

Additional surface characterization techniques can be employed to further study the investigated changes in cell surface properties. For example, X-ray photoelectron spectroscopy (XPS) can be used the cells surface during growth and aggregation. This technique measures the elemental composition of a material top 1 to 10 nm (44). Hence unlike the FTIR the information obtained from the XPS, only relates to the surface. This thesis revealed that outer membrane proteins (OMP) play a crucial role in *E.coli* by altering cell surface properties. This thesis recommends that OMP should be investigated further. This could be done by further characterizing the OMP by a colloidal approach. For example,

electrokinetic properties of OMP extracted during aggregation process and growth phase can be elucidated using dynamic light scattering.

Finally, this work specifically addressed cell-to-cell interactions leading to aggregation and not cell-to-surface interactions (i.e. biofilms) although it is anticipated that similar processes are involved. In addition, bacterial aggregation processes involving bacteria from the same strain (autoaggregation), and not bacteria from different strain (coaggregation) as seen in oral bacteria, was the focus of this thesis. Hence, it will be interesting if the experimental approaches used in this thesis (e.g. EPS production and characterization, potentiometric titration, electrophoretic mobility and proteomics) were applied to microorganisms that are known to form biofilms and co-aggregates of oral biofilm bacteria. This would enable the possibility of any general observations of bacterial aggregation to be developed.

References

1. O'Toole, G., H. B. Kaplan, and R. Kolter. Biofilm formation as microbial development. Annual Review of Microbiology.**2000** 54:49-79.

2. Costerton, J. W., P. S. Stewart, and E. P. Greenberg. Bacterial Biofilms: A Common Cause of Persistent Infections. Science.**1999** 284:1318-1322.

3. Hall-Stoodley, L., J. W. Costerton, and P. Stoodley. Bacterial Biofilms: From The Natural Environment To Infectious Diseases. Nature Reviews Microbiology.**2004** 2:95-108.

4. Coulon, J., L. Matoub, M. Dossot, S. Marchand, G. Bartosz, and P. Leroy. Potential relationship between glutathione metabolism and flocculation in the yeast *Kluyveromyces lactis*. FEMS Yeast Research.**2007** 7:93-101.

5. Calleja, G. B. Microbial Aggregation, p. 1-9, **1984**. CRC Press, Inc, Florida.

6. Calleja, G. B. Aggregation, p. 303-321. *In* K. C. Marshall (ed.), Microbial Adhesion and Aggregation, **1984**. Springer, Berlin.

7. Marshall, K. C. Microbial Adhesion and Aggregation,**1984** vol. Springer-Verlag, New York.

8. Verstrepen, K. J., G. Derdelinckx, H. Verachtert, and F. R. Delvaux. Yeast flocculation: what brewers should know. Applied Microbiology and Biotechnology.**2003** 61:197-205.

9. Touhami, A., B. Hoffmann, A. Vasella, F. A. Denis, and Y. F. Dufrene. Aggregation of yeast cells: direct measurement of discrete lectin-carbohydrate interactions. Microbiology.**2003** 149:2873-2878.

10. Jin, Y.-L., and R. Alex Speers. Flocculation of *Saccharomyces cerevisiae*. Food Research International.**1998** 31:421-440.

11. Buswell, C. M., Y. M. Herlihy, P. D. Marsh, C. W. Keevil, and S. A. Leach. Coaggregation amongst aquatic biofilm bacteria. Journal of Applied Microbiology.**1997** 83:477-484.

12. Kolenbrander, P. E. Coaggregations among oral bacteria. Methods Enzymol.**1995** 253:385-97.

13. Khemaleelakul, S., J. C. Baumgartner, and S. Pruksakom. Autoaggregation and Coaggregation of Bacteria Associated with Acute Endodontic Infections. Journal of Endodontics.**2006** 32:312-318.

14. Ward, M. J., and D. R. Zusman. Motility in *Myxococcus xanthus* and its role in developmental aggregation. Current Opinion in Microbiology.**1999** 2:624-629.

15. Curtiss, R. Bacterial Conjugation. Annual Review of Microbiology.**1969** 23:69-136.

16. **Riedewald, F., and A. Sexton.** 2006. The biofilm busters, p. 27-29, TCE, vol. February 2006.

17. McDevitt, D., P. Francois, P. Vaudaux, and T. J. Foster. Molecular characterization of the clumping factor (fibrinogen receptor) of *Staphylococcus aureus*. Molecular Microbiology.**1994** 11:237-248.

18. Menozzi, F. D., P. E. Boucher, G. Riveau, C. Gantiez, and C. Locht. Surface-associated filamentous hemagglutinin induces autoagglutination of *Bordetella pertussis*. Infect. Immun.**1994** 62:4261-4269.

19. Sherlock, O., R. M. Vejborg, and P. Klemm. The TibA Adhesin/Invasin from Enterotoxigenic *Escherichia coli* Is Self Recognizing and Induces Bacterial Aggregation and Biofilm Formation. Infect. Immun.**2005** 73:1954-1963.

20. Miyamoto, Y., T. Mukai, F. Takeshita, N. Nakata, Y. Maeda, M. Kai, and M. Makino. Aggregation of mycobacteria caused by disruption of fibronectin-

attachment protein-encoding gene. FEMS Microbiology Letters.**2004** 236:227-234.

21. Jucker, B. A., H. Harms, and A. J. Zehnder. Adhesion of the positively charged bacterium *Stenotrophomonas (Xanthomonas) maltophilia* 70401 to glass and Teflon. Journal of Bacteriology.**1996** 178:5472-9.

22. Resch, A., R. Rosenstein, C. Nerz, and F. Gotz. Differential gene expression profiling of *Staphylococcus aureus* cultivated under biofilm and planktonic conditions. Appl Environ Microbiol.**2005** 71:2663-76.

23. van Loosdrecht, M. C., J. Lyklema, W. Norde, and A. J. Zehnder. Influence of interfaces on microbial activity. Microbiological Reviews.**1990** 54:75-87.

24. Bossier, P., and W. Verstraete. Triggers for microbial aggregation in activated sludge? Applied Microbiology and Biotechnology.**1996** 45:1-6.

25. Burdman, S., E. Jurkevitch, B. Schwartsburd, M. Hampel, and Y. Okon. Aggregation in *Azospirillum brasilense*: effects of chemical and physical factors and involvement of extracellular components. Microbiology.**1998** 144:1989-1999.

26. Burdman, S., E. Jurkevitch, M. E. Soria-Diaz, A. M. G. Serrano, and Y. Okon. Extracellular polysaccharide composition of *Azospirillum brasilense* and its relation with cell aggregation. FEMS Microbiology Letters.**2000** 189:259-264.

27. Zhang, Z., and L. S. Pierson, 3rd. A second quorum-sensing system regulates cell surface properties but not phenazine antibiotic production in *Pseudomonas aureofaciens*. Applied And Environmental Microbiology.**2001** 67:4305-4315.

28. Park, S., P. M. Wolanin, E. A. Yuzbashyan, P. Silberzan, J. B. Stock, and R. H. Austin. Motion to form a quorum. Science.**2003** 301:188.

29. van Loosdrecht, M. C., J. Lyklema, W. Norde, G. Schraa, and A. J. Zehnder. The role of bacterial cell wall hydrophobicity in adhesion. Applied And Environmental Microbiology.**1987** 53:1893-1897.

30. van Loosdrecht, M. C., J. Lyklema, W. Norde, G. Schraa, and A. J. Zehnder. Electrophoretic mobility and hydrophobicity as a measured to predict the initial steps of bacterial adhesion. Applied And Environmental Microbiology.**1987** 53:1898-901.

31. Hong, Y., and D. G. Brown. Cell surface acid-base properties of *Escherichia coli* and *Bacillus brevis* and variation as a function of growth phase, nitrogen source and C:N ratio. Colloids and Surfaces B: Biointerfaces.**2006** 50:112-119.

32. Flemming, H. C., and J. Wingender. Relevance of microbial extracellular polymeric substances (EPSs)--Part II: Technical aspects. Water Sci Technol.**2001** 43:9-16.

33. Flemming, H. C., and J. Wingender. Relevance of microbial extracellular polymeric substances (EPSs)--Part I: Structural and ecological aspects. Water Sci Technol.**2001** 43:1-8.

34. Bassler, B. L. How bacteria talk to each other: regulation of gene expression by quorum sensing. Current Opinion in Microbiology.**1999** 2:582-587.

35. Bassler, B. L. Small talk. Cell-to-cell communication in bacteria. Cell.**2002** 109:421-424.

36. Miller, M. B., and B. L. Bassler. Quorum sensing in bacteria. Annu Rev Microbiol.**2001** 55:165-99.

37. Schauder, S., and B. L. Bassler. The languages of bacteria. Genes & Dev.**2001** 15:1468-1480.

38. Whitehead, N. A., A. M. Barnard, H. Slater, N. J. Simpson, and G. P. Salmond. Quorum-sensing in Gram-negative bacteria. FEMS Microbiology Reviews.**2001** 25:365-404.

39. Pratt, L. A., and R. Kolter. Genetic analysis of *Escherichia coli* biofilm formation: roles of flagella, motility, chemotaxis and type I pili. Mol Microbiol.**1998** 30:285-293.

40. Valverde, A., Y. Okon, and S. Burdman. cDNA-AFLP reveals differentially expressed genes related to cell aggregation of Azospirillum brasilense. FEMS Microbiology Letters.**2006** 265:186-194.

41. Rowan Orme, C. W. I. D., Stephen Rimmer, Michelle Webb,. Proteomic analysis of *Escherichia coli* biofilms reveals the overexpression of the outer membrane protein OmpA. PROTEOMICS.**2006** 6:4269-4277.

42. De Windt, W., H. Gao, W. Kromer, P. Van Damme, J. Dick, J. Mast, N. Boon, J. Zhou, and W. Verstraete. AggA is required for aggregation and increased biofilm formation of a hyper-aggregating mutant of *Shewanella oneidensis* MR-1. Microbiology.**2006** 152:721-729.

43. Fein, J. B., J.-F. Boily, N. Yee, D. Gorman-Lewis, and B. F. Turner. Potentiometric titrations of *Bacillus subtilis* cells to low pH and a comparison of modeling approaches. Geochimica et Cosmochimica Acta.**2005** 69:1123-1132.

44. van der Mei, H. C., J. de Vries, and H. J. Busscher. X-ray photoelectron spectroscopy for the study of microbial cell surfaces. Surface Science Reports.**2000** 39:1-24.

45. Schmitt, J., and H.-C. Flemming. FTIR-spectroscopy in microbial and material analysis. International Biodeterioration & Biodegradation.**1998** 41:1-11.

46. Wilson, W. W., M. M. Wade, S. C. Holman, and F. R. Champlin. Status of methods for assessing bacterial cell surface charge properties based on zeta potential measurements. Journal of Microbiological Methods.**2001** 43:153-164.

47. Puskas, A., E. Greenberg, S. Kaplan, and A. Schaefer. A quorum-sensing system in the free-living photosynthetic bacterium *Rhodobacter sphaeroides*. J. Bacteriol.**1997** 179:7530-7537.

48. Asakura, S., and F. Oosawa. On interaction between two bodies immersed in a solution of macromolecules. J. Chem. Phys.**1954** 22:1255-1256.

49. Asakura, S., and F. I. Oosawa. Interaction between particles suspended in solutions of macromolecules. J. of Poly. Sci.**1958:**183-92.

50. Calleja, G. B. Cell Aggregation, p. 165–238. *In* A. H. R. a. J. S. Harrison (ed.), The Yeast, **1987**. vol. 2. Academic Press, London.

51. Wilen, B.-M., K. Keiding, and P. H. Nielsen. Flocculation of activated sludge flocs by stimulation of the aerobic biological activity. Water Research.**2004** 38:3909-3919.

52. Liu, Y., S.-F. Yang, J.-H. Tay, Q.-S. Liu, L. Qin, and Y. Li. Cell hydrophobicity is a triggering force of biogranulation. Enzyme and Microbial Technology.**2004** 34:371-379.

53. Liu, Y., and J.-H. Tay. State of the art of biogranulation technology for wastewater treatment. Biotechnology Advances.**2004** 22:533-563.

54. Kolenbrander, P. E. Intergeneric coaggregation among human oral bacteria and ecology of dental plaque. Annu. Rev. Microbiol.**1988** 42:627-656.

55. Rickard, A. H., P. Gilbert, N. J. High, P. E. Kolenbrander, and P. S. Handley. Bacterial coaggregation: an integral process in the development of multi-species biofilms. Trends Microbiol.**2003** 11:94-100.

56. Kolenbrander, P. E., R. N. Andersen, D. S. Blehert, P. G. Egland, J. S. Foster, and R. J. Palmer Jr. Communication among oral bacteria. Microbiology and Molecular Biology Reviews.**2002** 66:486-505.

57. Kolenbrander, P. E. Oral microbial communities: biofilms, interactions, and genetic systems. Annu Rev Microbiol.**2000** 54:413-37.

58. Kinder, S. A., and S. C. Holt. Coaggregation between bacterial species, p. 254-270, Methods in Enzymology, **1994**.Volume 236 ed. Academic Press.

59. Calleja, G. B. Hooks, loops, and the shallow minimum: mechanistic aspects of yeast flocculation. Colloids and Surfaces B: Biointerfaces.**1994** 2:133-149.

60. Shen, S., L. P. Samaranayake, and H.-K. Yip. Coaggregation profiles of the microflora from root surface caries lesions. Archives of Oral Biology.**2005** 50:23-32.

61. Cisar, J. O., P. E. Kolenbrander, and F. C. McIntire. Specificity of coaggregation reactions between human oral *streptococci* and strains of *Actinomyces viscosus* or *Actinomyces naeslundii*. Infection And Immunity.**1979** 24:742-752.

62. Rickard, A. H., P. Gilbert, and P. S. Handley. Influence of growth environment on coaggregation between freshwater biofilm bacteria. J Appl Microbiol.**2004** 96:1367-1373.

63. Eboigbodin, K. E., J. R. Newton, A. F. Routh, and C. A. Biggs. Role of nonadsorbing polymers in bacterial aggregation. Langmuir.**2005** 21:12315-12319.

64. Kjargaard, K., M. A. Schembri, H. Hasman, and P. Klemm. Antigen 43 from *Escherichia coli* Induces Inter- and Intraspecies Cell Aggregation and Changes in Colony Morphology of *Pseudomonas fluorescens*. J. Bacteriol.**2000** 182:4789-4796.

65. Helm E, Nohr B, and T. RSW. The measurement of yeast flocculence and its significance in brewing. Wallerstein Lab Commun.**1953** 16:315–326.

66. Malik, A., M. Sakamoto, T. Ono, and K. Kakii. Coaggregation between *Acinetobacter johnsonii* S35 and *Microbacterium esteraromaticum* strains

isolated from sewage activated sludge. Journal of Bioscience and Bioengineering.**2003** 96:10-15.

67. Borrego, S., E. Niubo, O. Ancheta, and M. E. Espinosa. Study of the microbial aggregation inmycobacterium using image analysis and electron microscopy. Tissue and Cell.**2000** 32:494-500.

68. Angert, E. R. Alternatives to binary fission in bacteria. **2005** 3:214-224.

69. Weiss, D. S. Bacterial cell division and the septal ring. Mol Microbiol.**2004** 54:588-97.

70. Madigan, M., and M. J. Brock Biology of Microorganisms, **2006**.11th edition ed. Prentice Hall.

71. Olsson, J., S. Dasgupta, O. G. Berg, and K. Nordstrom. Eclipse period without sequestration in *Escherichia coli*. Mol Microbiol.**2002** 44:1429-1440.

72. Olsson, J. A., K. Nordstrom, K. Hjort, and S. Dasgupta. Eclipse-Synchrony Relationship in *Escherichia coli* Strains with Mutations Affecting Sequestration, Initiation of Replication and Superhelicity of the Bacterial Chromosome. Journal of Molecular Biology.**2003** 334:919-931.

73. Cowell, B. A., P. Willcox, B. Herbert, and R. P. Schneider. Effect of nutrient limitation on adhesion characteristics of *Pseudomonas aeruginosa*. Journal of Applied Microbiology.**1999** 86:944-954.

74. Sokolov, I., D. S. Smith, G. S. Henderson, Y. A. Gorby, and F. G. Ferris. Cell Surface Electrochemical Heterogeneity of the Fe(III)-Reducing Bacteria *Shewanella putrefaciens*. Environ. Sci. Technol.**2001** 35:341-347.

75. Walker, S. L. The role of nutrient presence on the adhesion kinetics of *Burkholderia cepacia* G4g and ENV435g. Colloids and Surfaces B: Biointerfaces.**2005** 45:181-188.

76. Strevett, K. A., and G. Chen. Microbial surface thermodynamics and applications. Research in Microbiology.**2003** 154:329-335.

77. Song, B., and L. G. Leff. Influence of magnesium ions on biofilm formation by *Pseudomonas fluorescens*. Microbiological Research.**2006** 161:355-361.

78. Hayashi, H., H. Seiki, S. Tsuneda, A. Hirata, and H. Sasaki. Influence of growth phase on bacterial cell electrokinetic characteristics examined by soft particle electrophoresis theory. Journal of Colloid and Interface Science.**2003** 264:565-568.

79. Walker, S. L., J. E. Hill, J. A. Redman, and M. Elimelech. Influence of growth phase on adhesion kinetics of *Escherichia coli* D21g. Applied And Environmental Microbiology.**2005** 71:3093-3099.

80. Rickard, A. H., S. A. Leach, C. M. Buswell, N. J. High, and P. S. Handley. Coaggregation between Aquatic Bacteria Is Mediated by Specific-Growth-Phase-Dependent Lectin-Saccharide Interactions. Applied And Environmental Microbiology.**2000** 66:431-434.

81. Wingender, J., T. R. Neu, and H. C. Flemming. Microbial Extracellular polymeric substanaces,**1999** vol. Springer, Berlin.

82. Bramhachari, P. V., and S. K. Dubey. Isolation and characterization of exopolysaccharide produced by *Vibrio harveyi* strain VB23. Letters in Applied Microbiology.**2006** 43:571–577.

83. John, A., and P. H. Nielsen. Extraction of extracellular polymeric substances (eps) from biofilms using a cation exchange resin. Water Science and Technology.**1995** 32:157-164.

84. Sheng, G.-P., H.-Q. Yu, and Z. Yu. Extraction of extracellular polymeric substances from the photosynthetic bacterium *Rhodopseudomonas acidophila*. Applied Microbiology and Biotechnology.**2005** 67:125-130.

85. Liu, H., and H. H. P. Fang. Extraction of extracellular polymeric substances (EPS) of sludges. Journal of Biotechnology.**2002** 95:249-256.

86. Frolund, B., R. Palmgren, K. Keiding, and P. H. Nielsen. Extraction of extracellular polymers from activated sludge using a cation exchange resin. Water Research.**1996** 30:1749-1758.

87. Kristina D. Rinker, R. M. K. Effect of carbon and nitrogen sources on growth dynamics and exopolysaccharide production for the hyperthermophilic archaeon *Thermococcus litoralis* and bacterium *Thermotoga maritima*. Biotechnology and Bioengineering.**2000** 69:537-547.

88. Macedo, M. G., C. Lacroix, and C. P. Champagne. Combined Effects of Temperature and Medium Composition on Exopolysaccharide Production by *Lactobacillus rhamnosus* RW-9595M in a Whey Permeate Based Medium. Biotechnol. Prog.**2002** 18:167-173.

89. Bayer, A. S., F. Eftekhar, J. Tu, C. C. Nast, and D. P. Speert. Oxygen-dependent up-regulation of mucoid exopolysaccharide (alginate) production in *Pseudomonas aeruginosa*. Infect Immun.**1990** 58:1344-9.

90. Bayer, A. S., T. O'Brien, D. C. Norman, and C. C. Nast. Oxygen-dependent differences in exopolysaccharide production and aminoglycoside inhibitory-bactericidal interactions with *Pseudomonas aeruginosa*--implications for endocarditis. J Antimicrob Chemother.**1989** 23:21-35.

91. Degeest, B., and L. De Vuyst. Indication that the Nitrogen Source Influences Both Amount and Size of Exopolysaccharides Produced by *Streptococcus thermophilus* LY03 and Modelling of the Bacterial Growth and Exopolysaccharide Production in a Complex Medium. Appl. Environ. Microbiol.**1999** 65:2863-2870.

92. Dunne, W. M., Jr., and F. L. Buckmire. Effects of divalent cations on the synthesis of alginic acid-like exopolysaccharide from mucoid *Pseudomonas aeruginosa*. Microbios.**1985** 43:193-216.

93. Zhang, X., P. L. Bishop, and B. K. Kinkle. Comparison of extraction methods for quantifying extracellular polymers in biofilms. Water Science and Technology.**1999** 39:211-218.

94. Bhaskar, P. V., and N. B. Bhosle. Microbial extracellular polymeric substances in marine biogeochemical processes. Current Science.**2005** 88:45-53.

95. Wingender, J., and H.-C. Flemming. Autoaggregation in flocs and biofilms, p. 63–86. *In* J. Winter (ed.), Biotechnology, **1999**. vol. 8.

96. Kreft, J. U., and J. W. Wimpenny. Effect of EPS on biofilm structure and function as revealed by an individual-based model of biofilm growth. Water Science and Technology.**2001** 43:135-141.

97. Sutherland, I. W. Exopolysaccharides in biofilms, flocs and related structures. Water Science and Technology.**2001** 43:77-86.

98. Sand, W., and T. Gehrke. Extracellular polymeric substances mediate bioleaching/biocorrosion via interfacial processes involving iron(III) ions and acidophilic bacteria. Research in Microbiology.**2006** 157:49-56.

99. Bahat-Samet, E., S. Castro-Sowinski, and Y. Okon. Arabinose content of extracellular polysaccharide plays a role in cell aggregation of *Azospirillum brasilense*. FEMS Microbiology Letters.**2004** 237:195-203.

100. Ledeboer, N. A., and B. D. Jones. Exopolysaccharide Sugars Contribute to Biofilm Formation by *Salmonella enterica Serovar Typhimurium* on HEp-2 Cells and Chicken Intestinal Epithelium. J. Bacteriol.**2005** 187:3214-3226.

101. Tsuneda, S., H. Aikawa, H. Hayashi, A. Yuasa, and A. Hirata. Extracellular polymeric substances responsible for bacterial adhesion onto solid surface. FEMS Microbiology Letters.**2003** 223:287-292.

102. Weiner, R., S. Langille, and E. Quintero. Structure, function and immunochemistry of bacterial exopolysaccharides. Journal of Industrial Microbiology and Biotechnology.**1995** V15:339-346.

103. Laurent, M., G. Johannin, N. Gilbert, L. Lucas, D. Cassio, P. X. Petit, and A. Fleury. Power and limits of laser scanning confocal microscopy. Biology of the Cell.**1994** 80:229-240.

104. Lavoie, D. M., B. J. Little, R. I. Ray, R. H. Bennett, M. W. Lambert, V. Asper, and R. J. Baerwald. Environmental Scanning Electron-Microscopy of Marine Aggregates. Journal of Microscopy-Oxford.**1995** 178:101-106.

105. Lawrence, J. R., Y. T. J. Kwong, and G. D. W. Swerhone. Colonization and weathering of natural sulfide mineral assemblages by *Thiobacillus ferrooxidans*. Canadian Journal of Microbiology.**1997** 43:178-188.

106. Nealson, K. H., T. Platt, and J. W. Hastings. Cellular control of the synthesis and activity of the bacterial luminescent system. Journal Of Bacteriology.**1970** 104:313-322.

107. Nealson, K. H., and J. W. Hastings. Bacterial bioluminescence: its control and ecological significance. Microbiological Reviews.**1979** 43:496-518.

108. Whitehead, N. A., A. M. L. Barnard, H. Slater, N. J. L. Simpson, and G. P. C. Salmond. Quorum-sensing in Gram-negative bacteria. FEMS Microbiology Reviews.**2001** 25:365-404.

109. Waters, C. M., and B. L. Bassler. Quorum sensing: Cell-to-Cell Communication in Bacteria. Annual Review of Cell and Developmental Biology.**2005** 21:319-346.

110. Mok, K. C., N. S. Wingreen, and B. L. Bassler. Vibrio harveyi quorum sensing: a coincidence detector for two autoinducers controls gene expression. Embo J.**2003** 22:870-81.

111. Miller, M. B., and B. L. Bassler. QUORUM SENSING IN BACTERIA. Annual Review of Microbiology.**2001** 55:165-199.

112. Winson, M. K., M. Camara, A. Latifi, M. Foglino, S. R. Chhabra, M. Daykin, M. Bally, V. Chapon, G. P. Salmond, and a. Bycroft et. Multiple N-acyl-L-homoserine lactone signal molecules regulate production of virulence determinants and secondary metabolites in *Pseudomonas aeruginosa*. Proceedings Of The National Academy Of Sciences Of The United States Of America.**1995** 92:9427-9431.

113. Derzelle, S., E. Duchaud, F. Kunst, A. Danchin, and P. Bertin. Identification, Characterization, and Regulation of a Cluster of Genes Involved in Carbapenem Biosynthesis in *Photorhabdus luminescens*. Appl. Environ. Microbiol.**2002** 68:3780-3789.

114. Anand, S. K., and M. W. Griffiths. Quorum sensing and expression of virulence in *Escherichia coli* O157:H7. International Journal of Food Microbiology.**2003** 85:1-9.

115. Beck von Bodman, S., and S. K. Farrand. Capsular polysaccharide biosynthesis and pathogenicity in *Erwinia stewartii* require induction by an N-acylhomoserine lactone autoinducer. J Bacteriol.**1995** 177:5000-8.

116. Davies, D. G., M. R. Parsek, J. P. Pearson, B. H. Iglewski, J. W. Costerton, and E. P. Greenberg. The involvement of cell-to-cell signals in the development of a bacterial biofilm. Science.**1998** 280:295-8.

117. de Kievit, T., P. C. Seed, J. Nezezon, L. Passador, and B. H. Iglewski. RsaL, a Novel Repressor of Virulence Gene Expression in *Pseudomonas aeruginosa*. J. Bacteriol.**1999** 181:2175-2184.

118. Pearson, J., L. Passador, B. Iglewski, and E. Greenberg. A Second N-Acylhomoserine Lactone Signal Produced by *Pseudomonas aeruginosa*. PNAS.**1995** 92:1490-1494.

119. Fuqua, W. C., S. C. Winans, and E. P. Greenberg. Quorum sensing in bacteria: The LuxR-LuxI family of cell density- responsive transcriptional regulators. Journal of Bacteriology.**1994** 176:269-275.

120. Yao, Y., M. A. Martinez-Yamout, T. J. Dickerson, A. P. Brogan, P. E. Wright, and H. J. Dyson. Structure of the *Escherichia coli* Quorum Sensing Protein SdiA: Activation of the Folding Switch by Acyl Homoserine Lactones. Journal of Molecular Biology.**2006** 355:262-273.

121. Xavier, K. B., and B. L. Bassler. LuxS quorum sensing: more than just a numbers game. Current Opinion in Microbiology.**2003** 6:191-197.

122. De Keersmaecker, S. C. J., K. Sonck, and J. Vanderleyden. Let LuxS speak up in AI-2 signaling. Trends in Microbiology.**2006** 14:114-119.

123. Schauder, S., K. Shokat, M. G. Surette, and B. L. Bassler. The LuxS family of bacterial autoinducers: biosynthesis of a novel quorum-sensing signal molecule. Molecular Microbiology.**2001** 41:463-476.

124. Xavier, K. B., and B. L. Bassler. LuxS quorum sensing: more than just a numbers game. Curr Opin Microbiol.**2003** 6:191-7.

125. Winzer, K., K. R. Hardie, and P. Williams. Bacterial cell-to-cell communication: sorry, can't talk now - gone to lunch! Current Opinion in Microbiology.**2002** 5:216-22.

126. Chen, X., S. Schauder, N. Potier, A. Van Dorsselaer, I. Pelczer, B. L. Bassler, and F. M. Hughson. Structural identification of a bacterial quorum-sensing signal containing boron. Nature.**2002** 415:545-549.

127. Miller, S. T., K. B. Xavier, S. R. Campagna, M. E. Taga, M. F. Semmelhack, B. L. Bassler, and F. M. Hughson. *Salmonella typhimurium* Recognizes a Chemically Distinct Form of the Bacterial Quorum-Sensing Signal AI-2. Molecular Cell.**2004** 15:677-687.

128. Surette, M. G., and B. L. Bassler. Quorum sensing in *Escherichia coli and Salmonella typhimurium*. PNAS.**1998** 95:7046-7050.

129. Xavier, K. B., and B. L. Bassler. Interference with AI-2-mediated bacterial cell-cell communication. Nature.**2005** 437:750-753.

130. Wang, L., Y. Hashimoto, C.-Y. Tsao, J. J. Valdes, and W. E. Bentley. Cyclic AMP (cAMP) and cAMP Receptor Protein Influence both Synthesis and Uptake of Extracellular Autoinducer 2 in *Escherichia coli*. J. Bacteriol.**2005** 187:2066-2076.

131. Atkinson, S., J. P. Throup, G. S. A. B. Stewart, and P. Williams. A hierarchical quorum-sensing system in *Yersinia pseudotuberculosis* is involved in the regulation of motility and clumping. Molecular Microbiology.**1999** 33:1267-1277.

132. Gonzalez Barrios, A. F., R. Zuo, Y. Hashimoto, L. Yang, W. E. Bentley, and T. K. Wood. Autoinducer 2 Controls Biofilm Formation in *Escherichia coli* through a Novel Motility Quorum-Sensing Regulator (MqsR, B3022). Journal of Bacteriology.**2006** 188:305-316.

133. Xu, L., H. Li, C. Vuong, V. Vadyvaloo, J. Wang, Y. Yao, M. Otto, and Q. Gao. Role of the luxS Quorum-Sensing System in Biofilm Formation and Virulence of *Staphylococcus epidermidis*. Infect. Immun.**2006** 74:488-496.

134. Yazdankhah, S. P., H. Sorum, H. J. S. Larsen, and G. Gogstad. Rapid Method for Detection of Gram-Positive and -Negative Bacteria in Milk from Cows with Moderate or Severe Clinical Mastitis. J. Clin. Microbiol.**2001** 39:3228-3233.

135. Cabeen, M. T., and C. Jacobs-Wagner. Bacterial cell shape. **2005** 3:601-610.

136. Chaput, C., and I. G. Boneca. Peptidoglycan detection by mammals and flies. Microbes and Infection.**2007** 9:637-647.

137. Neuhaus, F. C., and J. Baddiley. A Continuum of Anionic Charge: Structures and Functions of D-Alanyl-Teichoic Acids in Gram-Positive Bacteria. Microbiol. Mol. Biol. Rev.**2003** 67:686-723.

138. Delcour, J., T. Ferain, M. Deghorain, E. Palumbo, and P. Hols. The biosynthesis and functionality of the cell-wall of lactic acid bacteria. Antonie van Leeuwenhoek.**1999** 76:159-184.

139. Ruiz, N., D. Kahne, and T. J. Silhavy. Advances in understanding bacterial outer-membrane biogenesis. Nat. Rev. Microbiol.**2006** 4:57-66.

140. Nikaido, H. Molecular Basis of Bacterial Outer Membrane Permeability Revisited. Microbiology and Molecular Biology Reviews.**2003** 67:593-656.

141. Bos, M. P., and J. Tommassen. Biogenesis of the Gram-negative bacterial outer membrane. Current Opinion in Microbiology.**2004** 7:610-616.

142. Walker, S. L., J. A. Redman, and M. Elimelech. Role of Cell Surface Lipopolysaccharides in *Escherichia coli* K12 Adhesion and Transport. Langmuir.**2004** 20:7736-7746.

143. Schulz, G. E. The structure of bacterial outer membrane proteins. **2002** 1565:308-317.

144. Scott, J. R., and T. C. Barnett. Surface Proteins of Gram-Positive Bacteria and How They Get There. Annual Review of Microbiology.**2006** 60:397-423.

145. Sonohara, R., N. Muramatsu, H. Ohshima, and T. Kondo. Difference in surface properties between *Escherichia coli and Staphylococcus aureus* as revealed by electrophoretic mobility measurements. Biophysical Chemistry.**1995** 55:273-277.

146. Burdman, S., E. Jurkevitch, B. Schwartsburd, and Y. Okon. Involvement of outer-membrane proteins in the aggregation of *Azospirillum brasilense*. Microbiology.**1999** 145:1145-1152.

147. Hasman, H., T. Chakraborty, and P. Klemm. Antigen-43-Mediated Autoaggregation of *Escherichia coli* Is Blocked by Fimbriation. J. Bacteriol.**1999** 181:4834-4841.

148. Andrés F. González Barrios, R. Z., Dacheng Ren, Thomas K. Wood,. Hha, YbaJ, and OmpA regulate Escherichia coli K12 biofilm formation and conjugation plasmids abolish motility. Biotechnology and Bioengineering.**2006** 93:188-200.

149. Wilkins, M. R., C. Pasquali, R. D. Appel, K. Ou, O. Golaz, J. C. Sanchez, J. X. Yan, A. A. Gooley, G. Hughes, I. Humphery-Smith, K. L. Williams, and D. F. Hochstrasser. From proteins to proteomes: large scale protein identification by two-dimensional electrophoresis and amino acid analysis. Biotechnology (N Y).**1996** 14:61-5.

150. Tyers, M., and M. Mann. From genomics to proteomics. **2003** 422:193-197.

151. Angelika Görg, W. W., Michael J. Dunn,. Current two-dimensional electrophoresis technology for proteomics. PROTEOMICS.**2004** 4:3665-3685.

152. Cordwell, S. J. Technologies for bacterial surface proteomics. Current Opinion in Microbiology.**2006** 9:320-329.

153. Nandakumar, M. P., A. Cheung, and M. R. Marten. Proteomic Analysis of Extracellular Proteins from *Escherichia coli* W3110. J. Proteome Res.**2006** 5:1155-1161.

154. Twine, S. M., N. C. S. Mykytczuk, M. Petit, T.-L. Tremblay, J. W. Conlan, and J. F. Kelly. *Francisella tularensis* Proteome: Low Levels of ASB-14 Facilitate the Visualization of Membrane Proteins in Total Protein Extracts. J. Proteome Res.**2005** 4:1848-1854.

155. Changxin Xu, S. W., Haixia Ren, Xiangmin Lin, Lina Wu, Xuanxian Peng,. Proteomic analysis on the expression of outer membrane proteins of *Vibrio*

alginolyticus at different sodium concentrations. PROTEOMICS.**2005** 5:3142-3152.

156. Thomas A. Rhomberg, O. K., Thierry Mini, Ursula Zimny-Arndt, Ulrika Wickenberg, Marlene Röttgen, Peter R. Jungblut, Paul Jenö, Siv G. E. Andersson, Christoph Dehio,. Proteomic analysis of the sarcosine-insoluble outer membrane fraction of the bacterial pathogen Bartonella henselae. PROTEOMICS.**2004** 4:3021-3033.

157. Xiong, Y., M. J. Chalmers, F. P. Gao, T. A. Cross, and A. G. Marshall. Identification of *Mycobacterium tuberculosis* H37Rv Integral Membrane Proteins by One-Dimensional Gel Electrophoresis and Liquid Chromatography Electrospray Ionization Tandem Mass Spectrometry. J. Proteome Res.**2005** 4:855-861.

158. Barrios-Llerena, M. E., P. K. Chong, C. S. Gan, A. P. L. Snijders, K. F. Reardon, and P. C. Wright. Shotgun proteomics of cyanobacteria--applications of experimental and data-mining techniques. Brief Funct Genomic Proteomic.**2006** 5:121-132.

159. Severin, A., E. Nickbarg, J. Wooters, S. A. Quazi, Y. V. Matsuka, E. Murphy, I. K. Moutsatsos, R. J. Zagursky, and S. B. Olmsted. Proteomic Analysis and Identification of Streptococcus pyogenes Surface-Associated Proteins. J. Bacteriol.**2007** 189:1514-1522.

160. Kalmokoff, M., P. Lanthier, T.-L. Tremblay, M. Foss, P. C. Lau, G. Sanders, J. Austin, J. Kelly, and C. M. Szymanski. Proteomic Analysis of *Campylobacter jejuni* 11168 Biofilms Reveals a Role for the Motility Complex in Biofilm Formation. J. Bacteriol.**2006** 188:4312-4320.

161. Cohen, D. P., J. Renes, F. G. Bouwman, E. G. Zoetendal, E. Mariman, W. M. de Vos, and E. E. Vaughan. Proteomic analysis of log to stationary growth phase *Lactobacillus plantarum* cells and a 2-DE database. Proteomics.**2006** 6:6485-93.

162. Kim, E.-J., W. Wang, W.-D. Deckwer, and A.-P. Zeng. Expression of the quorum-sensing regulatory protein LasR is strongly affected by iron and oxygen concentrations in cultures of *Pseudomonas aeruginosa* irrespective of cell density. Microbiology.**2005** 151:1127-1138.

163. Bos, R., H. C. van der Mei, and H. J. Busscher. Physico-chemistry of initial microbial adhesive interactions - its mechanisms and methods for study. FEMS Microbiology Reviews.**1999** 23:179-229.

164. Hoek, E. M. V., and G. K. Agarwal. Extended DLVO interactions between spherical particles and rough surfaces. Journal of Colloid and Interface Science.**2006** 298:50-58.

165. Vitte, J., A. M. Benoliel, A. Pierres, and P. Bongrand. Is There A Predictable Relationship Between Surface Physical-Chemical Properties And Cell Behaviour At The Interface? European Cells and Materials.**2004** 7:52-63.

166. Rijnaarts, H. H. M., W. Norde, J. Lyklema, and A. J. B. Zehnder. DLVO and steric contributions to bacterial deposition in media of different ionic strengths. Colloids and Surfaces B: Biointerfaces.**1999** 14:179-195.

167. Hermansson, M. The DLVO theory in microbial adhesion. Colloids and Surfaces B: Biointerfaces.**1999** 14:105-119.

168. Burnett, P.-G., H. Heinrich, D. Peak, P. J. Bremer, A. J. McQuillan, and C. J. Daughney. The effect of pH and ionic strength on proton adsorption by the thermophilic bacterium *Anoxybacillus flavithermus*. Geochimica et Cosmochimica Acta.**2006** 70:1914-1927.

169. Turner, B. F., and J. B. Fein. Protofit: A program for determining surface protonation constants from titration data. Computers & Geosciences.**2006** 32:1344-1356.

170. Herbelin, A. L., and J. C. Westall. 1999. FITEQL 4.0: a computer program for determination of chemical equilibrium constants from experimental data.. Department of Chemistry, Oregon State University, Corvallis.

171. Dittrich, M., and S. Sibler. Cell surface groups of two picocyanobacteria strains studied by zeta potential investigations, potentiometric titration, and infrared spectroscopy. Journal of Colloid and Interface Science.**2005** 286:487-495.

172. Ngwenya B.T, S. I.W., and K. L. Comparison of the acid-base behaviour and metal adsorption characteristics of a gram-negative bacterium with other strains. Applied Geochemistry.18:527-538.

173. Haas J.R., D. T.J., and W. R. Thermodynamics of U(VI) sorption onto Shewanella putrefaciens. Chemical Geology.180:33-54.

174. Yee, N., L. G. Benning, V. R. Phoenix, and F. G. Ferris. Characterization of Metal-Cyanobacteria Sorption Reactions: A Combined Macroscopic and Infrared Spectroscopic Investigation. Environ. Sci. Technol.**2004** 38:775-782.

175. Fein, J. B., C. J. Daughney, N. Yee, and T. A. Davis. A chemical equilibrium model for metal adsorption onto bacterial surfaces. Geochimica et Cosmochimica Acta.**1997** 61:3319-3328.

176. Hayashi, H., S. Tsuneda, A. Hirata, and H. Sasaki. Soft particle analysis of bacterial cells and its interpretation of cell adhesion behaviors in terms of DLVO theory. Colloids and Surfaces B: Biointerfaces.**2001** 22:149-157.

177. Poortinga, A. T., R. Bos, W. Norde, and H. J. Busscher. Electric double layer interactions in bacterial adhesion to surfaces. Surface Science Reports.**2002** 47:1-32.

178. Tsuneda, S., H. Aikawa, H. Hayashi, and A. Hirata. Significance of cell electrokinetic properties determined by soft-particle analysis in bacterial adhesion onto a solid surface. Journal of Colloid and Interface Science.**2004** 279:410-417.

179. van der Mei, H. C., and H. J. Busscher. Electrophoretic mobility distributions of single-strain microbial populations. Applied And Environmental Microbiology.**2001** 67:491-4.

180. Tsuneda, S., J. Jung, H. Hayashi, H. Aikawa, A. Hirata, and H. Sasaki. Influence of extracellular polymers on electrokinetic properties of heterotrophic bacterial cells examined by soft particle electrophoresis theory. Colloids and Surfaces B: Biointerfaces.**2003** 29:181-188.

181. Ohshima, H., and T. Kondo. Approximate analytic expression for the electrophoretic mobility of colloidal particles with surface-charge layers. Journal of Colloid and Interface Science.**1989** 130:281-282.

182. Ohshima, H., and T. Kondo. Electrophoretic mobility and Donnan potential of a large colloidal particle with a surface charge layer. Journal of Colloid and Interface Science.**1987** 116:305-311.

183. Ohshima, H. Electrophoretic mobility of soft particles. Colloids and Surfaces A: Physicochemical and Engineering Aspects.**1995** 103:249-255.

184. Ohshima, H. Electrophoresis of soft particles. Advances in Colloid and Interface Science.**1995** 62:189-235.

185. Ducel, V., P. Saulnier, J. Richard, and F. Boury. Plant protein-polysaccharide interactions in solutions: application of soft particle analysis and light scattering measurements. Colloids and Surfaces B: Biointerfaces.**2005** 41:95-102.

186. Skvarla, J., Kupka D, Navesnakova Y, and S. A. An evaluation of the outer membrane charge and softness of *Thiobacillus ferrooxidans* by the Ohshima's electrophoretic model of a "soft" particle. Folia Microbiologica.**2002** 47: 218-224 2002.

187. Zita, A., and M. Hermansson. Effects of bacterial cell surface structures and hydrophobicity on attachment to activated sludge flocs. Applied and Environmental Microbiology.**1997** 63:1168-1170.

188. Kos, B., J. Suskovic, S. Vukovic, M. Simpraga, J. Frece, and S. Matosic. Adhesion and aggregation ability of probiotic strain *Lactobacillus acidophilus* M92. J Appl Microbiol.**2003** 94:981-987.

189. Kos, B., Suskovicacute, J. , Vukovicacute, S. , M. Simpraga, J. Frece, Matosicacute, and S. . Adhesion and aggregation ability of probiotic strain *Lactobacillus acidophilus* M92. Journal Of Applied Microbiology.**2003** 94:981-987.

190. Del Re, B., B. Sgorbati, M. Miglioli, and D. Palenzona. Adhesion, autoaggregation and hydrophobicity of 13 strains of *Bifidobacterium longum*. Lett Appl Microbiol.**2000** 31:438-442.

191. Mozes, N., and P. G. Rouxhet. Methods for measuring hydrophobicity of microorganisms. Journal of Microbiological Methods.**1987** 6:99-112.

192. Daffonchio, D., J. Thaveesri, and W. Verstraete. Contact angle measurement and cell hydrophobicity of granular sludge from upflow anaerobic sludge bed reactors. Applied and Environmental Microbiology.**1995** 61:3676-3680.

193. van der Mei, H. C., A. H. Weerkamp, and H. J. Busscher. A comparison of various methods to determine hydrophobic properties of streptococcal cell surfaces. Journal of Microbiological Methods.**1987** 6:277-287.

194. Van der Mei, H. C., J. De Vries, and H. J. Busscher. Hydrophobic and electrostatic cell surface properties of thermophilic dairy streptococci. Applied and Environmental Microbiology.**1993** 59:4305-4312.

195. Bunt, C. R., D. S. Jones, and I. G. Tucker. The effects of pH, ionic strength and organic phase on the bacterial adhesion to hydrocarbons (BATH) test. International Journal of Pharmaceutics.**1993** 99:93-98.

196. Rosenberg, M., D. Gutnick, and E. Rosenberg. Adherence of bacteria to hydrocarbons: A simple method for measuring cell-surface hydrophobicity. FEMS Microbiology Letters.**1980** 9:29-33.

197. Ahimou, F., M. Paquot, P. Jacques, P. Thonart, and P. G. Rouxhet. Influence of electrical properties on the evaluation of the surface hydrophobicity of *Bacillus subtilis*. Journal of Microbiological Methods.**2001** 45:119-126.

198. Lindahl, M., A. Faris, T. Wadstrom, and S. Hjerten. A new test based on 'salting out' to measure relative hydrophobicity of bacterial cells. Biochimica et Biophysica Acta (BBA) - General Subjects.**1981** 677:471-476.

199. Sklodowska A, and M. R. . Relative surface charge, hydrophobicity of bacterial cells and their affinity to substrate during copper bioleaching from post-flotation wastes. Biotechnol.**1998** 20:229-233.

200. Hazen, B. W., and K. C. Hazen. Modification and application of a simple, surface hydrophobicity detection method to immune cells. Journal of Immunological Methods.**1988** 107:157-163.

201. Jabra-Rizk, M. A., W. A. Falkler, Jr., W. G. Merz, and T. F. Meiller. New assay for measuring cell surface hydrophobicities of *Candida dubliniensis* and *Candida albicans*. Clin Diagn Lab Immunol.**2001** 8:585-7.

202. Geertsema-Doornbusch, G. I., H. C. van der Mei, and H. J. Busscher. Microbial cell surface hydrophobicity The involvement of electrostatic interactions in microbial adhesion to hydrocarbons (MATH). Journal of Microbiological Methods.**1993** 18:61-68.

203. Rosenberg, M. Microbial adhesion to hydrocarbons: twenty-five years of doing MATH. FEMS Microbiology Letters.**2006** 262:129-134.

204. van der Mei, H. C., B. van de Belt-Gritter, and H. J. Busscher. Implications of microbial adhesion to hydrocarbons for evaluating cell surface hydrophobicity 2. Adhesion mechanisms. Colloids and Surfaces B: Biointerfaces.**1995** 5:117-126.

205. van der Mei, H. C., P. Brokke, J. Dankert, F. J. Jan, P. G. Rouxhet, and H. J. Busscher. Physicochemical surface properties of nonencapsulated and

encapsulated coagulase-negative staphylococci. Appl Environ Microbiol.**1989** 55:2806-14.

206. Tomeczek, L., G. Reid, P. L. Cuperus, J. A. McGroarty, H. C. van der Mei, A. W. Bruce, A. E. Khoury, and H. J. Busscher. Correlation between hydrophobicity and resistance to nonoxynol-9 and vancomycin for urogenital isolates of *lactobacilli*. FEMS Microbiology Letters.**1992** 94:101-104.

207. Sheng, G.-P., and H.-Q. Yu. Relationship between the extracellular polymeric substances and surface characteristics of *Rhodopseudomonas acidophila*.. Applied Microbiology and Biotechnology.**2006** 72:126-131.

208. Liu, Y.-Q., Y. Liu, and J.-H. Tay. The effects of extracellular polymeric substances on the formation and stability of biogranules. Applied Microbiology and Biotechnology.**2004** 65:143-148.

209. Wang, Z.-W., Y. Liu, and J.-H. Tay. Distribution of EPS and cell surface hydrophobicity in aerobic granules. Applied Microbiology and Biotechnology.**2005** 69:469-473.

210. van der Mei, H. C., B. van de Belt-Gritter, P. H. Pouwels, B. Martinez, and H. J. Busscher. Cell surface hydrophobicity is conveyed by S-layer proteins--a study in recombinant *lactobacilli*. Colloids and Surfaces B: Biointerfaces.**2003** 28:127-134.

211. Gennis, R. B. Some recent contributions of FTIR difference spectroscopy to the study of cytochrome oxidase. FEBS Letters.**2003** 555:2-7.

212. Schuster, K. C., F. Mertens, and J. R. Gapes. FTIR spectroscopy applied to bacterial cells as a novel method for monitoring complex biotechnological processes. Vibrational Spectroscopy.**1999** 19:467-477.

213. Essendoubi, M., D. Toubas, M. Bouzaggou, J.-M. Pinon, M. Manfait, and G. D. Sockalingum. Rapid identification of *Candida* species by FT-IR

microspectroscopy. Biochimica et Biophysica Acta (BBA) - General Subjects.**2005** 1724:239-247.

214. Sockalingum, G. D., W. Bouhedja, P. Pina, P. Allouch, C. Mandray, R. Labia, J. M. Millot, and M. Manfait. ATR-FTIR Spectroscopic Investigation of Imipenem-Susceptible and -Resistant *Pseudomonas aeruginosa* Isogenic Strains. Biochemical and Biophysical Research Communications.**1997** 232:240-246.

215. Maquelin, K., C. Kirschner, L.-P. Choo-Smith, N. A. Ngo-Thi, T. van Vreeswijk, M. Stammler, H. P. Endtz, H. A. Bruining, D. Naumann, and G. J. Puppels. Prospective Study of the Performance of Vibrational Spectroscopies for Rapid Identification of Bacterial and Fungal Pathogens Recovered from Blood Cultures. J. Clin. Microbiol.**2003** 41:324-329.

216. Kim, S., B. L. Reuhs, and L. J. Mauer. Use of Fourier transform infrared spectra of crude bacterial lipopolysaccharides and chemometrics for differentiation of *Salmonella enterica* serotypes. Journal of Applied Microbiology.**2005** 99:411-417.

217. Kim, S., H. Kim, B. L. Reuhs, and L. J. Mauer. Differentiation of outer membrane proteins from *Salmonella enterica* serotypes using Fourier transform infrared spectroscopy and chemometrics. Letters in Applied Microbiology.**2006** 42:229-234.

218. Omoike, A., and J. Chorover. Spectroscopic Study of Extracellular Polymeric Substances from *Bacillus subtilis*: Aqueous Chemistry and Adsorption Effects. Biomacromolecules.**2004** 5:1219-1230.

219. Serra, D., A. Bosch, D. M. Russo, M. a. E. RodrÃ-guez, Ã. n. Zorreguieta, J. Schmitt, D. Naumann, and O. Yantorno. Continuous nondestructive monitoring of *Bordetella pertussis* biofilms by Fourier transform infrared spectroscopy and other corroborative techniques. Analytical and Bioanalytical Chemistry.**2007** V387:1759-1767.

220. Blattner, F. R., G. Plunkett, 3rd, C. A. Bloch, N. T. Perna, V. Burland, M. Riley, J. Collado-Vides, J. D. Glasner, C. K. Rode, G. F. Mayhew, J. Gregor, N. W. Davis, H. A. Kirkpatrick, M. A. Goeden, D. J. Rose, B. Mau, and Y. Shao. The complete genome sequence of *Escherichia coli* K-12. Science.**1997** 277:1453-74.

221. Hardie, K. R., C. Cooksley, A. D. Green, and K. Winzer. Autoinducer 2 activity in *Escherichia coli* culture supernatants can be actively reduced despite maintenance of an active synthase, LuxS. Microbiology.**2003** 149:715-728.

222. Greenberg, E. P., J. W. Hastings, and S. Ulitzur. Induction of luciferase synthesis in *Beneckea harveyi* by other marine bacteria. Arch. Microbiol.**1979** 120:87-91.

223. Rozen, S., and H. Skaletsky. Primer3 on the WWW for general users and for biologist programmers. Methods Mol Biol.**2000** 132:365-86.

224. Thompson, J. D., D. G. Higgins, and T. J. Gibson. CLUSTAL W: Improving the sensitivity of progressive multiple sequence alignment through sequence weighting, position-specific gap penalties and weight matrix choice. Nucleic Acids Research.**1994** 22:4673-4680.

225. Saito, N., and M. Nei. The neighbor-joining method: a new method for constructing phylogenetic trees. Mol. Biol. Evol.**1987** 4:406-425.

226. Page, R. D. TreeView: an application to display phylogenetic trees on personal computers. Computer Applications In The Biosciences: CABIOS.**1996** 12:357-358.

227. Schauder, S., K. Shokat, M. G. Surette, and B. L. Bassler. The LuxS family of bacterial autoinducers: biosynthesis of a novel quorum-sensing signal molecule. Mol Microbiol.**2001** 41:463-476.

228. Xavier, K. B., and B. L. Bassler. Regulation of Uptake and Processing of the Quorum-Sensing Autoinducer AI-2 in *Escherichia coli*. J. Bacteriol.**2005** 187:238-248.

229. Rutter, P. R., and B. Vincent. Microbial Adhesion and Aggregation, p. 21. *In* K. C. Marshall (ed.), **1984**. Springer-Verlag, New York.

230. Smyth, C. J., P. Jönsson, E. Olsson, and a. et. Differences in hydrophobic surface characteristics of porcine enteropathogenic *Escherichia coli* with or without K88 antigen as revealed by hydrophobic interaction chromatography. Infect. Immun.**1978** 22:462-472.

231. Liu, Y., S.-F. Yang, Q.-S. Liu, and J.-H. Tay. The role of cell hydrophobicity in the formation of aerobic granules. Current Microbiology.**2003** 46:270-274.

232. Liu, Y., and H. H. P. Fang. Influences of Extracellular Polymeric Substances (EPS) on Flocculation, Settling, and Dewatering of Activated Sludge. Critical Reviews in Environmental Science and Technology.**2003** 33:237-273.

233. Hammer, B. K., and B. L. Bassler. Quorum sensing controls biofilm formation in Vibrio cholerae. Molecular Microbiology.**2003** 50:101-104.

234. Petry, S., S. Furlan, M.-J. Crepeau, J. Cerning, and M. Desmazeaud. Factors Affecting Exocellular Polysaccharide Production by *Lactobacillus delbrueckii* subsp. bulgaricus Grown in a Chemically Defined Medium. Applied And Environmental Microbiology.**2000** 66:3427-3431.

235. Wolfstein, K., and L. Stal. Production of extracellular polymeric substances (EPS) by benthic diatoms: effect of irradiance and temperature. Marine Ecology Progress Series.**2002** 236:13–22.

236. Jenkins, P., and M. Snowden. Depletion flocculation in colloidal dispersions. Advances in Colloid and Interface Science.**1996** 68:57-96.

237. Tuinier, R., J. Rieger, and C. G. de Kruif. Depletion-induced phase separation in colloid-polymer mixtures. Advances in Colloid and Interface Science.**2003** 103:1-31.

238. Cerda, J. J., T. Sintes, C. M. Sorensen, and A. Chakrabarti. Kinetics of phase transformations in depletion-driven colloids. Phys Rev E Stat Nonlin Soft Matter Phys.**2004** 70:011405.

239. Traube, J. Gummi-Ztg.**1925** 39:434-5.

240. Vrij, A. Polymers at interfaces and the interaction in colloidal dispersions. Pure Applied. Chemistry.**1976** 48:471-483.

241. Vincent, B., J. Edwards, S. Emmett, and A. Jones. Depletion flocculation in dispersions of sterically-stabilised particles ("soft spheres"). Colloids and Surfaces.**1986** 18:261-281.

242. Richetti, P., and P. Kekicheff. Direct measurement of depletion and structural forces in a micellar system. Physical Review Letters.**1992** 68:1951-1954.

243. Milling, A., and S. Biggs. Direct Measurement of the Depletion Force Using an Atomic Force Microscope. Journal of Colloid and Interface Science.**1995** 170:604-606.

244. Mondain-Monval, O., F. Leal-Calderon, J. Phillip, and J. Bibette. Depletion forces in the presence of electrostatic double layer repulsion. Physical Review Letters.**1995** 75:3364-3367.

245. Burns, J. L., Y.-d. Yan, G. J. Jameson, and S. Biggs. The Effect of Molecular Weight of Nonadsorbing Polymer on the Structure of Depletion-Induced Flocs. Journal of Colloid and Interface Science.**2002** 247:24-32.

246. Yan, Y.-d., J. L. Burns, G. J. Jameson, and S. Biggs. The structure and strength of depletion force induced particle aggregates. Chemical Engineering Journal.**2000** 80:23-30.

247. Tuinier, R., and C. G. de Kruif. Phase Separation, Creaming, and Network Formation of Oil-in-Water Emulsions Induced by an Exocellular Polysaccharide. Journal of Colloid and Interface Science.**1999** 218:201-210.

248. Tuinier, R., E. ten Grotenhuis, C. Holt, P. A. Timmins, and C. G. de Kruif. Depletion interaction of casein micelles and an exocellular polysaccharide. Physical Review E (Statistical Physics, Plasmas, Fluids, and Related Interdisciplinary Topics).**1999** 60:848-856.

249. Tuinier, R., and C. G. de Kruif. Phase behavior of casein micelles/exocellular polysaccharide mixtures: Experiment and theory. Journal of Chemical Physics.**1999** 110:9296-9304.

250. de Bont, P. W., G. M. P. van Kempen, and R. Vreeker. Phase separation in milk protein and amylopectin mixtures. Food Hydrocolloids.**2002** 16:127-138.

251. Anderson, V. J., E. H. A. de Hoog, and H. N. W. Lekkerkerker. Mechanisms of phase separation and aggregation in colloid-polymer mixtures. Phys. Rev. E.**2002** 65:011403-1-011403-8.

252. Jenkins, P., and V. B. Depletion Flocculation of Nonaqueous Dispersions Containing Binary Mixtures of Nonadsorbing Polymers. Evidence for Nonequilibrium Effects. Langmuir.**1996** 12:3107-3113.

253. deKerchove, A. J., and M. Elimelech. Relevance of Electrokinetic Theory for "Soft" Particles to Bacterial Cells: Implications for Bacterial Adhesion. Langmuir.**2005** 21:6462-6472.

254. Packer, L., B. Arrio, G. Johannin, and P. Volfin. Surface charge of purple membranes measured by laser Doppler velocimetry. Biochemical and Biophysical Research Communications.**1984** 122:252-258.

255. Feigin, R. I., and D. H. Napper. Depletion stabilization and depletion flocculation. Journal of Colloid and Interface Science.**1980** 75:525-541.

256. Jucker, B. A., H. Harms, S. J. Hug, and A. J. B. Zehnder. Adsorption of bacterial surface polysaccharides on mineral oxides is mediated by hydrogen bonds. Colloids and Surfaces B: Biointerfaces.**1997** 9:331-343.

257. Jucker, B. A., H. Harms, and A. J. B. Zehnder. Polymer interactions between five gram-negative bacteria and glass investigated using LPS micelles and vesicles as model systems. Colloids and Surfaces B: Biointerfaces.**1998** 11:33-45.

258. Eboigbodin, K. E., J. R. A. Newton, A. F. Routh, and C. A. Biggs. Bacterial quorum sensing and cell surface electrokinetic properties. Applied Microbiology and Biotechnology.**2006** 73:669-675.

259. Lowry, O. H., N. J. Rosebrough, A. L. Farr, and R. J. Randall. Protein Measurement With The Folin Phenol Reagent. J. Biol. Chem.**1951** 193:265-275.

260. Gaudy, A. F. Colorimetric determination of protein and carbohydrate. Industrial Water and Wastes.**1962** 7:17-22.

261. Eboigbodin, K. E., J. Newton, A. Routh, and C. Biggs. Bacterial quorum sensing and cell surface electrokinetic properties. Applied Microbiology and Biotechnology.**2006** 73:669-675.

262. Razatos, A., Y.-L. Ong, M. M. Sharma, and G. Georgiou. Molecular determinants of bacterial adhesion monitored by atomic force microscopy. PNAS.**1998** 95:11059-11064.

263. Han, L., S.-O. Enfors, and L. HÃ¤ggstrÃ¶m. *Escherichia coli* high-cell-density culture: carbon mass balances and release of outer membrane components. Bioprocess and Biosystems Engineering.**2003** 25:205-212.

264. Lin, M., M. Al-Holy, S.-S. Chang, Y. Huang, A. G. Cavinato, D.-H. Kang, and B. A. Rasco. Rapid discrimination of *Alicyclobacillus* strains in apple juice by Fourier transform infrared spectroscopy. International Journal of Food Microbiology.**2005** 105:369-376.

265. Maquelin, K., C. Kirschner, L.-P. Choo-Smith, N. van den Braak, H. P. Endtz, D. Naumann, and G. J. Puppels. Identification of medically relevant microorganisms by vibrational spectroscopy. Journal of Microbiological Methods.**2002** 51:255-271.

266. Danese, P. N., L. A. Pratt, and R. Kolter. Exopolysaccharide production is required for development of *Escherichia coli* K-12 biofilm architecture. J Bacteriol.**2000** 182:3593-6.

267. Nielsen PH, and A. Jahn. Extraction of extracellular polymeric substances, p. 21–47. *In* N. T. Wingender J, Flemming HC (ed.), **1999**. Springer, Berlin Heidelberg New York.

268. Costerton, J. W., R. T. Irvin, and K. J. Cheng. The bacterial glycocalyx in nature and disease. Annu Rev Microbiol.**1981** 35:299-324.

269. Nielsen, P. H., A. Jahn, and R. Palmgren. Conceptual model for production and composition of exopolymers in biofilms. Water Science and Technology.**1997** 36:11-19.

270. Dignac, M.-F., V. Urbain, D. Rybacki, A. Bruchet, D. Snidaro, and P. Scribe. Chemical description of extracellular polymers: implication on activated sludge floc structure. Water Science and Technology.**1998** 38:45-53.

271. Sandkvist, M. Type II Secretion and Pathogenesis. Infect. Immun.**2001** 69:3523-3535.

272. Hartl, F.-U., S. Lecker, E. Schiebel, J. P. Hendrick, and W. Wickner. The binding cascade of SecB to SecA to SecY/E mediates preprotein targeting to the *E. coli* plasma membrane. Cell.**1990** 63:269-279.

273. Wick, L. M., M. Quadroni, and T. Egli. Short- and long-term changes in proteome composition and kinetic properties in a culture of *Escherichia coli* during transition from glucose-excess to glucose-limited growth conditions in

continuous culture and vice versa. Environmental Microbiology.**2001** 3:588-599.

274. Pei-Wen Chu, M.-N. Y., Chi-Yue Wu, Chun-Ming Huang, Fu-Ming Pan, Min-Jen Tseng, Shui-Tein Chen,. A proteomic analysis of secreted proteins from xylan-induced Bacillus sp. strain K-1. Electrophoresis.**2000** 21:1740-1745.

275. Li, M., I. Rosenshine, S. L. Tung, X. H. Wang, D. Friedberg, C. L. Hew, and K. Y. Leung. Comparative proteomic analysis of extracellular proteins of enterohemorrhagic and enteropathogenic *Escherichia coli* strains and their ihf and ler mutants. Appl Environ Microbiol.**2004** 70:5274-82.

276. Laemmli, U. K. Cleavage of Structural Proteins during the Assembly of the Head of Bacteriophage T4. Nature.**1970** 227:680-685.

277. Chee Sian Gan, K. F. R., Phillip C. Wright,. Comparison of protein and peptide prefractionation methods for the shotgun proteomic analysis of *Synechocystis sp.* PCC 6803. PROTEOMICS.**2005** 5:2468-2478.

278. Kyte, J., and R. F. Doolittle. A simple method for displaying the hydropathic character of a protein. Journal of Molecular Biology.**1982** 157:105-132.

279. Gasteiger E., Hoogland C., Gattiker A., Duvaud S., Wilkins M.R., Appel R.D., and B. A.;. Protein Identification and Analysis Tools on the ExPASy Server, p. 571-607. *In* J. M. Walker (ed.), The Proteomics Protocols Handbook, **2005**. Humana Press., Hatfield, Herts, UK.

280. Gardy, J. L., M. R. Laird, F. Chen, S. Rey, C. J. Walsh, M. Ester, and F. S. L. Brinkman. PSORTb v.2.0: Expanded prediction of bacterial protein subcellular localization and insights gained from comparative proteome analysis. Bioinformatics.**2005** 21:617-623.

281. Juncker, A. S., H. Willenbrock, G. von Heijne, S. Brunak, H. Nielsen, and A. Krogh. Prediction of lipoprotein signal peptides in Gram-negative bacteria. Protein Sci.**2003** 12:1652-1662.

282. Martinez, A., and R. Kolter. Protection of DNA during oxidative stress by the nonspecific DNA- binding protein Dps. J. Bacteriol.**1997** 179:5188-5194.

283. Fekkes, P., J. G. de Wit, J. P. W. van der Wolk, H. H. Kimsey, C. A. Kumamoto, and A. J. M. Driessen. Preprotein transfer to the *Escherichia coli* translocase requires the co-operative binding of SecB and the signal sequence to SecA. Molecular Microbiology.**1998** 29:1179-1190.

284. Baars, L., A. J. Ytterberg, D. Drew, S. Wagner, C. Thilo, K. J. van Wijk, and J.-W. de Gier. Defining the Role of the *Escherichia coli* Chaperone SecB Using Comparative Proteomics. J. Biol. Chem.**2006** 281:10024-10034.

285. Jackson, D. W., J. W. Simecka, and T. Romeo. Catabolite Repression of *Escherichia coli* Biofilm Formation. J. Bacteriol.**2002** 184:3406-3410.

286. Sterkenburg, A., E. Vlegels, and J. T. Wouters. Influence of nutrient limitation and growth rate on the outer membrane proteins of *Klebsiella aerogenes* NCTC 418. J Gen Microbiol.**1984** 130:2347-55.

287. Liu, X., and T. Ferenci. Regulation of Porin-Mediated Outer Membrane Permeability by Nutrient Limitation in *Escherichia coli*. J. Bacteriol.**1998** 180:3917-3922.

288. Nandi, B., R. K. Nandy, A. Sarkar, and A. C. Ghose. Structural features, properties and regulation of the outer-membrane protein W (OmpW) of *Vibrio cholerae*. Microbiology.**2005** 151:2975-2986.

289. Gavin, R., A. A. Rabaan, S. Merino, J. M. Tomas, I. Gryllos, and J. G. Shaw. Lateral flagella of *Aeromonas* species are essential for epithelial cell adherence and biofilm formation. Molecular Microbiology.**2002** 43:383-397.

290. Wai, S. N., Y. Mizunoe, A. Takade, S.-I. Kawabata, and S.-I. Yoshida. *Vibrio cholerae* O1 Strain TSI-4 Produces the Exopolysaccharide Materials That Determine Colony Morphology, Stress Resistance, and Biofilm Formation. Appl. Environ. Microbiol.**1998** 64:3648-3655.

291. Kolenbrander, P., N. Ganeshkumar, F. Cassels, and C. Hughes. Coaggregation: specific adherence among human oral plaque bacteria. FASEB J.**1993** 7:406-413.

292. O'Toole, G., and R. Kolter. Flagellar and twitching motility are necessary for *Pseudomonas aeruginosa* biofilm development. Mol Microbiol.**1998** 30:295 - 304.

293. Torimura, M., S. Ito, K. Kano, T. Ikeda, Y. Esaka, and T. Ueda. Surface characterization and on-line activity measurements of microorganisms by capillary zone electrophoresis. Journal of Chromatography B: Biomedical Sciences and Applications.**1999** 721:31-37.

294. Takashima, S., and H. Morisaki. Surface characteristics of the microbial cell of *Pseudomonas* syringae and its relevance to cell attachment. Colloids and Surfaces B: Biointerfaces.**1997** 9:205-212.

295. Kolenbrander, P. E., N. Ganeshkumar, F. J. Cassels, and C. V. Hughes. Coaggregation: specific adherence among human oral plaque bacteria. Faseb J.**1993** 7:406-13.

296. Yee, N., and J. Fein. Cd adsorption onto bacterial surfaces: A universal adsorption edge? Geochimica et Cosmochimica Acta.**2001** 65:2037-2042.

297. Borrok, D., M. J. Borrok, J. B. Fein, and L. L. Kiessling. Link between Chemotactic Response to Ni^{2+} and its Adsorption onto the *Escherichia coli* Cell Surface. Environ. Sci. Technol.**2005** 39:5227-5233.

298. Manas, P., and B. M. Mackey. Morphological and Physiological Changes Induced by High Hydrostatic Pressure in Exponential- and Stationary-Phase Cells of *Escherichia coli*: Relationship with Cell Death. Appl. Environ. Microbiol.**2004** 70:1545-1554.

299. O'Toole, G. A., and R. Kolter. Initiation of biofilm formation in *Pseudomonas fluorescens* WCS365 proceeds via multiple, convergent signalling pathways: a genetic analysis. Molecular Microbiology.**1998** 28:449-461.

300. Filip, C., G. Fletcher, J. L. Wulff, and C. F. Earhart. Solubilization of the Cytoplasmic Membrane of *Escherichia coli* by the Ionic Detergent Sodium-Lauryl Sarcosinate. J. Bacteriol.**1973** 115:717-722.

301. Banerjee, U. C., Y. Chisti, and M. Moo-Young. Spectrophotometric determination of mycelial biomass. Biotechnology Techniques.**1993** V7:313-316.

302. Stanley, N. R., R. A. Britton, A. D. Grossman, and B. A. Lazazzera. Identification of Catabolite Repression as a Physiological Regulator of Biofilm Formation by *Bacillus subtilis* by Use of DNA Microarrays. J. Bacteriol.**2003** 185:1951-1957.

303. Sperandio, V., A. G. Torres, J. A. Giron, and J. B. Kaper. Quorum Sensing Is a Global Regulatory Mechanism in Enterohemorrhagic *Escherichia coli* O157:H7. J. Bacteriol.**2001** 183:5187-5197.

304. DeLisa, M. P., C.-F. Wu, L. Wang, J. J. Valdes, and W. E. Bentley. DNA Microarray-Based Identification of Genes Controlled by Autoinducer 2-Stimulated Quorum Sensing in *Escherichia coli*. Journal of Bacteriology.**2001** 183:5239-5247.

305. Martinez, R. E., D. S. Smith, E. Kulczycki, and F. G. Ferris. Determination of Intrinsic Bacterial Surface Acidity Constants using a Donnan Shell Model and a Continuous pKa Distribution Method. Journal of Colloid and Interface Science.**2002** 253:130-139.

306. Walker, S. L., J. A. Redman, and M. Elimelech. Influence of growth phase on bacterial deposition: interaction mechanisms in packed-bed column and radial stagnation point flow systems. Environ Sci Technol.**2005** 39:6405-6411.

307. Vinchurkar, M. S., K. H.-C. Chen, S. S.-F. Yu, S.-J. Kuo, H.-C. Chiu, S.-H. Chien, and S. I. Chan. Polarized ATR-FTIR Spectroscopy of the Membrane-Embedded Domains of the Particulate Methane Monooxygenase. Biochemistry.**2004** 43:13283-13292.

308. Alexander, D. M., and A. C. St John. Characterization of the carbon starvation-inducible and stationary phase-inducible gene slp encoding an outer membrane lipoprotein in *Escherichia coli*. Mol Microbiol.**1994** 11:1059-71.

309. Pollitt, S., S. Inouye, and M. Inouye. Effect of amino acid substitutions at the signal peptide cleavage site of the **Escherichia coli** major outer membrane lipoprotein. J. Biol. Chem.**1986** 261:1835-1837.

310. Hussain, M., S. Ichihara, and S. Mizushima. Accumulation of glyceride-containing precursor of the outer membrane lipoprotein in the cytoplasmic membrane of *Escherichia coli* treated with globomycin. J. Biol. Chem.**1980** 255:3707-3712.

311. Caroff, M., and D. Karibian. Structure of bacterial lipopolysaccharides. Carbohydrate Research.**2003** 338:2431-2447.

312. Eboigbodin, K. E., J. R. A. Newton, A. F. Routh, and C. A. Biggs. Role of Nonadsorbing Polymers in Bacterial Aggregation. Langmuir.**2005** 21:12315-12319.

313. Puskas, A., E. P. Greenberg, S. Kaplan, and A. L. Schaefer. A quorum-sensing system in the free-living photosynthetic bacterium Rhodobacter sphaeroides. Journal Of Bacteriology.**1997** 179:7530-7537.

314. Merritt, J., F. Qi, S. D. Goodman, M. H. Anderson, and W. Shi. Mutation of luxS affects biofilm formation in *Streptococcus mutans*. Infection And Immunity.**2003** 71:1972-1979.

315. Yoshida, A., T. Ansai, T. Takehara, and H. K. Kuramitsu. LuxS-Based Signaling Affects *Streptococcus mutans* Biofilm Formation. Applied And Environmental Microbiology.**2005** 71:2372-2380.

316. Winzer, K., C. Falconer, N. C. Garber, S. P. Diggle, M. Camara, and P. Williams. The *Pseudomonas aeruginosa* lectins PA-IL and PA-IIL are controlled by quorum sensing and by RpoS. Journal of Bacteriology.**2000** 182:6401-6411.

317. Asanuma, N., T. Yoshii, and T. Hino. Molecular Characterization and Transcription of the *luxS* Gene That Encodes LuxS Autoinducer 2 Synthase in *Streptococcus bovis*. Current Microbiology.**2004** 49:366-371.

318. Taga, M. E., S. T. Miller, and B. L. Bassler. Lsr-mediated transport and processing of AI-2 in *Salmonella typhimurium*. Molecular Microbiology.**2003** 50:1411-1427.

319. de Kerchove, A. J., and M. Elimelech. Relevance of electrokinetic theory for "soft" particles to bacterial cells: implications for bacterial adhesion. Langmuir.**2005** 21:6462-72.

320. Ricq, L., A. Pierre, J.-C. Reggiani, J. Pagetti, and A. Foissy. Use of electrophoretic mobility and streaming potential measurements to characterize electrokinetic properties of ultrafiltration and microfiltration membranes. Colloids and Surfaces A: Physicochemical and Engineering Aspects.**1998** 138:301-308.

Appendices

Appendix A

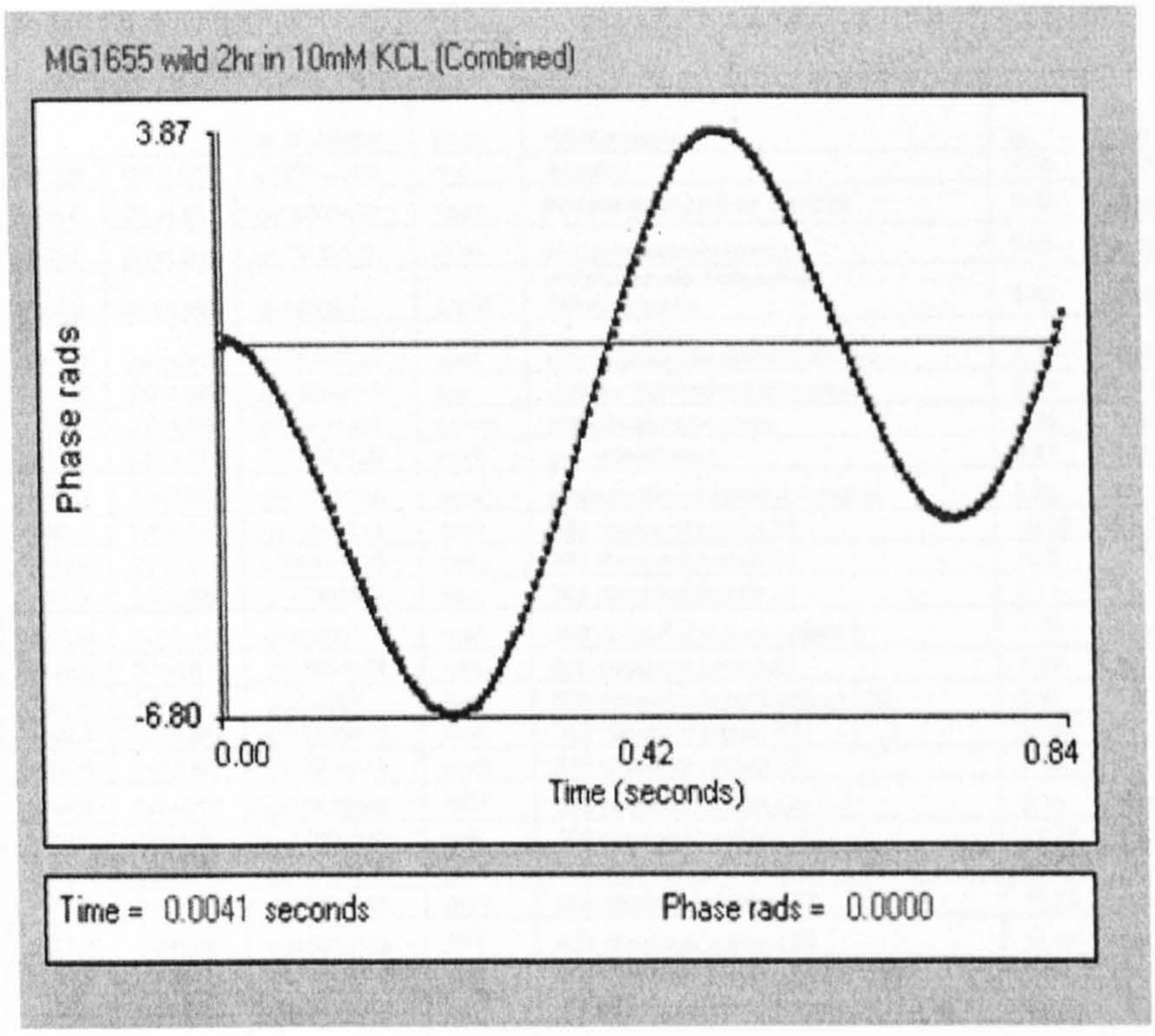

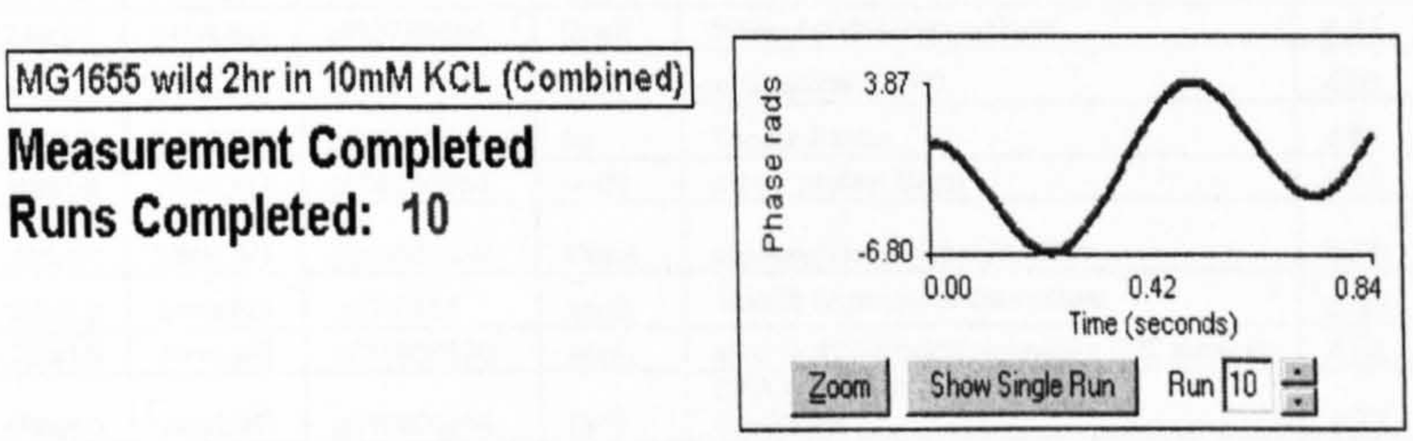

Run	Mobility	Zeta Potential (mV)	Rel. Residual
1	-2.62	-33.50	0.0135
2	-2.75	-35.15	0.0115
3	-2.65	-33.93	0.0124
4	-2.57	-32.83	0.0087
5	-2.52	-32.32	0.0152
6	-2.50	-31.94	0.0133
7	-2.26	-28.93	0.0068
8	-2.45	-31.33	0.0108
9	-2.54	-32.47	0.0160
10	-2.34	-29.94	0.0099
Mean	-2.52	-32.23	0.0118
Std. Error	0.05	0.58	0.0009
Combined	-2.52	-32.21	0.0052

Measurement Parameters:	
Conductance	= 9 µS
Electric Field	= 9.95 V/cm
Sample Count Rate	= 456 kcps
Ref. Count Rate	= 1248 kcps

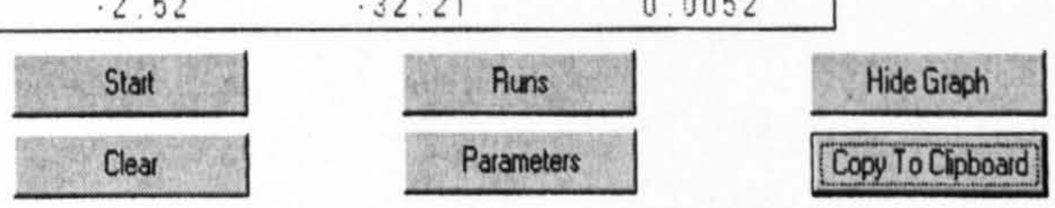

Appendix A Display of Zeta PALS utilizing phase analysis light scattering to determine the electrophoretic mobility of charged bacteria

Appendix B. Summary of major *E.coli* MG1655 extracellular proteins common to all growth conditions

Growth condition				GI NUMBER	Gene	*Protein name*	pI	Mr (Da)	GRAVY	LOCATION (PSORTb)	score
6hrLB	6hrLBG	24hrLB	24hrLBG	gi|15803300	eno	enolase	5.36	45574	-0.155	Cytoplasmic	1996
6hrLB	6hrLBG	24hrLB	24hrLBG	gi|15803459	FbaA	fructose-bisphosphate aldolase	5.52	38966	-0.349	UNKNOWN	1374
6hrLB	6hrLBG	24hrLB	24hrLBG	gi|16130827	PGK	phosphoglycerate kinase	5.08	41093	0 072	Cytoplasmic	5084
6hrLB	6hrLBG	24hrLB	24hrLBG	gi|146099	GapA	glyceraldehyde-3-phosphate dehydrogenase	6.02	33070	-0.162	Cytoplasmic	1090
6hrLB	6hrLBG	24hrLB	24hrLBG	gi|15799799	aceF	dihydrolipoamide acetyltransferase	5.09	66055	-0 008	Cytoplasmic Membrane	1065
6hrLB	6hrLBG	24hrLB	24hrLBG	gi|15804618	pgi	glucose-6-phosphate isomerase	5 85	61749	-0.268	Cytoplasmic	823
6hrLB	6hrLBG	24hrLB	24hrLBG	gi|16131483	GpmA	phosphoglyceromutase	5.85	28571	-0.195	Cytoplasmic	650
6hrLB	6hrLBG	24hrLB	24hrLBG	gi|26247926	pykF	pyruvate kinase I	5 77	50276	-0 071	UNKNOWN	592
6hrLB	6hrLBG	24hrLB	24hrLBG	gi|15799798	aceE	pyruvate dehydrogenase complex	5 46	99606	-0.437	UNKNOWN	2452
6hrLB	6hrLBG	24hrLB	24hrLBG	gi|15803823	rpsD	30S ribosomal protein S4	10.05	23455	-0.664	Cytoplasmic	1904
6hrLB	6hrLBG	24hrLB	24hrLBG	gi|16131220	rpsG	30S ribosomal protein S7	10.3	17593	-0.46	UNKNOWN	1703
6hrLB	6hrLBG	24hrLB	24hrLBG	gi|15803832	RplF	50S ribosomal protein L6	9.71	18892	-0 227	Cytoplasmic	1511
6hrLB	6hrLBG	24hrLB	24hrLBG	gi|42900	rpsA	30S ribosomal subunit protein S1	4.86	60979	-0 288	Cytoplasmic	1497
6hrLB	6hrLBG	24hrLB	24hrLBG	gi|15804574	rplA	50S ribosomal protein L1	9 64	24714	-0.109	UNKNOWN	1219
6hrLB	6hrLBG	24hrLB	24hrLBG	gi|223035	RplJ	50S ribosomal subunit protein L10	9 27	17725	0.007	UNKNOWN	760
6hrLB	6hrLBG	24hrLB	24hrLBG	gi|15803841	rpsC	30S ribosomal protein S3	10.27	26021	-0.422	Cytoplasmic	714
6hrLB	6hrLBG	24hrLB	24hrLBG	gi|26246115	rpsB	30S ribosomal protein S2	7.16	34405	-0.27	Cytoplasmic	646
6hrLB	6hrLBG	24hrLB	24hrLBG	gi|15803846	rplD	50S ribosomal protein L4	9 72	22073	-0 235	UNKNOWN	500
6hrLB	6hrLBG	24hrLB	24hrLBG	gi|15803840	rplP	50S ribosomal protein L16	11.22	15271	-0.384	UNKNOWN	449
6hrLB	6hrLBG	24hrLB	24hrLBG	gi|15803830	rpsE	30S ribosomal protein S5	10.11	17592	-0.101	UNKNOWN	408
6hrLB	6hrLBG	24hrLB	24hrLBG	gi|15803825	rpsM	30S ribosomal protein S13	10.78	13091	-0 424	Cytoplasmic	354
6hrLB	6hrLBG	24hrLB	24hrLBG	gi|15802128 •	rplT	50S ribosomal protein L20	11.47	13489	-0.336	UNKNOWN	303
6hrLB	6hrLBG	24hrLB	24hrLBG	gi|15804573	rplK	50S ribosomal subunit protein L11	9.64	14866	-0.061	UNKNOWN	265
6hrLB	6hrLBG	24hrLB	24hrLBG	gi|15799852	tsf	Elongation Factor Complex Ef-TuEF-Ts	5.22	30273	-0.118	Cytoplasmic	445
6hrLB	6hrLBG	24hrLB	24hrLBG	gi|16131218	tufA/B	elongation factor Tu	6.03	5658	-0.196	Cytoplasmic	255
6hrLB	6hrLBG	24hrLB	24hrLBG	gi|15799694	DnaK	molecular chaperone DnaK	4.83	69072	-0.409	Cytoplasmic	1209
6hrLB	6hrLBG	24hrLB	24hrLBG	gi|15834378	GroL	chaperone Hsp60	4.85	57404	-0.009	Cytoplasmic	105
6hrLB	6hrLBG	24hrLB	24hrLBG	gi|16128421	tig	Trigger Factor	4 83	48163	-0 428	Cytoplasmic	64
6hrLB	6hrLBG	24hrLB	24hrLBG	gi|26250254	secB	export protein SecB	4.61	19518	-0.11	Cytoplasmic	272
6hrLB	6hrLBG	24hrLB	24hrLBG	gi|15801469	OppA	oligopeptide transport protein	5.95	60985	-0.435	Periplasmic	926
6hrLB	6hrLBG	24hrLB	24hrLBG	gi|640114	sodB	Iron(Ii) Superoxide Dismutase	5.58	21121	-0.18	UNKNOWN	1565
6hrLB	6hrLBG	24hrLB	24hrLBG	gi|15800320	ahpC	alkyl hydroperoxide reductase C22 subunit	5.03	20748	-0 278	Cytoplasmic	973
6hrLB	6hrLBG	24hrLB	24hrLBG	gi|15800564	DPS	DNA protection during starvation conditions	5.72	18684	-0 214	UNKNOWN	6564
6hrLB	6hrLBG	24hrLB	24hrLBG	gi|15800816	OmpA	outer membrane Porin protein A	5.99	37178	-0 339	Outer Membrane	3282
6hrLB	6hrLBG	24hrLB	24hrLBG	gi|16130152	ompC	outer membrane porin protein C	4 58	40343	-0.533	Outer Membrane	4336
6hrLB	6hrLBG	24hrLB	24hrLBG	gi|16128970	wrbA	trp repressor binding protein	5 59	20832	-0 082	UNKNOWN	1337
6hrLB	6hrLBG	24hrLB	24hrLBG	gi|15802089	lpp	murein lipoprotein	9 3	8318	-0.314	SpII	802
6hrLB	6hrLBG	24hrLB	24hrLBG	gi|16128870	pflB	pyruvate formate lyase	5.69	85303	-0 38	Cytoplasmic	3319
6hrLB	6hrLBG	24hrLB	24hrLBG	gi|75236334	rpoA	DNA-directed RNA polymerase, alpha subunit	5 02	36452	-0 182	Cytoplasmic	544
6hrLB	6hrLBG	24hrLB	24hrLBG	gi|26246432	yajQ	hypothetical protein c0537	8.12	24680	-0.52	UNKNOWN	692

Appendix C The list of extracellular proteins identified under different growth conditions

Growth condition				GI NUMBER	Gene	*Protein name*	pI	Mr (Da)	GRAVY	LOCATION (PSORTb)
						1. Metabolism of Carbohydrates				
						1.1.specific Pathways				
		24hrLB		gi|15802569	gatA	galactitol PTS permease	5 2	16897	0.003	Cytoplasmic
6hrLB		24hrLB		gi|15802949	ptsI	PTS enzyme I	4 8	63494	-0.12	Cytoplasmic
		24hrLB		gi|16129197	galU	glucose-1-phosphate uridylyltransferase	5.1	32921	0 031	Cytoplasmic
		24hrLB		gi|51247222	Glk	glucokinase	6 2	35778	0 047	Cytoplasmic
			24hrLBG	gi|16130232	pta	Phosphate acetyltransferase	5 2	77110	-0.08	**UNKNOWN**
		24hrLB		gi|16129341	ldhA	D-lactate dehydrogenase	5.3	36497	-0.101	Cytoplasmic
6hrLB	6hrLBG	24hrLB		gi|15802569	crr	PTS system enzyme IIA component	4.7	18240	0 003	Cytoplasmic
		24hrLB		gi|90111527	DkgA	methylglyoxal reductas		27012	-0.375	Cytoplasmic
		24hrLB	24hrLBG	gi|15802566	GatD	galactitol-1-phosphate dehydrogenase	5.9	37366	0 139	Cytoplasmic
		24hrLB	24hrLBG	gi|15804128	aldB	Aldehyde dehydrogenase B	5 5	59687	-0.141	Cytoplasmic
		24hrLB	24hrLBG	gi|15803603	ttdA	L-tartrate dehydratase, α subunit ,	5.9	32656	-0.048	Cytoplasmic
			24hrLBG	gi|75187872	ttdB	L-tartrate dehydratase, β subunit	6.2	22665	-0.13	Cytoplasmic
			24hrLBG	gi|16131619	rbsB	ribose ABC transporter subunit	6 9	30931	-0.031	**Periplasmic**
	6hrLBG	24hrLB	24hrLBG	gi|16131841	gatZ	D-tagatose 1,6-bisphosphate aldolase 2, subunit	5.5	47079	-0 224	Cytoplasmic
	6hrLBG	24hrLB	24hrLBG	gi|15802571	gatY	tagatose 1,6-diphosphate aldolase	6	31093	-0.116	Cytoplasmic
						1.2 Main Glycolytic Pathways				
6hrLB	6hrLBG	24hrLB	24hrLBG	gi|15803300	eno	phosphopyruvate hydratase or enolase	5 4	45574	-0.155	Cytoplasmic
		24hrLB	24hrLBG	gi|16131754	PFK	Phosphofructokinase	5 6	46791	0.000	Cytoplasmic
	6hrLBG	24hrLB	24hrLBG	gi|16129733	GapA	Glyceraldehyde 3-Phosphate Dehydrogenase	6 6	35239	-0.133	Cytoplasmic
6hrLB	6hrLBG	24hrLB	24hrLBG	gi|15803459	FbaA	fructose-bisphosphate aldolase	5.5	38966	-0.349	**UNKNOWN**
6hrLB	6hrLBG	24hrLB	24hrLBG	gi|16130827	PGK	phosphoglycerate kinase	5.1	41093	0 072	Cytoplasmic
6hrLB	6hrLBG	24hrLB	24hrLBG	gi|146099	GapA	glyceraldehyde-3-phosphate dehydrogenase	6	33070	-0.162	Cytoplasmic
6hrLB	6hrLBG	24hrLB	24hrLBG	gi|15799799	aceF	dihydrolipoamide acetyltransferase	5.1	66055	-0.008	**Cytoplasmic Membrane**
6hrLB	6hrLBG	24hrLB	24hrLBG	gi|15804618	pgi	glucose-6-phosphate isomerase	5.9	61749	-0.268	Cytoplasmic
6hrLB	6hrLBG	24hrLB	24hrLBG	gi|16131483	GpmA	phosphoglyceromutase	5.9	28571	-0.195	Cytoplasmic
6hrLB		24hrLB	24hrLBG	gi|26247926	pykF	Pyruvate Kinase	6.7	58651	-0 071	**UNKNOWN**
6hrLB	6hrLBG	24hrLB	24hrLBG	gi|26247926	pykF	pyruvate kinase I	5.8	50276	-0.071	**UNKNOWN**
6hrLB	6hrLBG		24hrLBG	gi|15804508	Tim	Triosephosphate Isomerase Tim	5 6	26955	0.010	**UNKNOWN**
						1.3 Gluconeogenesis				
		24hrLB	24hrLBG	gi|15803907	pckA	phosphoenolpyruvate carboxykinase	8.2	59590	-0 309	**UNKNOWN**
		24hrLB		gi|16129658	pps	phosphoenolpyruvate synthase	5	87347	-0.243	Cytoplasmic
						1.4 glycolate metabolism				
	6hrLBG	24hrLB	24hrLBG	gi|15801728	aldA	aldehyde dehydrogenase A, NAD-linked	5.1	52206	-0.054	Cytoplasmic
6hrLB	6hrLBG			gi|16129803	eda	oxaloacetate decarboxylase	5 6	22300	0.322	Cytoplasmic
		24hrLB	24hrLBG	gi|16131841	aceA	isocitrate lyase	5.4	47200	-0.224	Cytoplasmic
						1.5 TCA cycle				
	6hrLBG	24hrLB	24hrLBG	gi|15803770	mdh	malate dehydrogenase	5 6	32317	0.194	**UNKNOWN**
	6hrLBG	24hrLB	24hrLBG	gi|33383669	Icd	isocitrate dehydrogenase	5.3	42907	-0.171	Cytoplasmic
	6hrLBG	24hrLB	24hrLBG	gi|16128111	acnB	aconitate hydratase aconitase B	5 2	93439	-0.117	Cytoplasmic
		24hrLB		gi|226907	Mdh	malate dehydrogenase	5 6	32246	0 204	**UNKNOWN**
		24hrLB	24hrLBG	gi|15800424	GltA	citrate synthase	6 2	47934	-0.221	Cytoplasmic
		24hrLB	24hrLBG	gi|15800432	sucC	succinyl-CoA synthetase beta subunit	5 4	41367	0.024	Cytoplasmic
		24hrLB	24hrLBG	gi|16131840	AceB	malate synthase A	5 4	60236	-0.316	Cytoplasmic
	6hrLBG	24hrLB		gi|16129237	AcnA	aconitate hydratase OR aconitase	5.6	97616	-0.234	Cytoplasmic
		24hrLB	24hrLBG	gi|15799800	lpdA	dihydrolipoamide dehydrogenase	5 8	50657	-0 011	Cytoplasmic
			24hrLBG	gi|16128704	sucD	Succinyl-CoA synthetase, alpha subunit	6.2	29601	0.162	**UNKNOWN**
	6hrLBG	24hrLB	24hrLBG	gi|16131978	frdB	fumarate reductase (anaerobic)	6.1	27105	-0 224	Cytoplasmic
		24hrLB		gi|16128108	sucB	dihydrolipoamide acetyltransferase	5 6	43984	0 004	**Cytoplasmic Membrane**
		24hrLB	24hrLBG	gi|15800430	sucA	2-oxoglutarate decarboxylase		104993	-0 446	Cytoplasmic
				gi|16128699	sdhB	succinate dehydrogenase iron-sulfur protein	6.3	26752	-0 299	**UNKNOWN**
6hrLB	6hrLBG	24hrLB	24hrLBG	gi|15799798	aceE	pyruvate dehydrogenase complex	5.5	99606	-0 437	**UNKNOWN**

						1.6 pentose phosphate pathway				
		24hrLB	24hrLBG	gı|15802986	talA	transaldolase	5.9	35636	-0.315	UNKNOWN
		24hrLB	24hrLBG	gı|16130390	TktB	transketolase 2, thiamin-binding	5.9	72997	-0 309	Cytoplasmic
	6hrLBG	24hrLB	24hrLBG	gı|1941982	talB	Transaldolase B	5.1	35066	-0.216	UNKNOWN
6hrLB		24hrLB	24hrLBG	gi|11464528	gnd	6-phosphogluconate dehydrogenase	5.1	48744	-0.179	UNKNOWN
						2. TRANSLATION				
						2.1 Ribosomal Proteins				
6hrLB	6hrLBG	24hrLB	24hrLBG	gi|15803823	rpsD	30S ribosomal protein S4	10	23455	-0.664	Cytoplasmic
6hrLB	6hrLBG	24hrLB	24hrLBG	gi|16131220	rpsG	30S ribosomal protein S7	10	17593	-0.46	UNKNOWN
6hrLB	6hrLBG	24hrLB	24hrLBG	gi|15803832	RplF	50S ribosomal protein L6	9.7	18892	-0.227	Cytoplasmic
6hrLB	6hrLBG	24hrLB	24hrLBG	gı|42900	rpsA	30S ribosomal subunit protein S1	4.9	60979	-0 288	Cytoplasmic
6hrLB	6hrLBG	24hrLB	24hrLBG	gi|15804574	rplA	50S ribosomal protein L1	9.6	24714	-0.109	UNKNOWN
6hrLB	6hrLBG	24hrLB	24hrLBG	gı|223035	RplJ	50S ribosomal subunit protein L10	9.3	17725	0.007	UNKNOWN
6hrLB	6hrLBG	24hrLB	24hrLBG	gi|15803841	rpsC	30S ribosomal protein S3	10	26021	-0.422	Cytoplasmic
6hrLB	6hrLBG	24hrLB	24hrLBG	gi|26246115	rpsB	30S ribosomal protein S2	7.2	34405	-0.27	Cytoplasmic
6hrLB	6hrLBG		24hrLBG	gi|15804792	rplI	50S ribosomal protein L9	6 2	15759	0.091	Cytoplasmic
6hrLB	6hrLBG	24hrLB	24hrLBG	gı|15803846	rplD	50S ribosomal protein L4	9.7	22073	-0 235	UNKNOWN
6hrLB	6hrLBG		24hrLBG	gi|15803835	rplE	50S ribosomal protein L5	9 5	20289	-0.282	Cytoplasmic
6hrLB	6hrLBG	24hrLB	24hrLBG	gi|15803840	rplP	50S ribosomal protein L16	11	15271	-0.384	UNKNOWN
6hrLB	6hrLBG	24hrLB	24hrLBG	gi|15803830	rpsE	30S ribosomal protein S5	10	17592	-0.101	UNKNOWN
6hrLB	6hrLBG	24hrLB	24hrLBG	gi|15803825	rpsM	30S ribosomal protein S13	11	13091	-0.424	Cytoplasmic
	6hrLBG		24hrLBG	gi|15803844	rplB	50S ribosomal protein L2	11	29842	-0.699	UNKNOWN
6hrLB	6hrLBG	24hrLB	24hrLBG	gı|15802128	rplT	50S ribosomal protein L20	11	13489	-0 336	UNKNOWN
6hrLB	6hrLBG	24hrLB	24hrLBG	gi|15804573	rplK	50S ribosomal subunit protein L11	9.6	14866	-0.061	UNKNOWN
6hrLB	6hrLBG		24hrLBG	gi|15803847	rplC	50S ribosomal protein L3		22230	-0.235	UNKNOWN
6hrLB	6hrLBG		24hrLBG	gi|15803821	rplQ	50S ribosomal protein L17	11	14356	-0.565	UNKNOWN
6hrLB	6hrLBG		24hrLBG	gi|16131194	rplV	50S ribosomal protein L22	10	12219	-0.349	Cytoplasmic
6hrLB	6hrLBG			gi|15803765	rplM	50S ribosomal protein L13	9 9	16009	-0.54	Cytoplasmic
	6hrLBG	24hrLB	24hrLBG	gı|16131120	rpsI	30S ribosomal protein S9	11	14847	-0 687	Cytoplasmic
6hrLB	6hrLBG		24hrLBG	gi|606235	rplO	50S ribosomal subunit protein L15	11	15025	-0.249	Cytoplasmic
6hrLB		24hrLB		gı|11120595	rpsL	30S ribosomal protein S12	11	13729	-0.627	UNKNOWN
	6hrLBG	24hrLB		gı|133976	rpsF	30S ribosomal protein S6	4 9	15694	-0.827	Cytoplasmic
6hrLB				gi|15803128	rplS	50S ribosomal protein L19	11	13125	-0.527	Cytoplasmic
	6hrLBG			gi|15803824	rpsK	30S ribosomal protein S11	11	13836	-0.446	UNKNOWN
	6hrLBG			gı|15804178	rpmB	50S ribosomal protein L28	11	9058	-0.65	Cytoplasmic
						2.2 Aminoacyl-tRNA biosynthesis				
	6hrLBG	24hrLB		gi|16130792	LysS	lysyl-tRNA synthetase	5.1	57790	-0.396	Cytoplasmic
6hrLB	6hrLBG	24hrLB		gi|16129819	aspS	aspartyl-tRNA synthetase	5 5	65872	-0.265	Cytoplasmic
	6hrLBG	24hrLB		gı|16131430	glyS	glycyl-tRNA synthetase subunit beta	5.3	76765	-0.219	Cytoplasmic
	6hrLBG	24hrLB	24hrLBG	gi|15831679	infC	translation initiation factor IF-3	9.5	20551	-0.671	Cytoplasmic
		24hrLB	24hrLBG	gı|15800356	leuS	leucyl-tRNA synthetase	5 2	97171	-0 368	Cytoplasmic
		24hrLB		.gı|16129669	pheT	phenylalanyl-tRNA synthetase β-chain		87323	-0.097	Cytoplasmic
		24hrLB		gı|75212974	TyrS	Tyrosyl-tRNA synthetase	5.5	47996	-0.293	Cytoplasmic
		24hrLB	24hrLBG	gi|75190755	thrS	Threonyl-tRNA synthetase	5 8	71738	-0.494	Cytoplasmic
	6hrLBG			gi|75189130	ileS	Isoleucyl-tRNA synthetase	5.7	104215	-0 26	Cytoplasmic
				gi|16130330	gltX	glutamyl-tRNA synthetase	5.7	53722	-0 528	Cytoplasmic
	6hrLBG	24hrLB		gı|16128187	proS	Prolyl-tRNA synthetase	5.1	63657	-0.243	Cytoplasmic
						2.3 Elongation				
	6hrLBG	24hrLB	24hrLBG	gi|15803853	FusA	elongation factor EF-2 (G)	5 2	77532	-0.286	Cytoplasmic
6hrLB	6hrLBG	24hrLB	24hrLBG	gı|15799852	tsf	Elongation Factor Complex Ef-TuEF-Ts	5.2	30273	-0 118	Cytoplasmic
6hrLB	6hrLBG	24hrLB	24hrLBG	gi|16131218	tufA/B	elongation factor Tu	6	5658	-0.196	Cytoplasmic
6hrLB	6hrLBG	24hrLB		gi|1790590	efp	elongation factor EF-P	5	20578	-0.221	Cytoplasmic
						2.4posttranslation				
6hrLB	6hrLBG	24hrLB		gi|37926485	frr	ribosome recycling factor	6 4	20683	-0.512	Cytoplasmic
						Protein transport,secretion and folding				
						2.1 Protein Foldingand binding				
		24hrLB	24hrLBG	gi|15802400	yedU	chaperone protein (Hsp) 31	5 5	31145	-0 213	UNKNOWN
		24hrLB	24hrLBG	gi|16130533	grpE	GrpE nucleotide exchange factor/heat shock protein	4.7	21784	-0.372	Cytoplasmic
6hrLB	6hrLBG	24hrLB	24hrLBG	gi|15799694	DnaK	molecular chaperone DnaK	4 8	69072	-0.409	Cytoplasmic
		24hrLB	gi|16128509	gi|16128509	ppiB	peptidyl-prolyl cis-trans isomerase B	5.5	18142	-0.312	Cytoplasmic
6hrLB	6hrLBG	24hrLB		gi|16128422	clpP	ClpB chaperone	5.5	23172	-0.154	Cytoplasmic
6hrLB	6hrLBG	24hrLB	24hrLBG	gi|15834378	GroL	chaperone Hsp60	4.9	57404	-0 009	Cytoplasmic
6hrLB	6hrLBG	24hrLB	24hrLBG	gi|16128421	tig	Trigger Factor	4.8	48163	-0.428	Cytoplasmic
						2.2 Protein turnovwer				
		24hrLB		gi|15800793	pepN	aminopeptidase N	5.1	98819	-0.336	**Cytoplasmic Membrane**

				gi|16130810	pepP	Aminopeptidase P	5 2	49653	-0.308	Cytoplasmic
		24hrLB		gi|16131370	prlC	oligopeptidase A	5.2	77119	-0.416	Cytoplasmic
						2.3Protein transport and secretion				
6hrLB	6hrLBG	24hrLB	24hr	gi|26250254	secB	export protein SecB	4.6	19518	-0.11	Cytoplasmic
6hrLB	6hrLBG	24hrLB	24hrLBG	gi|15801469	OppA	oligopeptide transport protein	6	60985	-0.435	**Periplasmic**
		24hrLB		gi|16129867	fliY	periplasmic cystine-binding protein	6 2	29021	-0.302	**Periplasmic**
						4 Cell process				
						3.1 Cell protection				
6hrLB	6hrLBG	24hrLB	24hrLBG	gi|640114	sodB	Iron(Ii) Superoxide Dismutase	5 6	21121	-0.18	**UNKNOWN**
	6hrLBG	24hrLB	24hrLBG	gi|15802143	katE	catalase; hydroperoxidase HPII(III)	5.5	84060	-0 493	Cytoplasmic
		24hrLB	24hrLBG	gi|16131780	KatG	Catalase/hydroperoxidase	5.5	84150	-0.372	Cytoplasmic
	6hrLBG	24hrLB	24hrLBG	gi|15801846	tpx	thiol peroxidase	4 8	17824	0.256	**UNKNOWN**
6hrLB	6hrLBG	24hrLB	24hrLBG	gi|15800320	ahpC	alkyl hydroperoxide reductase C22 subunit	5	20748	-0 278	Cytoplasmic
					katE	Catalase (peroxidase I)	5.1	79978		
		24hrLB	24hrLBG	gi|16129666	btuE	Glutathione peroxidase	4 7	20397	-0 131	**Periplasmic**
	6hrLBG	24hrLB	24hrLBG	gi|38703898	gst	Glutathione S-transferase	5 1	23714	-0 198	Cytoplasmic
		24hrLB		gi|49176442	sodA	Manganese Superoxide Dismutase	6.4	22952	-0.429	**UNKNOWN**
						3 2 Adaptation to specific condtions				
6hrLB	6hrLBG	24hrLB	24hrLBG	gi|15800564	DPS	DNA protection during starvation conditions	5.7	18684	-0.214	**UNKNOWN**
	6hrLBG	24hrLB		gi|15803116	clpB	heat shock protein/ClpB chaperone	5.4	95870	-0.35	Cytoplasmic
6hrLB	6hrLBG		24hrLBG	gi|26247992	osmE	Osmotically inducible lipoprotein E precursor	7.7	11526	-0 288	**SpII**
6hrLB	6hrLBG	24hrLB		gi|15804041	Slp	Starvation-inducible outer membrane lipoprotein	6.8	20887	-0.088	**SpII**
			24hrLBG	gi|16131215	bfr	bacterioferritin	4.6	18326	-0.472	Cytoplasmic
	6hrLBG	24hrLB		gi|15804947	osmY	hyperosmotically inducible periplasmic protein	6	21056	-0.248	Cytoplasmic
				gi|16131119	sspA	stringent starvation protein A	5.2	24289	-0 265	Cytoplasmic
		24hrLB	24hrLBG	gi:16128457	htpG	Molecular chaperone, HSP90	5.1	71374	-0.521	Cytoplasmic
	6hrLBG	24hrLB		gi|15804972	arcA	ArcA transcriptional dual regulato	5 2	27275	-0.487	Cytoplasmic
	6hrLBG	24hrLB	24hrLBG	gi|15803106	yfiD	putative formate acetyltransferase	5.1	14283	-0.355	Cytoplasmic
						3.3 cell communication				
	6hrLBG			gi|16130599	LuxS	autoinducer 2 (AI-2) synthase/S-ribosylhomocysteinase	5 2	19430	-0 323	Cytoplasmic
6hrLB				gi|16130843	metK	S-adenosylmethionine synthetase 1		42153	-0.189	Cytoplasmic
						3.4 motility				
		24hrLB		gi|16129045	flgK	flagellar hook-associated protein K	4.5	57895	-0.25	**Outer Membrane**
						5 Cell wall and Membrane proteins				
6hrLB	6hrLBG	24hrLB	24hrLBG	gi|15800816	OmpA	outer membrane Porin protein A	6	37178	-0.339	**Outer Membrane**
6hrLB	6hrLBG	24hrLB	24hrLBG	gi|16128782	OmpX	Outer Membrane Protein Ompx	5	16350	-0.32	**Outer Membrane**
6hrLB	6hrLBG	24hrLB	24hrLBG	gi|16128924	OmpA	OmpA-like transmembrane	5.7	37414	-0 339	**Outer Membrane**
	6hrLBG	24hrLB	24hrLBG	gi|16128896	Ompf	outer membrane porin OmpF	4 6	37120	-0.398	**Outer Membrane**
6hrLB	6hrLBG	24hrLB	24hrLBG	gi|88192831	OmpW	Outer Membrane Protein Ompw	6 2	21661	-0.255	**Outer Membrane**
				gi|15802711	tonB	Outer Membrane Transporter Feca	5.5	84968	-0 584	**Outer Membrane**
	6hrLBG			gi|1786777	ompT	outer membrane protein 3b (a)	5 6	35626	-0.645	**Outer Membrane**
6hrLB	6hrLBG			gi|15803582	tolC	outer membrane channel precursor protein	5.5	53953	-0 429	**Outer Membrane**
		24hrLB		gi|1788120	manX	PTS enzyme IIAB	5.7	35079	-0.058	Cytoplasmic
	6hrLBG			gi|16131604	atpF	ATP synthase subunit B	6	17253	-0.213	Cytoplasmic
	6hrLBG			gi|15802711	cirA	outer membrane receptor for iron-regulated	5.1	73352	-0.584	**Outer Membrane**
6hrLB	6hrLBG	24hrLB	24hrLBG	gi|16130152	ompC	outer membrane porin protein C	4 6	40343	-0 533	**Outer Membrane**
6hrLB				gi|16130277	fadL	long-chain fatty acid outer membrane transporter	5.1	48742	-0 3	**Outer Membrane**
	6hrLBG		24hrLBG	gi|16129736	mipA	scaffolding protein	5.5	27813	-0.402	**Outer Membrane**
	6hrLBG	24hrLB	24hrLBG	gi|33112659	nmpC	outer membrane porin protein	4.9	41501	-0 421	**Outer Membrane**
	6hrLBG	24hrLB	24hrLBG	gi|16129338	ompN	outer membrane pore protein N	4 5	41210	-0 546	**Outer Membrane**
	6hrLBG		24hrLBG	gi|16132112	fecA	outer membrane receptor; citrate-dependent	5 5	85224	-0 517	**Outer Membrane**
6hrLB	6hrLBG	24hrLB	24hrLBG	gi|16128970	wrbA	trp repressor binding protein	5.6	20832	-0.082	**UNKNOWN**
		24hrLB	24hrLBG	gi|16131860	malE	Maltose-binding periplasmic proteins	5.2	41591	-0 251	**Periplasmic**
			24hrLBG	gi|49176129	slyB	Outer membrane lipoprotein	9 4	15649	0.114	**/SpII**
			24hrLBG	gi|49176177	flu	antigen 43 autotransporter	5.8	106818	-0 275	**Outer Membrane**
			24hrLBG	gi|16131862	lamB	maltose outer membrane porin	4.8	50042	-0.516	**Outer**

										Membrane
6hrLB	6hrLBG		24hrLBG	gi|15800457	pal	peptidoglycan-associated lipoprotein	6.3	18812	-0.454	**Outer Membrane**
6hrLB	6hrLBG	24hrLB	24hrLBG	gi|15802089	lpp	murein lipoprotein	9.3	8318	-0.314	**SpII**
						6 Metabolism of Amino Acids				
6hrLB			24hrLBG	gi|26247778	gadB	glutamate decarboxylase B subunit	5 7	55405	-0.287	**Periplasmic**
		24hrLB	24hrLBG	gi|16131389	gadA	glutamate decarboxylase A subunit	5 3	32152	-0.278	**Periplasmic**
			24hrLBG	gi|26249699	tdcE	Keto-acid formate acetyltransferase	5 5	85931	-0.293	Cytoplasmic
6hrLB	6hrLBG		24hrLBG	gi|15800563	glnH	glutamineABC transporter periplasmic-binding protein	8.4	27173	-0 233	**Periplasmic**
	6hrLBG			gi|26248790	cysK	Cysteine synthase A	5.8	34865	-0 087	**UNKNOWN**
		24hrLB		gi|9257156	aspC	Aspartate Aminotransferase	5.4	43586	-0.216	Cytoplasmic
		24hrLB		gi|15804731	aspA	aspartate ammonia-lyase	5.5	54030	-0 061	Cytoplasmic
		24hrLB	24hrLBG	gi|882433	gcvP	glycine dehydrogenase (decarboxylating)	5 6	104334	-0.065	**UNKNOWN**
			24hrLBG	gi|16131416	dppA	dipeptide transporter	6 2	60255	-0.463	**Periplasmic**
	6hrLBG			gi|15804455	glnA	glutamine synthetase	5.3	51873	-0 302	Cytoplasmic
6hrLB	6hrLBG			gi|16128223	pepD	aminoacyl-histidine dipeptidase (peptidase D)	5.2	52884	-0.146	Cytoplasmic
	6hrLBG	24hrLB		gi|16128159	dapD	succinyltransferase	5 6	29859	-0.054	Cytoplasmic
			24hrLBG	gi|16130575	gabD	succinate-semialdehyde dehydrogenase I	5.4	51688	-0 071	Cytoplasmic
	6hrLBG			gi|75189962	serC	phosphoserine transaminase	5 5	38592	-0.149	Cytoplasmic
		24hrLB	24hrLBG	gi|48425743	prpD	2-Methylcitrate Dehydratase	5.7	53677	-0.188	**UNKNOWN**
		24hrLB		gi|15803496	ansB	periplasmic L-asparaginase II	5.7	36828	-0.128	**Periplasmic**
		24hrLB		gi|16129498	ydfG	3-hydroxy acid dehydrogenase	5.7	27232	-0.175	Cytoplasmic
		24hrLB	24hrLBG	gi|26247036	putA	Delta-1-pyrroline-5-carboxylate dehydrogenase	5.7	146401	-0.145	Cytoplasmic
6hrLB				gi|1787088	artI	arginine transporter subunit	5.8	26913	-0.329	**Periplasmic**
		24hrLB		gi|16131487	tdh	L-threonine 3-dehydrogenase	5.9	37215	0.051	Cytoplasmic
		24hrLB		gi|26248185	yedO	D-cysteine desulfhydrase	5.2	38727	0.147	Cytoplasmic
		24hrLB		gi|16131488	kbl	2-amino-3-ketobutyrate CoA ligase/glycine C-acetyltransferase	5.7	43130	-0 049	Cytoplasmic
		24hrLB		gi|3005594	nagB	glucosamine-6-phosphate deaminase	6.8	29719	-0.161	Cytoplasmic
				gi|73671334	glmS	glucosamine fructose-6-phosphate aminotransferase	5.6	66865	-0.093	Cytoplasmic
6hrLB	6hrLBG	24hrLB	24hrLBG	gi|16128870	pflB	pyruvate formate lyase	5.7	85303	-0.38	Cytoplasmic
		24hrLB		gi|49176235	YfhO	cysteine desulfurase	94	46203	-0.273	Cytoplasmic
		24hrLB	24hrLBG	gi|15804305	TnaA	tryptophanase	5.9	53392	-0.225	Cytoplasmic
						7 TRANSCRIPTION				
		24hrLB	24hrLBG	gi|15801327	phoP	transcriptional regulatory protein	5	25466	-0.228	Cytoplasmic
		24hrLB		gi|16131236	crp	CRP transcriptional dual regulator/cyclic AMP receptor protein	8 4	23494	-0 21	Cytoplasmic
	6hrLBG			gi|16129198	hns	H-NS transcriptional dual regulator	5 2	15331	-0.751	Cytoplasmic
		24hrLB		gi|16130166	gyrA	DNA gyrase, subunit A	5.1	97132	-0.24	Cytoplasmic
		24hrLB	24hrLBG	gi|15804577	rpoB	DNA-directed RNA polymerase beta subunit	5 2	150536	-0.398	Cytoplasmic
6hrLB	6hrLBG	24hrLB	24hrLBG	gi|75236334	rpoA	DNA-directed RNA polymerase, alpha subunit	5	36452	-0.182	Cytoplasmic
						8. nucleotide and nucleoside conversions and biosynthesis				
		24hrLB	24hrLBG	gi|15804956	deoD	purine nucleoside phosphorylase	5.7	27924	0.07	Cytoplasmic
6hrLB	6hrLBG			gi|15803021	upp	uracil phosphoribosyltransferase	5.9	23545	0.009	Cytoplasmic
6hrLB	6hrLBG	24hrLB		gi|15800203	adk	adenylate kinase	5.6	23571	-0.383	Cytoplasmic
6hrLB		24hrLB		gi|15804955	deoB	phosphopentomutase		44342	-0 271	Cytoplasmic
	6hrLBG	24hrLB		gi|75255057	prsA	Phosphoribosylpyrophosphate synthetase	5 6	36699	0 082	Cytoplasmic
	6hrLBG		24hrLBG	gi|26246416	tsx	protein tsx precursor	5 8	32216	-0 54	**Outer Membrane**
		24hrLB	24hrLBG	gi|147406	purA	adenylosuccinate synthetase	5 2	47373	-0.207	Cytoplasmic
	6hrLBG			gi|15800198	apt	adenine phosphoribosyltransferase	5 3	19860	0.008	Cytoplasmic
		24hrLB		gi|16132198	deoC	deoxyribose-phosphate aldolase	5.5	27730	-0.014	Cytoplasmic
		24hrLB		gi|15799809	hpt	guanine phosphoribosyltransferase	5 1	20604	-0 077	Cytoplasmic
	6hrLBG			gi|16130401	purC	succinocarboxamide synthase	5.1	27149	-0 37	**UNKNOWN**
		24hrLB		gi|16130433	guaB	inositol-5-monophosphate dehydrogenase	6	52275	-0.098	Cytoplasmic
		24hrLB		gi|16129581	add	deoxyadenosine deaminase	5 4	36546	-0 024	Cytoplasmic
		24hrLB	24hrLBG	gi|16130432	guaA	GMP synthetase	5 2	59041	-0.096	Cytoplasmic
		24hrLB		gi|16130687	pyrG	CTP synthetase	5 6	60806	-0.139	Cytoplasmic
						nucleic acid synthesis and replication				
		24hrLB		gi|15803706	pnp	polynucleotide phosphorylase	5 4	79797	-0.169	Cytoplasmic
		24hrLB		gi|16131704	polA	DNA polymerase I	5.4	103054	-0 817	**UNKNOWN**
						9. Metabolism of Fatty and Related Molecules				
	6hrLBG	24hrLB	24hrLBG	gi|145881	fabG	β-ketoacyl-[acyl-carrier-protein] reductase	6 8	25530	0.091	Cytoplasmic

		24hrLB	24hrLBG	gi|15801888	fabI	enoyl-(acyl carner protein) reductase	5 6	27846	0.163	UNKNOWN
				gı|15800061	prpC	citrate synthase-2 /2-methylcitrate synthase	6.4	43075	-0.286	Cytoplasmic
		24hrLB		gi|16128921	fabA	3-hydroxydecanoyl-(acyl carrier protein) dehydratases	7	17249	-0.012	Cytoplasmic
		24hrLB		gi|16128316	prpB	putative phosphonomutase 2 /2-methylisocitrate lyase	5 4	32114	-0 015	Cytoplasmic
		24hrLB	24hrLBG	gi|26250876	acsA	acetyl-coenzyme A synthetase	5.5	71922	-0.277	Cytoplasmic
						10. Metabolism of lipopolysaccharides/lipoprotein				
6hrLB	6hrLBG	24hrLB		gı|15799927	gmhA	phosphoheptose isomerase	6	20802	-0 062	Cytoplasmic
		24hrLB	24hrLBG	gi|16131490	rfaD	ADP-L-glycero-D-mannoheptose-6-epimerase	4.8	34871	-0.284	UNKNOWN
	6hrLBG			gi|15799879	yaeC	putative lipoprotein	5 2	29399	-0.138	SpII
						11.Energy metabolim and transport				
	6hrLBG	24hrLB	24hrLBG	gı|75238587	Qor	NADP-dependent quinone oxidoreductase	5.6	41006	-0.105	UNKNOWN
	6hrLBG			gi|15800387	fldA	flavodoxin	4 2	19725	-0 285	Cytoplasmic
						12.0 metabolism of other compounds				
		24hrLB	24hrLBG	gi|16132048	ppa	inorganic pyrophosphatase	5.1	19691	-0 272	Cytoplasmic
		24hrLB		gi|15801181	grxB	Glutaredoxin 2	7.7	24335	-0.264	UNKNOWN
		24hrLB		gi|16129403	ydcW	γ-aminobutyraldehyde dehydrogenase	5.7	50798	-0.029	Cytoplasmic
				gi|16130843	metK	S-Adenosylmethionine Synthetase/methionine adenosyltransferase	5.1	41614	-0.189	Cytoplasmic
		24hrLB	24hrLBG	gi|16128126	panC	pantoate-β-alanine ligase	5.9	31578	-0.108	Cytoplasmic
						cofactors, small molecule carriers				
		24hrLB		gi|16128127	panB	3-methyl-2-oxobutanoate hydroxymethyltransferase	5.2	28219	0.137	UNKNOWN
6hrLB				gi|26246420	ribH	riboflavin synthase subunit beta	9.6	19798	0.038	UNKNOWN
		24hrLB		gi|16128147	hemL	glutamate-1-semialdehyde 2,1-aminomutase	4.8	45383	0 202	Cytoplasmic
						13. Hypothetical protein				
						Chain A, Designed Helical Protein Fusion Mbp	5 6	54193	-0 619	Cytoplasmic
	6hrLBG	24hrLB	24hrLBG	gi|26247251	ycfP	hypothetical protein c1381	6.5	23336	-0.323	Cytoplasmic
6hrLB	6hrLBG	24hrLB	24hrLBG	gi|26246432	yajQ	hypothetical protein c0537	8.1	24680	-0.52	UNKNOWN
6hrLB		24hrLB	24hrLBG	gi|15802817	elaB	hypothetical protein Z3526	5.4	11299	-0.416	UNKNOWN
6hrLB		24hrLB	24hrLBG	gi|16131082	yrbC	predicted ABC-type organic solvent transporter	9.4	23947	-0.459	UNKNOWN
6hrLB				gi|16128833	ybjP	predicted lipoprotein	6.1	18979	-0.579	SpII
		24hrLB		gi|15800183	ybaY	predicted outer membrane lipoprotein (YbaY)	7.9	19429	0.172	UNKNOWN
		24hrLB		gi|90111415	YfbU	hypothetical protein Z3555	5.9	20213	-0.579	Cytoplasmic
		24hrLB		gi|16129901	yedP	hypothetical protein Z3045	4.9	30451	-0.256	Cytoplasmic
			24hrLBG	gi|16129679	yniA	/predicted phosphotransferase	5	32438	-0.314	UNKNOWN
		24hrLB		gi|16128864	ycaC	predicted hydrolase	5.2	23128	-0 127	UNKNOWN
		24hrLB		gi|90111476	ygaT	hypothetical protein	5.8	37394	-0 375	UNKNOWN
		24hrLB		gı|1742405	YddL	putative outer membrane porin protein/predicted lipoprotein	6.1	10729	-0.592	Outer Membrane
		24hrLB	24hrLBG	gı|16129577	HdhA	7-α-hydroxysteroid dehydrogenase	4.3	9316	0.139	Cytoplasmic
		24hrLB		gi|15801204	maf	Maf-like protein	5.8	23193	-0.249	Cytoplasmic